UNIVERSITY OF SOUTHAMPTON

Faculty of Medicine

Cancer Sciences Unit

B-cell receptor signalling, receptor cross-talk and the SHIP1 phosphatase in malignant B cells

by

Yohannes Gebreselassie

Thesis for the degree of Doctor of Philosophy

October 2019

University of Southampton

Abstract

Faculty of Medicine
Cancer Sciences Unit

Thesis for the degree of Doctor of Philosophy

B-cell receptor signalling, receptor cross-talk and the SHIP1 phosphatase in malignant B cells

Yohannes Gebreselassie

B-cell receptor (BCR) signalling plays a major role in the pathogenesis of chronic lymphocytic leukaemia (CLL) and other B-cell malignancies. In addition to its ability to promote cell accumulation, BCR signalling also influences the function of other cell surface receptors (receptor cross-talk), including G-protein couple receptors (GPCR). This project addresses two inter-connected areas related to BCR signalling in malignant B cells. First, it explores pathways of cross-talk between the BCR and the GPCRs CXCR4 and EBI2, including the role of kinases and the inositol lipid phosphatase SHIP1. Second, it identifies novel pathways regulated by a chemical SHIP1 activator, AQX-435.

Established B-cell lines were selected to investigate BCR→CXCR4 to extend previous studies performed using primary CLL cells. This revealed that, similar to CLL cells, anti-IgM-induced CXCR4 down-modulation was dependent primarily on SYK and PI3K, but not BTK. However, in contrast to CLL cells, activation of SHIP1 using AQX-435 was not sufficient to down-modulate CXCR4 in B-cell lines. One aim of these cell line studies was to perform RNAi transfection studies to investigate the role of individual signalling intermediates in BCR→CXCR4 cross-talk. However, it was not possible to achieve sufficient target knock-down with RNAi for reliable characterisation. Investigation of cross-talk was extended to EBI2 which, like CXCR4, is involved in positioning B cells during immune responses. Overall, EBI2 was expressed at low levels on CLL cells compared to normal B cells and this low level did not seem to be sufficient to support signalling or survival responses following ligand stimulation. In contrast to CXCR4, there was no strong evidence that EBI2 was subject to regulation either by anti-IgM or AQX-435.

Analysis of RNA-seq data demonstrated that AQX-435 and the PI3K inhibitor idelalisib shared the ability to reduce anti-IgM-induced changes in gene expression in CLL cells. However, AQX-435 also triggered a unique transcriptional response driven by activation of liver X receptor (LXR), potentially linked to SHIP1 activation. LXR activation drives cholesterol efflux and functional experiments demonstrated that supplementation of cholesterol using mevalonic acid significantly reduced AQX-435-induced CLL cell apoptosis.

Overall, these experiments shed important new light on BCR signalling in malignant B cells, and support the idea that SHIP1 activators, such as AQX-435, are attractive potential therapeutic agents.

Table of Contents

Table of Tables

List of Figures

Academic Thesis: Declaration Of Authorship

I, Yohannes gebreselassie declare that this thesis and the work presented in it are my own and has been generated by me as the result of my own original research.

B-cell receptor signalling, receptor cross-talk and the SHIP1 phosphatase in malignant B cells

I confirm that:

1. This work was done wholly or mainly while in candidature for a research degree at this University;

2. Where any part of this thesis has previously been submitted for a degree or any other qualification at this University or any other institution, this has been clearly stated;

3. Where I have consulted the published work of others, this is always clearly attributed;

4. Where I have quoted from the work of others, the source is always given. With the exception of such quotations, this thesis is entirely my own work;

5. I have acknowledged all main sources of help;

6. Where the thesis is based on work done by myself jointly with others, I have made clear exactly what was done by others and what I have contributed myself;

7. Either none of this work has been published before submission, or parts of this work have been published as: [please list references below]:

Signed: ……

Date: ……

Acknowledgements

Firstly, I would like to thank my supervisor Professor Graham Packham, Dr Andy Steele, Dr Francesco Forconi and Professor Mark Cragg for giving me the opportunity to carry out this research in his laboratory and his support and guidance throughout my PhD.

I am also grateful to the members of the CLL lab group for their support and encouragement during my PhD for always providing a pleasant work environment. I want to particularly to thank Dr Elizabeth Lemm and Dr Nicki Weston-bell for mentoring me in the lab. I want to also thank Andrea Sailer for his kind gift of reagents which are not commercially available.

Furthermore, I would especially like to thank my parents and family for their unconditional continued support in every venture I undertake. Particular thanks must go to my partner Angelina for her patience, support and computer help. Without these people I would not have been able to achieve completing my PhD.

Finally I would like to acknowledge and thank Bloodwise and the University of Southampton for providing me with a scholarship to pursue my studies.

Definition and Abbreviation

7α25-OHC	7α,25-dihydroxycholesterol
AACS	Acetoacetyl-CoA Synthetase
ABCA1	ATP-binding cassette transporter
ABCG1	ATP Binding Cassette Subfamily G Member 1
ABC-DLBCL	Activated B cell like Diffuse Large B cell Lymphoma
ACAT1	Acetyl-CoA acetyltransferase
AID	Activation Induced Cytidine Deaminase
AKT	Protein Kinase B
ALL	Acute Lymphoblastic Leukeamia
AML	Acute Myeloid Leukeamia
ATF3	Activating Transcription Factor 3
AQX-435	Aquinox 435
BAFF	B-Cell Activating Factor
BAX	BCL-2 Associated X Protein
BCL-6	B-Cell Lymphoma 6 Protein
BcL-xL	B-Cell Lymphoma-extra large
BCL2	B-Cell Lymphoma 2
BCMA	B-Cell Maturation Antigen
BCR	B-Cell Receptor
BLNK	B-Cell Linker Protein
BM	Bone Marrow
BPS/IC	Bladder Pain Syndrome/Interstitial Cystitis
BSA	Bovine Serum Albumin
BTK	Bruton Tyrosine Kinase
CA^{2+}	Calcium
CCL2	Chemokine (C-C motif) Ligand 2
CCL7	Chemokine (C-C motif) Ligand 7
CCL17	Chemokine (C-C motif) Ligand 17
CCL19	Chemokine (C-C motif) Ligand 19
CCL21	Chemokine (C-C motif) ligand 21
CCL22	Chemokine (C-C motif) Ligand 22
CCR7	Chemokine Receptor Type 7
CD19	Cluster of Differentiation 19
CD20	Cluster of Differentiation 20
CD22	Cluster of Differentiation 22
CD23	Cluster of Differentiation 23
CD38	Cluster of Differentiation 38
CD40	Cluster of Differentiation 40
CD40L	Cluster of Differentiation 40 Ligand
CD40R	Cluster of Differentiation 40 Receptor

CD44	Cluster of Differentiation 44
CD49d	Cluster of Differentiation 49d
CD5	Cluster of Differentiation 5
CD79A	Cluster of Differentiation 79A
CD79B	Cluster of Differentiation 79B
cDNA	Complimentary DNA
CH25H	Cholesterol 25-Hydroxylase
CLL	Chronic Lymphocytic Leukeamia
CML	Chronic Myeloid Leukeamia
CME	Clathrin Mediated Endocytosis
COPD	Chronic Obstructive Pulmonary Disease
cRPMI	Complete RPMI
CXCL12	C-X-C Motif Chemokine Ligand 12
CXCL13	C-X-C Motif Chemokine Ligand 13
CXCR4	CXC Chemokine Receptor 4
CXCR5	CXC Chemokine Receptor 5
CYP7B1	25-Hydroxycholesterol 7-alpha-Hydroxylase
DAG	Diacylglycerol
DC	Dendritic Cells
DCSIGN	Dendritic Cell-Specific Intercellular adhesion molecule-3-Grabbing Non integrin
DDX11	DEAD/H-Box Helicase 11
DDX11L2	DEAD/H-Box Helicase 11 Like 2
DHCR24	24-Dehydrocholesterol Reductase
DOK	Docking Protein
DNA	Deoxyribonucleic Acid
EBI2	Epstein Barr virus induced G coupled protein receptor 2
ER	Endoplasmic Reticulum
FBS	Fetal Bovine Serum
FCR	Fludarabine, Cyclophosphamide Retuximab
FCS	Fetal Calf Serum
FDA	Food and Drug Administration
FDC	Follicular Dendritic cells
g	Gravitational Force
GC	Germinal Centre
GFP	Green Fluorescent Protein
GPCR	G Coupled Protein Receptor
Grb2	Growth Factor Receptor-bound Protein 2
GSK3-β	Glycogen Synthase Kinase 3 Beta
HCL	Hydrochloric Acid
HEL	Hen egg Lysozyme
HEV	High Endothelial Venules
HMGB1	High Mobility Group Box 1
HMGR1	3-hydroxy-3-methylglutaryl CoA reductase 1

HSC	Hematopoietic Stem Cells
IFN α	Interferon Alpha
IFN γ	Interferon Gamma
Ig	Immmunoglobulin
IGHV	Immunoglobulin Heavy chain Variable region Gene
IL-2	Interleukin-2
IL-4	Interleukin-4
IL-5	Interleukin-5
IL-6	Interleukin-6
IPA	Ingenuity Pathway Analysis
ITAM	Immunoreceptor Tyrosine-based Activation Motifs
ITIM	Immunoreceptor tyrosine-based Inhibition Motif
JNK	c-Jun N-terminal Kinases
LAM	Lymphoid Associated Macrophages
LXR	Liver X Receptor
LYN	Lck/Yes novel tyrosine kinase
MALT	Mucosal-Associated Lymphoid Tissues
MAPK	Mitogen Activated Protein Kinase
MCL1	Myeloid Leukeamia Cell differentiation protein 1
MHC	Major Histocompatibility Complex
MMP9	Matrix MetalloPeptidase 9
MSC	Mesenchymal Stem Cells
mTOR	mammalian Target Of Rapamycin
MVA	Mevalonic acid
MVD	Mevalonate Diphosphate Decarboxylase
MVK	Mevalonate Kinase
NFAT	Nuclear factor of activated T-cells
NF-κB	Nuclear factor kappa-light-chain-enhancer of activated B cells
NLC	Nurse Like Cells
OS	Overall Survival
PBMC	Peripheral Blood Mononuclear Cells
PC	Proliferation centres
PDK	3-Phosphoinositide Dependent protein Kinase-1
PFS	Progression Free Survival
PIK3C3	Phosphatidylinositol 3-Kinase Catalytic Subunit Type 3
PKC	Protein Kinase C
PKD	Protein Kinase D
PLC-γ2	Phospholipase C Gamma 2
PTB	PhosphoTyrosine-Binding domains
PTEN	Phosphatase and Tensin Homolog
PTPN22	Protein Tyrosine Phosphatase, Non-receptor type 22
RNA	Ribonucleic acid
S1P	Sphingosine-1-Phosphate

S1PR1	Sphingosine-1-phosphate receptor
SCD	Stearoyl-CoA desaturase-1
SDF1	Stromal Derived Factor 1
SDS	Sodium Dodecyl Sulfate
SH2	Src Homology 2
SHIP1	Phosphatidylinositol-3,4,5-trisphosphate 5-phosphatase 1
SHIP2	Phosphatidylinositol 3,4,5-trisphosphate 5-phosphatase 2
SHP-1	Src Homology region 2 domain-containing Phosphatase-1
sIg	Surface Immunoglobulin
SLO	Secondary Lymphoid Organ
SMH	Somatic Hyper Mutation
SREBF1	Sterol Regulatory Element Binding Transcription Factor 1
SQLE	Squalene Epoxidase
STAT2	Signal Transducer and Activator of Transcription 2
STAT3	Signal Transducer and Activator of Transcription 3
SYK	Spleen Tyrosine Kinase
TACI	Transmembrane Activator and Calcium-modulator and Cytophilin Ligand Interactor
TAPP	Tandem PH (pleckstrin homology)-domain-containing protein
TBS	Tris-Buffered Saline
TCR	T Cell Receptor
TGF-B	Tumour Growth Factor Beta
TNF	Tumour Necrosis Factor
Treg	T Regulatory Cells
VCAM-1	Vascular Cell Adhesion Protein 1
VEGF	Vascular Endothelial Growth Factor
VLA-4	Very Late Activation Antigen 4
WHO	World Health Organisation
WT	Wild Type
XIAP	X-linked Inhibitor of Apoptosis Protein
α4β1	Alpha 4 Beta 1 integrin

Chapter 1 : Introduction

1.1 Overview

This project addresses two closely inter-related areas. First, cross-talk between the B-cell receptor (BCR) and other cell surface receptors which influence the response of chronic lymphocytic leukaemia (CLL) cells to microenvironmental factors, including the role of specific kinases and the inositol lipid phosphatase SHIP1. Second, pathways regulated by a novel chemical SHIP1 activator, AQX-435. This introduction, therefore, focuses on the following main areas; (i) the microenvironment and normal B-cell development, (ii) structure and function of the BCR, (iii) the role of BCR signalling and the microenvironment in CLL, and (iv) targeting of BCR signalling with kinase inhibitors and the SHIP1 agonist AQX-435.

1.2 Microenvironmental influences in normal B-cell development

Normal B cell are characterised by their ability to survey and identify antigen followed by their maturation and development of antigen-specific humoral responses (LeBien & Tedder, 2008). To orchestrate an effective immune response, normal B cells depend on specific signals and interactions to promote cell proliferation, differentiation and survival within structurally organised tissue microenvironments including the bone marrow (BM) and secondary lymph nodes (SLO).

1.2.1 The Bone Marrow and Secondary Lymphoid Organs and their role in B-cell development and differentiation

The BM microenvironment occupies the medullary cavities of the long bones and consists of two main components, the parenchyma which comprises the haematopoietic component and includes haematopoietic stem cells and progenitor stem cells, and the stroma which comprises the vascular component, including multipotent non-haematopoietic progenitor cells (LeBien & Tedder, 2008). In essence, the BM harbours a dense, complex

microenvironment that supports the creation of large numbers of various blood cells and is the primary lymphoid organ for the development of B cells.

Whitlock and Witte initially developed an *in vitro* culture system to study the early stages of B-cell maturation and confirmed the pivotal role of mesenchymal stem cells (MSC) (Whitlock & Witte, 1982). MSC act via expression of co-stimulatory/survival molecules, such as CD80, CD86 and CD40 ligand (Klyushnenkova et al., 2005), cytokines which promote growth (e.g. IL-6), as well as direct cell-to-cell contact-mediated growth signals (e.g. via VLA-4) (Minges et al., 2002). Therefore, the BM contributes to B-cell development and humoral immune responses by providing a highly supportive, stroma-dense microenvironment.

The BM microenvironment also allows for the development and maturation of B cells with appropriate antigen receptors before they egress into peripheral blood (Blackwell & Alt, 1988; Davis & Bjorkman, 1988). Initial BCR diversity is generated in the BM via the random recombination of heavy and light chain-encoding immunoglobulin (Ig) gene segments as cells progress through their initial antigen-independent developmental stages (Figure 1.1).

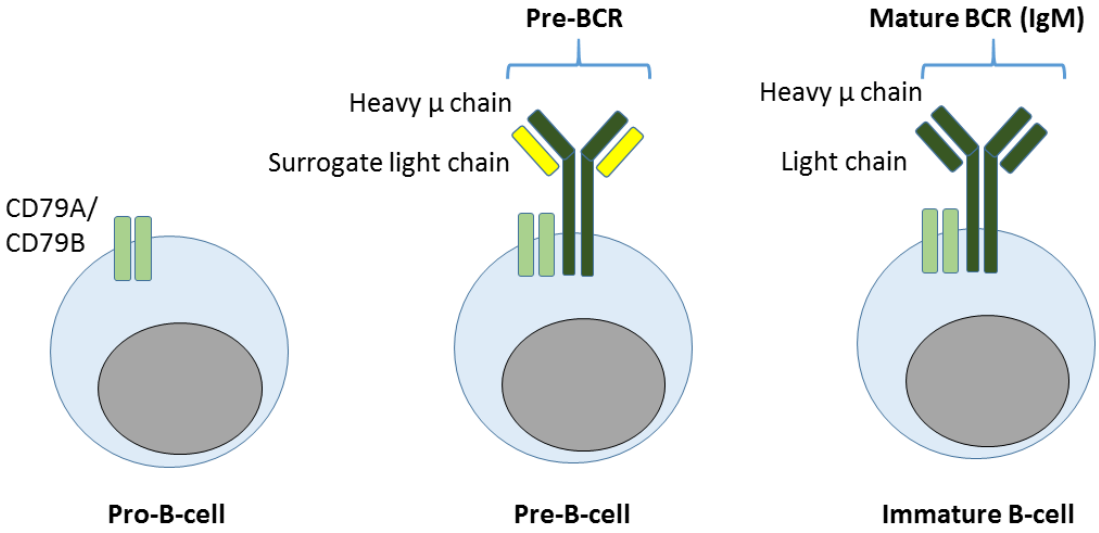

Figure 1.1. Maturation of the BCR and early B-cell development in the BM
Ig heavy chain gene rearrangement occurs with development of pro-B cells into pre-B cells, resulting in the expression of Ig heavy chains and surrogate light chains on the surface of the pre-B cell, which along with CD79A and CD79B, forms the pre-B cell receptor. The pre-B cell then undergoes light chain gene rearrangements as it differentiates into an immature B cell with a fully formed BCR. Illustration taken from Kuby immunology (Kindt et al., 2007).

The SLO includes the spleen, lymph node (LN) and mucosal-associated lymphoid tissues (MALT). The primary role of these tissues is to trap, process and present foreign antigens entering via from the bloodstream to initiate an adaptive immune response (Zhao et al., 2012). Migration of mature B cells to the germinal centres (GC) within the SLO allows further development of B cells and generation of BCR diversity in response to antigen, by promoting somatic hyper-mutation (SHM), class-switching and interactions with $CD4^+$ T follicular helper (TFH) cells and follicular dendritic cells (FDC) for antigen presentation and T-cell help (Cyster et al., 2000) (Figure 1.2). These finely regulated steps results in the proliferation, maturation, and differentiation of appropriate B cells into antigen-specific effector plasma cells or memory B cells (LeBien & Tedder, 2008), as well as tolerance and elimination of autoreactive/non-functional B cells.

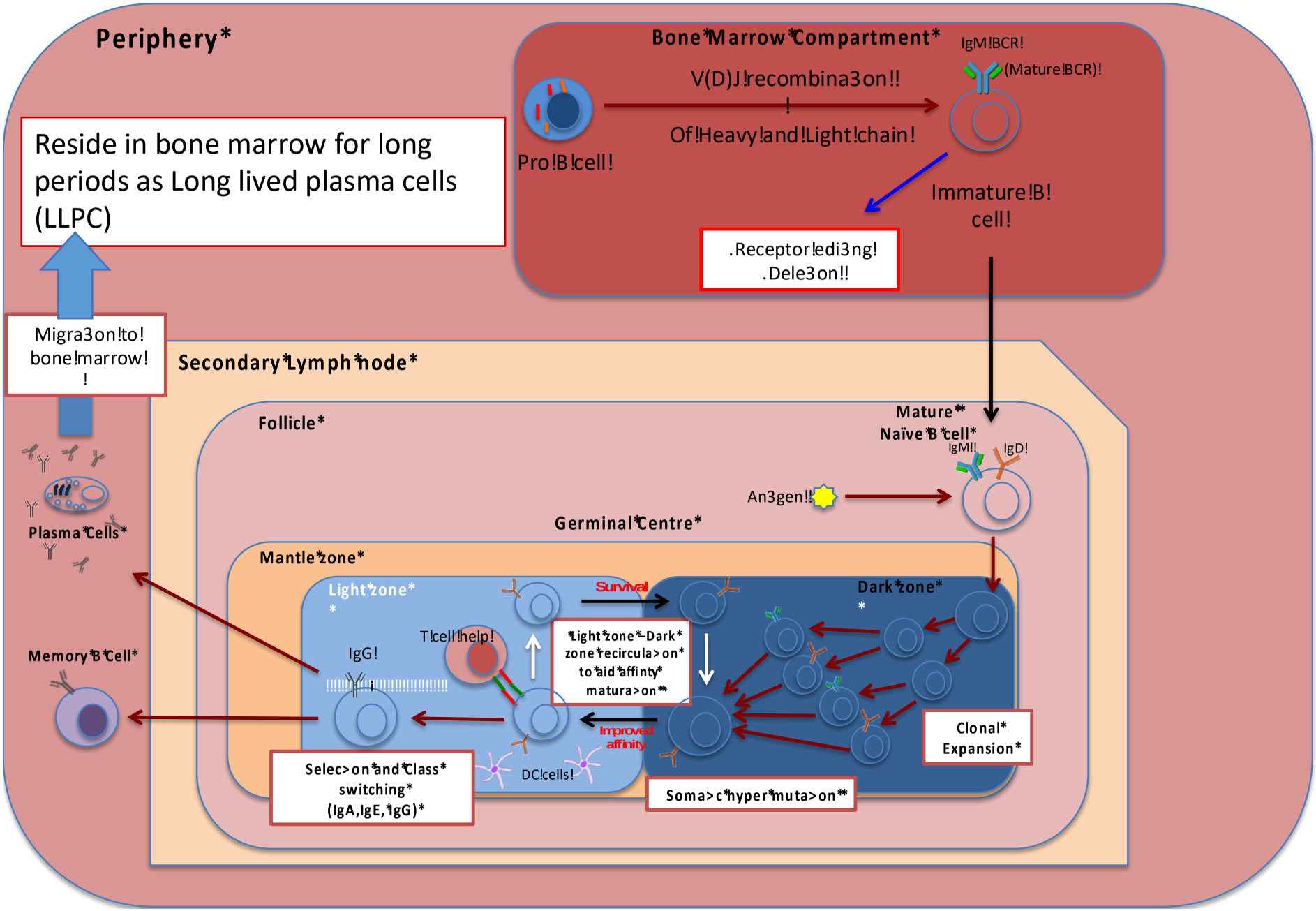
Periphery*
Bone*Marrow*Compartment*
IgM!BCR!
(Mature!BCR)!
V(D)J!recombina3on!!
!
Of!Heavy!and!Light!chain!
Pro!B!cell!
Immature!B!
cell!
.Receptor!edi3ng!
.Dele3on!!
Reside in bone marrow for long periods as Long lived plasma cells (LLPC)
Migra3on!to!
bone!marrow!
!
Secondary*Lymph*node*
Follicle*
Mature**
Naïve*B*cell*
IgM!!
IgD!
An3gen!!
Germinal*Centre*
Plasma*Cells*
Mantle*zone*
Light*zone*
*
Survival
Dark*zone*
*
T!cell!help!
IgG!
*Light*zone*–Dark*
zone*recircula>on*
to*aid*affinty*
matura>on**
Memory*B*Cell*
Improved
affinity
Clonal*
Expansion*
Selec>on*and*Class*
switching*
(IgA,IgE,*IgG)*
DC!cells!
Soma>c*hyper*muta>on**

Figure 1.2. B cell lymphopoiesis and generation of BCR diversity.
B-cell development occurs in both the BM and SLO. Recombination of Ig heavy and light chain gene segments within the BM results in the generation of immature B cells expressing a specific BCR. At this point, autoreactive cells may be removed from the repertoire through receptor editing or deletion. IgM/IgD-expressing mature naïve B cells then exit the BM and migrate to the SLO. Upon antigen stimulation, B cells enter the dark zone within germinal centres where B cells undergo clonal expansion (proliferation) and generate additional BCR diversity through somatic hypermutation (SHM) of Ig variable region genes. After SHM, B cells enter the light zone where BCRs are tested for their affinity by competing for antigen uptake and T-cell help. Cells which are relatively poor at internalising antigen do not receive adequate T-cell help and are eliminated by apoptosis. B cells bearing higher affinity BCRs are positively selected and may undergo class switching to generate BCRs with distinct constant regions (i.e, IgG, IgA, IgE). Mature B cells then receive differentiation signals to exit the germinal centre as (i) memory B cells that circulate in the periphery and can be reactivated in subsequent contacts with antigen or (ii) antibody producing plasma cells.

1.2.2 Lymphocyte trafficking : The role of chemokine-chemokine receptor interactions

Chemokines are key mediators of trafficking, homing and retention of lymphocytes in the BM and SLO. They are a family of small (8–10 kDa) proteins which are secreted to regulate trafficking, proliferation and adhesion to extracellular matrix molecules. Chemokines can be divided into two major groups (Dürig et al., 2001). The first group are homeostatic chemokines which are constitutively produced and secreted within tissue microenvironments and serve to maintain physiological trafficking. An example of homeostatic chemokines that are constitutively produced in certain tissues and are CCL19/CCL21, CXCL12 and CXCL13 that are responsible for basal leukocyte migration through the receptor CCR7, CXCR4 and CXCR5 respectively. The second group includes inflammatory chemokines, which are primarily induced in inflamed tissues under pathological conditions such as IL-1, TNF-Alpha, Lipopolysaccharides (LPS), or viruses to recruit and attract effector cells (Moser et al., 2001) include CCL2, CCL3 , CCL4, CCL5, CCL11, CXCL10. These chemokine actively participate in attracting immune cells to the site of inflammation in order to initiate an immune response or promote wound healing include (Zlotnik & Yoshie, 2012). Chemokines specifically act via binding to their respective receptors, which are seven transmembrane domain-containing G-protein-coupled cell surface receptors (GPCR) (Figure 1.3).

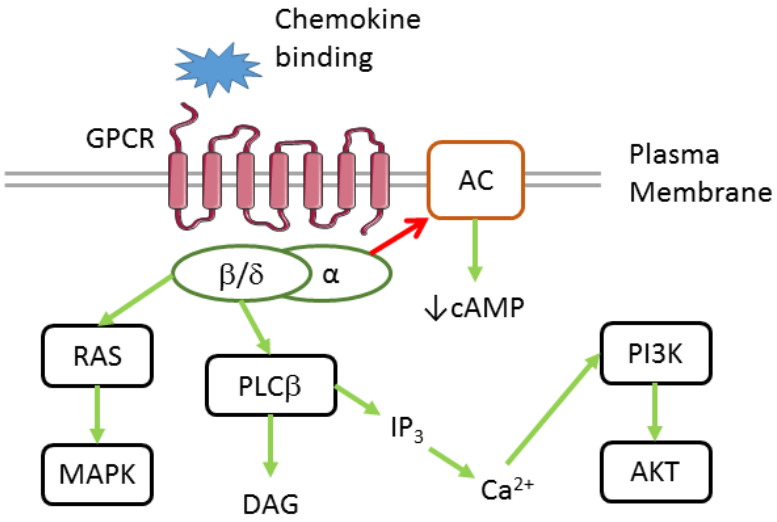

Figure 1.3 Chemokine -induced signalling via GPCR
Chemokine-induced activation of chemokine receptors results in a conformational change of the receptor and activation of the coupled G proteins. G proteins that associate with GPCRs are heterotrimeric comprising α, β and γ subunits. Upon ligand activation of GPCR, these proteins dissociate resulting in the exchange of GDP for GTP on the α subunit. The Gα proteins coupled with chemokine receptors are generally inhibitory Gα proteins (Gαi). The activated Gαi protein inhibits adenylyl cyclase (AC) which is enzyme that induces formation of cAMP, which in turn results in the activation of protein kinase A. However, stimulation of GPCR (Gαs) via the Gαs-coupled receptors promotes increased AC activity and cAMP accumulation to activate a downstream cAMP-responsive element- binding protein (CREB) via PKA to modulate gene transcription and regulates expression of cyclins and the CDK inhibitor p27Kip1. The β- and γ-subunits activate phospholipase C (PLCβ) which cleaves PI(4,5)P2 to produce diacylglycerol (DAG) and inositol triphosphate (IP3), resulting in mobilisation of intracellular Ca2+. Other pathways activated following GPCR stimulation include RAS→MAPK and PI3K→AKT signalling. Collectively these pathway modulate cytoskeleton dynamics, proliferation and cell migration. Illustration taken from Zarbock et al., 2012.

Homing and migration of lymphocytes during lymphopoiesis and immune responses involves co-operation between chemokines and adhesion molecules, such as integrins, CD44, and L-selectins (Springer et al., 1994). In normal B cells, trafficking and homing is mediated predominantly by interactions between B cells and accessory stromal cells (Burger et al., 2011). One well documented mediator is CXCL12 (Nagasawa et al., 1994) which binds to CXCR4 on hematopoietic cells to promote trafficking along CXCL12 concentration gradients that exist between the peripheral blood and microenvironmental niches.

The synchronized entry, movement and positioning of lymphocytes into and within tissue microenvironments is crucial to elicit specific immune responses. In line with Springer's multistep paradigm (Springer et al., 1994), circulating lymphocytes enter the SLO via transient and reversible interactions with high endothelial venules (HEV). The entry process involves chemokines displayed on the luminal endothelial surface which activates chemokine receptors on lymphocytes to induce selectin or integrin supported ''rolling''. This results in the arrest, firm adhesion and trans-endothelial migration into tissues where chemokine gradients guide localization and retention of the cells, also known as "homing" (Cyster et al., 1999). CCL21 is the predominant chemokine expressed by HEV and it is involved in lymphocyte trafficking via interaction with CCR7 (Gunn et al., 1998). CXCL12-CXCR4 and CXCL13-CXCR5 interactions also contribute to homing and trafficking to the LNs (Cyster et al., 2005).

1.2.3 Chemokines and movement and positioning of B cells within SLO

After lymphocytes enter the SLO from the blood they organise themselves within B-cell follicles and T-cell zones; this is mediated by chemokine-chemokine receptor mediated positioning (Figure 1.4). Naïve B cells home into follicles in a CXCR5-CXCL13 dependent manner, with CXCL13 being produced by stromal cells such as FDC within the follicles (Gunn et al., 1998; Cyster et al., 2000).

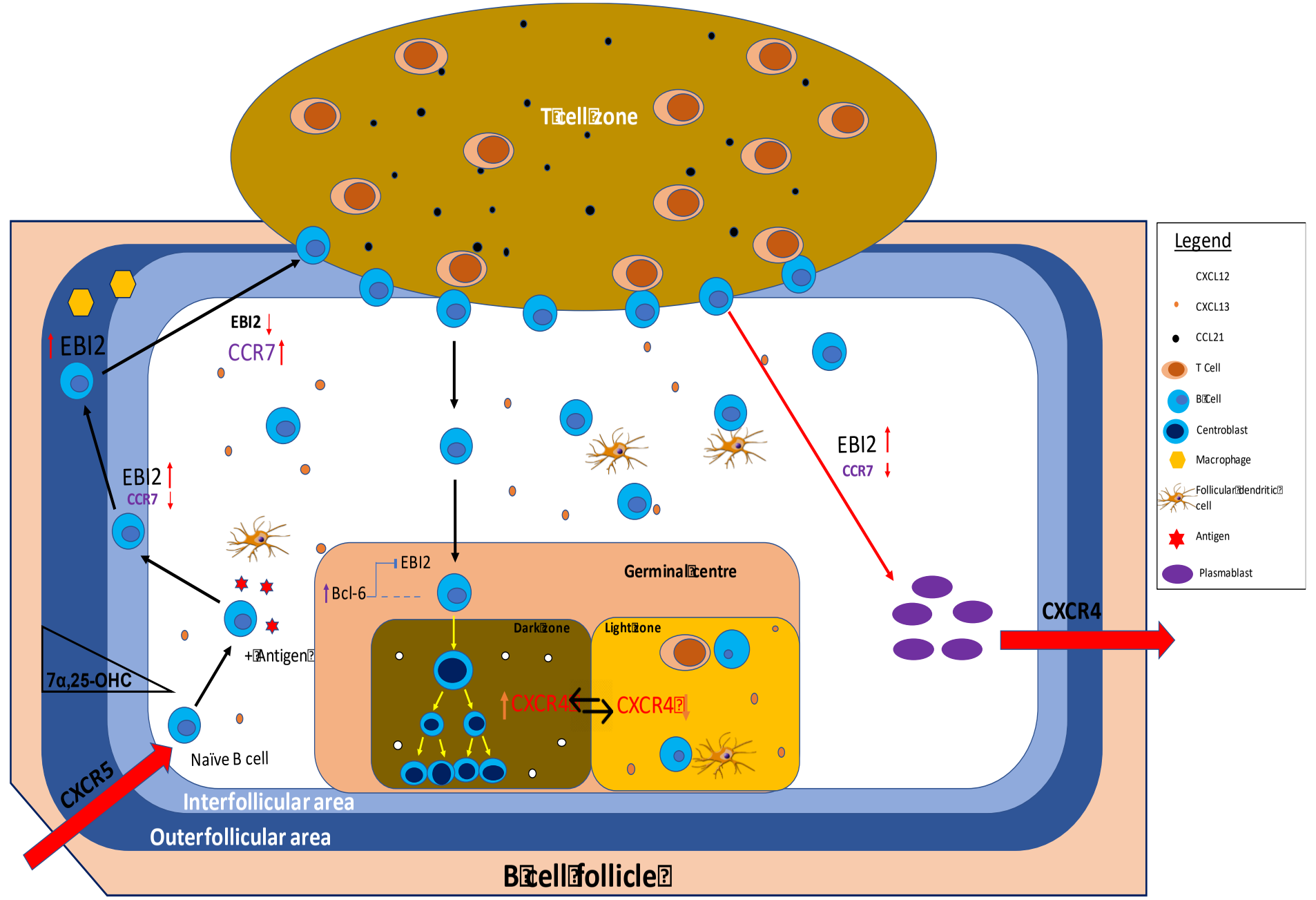
T cell zone
EBI2
EBI2
CCR7
EBI2
CCR7
EBI2
CCR7
EBI2
Bcl-6
Germinal centre
Dark zone
Light zone
CXCR4
CXCR4
+ Antigen
7α,25-OHC
Naïve B cell
CXCR5
CXCR4
Interfollicular area
Outerfollicular area
B cell follicle
Legend
CXCL12
CXCL13
CCL21
T Cell
B Cell
Centroblast
Macrophage
Follicular dendritic cell
Antigen
Plasmablast

Figure 1.4. The movement and positioning of B cells inside the lymphoid follicles during T-cell-dependent antibody responses
Figure illustrates the role of specific cytokines and their receptors in controlling movement and position of B-cells during a T-cell dependent antibody response. See text for further details.

Positioning and movement of B and T cells within the lymphoid structures in a cellular immune response is tightly controlled by chemo-attractants interacting with their receptors. For example, during an antigen-driven, T-cell dependent antibody response, EBI2, which belongs to the rhodopsin-like subfamily of GPCR, mediates migration of activated B cells to inter- and outer-follicular areas of the LN (Kelly et al., 2011). Although expressed constitutively in mature naive B cells, engagement of the BCR by antigen results in a substantial (5-fold) and rapid (within one hour) increase of *EBI2* mRNA expression (Glynne et al., 2000; Kelly et al., 2011; Gatto et al., 2013). Upregulated EBI2 receptor expression then mediates the immediate positioning of antigen-activated B-cell in the outer-follicular areas (Figure 1.4). This is thought to be required for B cells to gain additional antigen presented by macrophages present in either the marginal sinus or subscapular sinus of the spleen and LN, respectively (Phan et al., 2007). The major ligand for EBI2 which is responsible for directing activated B cells to inter- and outer-follicular areas is the oxygenated derivative of cholesterol, 7α,25-dihydroxycholesterol (7α25-OHC) (Hannedouche et al., 2011).

As the B-cell response proceeds, upregulation of chemokine receptor CCR7 (6-24 hours after BCR activation) results in increased responsiveness to its ligands CCL19 and CCL21 which are abundantly expressed in the T-cell zone causing B cells to relocate to the B/T-cell zone boundary (Reif et al., 2002). CCR7, plays an important role in homing and allowing entry of naïve B cells, T cells and activated mature dendritic cells (DC) into the LN (Gatto et al., 2013). In the context of T-cell dependent antibody responses, CCR7, acting in concert with EBI2, causes B cells to migrate and align at the T/B-cell border to allow effective T-cell/B-cell interactions. Studies using CCR7-deficient mice B cells demonstrate that there is a hierarchical relationship between CCR7 and EBI2, with CCR7 being dominant as deficient B cells move directly to outer-follicular areas after antigen engagement (Reif et al., 2002). This is consistent with the observation that 24-48 hours after antigen engagement, movement of splenic mice B cells to the inter-follicular area is dependent on CCR7 down-regulation (Gatto et al., 2013).

At 48-72 hours into the B-cell response, reduction in CCR7 expression allows B cells to regain sensitivity to 7α,25-OHC. Thus, sustained elevated EBI2 expression directs B cells to migrate towards the inter-follicular area where they undergo an initial burst of proliferation and differentiation. In addition, differential expression of enzymes that synthesise (CH25H, CYP7B1) and degrade (HSD3B7) 7α,25-OHC, scattered between the inner-/outer-follicular areas and the T cell zone, create a gradient in 7α,25O-HC which further aids the correct positioning of B cells (Cyster et al., 2014). This again highlights the complex and efficient coordination between EBI2 and CCR7 during the T-cell dependent antibody response. Additionally, EBI2 plays a key role during in influencing whether B cells commit to an early plasma blast response (maintained EBI2 expression) or become GC B cells (reduced EBI2 expression) (Gatto et al., 2013; Gatto et al., 2009).

Egress of lymphocytes from the SLO lymphoid structures is largely controlled by the sphingosine-1-phosphate (S1P) receptor (S1PR). Cyster et al., demonstrated that an increasing concentration gradient of S1P (high in blood and lymph circulation, low in tissue) exists between the interior of the lymphoid tissue and the adjacent blood or lymph circulation (Cyster et al., 2005). This is due to higher activity of S1P-degrading enzymes in tissues (Milstien & Spiegel, 2003). Inside the LN, B cells ready to exit upregulate S1PR to orchestrate tissue egression. By contrast, when B cells re-enter SLO, S1PR is transiently downregulated. Antigen engagement further down-modulates S1PR favouring tissue retention.

Collectively, positioning and migration of B cells during an immune response is as a result of a balanced network of stimuli that sequentially generate extra-follicular and GC responses, and LN entry/exit to provide protective immunity (Figure 1.4). Chemokine receptors and their modulation following antigen engagement of the BCR play a critical role in co-ordinating these events.

1.3 The B-cell receptor: structure and function

The fate of B cells is highly dependent on the function of the BCR. BCR-driven outcomes include activation, proliferation, differentiation, cell killing and/or induction of anergy (Woyach et al., 2012; Treanor, 2012; Packham et al., 2011). Selection of these different fates is dependent on the stage of B-cell differentiation, the nature of the engaging ligand and the presence or absence of supporting co-stimulation. As described above (section 1.2), cell autonomous effects of BCR signalling (e.g. proliferation/activation) are accompanied by BCR-dependent modulation of other cell surface receptors, including chemokine receptors, which influences how B-cells sense and respond to their microenvironment.

The BCR comprises a disulphide-linked tetramer of two Ig heavy and two Ig light chains molecules that comprise a transmembrane antigen-binding immunoglobulin (IgA, IgD, IgE, IgG or IgM) and a heterodimer of CD79A (Igα) and CD79B (Igβ), the signal transduction unit (Figure 1.5). Each B-cell clone carries a unique BCR due to variation in the variable region. This defines antigen specificity and is generated by Ig gene rearrangements in the BM and SHM within the GC (section 1.2.1)

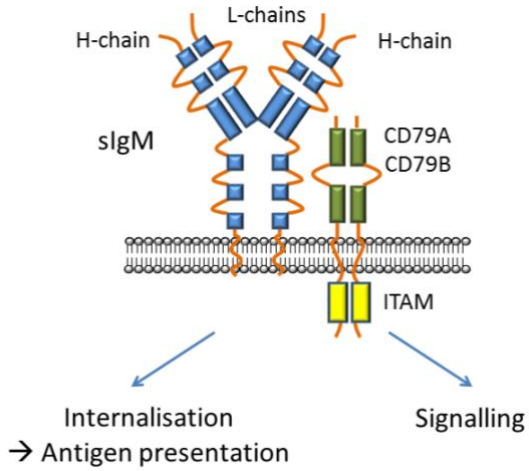

Figure 1.5. Structure and function of the BCR
The BCR comprises a tetramer of 2 heavy chains and 2 light chains, linked to the signal transduction molecules, CD79A and CD79B. Each BCR has two variable regions located on the end of the "arms" of the receptor which define antigen-binding specificity. The main functions of the BCR include induction of both positive and negative signalling as well as antigen internalisation which is critical for gaining cognate T-cell help. Signalling is initiated by phosphorylation of conserved tyrosine residues within the CD79A/B ITAM domains.

1.3.1 BCR function; antigen internalisation

BCR-mediated antigen internalisation is critical for effective B-cell responses. Following intracellular processing, antigen-derived peptides are loaded into major histocompatibility complex class II (MHC II) molecules and then presented at the B-cell surface where they are available for interaction with cognate T cells. Cognate T cells then provide secondary activation signals to B cells by expression of the B-cell stimulatory molecule CD40 ligand expressed on the surface of activated T cells which binds to the CD40 receptor (CD40R) expressed on the surface of B cell, to promote the clonal expansion (Maliszewski et al., 1993; Armitage et al., 1990) Additionally, T cells deliver help to B cells through secretion of regulatory cytokines (Hodgkin et al., 1990) such as IL-4 which promotes isotype switching (Snapper et al., 1993; Hodgkin et al., 1991; Coffman et al., 1990), increases surface IgM (sIgM) expression to enhance signalling capacity (Guo et al., 2009) and, like CD40, enhances B-cell survival and proliferation (Hasbold et al., 1998; Hodgkin et al., 1991).

1.3.2 BCR function; positive signalling

Antigen binding results in clustering of the BCR on the cell membrane and triggering of intracellular signalling (Figure 1.6). The initial step is phosphorylation of tyrosine residues within the immunoreceptor tyrosine-based activation motifs (ITAM) of the cytoplasmic tails of CD79A and CD79B by non-receptor tyrosine kinases. The two main proteins responsible for the initiation of the signalling cascade are the spleen tyrosine kinase (SYK) (Rolli et al., 2002) and Lck/Yes novel tyrosine kinase (LYN) (Monroe et al., 2006; Yamamoto et al., 2003).

CD79A/B ITAM dual-phosphorylation then allows recruitment of intracellular protein tyrosine kinases including Bruton's tyrosine kinase (BTK) and adaptor proteins such as the growth factor receptor-bound protein 2 (Grb2) and B-cell linker protein (BLNK). These proteins contribute to the ''signalosome'', a complex tethered at activated BCRs which is responsible for sustaining, amplifying and relaying BCR signal transduction to downstream pathways (Kurosaki et al., 2010; Dal Porto et al., 2005) (Figure 1.6).

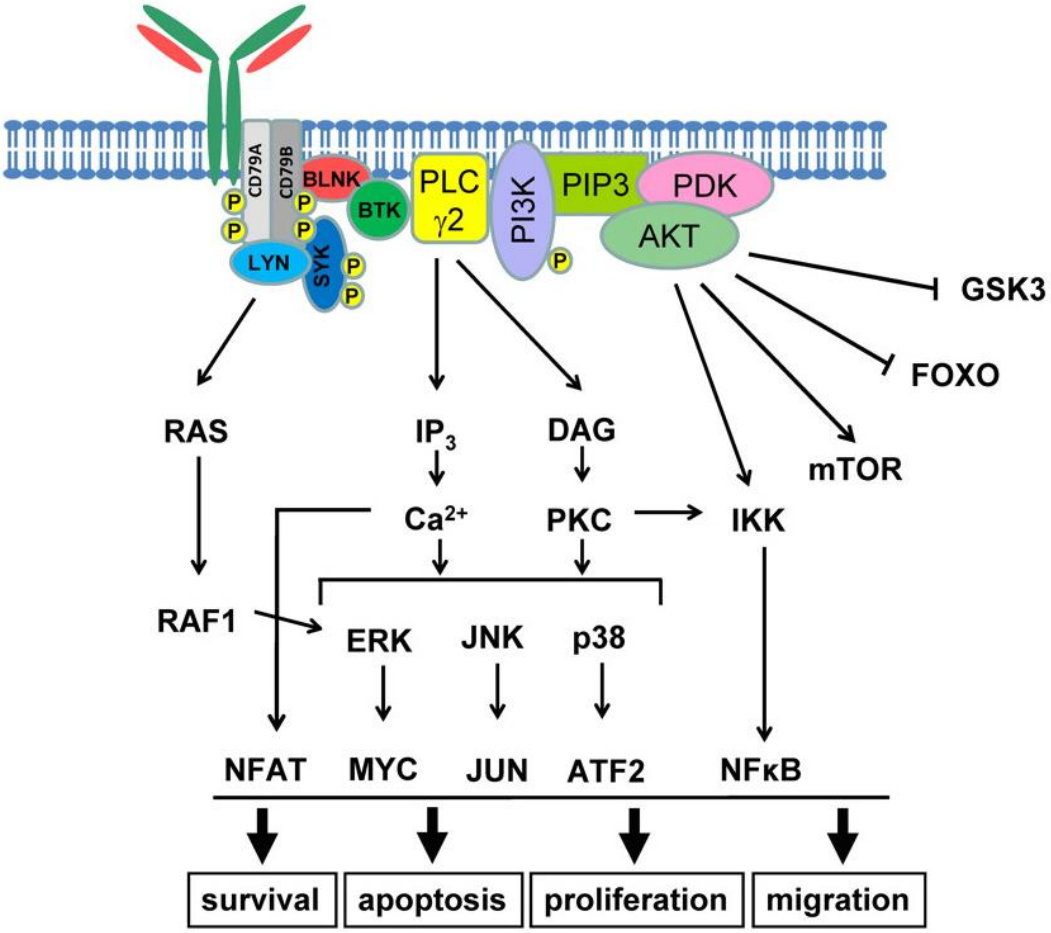

Figure 1.6. The BCR signalosome

ITAMS that are phosphorylated by LYN upon antigen engagement of BCR promote recruitment of SYK and assembly of a signalling complex consisting of BTK, BLNK, PLC-γ2, PI3K, Grb2 and other effector/adaptor molecules. Collectively, the signalosome triggers downstream cellular events via the action of second messengers and kinases/lipases that engage effector responses, including cell survival, apoptosis, proliferation and migration. See text for further details. Image taken from Packham et al., 2011.

Calcium (Ca^{2+}) is an important intracellular second messenger following BCR activation. Signalosome formation results in activation of phospholipase C- gamma 2 (PLC-γ2) which is recruited to the plasma membrane via its SH2 domain and then phosphorylated by BTK and SYK (Fu et al., 1998). Active PLC-γ2 catalyses the breakdown of the plasma membrane lipid phosphatidylinositol 4,5 bisphosphate ($PI(4,5)P_2$) into two second messenger molecules, inositol triphosphate (IP_3) and diacylglycerol (DAG). IP_3 promotes intracellular Ca^{2+} (iCa^{2+}) via IP_3-gated endoplasmic reticulum Ca^{2+} channels which then triggers influx of extracellular Ca^{2+} (Takata et al., 2004). DAG (along with Ca^{2+}) is a key activator of canonical protein kinase C (PKC) enzymes, leading to triggering of downstream pathways such as mitogen-activated

protein kinase (MAPK) (Hashimoto et al., 1998), nuclear factor kappa-light-chain-enhancer of activated B cells (NF-κB) and Nuclear factor of activated T-cells (NFAT) (Figure 1.6).

Another key pathway activated downstream of the BCR is mediated via phosphatidylinositol 3-kinases (PI3K) (Fruman et al., 2004). There are multiple PI3K isoforms, each comprising a catalytic and regulatory subunit. In B cells, the PI3kδ isoform is primarily responsible for signalling downstream of the BCR (Okkenhaug & Vanhaesebroeck, 2003). Phosphorylation of CD19 by LYN enables Gab-associated binder 2 (GAB2) to mediate recruitment of PI3K to the plasma membrane (Maus et al., 2009). PI3K then converts $PI(4,5)P_2$ to phosphatidylinositol 3,4,5-triphosphate ($PI(3,4,5)P_3$) which creates a docking site for various pleckstrin homology (PH) domain-containing proteins, including Protein Kinase B (AKT), PLC-y2 and BTK. Once at the membrane, AKT is phosphorylated and activated by phosphoinositide dependent protein kinase (PDK) resulting in activation of a cascade of growth, proliferation and survival promoting responses associated with activation of mammalian target of rapamycin (mTOR) signalling and other pathways.

Together, these BCR signalling pathways ultimately engage downstream effector pathways which promote cell growth, cell cycle entry/progression and survival to facilitate B-cell responses (positive signalling) (Figure 1.6).

1.3.3 BCR function; negative signalling

This "positive" BCR signalling is balanced by inhibitory signalling involving both protein and lipid phosphatases (Packard & Cambier, 2013). Inhibitory signalling is engaged following BCR ligation as a natural feedback mechanism to curtail antigen responses by limiting signalling, or by co-engagement of inhibitory co-receptors such as CD22 and FcγRIIb (Figure 1.7). Overall, the balance between positive and negative signalling determines B-cell outcomes. However, it is important to note that the distinction between kinases and phosphatases in signal control is complex. For example the CD45 phosphatase is considered as a positive regulator of signalling since it reverses inhibitory phosphorylation on several kinases

involved in BCR signalling (Coughlin et al., 2015). In addition to its role in positive signalling, LYN plays an important role in triggering negative signalling. In fact, deletion of LYN in mouse B cells results in hyper-activation indicating that LYN's negative role predominates (DeFranco et al., 1998).

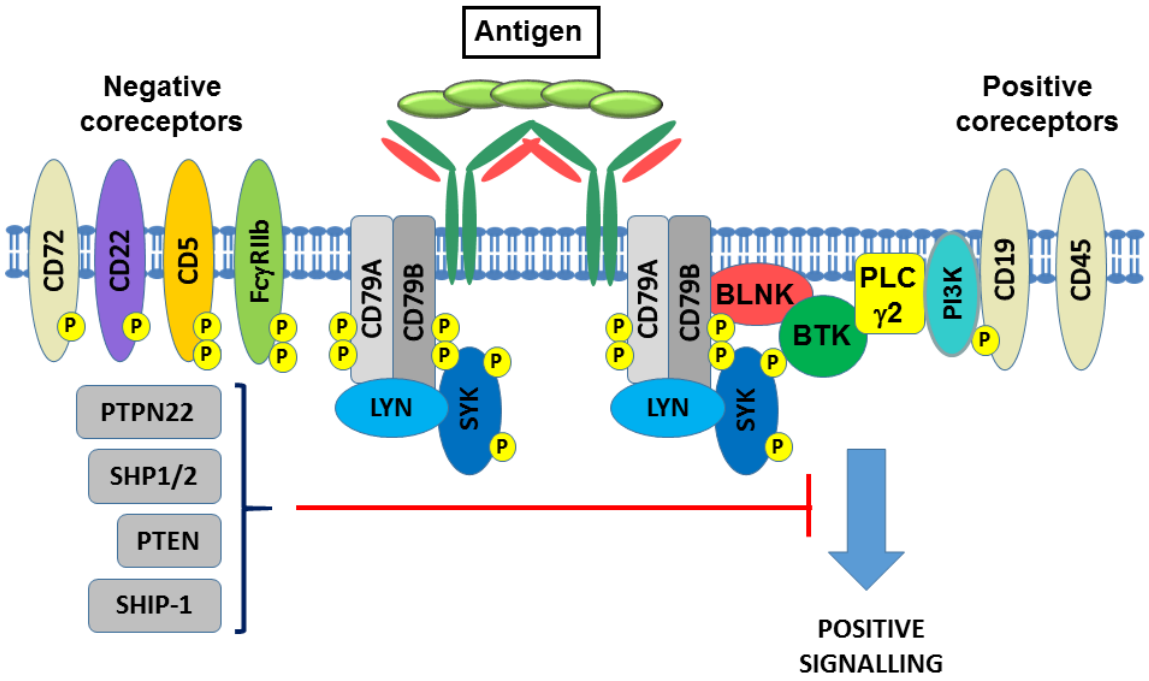

Figure 1.7. The balance between inhibitory and positive BCR signalling
Negatively acting co-receptors that regulate BCR responses include CD22 and FcγRIIb which suppress BCR signalling by activating downstream negative regulators such as protein tyrosine phosphatases SHP1, SHP2, and PTPN22, and the lipid phosphatases SHIP1 and PTEN (left side). Positive BCR signalling and associated receptors are shown on the (right side). Illustration taken from Packham et al., 2011.

One particularly interesting example of negative B-cell signalling is anergy which is a major pathway implemented in B cells to maintain tolerance (Cambier et al., 2007). It is induced as a result of chronic BCR engagement without secondary activation signals from $CD4^+$ helper T cells, for example, in response to engagement of BCR by autoantigens (Akerlund et al., 2015). They are cells that are left suspended in an unresponsive state and are prone to apoptosis due to upregulation of the proapoptotic BCL2 family protein, Bcl-2-like protein 11 (BIM) (Oliver et al., 2006; Enders et al., 2003). It is characterised by down-modulation of sIgM, but not sIgD, and reduction in sIg signalling capacity, in both mouse models and

humans (Duty et al., 2009; Cambier et al., 2007). Anergy is dependent on chronic antigen binding and is, therefore, rapidly reversible following removal of antigen (Gauld et al., 2005). Anergy appears to be mediated by biased activation of inhibitory pathways and is discussed in further detail below (section 1.3.4.3).

1.3.4 SH2 domain- containing phosphatidylinositol 5-phosphatase-1 (SHIP1)

Although multiple phosphatases are involved in negative signalling (Figure 1.7), Src homology 2 domain containing inositol polyphosphate 5-phosphatase 1 (SHIP1) appears to play a particularly important role. It is also a focus of research in my project and is therefore, covered in detail in the following sections. As described in detail below, SHIP1 appears to play a key inhibitory function in B cells; (i) following BCR/FcγRIIb co-ligation, (ii) for acute feed-back inhibition to limit B-cell responses and (iii) in anergy.

1.3.4.1 SH2 domain- containing phosphatidylinositol 5-phosphatase-1 (SHIP1)

SHIP1 was discovered as a phosphatase that binds to the adaptor molecules SHC and Grb2 in macrophages (Lioubin et al., 1996). It is expressed exclusively by haematopoietic cells (Lioubin et al., 1996) and comprises a SH2 domain, the active site and carboxy-terminal proline rich regions containing two tyrosine phosphorylation sites (Figure 1.8). Of particular note, SHIP1 contains a C2 domain which is adjacent to the catalytic domain and is important for allosteric activation of SHIP1 enzymatic activity. The natural ligand for the the C2 domain is the SHIP1 product $PI(3,4)P_2$ suggesting operation of a positive feedback loop whereby product ($PI(3,4)P_2$) further enhances SHIP1 activity (Fernandes et al., 2013). In contrast to SHIP1, the structurally related SHIP2 is expressed in both haematopoietic and non-haematopoietic cells.

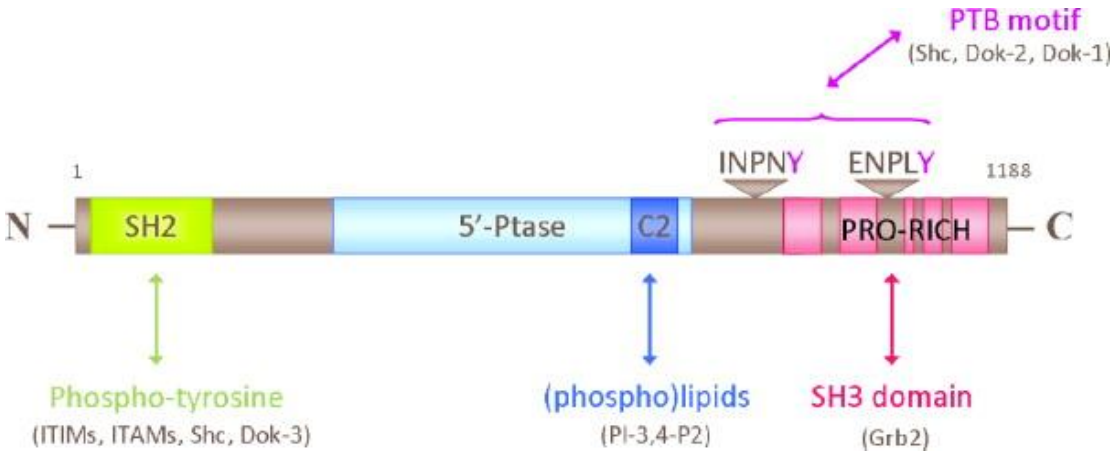

Figure 1.8. Structure of SHIP1

The SHIP1 protein is composed of 3 main functional domains. The N-terminal part of the protein contains an SH2-domain which mediates interaction with tyrosine-phosphorylated proteins, including SHC and DOK3, and receptors containing phosphorylated ITAM/ITIM domains. The catalytic domain (5'-inositol lipid phosphatase) and a C2 allosteric modulation domain are located at the centre of the protein. The known ligand for the C2 domain is the product of SHIP1 enzymatic activity, $PI(3,4)P_2$, suggesting that SHIP1 activity is subject to positive feedback control. The C-terminus includes a proline rich region (PRO-RICH) and two tyrosine residues which, when phosphorylated, bind phosphotyrosine-binding (PTB)/SH3-domain containing proteins such as Shc, Dok-2, Dok-1 and Grb2. Illustration taken from Condé et al., 2011.

SHIP1 is a 5'-inositol lipid phosphatase which acts at the plasma membrane to catalyse the hydrolysis of $PI(3,4,5)P_3$ into $PI(3,4)P_2$ (Damen et al., 1996) (Figure 1.9). Its enzymatic activity is distinct from the 3' phosphatase and Tensin Homolog (PTEN) which directly reverses the PI3K-catalysed reaction leading to production of $PI(4,5)P_2$.

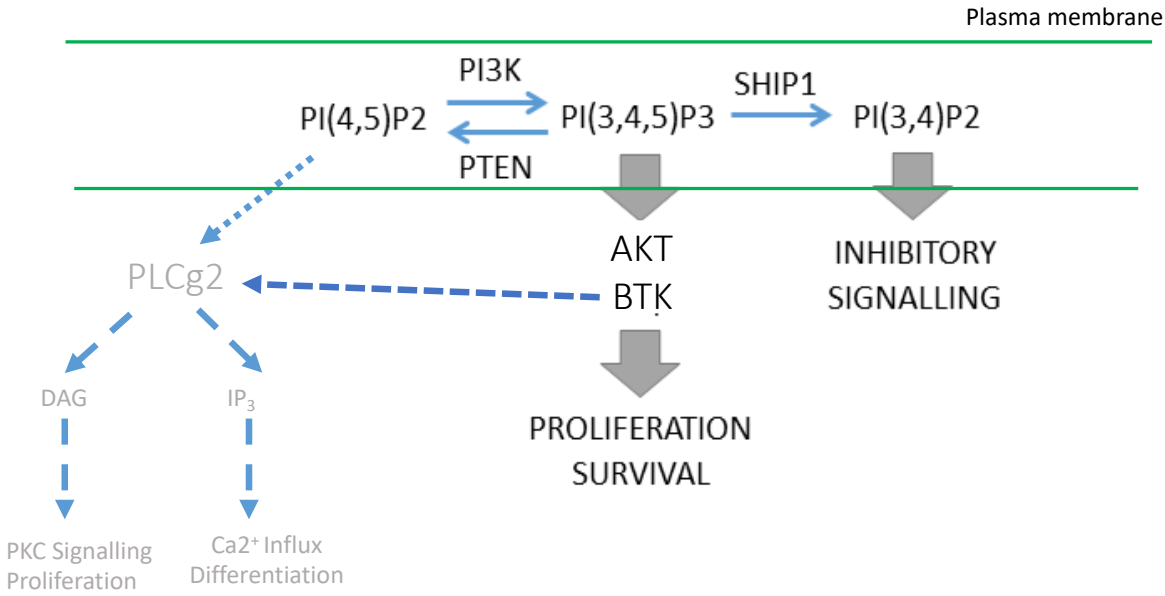

Figure 1.9. Summary of the role of SHIP1 and PTEN in countering PI3K activity
Activation of PI3K catalyses phosphorylation of PI(4,5)P_2 into PI(3,4,5)P_3. Production of PI(3,4,5)P_3 then activates growth promoting signalling molecules such as AKT, BTK and indirectly PLCγ2 which is also induced by PI(4,5)P_2 . Negative regulation is mediated by PTEN-dependent dephosphorylation which converts PI(3,4,5)P_3 back into PI(4,5)P_2. On the other hand, SHIP1 dephosphorylates PI(3,4,5)P_3 through removal of the 5'-phosphate to generate PI(3,4)P_3. PI(3,4)P_2 can act as an inhibitory second messenger to reduce B-cell responses (Landego et al., 2012).

1.3.4.2 SHIP1 and B-cell inhibitory responses

Initial analysis of SHIP1 function focused on effects following co-ligation BCR/FcγRIIB on B cells since it was known that FcγRIIB activation triggered recruitment of SHIP1 to FcγRIIB ITIMs. The inhibitory effects of BCR/FcγRIIB are thought to be important to control B cells by down-modulating responses to IgG-containing immune responses. In these experiments, BCR/FcγRIIB co-ligation of B cells from SHIP1-deficient mice was associated with prolonged iCa^{2+} release, MAPK signalling and proliferation compared to control cells demonstrating that SHIP1-deficient cells have reduced ability to down-modulate BCR signalling by FcγRIIB ligation (Liu et al., 1998). Similar results were obtained using SHIP1-deficient DT40 chicken B cells where deletion of SHIP1 abrogated FcγRIIB-mediated inhibition of BCR-induced iCa^{2+} release (Leung et al., 2009).

Although initial studies focused on the role of SHIP1 in mediating inhibition of BCR signalling following FcγRIIB/BCR co-ligation, it has become clear more recently that BCR activation alone also leads to SHIP1 activation (Paul & Marshal, 2017). Thus, SHIP1-deficient B cells

show increased activation of AKT, BTK and PLC-γ2 following stimulation with anti-IgM alone relative to control cells (Carver et al., 2000; Scharenberg et al., 1998; Bolland et al., 1998; Okada et al., 1998). Increased BCR signalling in SHIP1-deficient B cells was associated with over a five-fold elevation in levels of $PI(3,4,5)P_3$ which induced increased downstream effector activation to promote proliferation compared to wildtype cells. $SHIP1^{-/-}$ cells demonstrated increased survival as they were also more resistant to BCR-mediated cell death than their $SHIP1^{+/+}$ counterparts, especially at elevated concentrations of stimulus. Consistent with this, loss of B-cell inhibition revealed in *in vitro* experiments, mice lacking SHIP1 (specifically in B-cells) have enlarged spleen and LN, and a significant shorter life span (Helgason, 1988). These tissue effects were associated with increased numbers of mature B cells compared to control animals (Helgason et al., 2000).

The mechanisms by which SHIP1 reduces B-cell responses are likely to be complex. Although some effects of SHIP1 are clearly due to reducing $PI(3,4,5)P_3$-dependent signalling, other effects appear to be mediated via accumulation of $PI(3,4)P_2$ (Figure 1.8). $PI(3,4)P_2$ selectively recruits the tandem PH domain proteins TAPP1/2 proteins and these proteins further inhibit AKT activation (Landego et al., 2012). Moreover, TAPP1/2 also bind clathrins and clathrin associated adaptors (Landego, et al 2012; Jayachandran et al., 2017) suggesting that SHIP1 might modulate clathrin-mediated endocytosis (CME) of various receptors via accumulation of $PI(3,4)P_2$. Importantly, deletion of TAPP1/2 pheno-copies exacerbates the effects of SHIP1 deletion (O'Neill et al., 2011), suggesting that at least some of the inhibitory functions of SHIP1 are mediated via $PI(3,4)P_2$ rather than depletion of $PI(3,4,5)P_3$ (Landego et al., 2012).

Whilst binding of SHIP1 to phosphorylated ITIMs explains the ability of SHIP1 to mediate suppression of BCR signalling following co-ligation of FcγRIIb, the mechanisms by which SHIP1 is activated to the BCR in the absence of FcγRIIb are less clear. SHIP1 phosphorylation is increased in a SYK-dependent manner in normal B cells following BCR activation (Leung et al., 2010) and this may promote binding of SHIP1 to PTB-binding/SH3-domain containing proteins, such as Grb2, Shc and DOK1/2. SHIP1 recruitment to the BCR may also involve binding to phosphorylated CD79A/B ITAMs via the SHIP1 N-terminal SH2 domains (Pauls & Marshall, 2017).

1.3.4.3 SHIP1 and anergy

In addition to its roles in inhibitory signalling downstream of FcγRIIB and feedback inhibition of acute BCR responses in naïve B cells, SHIP1 may also play a central role in the establishment of anergy as well as curtailing continuous uncontrolled BCR activation and potential tumourigenesis (Cambier et al., 2007). Here, chronic BCR engagement appears to favour the selective mono-phosphorylation of CD79A/B ITAMs leading to attenuation of SYK activation but retained LYN activation. This is demonstrated by enhanced levels of LYN activation in anergic B cell, as well as the induced BCR hyperactivity and autoantibody production associated with LYN deletion (Spaargaren et al., 2003). ITAM mono-phosphorylation appears to lead to a bias towards inhibitory signals acting via the phosphatases SHIP1 (O'Neill et al., 2011), PTEN (Song et al., 2011) and/or SHP1 (Pao et al., 2007). The role of these phosphatase in cancer is discussed in section 1.3.4.5-7). The importance of SHIP1 in anergy is demonstrated by the fact it is constitutively phosphorylated in anergic cells of both the ARS/A1 transgenic model of anergy and MD4.ML-5 (HEL) models (Goodnow et al., 1998). Moreover, deletion of SHIP1 in mice is associated with rapid onset of autoimmunity in the HEL model as anergy is lost, allowing mechanisms that prevent expansion and differentiation of autoantibody production to be overridden (O'Neill et al., 2011). In other studies, both PTEN and SHIP1 an play important role in the inducing and maintaining anergy. This is supported by the fact that SHIP1 deficiency did not alter anergy induction in response to high avidity autoantigens soluble hen-egg lysozyme Ag in the MDA4 transgenic mode (Leung et al., 2013), suggesting anergic B cells are perhaps compensated by upregulation of PTEN to prevent accumulation of $PI(3,4,5)P_3$ (Leung et al., 2013; Browne et al., 2009). In support of this, reports have shown mice that are haploinsufficient for the PTEN gene develop spontaneous lupus-like autoimmunity (Di Cristofano et al., 1999). Furthermore, Moody et al., demonstrated that that haploinsufficiencies of both PTEN and SHIP1 lead to a more pronounced lupus-like autoimmunity than either single haploinsufficiency (Moody et al., 2003). Overall, these studies link together that suppression of $PI(3,4,5)P_3$ is vital to self-tolerance and suggests that PTEN and SHIP1 activation may act cooperatively in order to induce and maintain anergy.

An interesting feature of B-cell anergy is that desensitisation "spreads" from the (auto-antigen) engaged BCR to other cell surface receptors, imposing a broad lack of

responsiveness to multiple ligands (Cambier et al., 2007). Affected receptors include CXCR4, which is functionally inactivated in anergic B cells (Brauweiler et al., 2007). This remote CXCR4 desensitisation is mediated in part by SHIP1. Thus, the decrease in CXCR4-dependent migratory activity that is observed in anergic B cells is lost when cells lack expression of SHIP1 (Brauweiler et al., 2007). SHIP1 may interfere directly with CXCR4 signalling, via effects on PI3K-induced $PI(3,4,5)P_3$, but could also trigger CXCR4 internalisation, potentially via $PI(3,4)P_2$-dependent effects on CME.

1.3.4.5 SHIP1 in Cancer

Several tumours such as breast cancer and haematological malignancies are dependent on constitutive activation of the PI3K-Akt pathway (Alkan & Izban, 2002). Furthermore, several oncogenes, such as Her2/Neu and K-Ras, can enhance tumour growth by promoting activation of the PI3K pathway (Jiang & Liu, 2009). Given that PI3K pathway has been identified as a critical event in tumour development and the fact SHIP1 acts as a negative regulator of the PI3K pathway and is exclusively expressed in hematopoietic cells, I have reviewed below multiple studies that demonstrate that SHIP1 may act as a tumour suppressor in numerous hematological malignancies.

Numerous B cell malignancies have shown evidence to be dependent on deregulation of the PI3K pathway (Fukuda et al., 2005) (Vanderwinden et al., 2006). For instance, It is well documented that there is an inverse relationship between expression of SHIP1 and BCR-ABL, the oncogene responsible for chronic myeloid leukaemia (Fukuda et al., 2005; Jiang et al., 2003)). Consistent with this, the Sattler group showed hat that BCR-ABL reduces the SHIP1 protein levels (Sattler et al., 1997). Specifically BCR-ABL were found to tyrosine phosphorylate SHIP1 leading direct SRC family member mediated polyubiquitination and subsequent proteasomal degradation (Ruschmann et al., 2010). This conveyed that the overall level of the SHIP1 may determine its overall activity.

In nongerminal centre diffuse large b-cell lymphoma, reduction of SHIP1 expression was linked with overall survival of tumour cells (Pedersen et al., 2009). This was also observed in animal models as $SHIP^{-/-}$ mice result in generation B-cell lymphomas and reduced overall survival (Nakamura et al., 2009).

Moreover, a low SHIP1 expression has also been observed in non B cell malignancies such in adult T-cell leukaemia and lymphoma, as well as in Jurkat T cells (cell lines derived from a patient with acute lymphoblastic leukaemia) (Horn et al., 2004). Expectedly, reintroduction of SHIP1 activity in Jurkat T cells restricted cell growth through downregulation of Akt expression (Horn et al., 2004)

Additionally, microRNA regulation of SHIP1 levels (Pedersen et al., 2009) is vital in aiding in development and progression of hematopoietic cancers. Specifically, transgenic mice overexpressing miR-155 develop a mixed tumour phenotype with characteristics of ALL and high grade lymphoma (Costinean et al., 2006). Elevated levels of miR-155 are also observed in natural killer cell lymphoma/leukaemia (Yamanaka et al., 2009) and diffuse large B-cell lymphoma in humans Pedersen et al., 2009. Particularly, a study using DLBCL patients observed the more aggressive disease type (non-GC DLBCL) was associated with higher levels of miR-155, and consequently lower levels of SHIP1, compared to GC DLBCL. Patients with the least SHIP1 expression also had the worst survival outcome (Pedersen et al., 2009). In support of this, another study demonstrated that SHIP1 is often down-regulated in DLBCL patients (Miletic et al., 2010). The effect of miR-155 effect on SHIP1 in patients with CLL will be addressed in section 1.4.3.

SHIP1 is expressed at varying levels in different immune cells (Antignano et al., 2009) which function to promote or inhibit tumour development and thus can shape the immune response to cancer cells (Antignano et al., 2009). The figure below outline the biological role of SHIP1 in different white blood cells and on how this shapes the immune response to cancer (Figure 1.9.1)

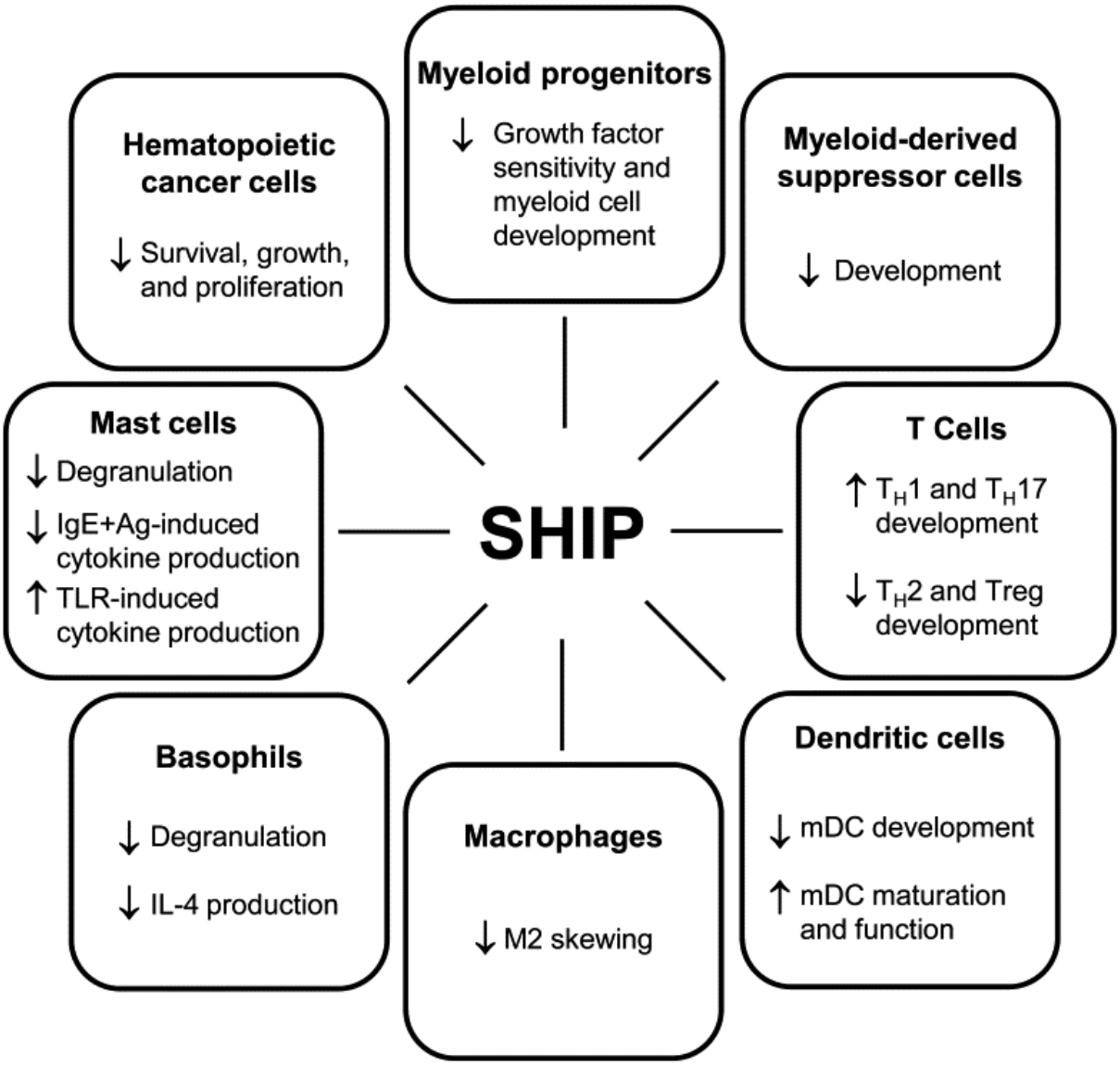

Figure 1.9.1 SHIP regulates immune cell functions and restricts tumour development and growth. SHIP1 plays a critical role in regulating the development and function of various hematopoietic cells. In general, SHIP restricts the development of immunosuppressive cells and promotes the development and function of TH1 and TH17 cells, which may reduce tumour growth and metastasis. Image taken from Hamilton et al., 2010.

Together this lends further support to SHIP1 being a tumour suppressor within haematopoietic cells (Costinean et al., 2006). Although SHIP1 is not expressed in non-haematopoietic cancers, there is a growing narrative that SHIP1 may regulates their development by manipulating the immune response. This is supported by the fact that certain solid tumours grew more rapidly in $SHIP^{-/-}$ mice (Rauh et al., 2005).

1.3.4.6 Role of the PTEN phosphatase in cancer

Activating mutations or gene amplifications of the catalytic p110α subunit of PI3K (Campbell et al., 2004) or AKT (Hennessy et al., 2005) results in abnormal cellular processes, including uncontrolled proliferation, differentiation, angiogenesis. This is generally vital in development and progression of various types of human cancers. Equally, alterations in expression or function of phosphatase that maintains the balanced equilibrium of kinase may exacerbate tumourogenesis.

The previously mentioned phosphatase PTEN (chapter 1.3.4.1) naturally, like SHIP-1 counteract the PI3K activity by the removal of a specific phosphate groups from PI(3,4,5)P3. Similar to SHIP1 the tumour suppressor activity of PTEN is based on the reduction of PI(3,4,5)P3 levels, repressing AKT activation and regulating a variety of downstream cellular effects including proliferation, survival energy metabolism, and cellular architecture (Hollander et al., 2011). Indeed inactivating mutations of the PTEN gene are frequently reported in 50% of all human cancers, including genomic locus deletions, missense/nonsense mutations, promoter methylation, and regulation of oncogenic microRNAs (Lee et al., 2018) (Eng et al., 2003). Perhaps the role of PTEN in hematological malignancies may be similar to the discussed role of decreased expression and activity of the tumour suppressor SHIP1 in B cell malignancies was discussed in section 1.3.4.5.

Nevertheless, there are multiple studies that show the role of PTEN as a tumour suppressive role in B cell malignancies. For example PTEN mutations were found in 5% of primary lymphoma (Gronbaek et al., 1998; Sakai et al., 1998) and in two primary effusion lymphoma cell lines but not in primary cells (Boulanger et al., 2009). Furthermore, several studies showed a reduction or loss of PTEN expression in DLBCL (Abubaker et al., 2007; Liu et al., 2010) and abnormal expression has been implicated in CLL (Cuní S, et al 2004; Leupin et al., 2003). In other cell line studies it was also observed that BJAB B cell lymphoma has no detectable PTEN protein and elevated generation of $PI(3,4,5)P_3$ and $PI(3,4)P_2$. This was consistent with (Cheung et al., 2007), however PTEN mRNA appeared to be expressed normally in these cells and contained no mutations.

Similar to mIR-155 which regulates the level of SHIP1, the function and expression of PTEN is regulated by microRNAs through phosphorylation, ubiquitination and subsequent oxidation. Comparable to mIR-155 , the mir17-92 microRNA cluster is over-expressed in several leukaemia's (Lenz et al., 2008) and lymphomas (Rao et al., 2011) providing a potential mechanism for PTEN down-regulation. Although no particular mutation was pinpointed, a proposed mechanism was via a NOTCH1 mutation that that results in overactivation the PI3K pathway by inhibiting PTEN transcription (Rossi et al., 2012). Moreover, PTEN enzymatic activity is reported to be deficient in CLL (Shehata et al., 2010), suggesting that PTEN post-translational regulation is also altered in haematological cancer.

1.3.4.7 Role of SHP-1 phosphatase in cancer

SHP-1, an SH2 domain-containing protein tyrosine phosphatase, is primarily expressed in heamatopoietic cells and behaves as a key regulator controlling. SHP-1 acts on the the immunoreceptor tyrosine-based inhibition motif (ITIM) of the inhibitory receptors (Figure 1.7), via its SH2 domains to dephosphorylate the downstream proteins and as a result and subsequently curtails the activated signal or induces apoptotic pathway (Christensen & Geisler, 2000).

Aberrant expression or function of SHP-1 can, therefore, cause abnormal cell growth and induce different kinds of cancers. Interestingly SHP-1 is over-expressed in some non-lymphocytic cell lines, such as prostate cancer, ovarian cancer and breast cancer cell lines but conversely decreased in some breast cancer cell lines with negative expression of oestrogen receptor as well as some prostate and colorectal cancer cell lines (Liu et al., 2017). Overall, these data suggest that SHP-1 can play either negative or positive roles in regulating signal transduction pathways and therefore the understanding of SHP1 in cancer is not very clear. However, there are studies which show an overall decreased or silenced expression of the SHP-1 gene which in turn are associated with tumourogenesis in B cell malignancies (Tabrizi et al., 1998). For instance, expression of SHP-1 in most of human Burkitt's lymphoma cell lines was dramatically decreased (Wu et al., 2003). Negative SHP-1 expression were also present in different leukaemia cell lines including T cell chronic lymphocyte leukaemia

(TCLL), and a k562 chronic myelogenous leukaemia (CML) cell line (Liu et al., 2017). In addition, B cell acute lymphoblastic leukaemia (B-ALL) cell lines and multiple myeloma (MM) cell lines demonstrated and overall decreased or absent SHP-1 expression (Liu et al., 2017). It is not clear why SHP-1 is expressed so differently in different leukemia cell lines, but the SHP-1 expression in various leukaemia and lymphoma cell lines have been attributed to either the methylation of the promoter region of the SHP-1 gene or the post-transcriptional block of SHP-1 protein synthesis and seem to be prevalent in to the progressive and aggressive stages of leukemia (Bruecher-Encke et al., 2001; Oka et al., 2001).

Taken together, SHP-1 seems plays an important role in the pathogenesis of a wide range of cancers including lymphoma/leukemia, although additional research is needed to generate mechanistic date to elucidate its tumour suppressive role combined with studies into its expression in observation studies of patients.

1.4 Haemeotological malignancies

Haematological neoplasms account for 9% of cancers world-wide according to the World Health Organisation (Swerdlow et al., 2016). This heterogeneous group of diseases comprises myeloma and subtypes of lymphomas and leukaemias, of which the B cell-derived neoplasia comprise the majority (~90%).

1.4.0.1 Lymphomas

Lymphoma's comprises a group of neoplasms arising from lymphoid cells. Lymphomas are classified clinically into Hodgkin's disease and non-Hodgkin's lymphomas ad can be caused by a variety of risk factors such as infection by Epstein–Barr virus (EBV), along with congenital or acquired immune deficiencies, organ transplantation, autoimmune disorders like Hashimoto's thyroiditis and Sjogren's syndrome, malaria, infection with human T-cell leukemia/lymphoma virus, or Kaposi's sarcoma-associated herpes virus (Baris & Zahm, 2000). Lymphomas are typically further classified according to their presumed normal counterpart. Therefore, some of the subtypes of aggressive B-cell lymphoma reflect different cellular origins, such as mature B cells versus more differentiated plasma cells. Diffuse large B-cell lymphoma (DLBCL) is the most common type of aggressive non-Hodgkin lymphoma originating from the germinal center, and it represents a heterogeneous group of diseases with variable outcomes that are differentially characterized by clinical features, cell of origin (COO), molecular features, and most recently, frequently recurring mutation Addition of the anti-CD20 monoclonal antibody rituximab to the standard cyclophosphamide, doxorubicin, vincristine, and prednisone CHOP resulted in significant improvements in progression-free survival and overall survival (OS) (Coiffier et al., 2010). Despite these improvements approximately 40% of patients with DLBCL who are treated with R-CHOP or R-CHOP–like chemotherapy will relapse or develop refractory disease (Sehn et al., 2012; Coiffier et al., 2002) and the majority of patients with relapsed or refractory DLBCL will succumb to the disease (Coiffier et al., 2010). Various strategies have been implemented to improve the outcome of DLBCL, including intensification of chemotherapy and use of maintenance therapy. Nevertheless the, standard front-line treatment for DLBCL still remains a combination of R-CHOP or CHOP-like chemotherapy (Liu & Barta, 2019)

On the other hand, approximately 352,000 people were diagnosed with leukaemia world-wide in 2011, comprising 2.5% of all cancers (Smith et al., 2011). In the UK alone, leukaemia is the 11th most common cancer with 3,200 people diagnosed annually. Leukaemias are sub-divided into large subgroups depending on whether the malignant clone arose from the myeloid or lymphoid lineages, and the time it takes for the malignancy to progress. The main forms of leukaemia are acute myeloid leukaemia (AML), chronic myelogenous leukaemia (CML), acute lymphoblastic leukaemia (ALL) and Chronic lymphocytic leukaemia CLL (Harris et al., 1999). In relevance to this project I shall focus on CLL.

1.4.1 Chronic lymphocytic leukeamia and **a summary of disease features and pathways**

CLL is the most common subtype of leukaemia and arises from the accumulation of clonal, mature B lymphocytes (Kipps et al., 2017). Disease manifests as a lymphocytosis but also typically involves accumulation of neoplastic cells in the BM and the lymphatic tissues. It is two times more prevalent in men than women (Nabhan et al., 2014) and incidence increases significantly with advancing age. The median age at diagnosis is ~70 years (Pulte et al., 2015).

The clinical manifestations of CLL are diverse. It can be indolent, not requiring immediate treatment, or relatively aggressive. Therefore, dependent on the disease subset, a patient may remain asymptomatic for years or be confronted by rapidly progressive and fatal disease. Symptoms associated with CLL include weight loss, fatigue, excessive perspiration during sleep, enlarged LN and hypogammaglobulinemia, with a resultant increase in incidence and severity of infections.

Physical and laboratory tests performed to diagnose CLL include full blood cell count (>3500 blood lymphocytes per microlitre of blood) and flow cytometry to detect the presence of small mature lymphocytes that express the typical immunophenotype ($CD5^+$, $CD19^+$, $CD23^+$) associated with CLL (Kipps et al., 2017). CLL cells typically express both sIgM and sIgD, although at low levels compared to non-malignant peripheral B cells. A minor fraction of cases (~10%) express sIgG (or more rarely sIgA). Additional diagnostic measures include microscopic morphological assessment of lymphocytes in Wright-Giemsa stained blood, BM (Montserrat & Rozman, 1983) and LN biopsies (Gupta et al., 1983), quantitation of Ig and/or a direct Coombs test (Kipps et al., 2017).

Traditional prognostic tools for staging CLL patient are the Binet and Rai systems (Binet et al., 1977; Rai et al., 1975). The Rai system is used more commonly in the US and is based on measures of lymphocyte accumulation and physiological development of disease, such as splenomegaly and hepatomegaly (Rai et al., 1975). The Binet system is more commonly used in Europe and is based on the number of involved areas (spleen, axillae, groin, liver, head & neck) as defined by the presence of enlarged LN, combined with the presence of thrombocytopenia and anaemia (Binet et al., 1981). Döhner et al., demonstrated that these staging tools are somewhat limited as they are not able to identify patients with poorer prognosis at an early stage of disease (Döhner et al., 2000).

Technological advancement has allowed application of modern day diagnostic and staging tools to more accurately identify patients at high risk of progression/poor response to treatment. The most notable of these is p53 dysfunction (through loss of 17p13 and/or inactivating mutations) which is associated with poor response to conventional chemoimmunotherapy and shorter overall survival (Döhner et al., 1995).

Other important chromosomal lesions include loss of 11q or 13q, and trisomy 12. Del(13q) is the most common genetic lesion in CLL (~70% of cases), is typically clonal, and is often detected in pre-malignant/early disease (such as monoclonal B-cell lymphocytosis, a precursor condition for CLL). Del13q results in upregulation of the BCL2 survival protein by deletion of down-modulatory miRNAs (Balatti et al., 2013).

IGHV mutation status (the extent of mutations introduced into Ig variable regions by SHM) is another key determinant of variability within CLL. Cases in which the malignant cells express unmutated μ-heavy chain genes (termed U-CLL) originate from pre-GC normal B cells that have not undergone SHM (Figure 1.10). Although U-CLL are pre-GC, they are still likely to be antigen influenced (Packham et al., 2014). This is perhaps most clearly revealed by biased V-gene usage and expression of B-cell activation markers, including CD23. On the other hand, CLL with mutated μ-heavy chain genes (M-CLL) originate from post-GC B cells that have undergone SHM. Importantly, these subsets have distinct outcomes; median survival for U-CLL (comprising ~40% of cases) is 95 months and 293 months for M-CLL (~60%

of cases) (Hamblin et al., 1999). The small subset of IgG-expressing CLL may represent a third (minor) subset, having derived from a normal B cell which has undergone both SHM and class-switching (Stevenson et al., 2011).

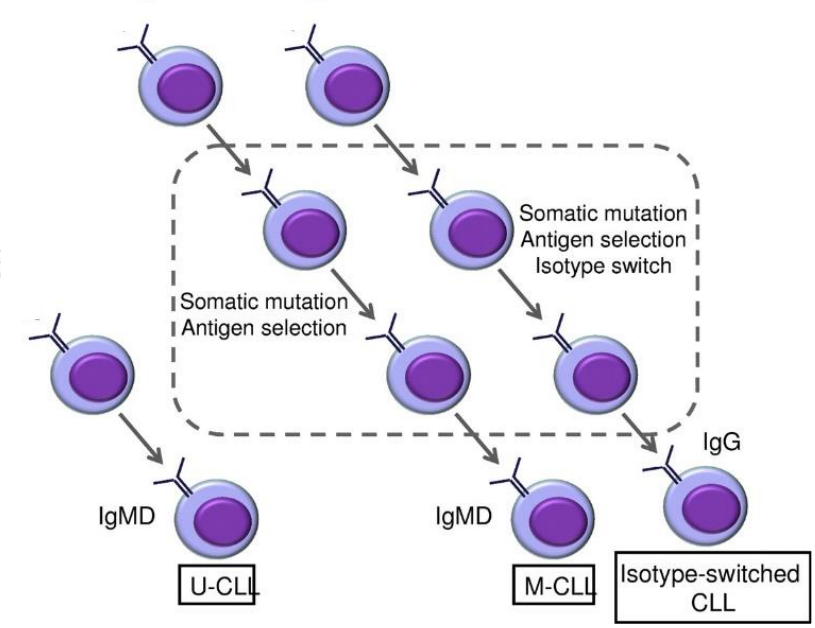

Figure 1.10. Formation of the 2 major subsets of CLL and a minor isotype switched variant
U-CLL is thought to derive from pre-GC B cells and lack SHM, whereas M-CLL derives from post-GC cells with SHM. A third smaller subset is thought to derive from infection or antigen engagement and a class-switched isotype. Illustration taken from Stevenson et al., 2011.

Other markers which are linked to outcome is CLL include expression of CD38 (Patten et al., 2008; Damle et al., 1999), the kinase ZAP70 (Dürig et al., 2003), CXCR4 (Pepper et al., 2015; Ganghammer et al., 2016) and CD49d (Gattei et al., 2008).

Somatic mutations associated with CLL have been identified by studies using whole-exome sequencing (Puente et al., 2011). However, it is important to note that the overall mutational burden in CLL is relatively low compared to solid tumours and more aggressive B-cell lymphomas. The pathways affected by these mutations are summarised in Figure 1.11. In general, these mutations (and other genomic alterations) are most common in U-CLL.

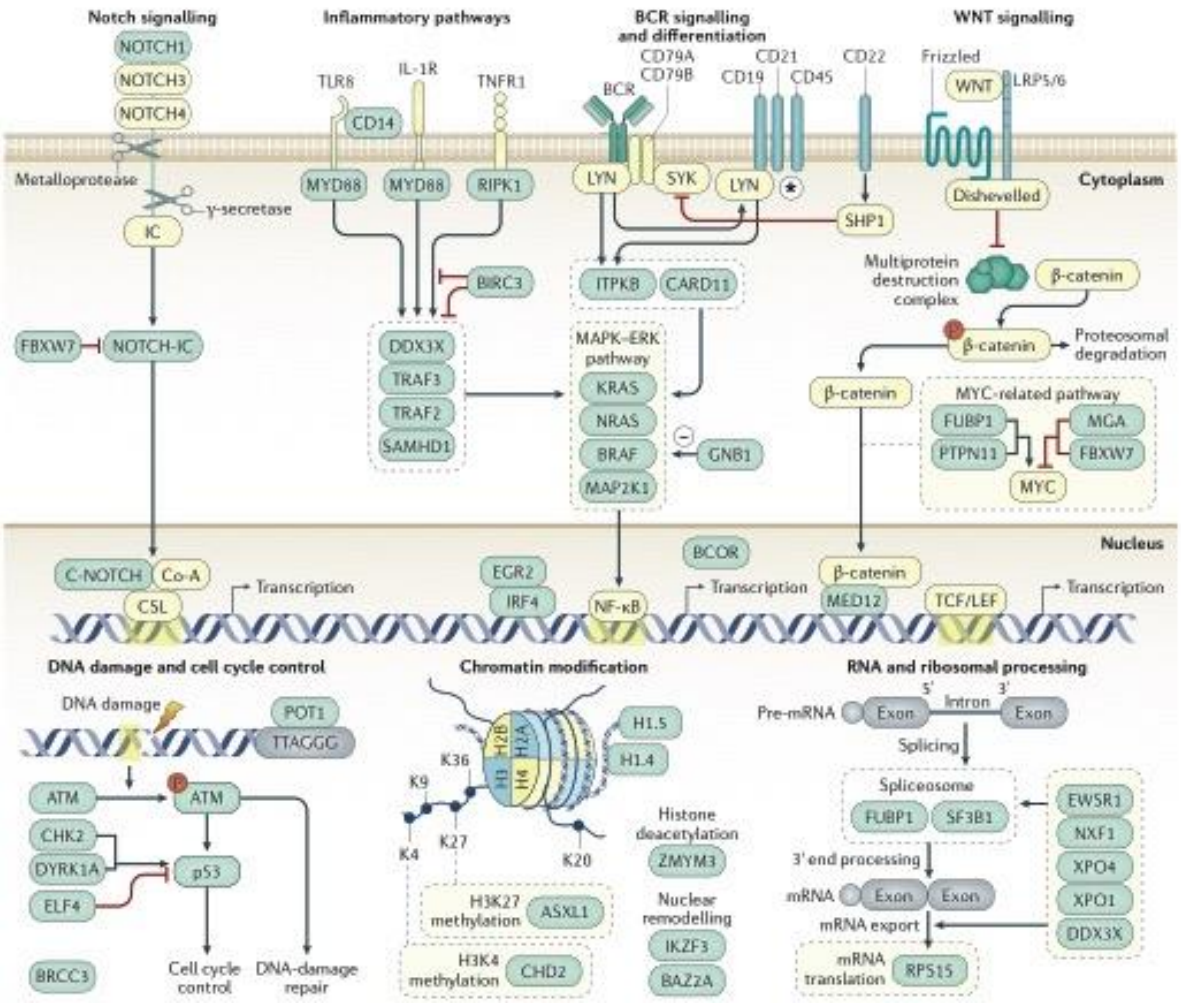

Figure 1.11. Somatic mutations in CLL

Recurrently mutated genes in CLL (Blue boxes)may influence a range of downstream cellular pathways including BCR signalling, cell cycle control, DNA repair, chromatin modification and RNA processing/translation. Illustration taken from Kipps et al., 2017.

In addition to p53 mutations described above, the most commonly mutated genes in CLL are *ATM*, *NOTCH1* 1 and *SF3B1*. ATM is involved in DNA damage responses and therefore, like p53 dysfunction, CLL cells with ATM mutations (and/or deletion of the *ATM* gene on chromosome 11q) respond poorly to chemotherapeutic agents. Mutations in the 3′ untranslated region of *NOTCH1* and a *PAX5* enhancer leads to constitutive activation of NOTCH1 and resultant increased and sustained expression of B cell-associated transcription factors such as Mcl-1 and increased activity of eIF4E which are implicated in apoptosis resistance and promote increased cell survival in CLL respectively (Ljungstrom et al., 2016; De Falco et al., 2015). Overall, patients with mutations in the 3′ untranslated region of *NOTCH1* have a shorter time from diagnosis to treatment and poorer overall survival, similar to that of patients with non-synonymous mutations, which alter the amino acid sequence of NOTCH1 (Villamor et al., 2013)

Mutations in mRNA processing molecules such SF3B1 have been found to be associated with aberrant RNA splicing an inducing altered DNA-damage response (Te Raa et al., 2015). Furthermore, evidence suggest SF3B1 mutation might be linked to genomic stability and epigenetic and found in ppredominantly sub clonal genetic events in CLL, and hence are likely later events in the progression of CLL. Modification in the SF3B1 are associated with faster disease progression and poor overall survival. More recent studies have revealed important variation in the epigenome and gene expression between normal B cells and CLL cells, and between distinct disease subsets. For example, U-CLL and M-CLL have distinct disease DNA methylation and mRNA/miRNA expression profiles (Kulis et al., 2012; Clin et al., 2005). This variation may partly reflect the differing cell-of-origin of these subsets and influence the variable disease behaviour. However, intermediate groups also exist (e.g. the intermediate group identified in analysis of DNA methylation).

Current treatment and management strategies of CLL is dependent on stage of disease, blood profile (leukocyte profile), severity of symptoms and disease progression. Another important factor taken into consideration is the age of patient, as more aggressive management approaches are generally limited to younger/fitter patients. Patients with indolent disease are typically monitored for progression of disease but not treated immediately, whereas options for patients with more aggressive disease include surgery, radiation and chemoimmunotherapy. Despite a range of management strategies, many

patients relapse from minimal residual disease and stem cell transplantation remains the only curative option.

Fludarabine in combination with cyclophosphamide and rituximab (anti-CD20 antibody) (FCR) is frequently used to treat newly diagnosed patients. Strikingly, Thompson et al., demonstrated that a subset of patients with M-CLL achieve long term progression free survival (PFS) on FCR treatment and remain in remission beyond 10 years (Thompson et al., 2016). This paper proposed that FCR could provide a curative option for this subset of CLL. By contrast, patients with p53 dysfunction do not respond well to FCR and are offered different treatment regimens, most commonly newer drugs targeted against either BCR signalling pathways or the anti-apoptosis protein BCL2 (see in section 1.5).

1.4.2 BCR function in CLL

Similar to its role in normal B cells, the BCR remains a key determinant of CLL development and progression (Packham & Stevenson, 2011). This is perhaps highlighted most clearly by the distinct clinical behaviour of the two main subsets of CLL (U-CLL and M-CLL) and dramatic clinical responses to inhibitors targeted against BCR-associated signalling kinases (see below section 1.5). Further evidence in support of a key role for the BCR in CLL is provided by the biased V-gene usage and BCR "stereotypy" (Kipps et al., 2017). Moreover, sIgM is variably and reversibly downregulated on CLL cells compared to normal B cells, indicative of on-going antigen engagement *in vivo* (Mockridge et al., 2007). Although the nature of antigens operating in CLL *in vivo* remains unclear identified candidates include viral, fungal and bacterial antigens as well as a diverse array of autoantigens (Niemann & Wiestner, 2013). "Autonomous" signalling via CLL BCRs has also been described, whereby cells are activated via binding to an intrinsic BCR motif (Dühren et al., 2012). However, the role of this *in vivo* is unclear. Antigen signalling is thought to occur within the LN and can, therefore, be considered as part of the microenvironment milieu which influences CLL cell behaviour (Herishanu et al., 2011).

In CLL, the main fate operating following BCR engagement *in vivo* appears to be anergy (Figure 1.12). This is evident by the variable but reversible down-modulation of sIgM, but not sIgD, expression and signalling capacity (Packham et al., 2014). Although normal anergic

cells tend to have a short survival span, anergy-associated apoptosis of CLL cells appears to be countered by overexpression of BCL2.

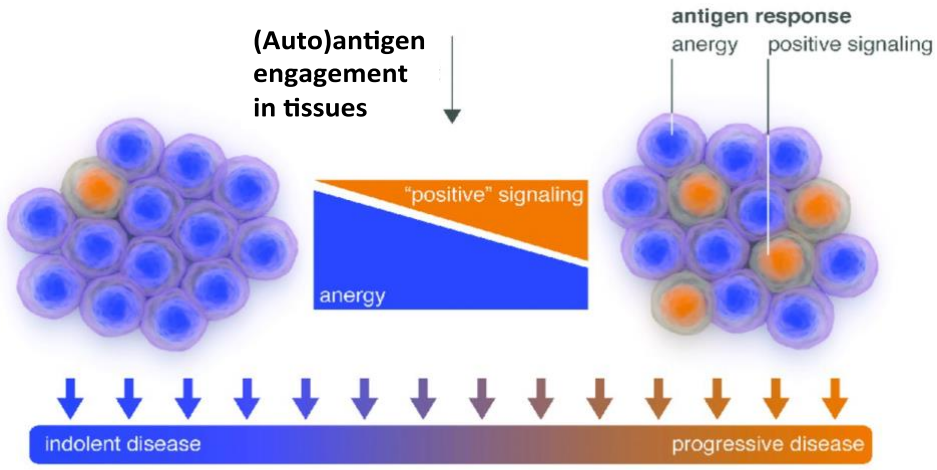

Figure 1.12. Clinical behaviour of CLL subsets depending on different antigen-driven responses influence variable.
The clinical outcome of CLL is subjective to CLL variability in BCR signalling effects on anergy and positive signalling. Continuous antigen engagement in CLL tends to result in predominantly in an anergic subtype, although low levels of growth promoting positive signalling may tip the balance towards progressive disease subtype. The balance between anergy and positive signalling is likely to be determined by both intrinsic and extrinsic factors. Illustration taken from Packham et al., 2014.

There also appears to be on-going BCR-driven proliferative signalling in some CLL cases, although this may be at a low level, consistent with the chronic nature of the disease. Some proliferation and pro-survival responses linked to BCR activation of CLL cells are summarised in Table 1.1. This positive signalling may be facilitated by low levels of "T-cell help" although it is unclear as to whether this might stem from classical cognate T-cell help, or a low level of non-cognate T-cell activation within LN with disrupted tissue architecture.

Overall the balance between BCR-induced anergy and positive signalling appears to influence disease behaviour. Anergy appears to be feature of all CLL, but is particularly prominent in M-CLL. By contrast, positive signalling leading to proliferation in U-CLL (even at low levels) may tip the balance towards accumulation of the malignant clone.

Table 1.1 Summary of proliferation/survival effector pathways activated downstream of sIgM in CLL cells

Target	Function	Reference
MCL1	Survival	Petlickovksi et al., 2005
BIM phosphorylation	Survival	Paterson et al., 2012
MYC	Growth	Krysov et al., 2013
Cyclin D2	Proliferation	Deglesne et al., 2006
RNA translation	Protein synthesis	Yeomans et al ., 2016
Unfolded protein response	Survival, Protein synthesis	Krysov et al., 2015
Metabolic pathways	ATP production	Vangapandu et al., 2018

Note, table is illustrative and does not list all known targets of BCR signalling in CLL cells.

1.4.3 SHIP1 in CLL

Despite the important role SHIP1 plays in determining B-cell responses, only two studies have focused on analysing its expression in CLL cells.

Gabelloni et al., published a small study demonstrating that SHIP1 was expressed and constitutively phosphorylated in CLL (Gabelloni et al., 2008). The number of samples analysed was small, but expression/phosphorylation appeared to be highest in ZAP70 positive samples. Cui et al., investigated potential regulation of SHIP1 by miRNAs (Cui et al., 2014). These authors collectively demonstrated that *miR155* down-regulated SHIP1 expression in CLL cells and that this was associated with increased sIgM signalling capacity. Furthermore, *miR155* expression was inversely correlated with SHIP1 expression and was associated with poor prognosis disease. Thus, both studies point to a potential association between higher expression of SHIP1 in more indolent disease subsets, consistent with the known link between SHIP1 and anergy.

Unpublished studies from the host laboratory have focused on regulation of SHIP1 following sIgM stimulation of CLL cells (E Lemm., Unpublished). This work confirmed that SHIP1 is constitutively expressed and phosphorylated in CLL cells. Interestingly, anti-IgM did not alter SHIP1 phosphorylation but promoted its relocalisation from the cytoplasm to the plasma membrane where it co-localised with activated BCRs. This relocalisation is likely to be key for SHIP1 function since its substrate $PI(3,4,5)P_3$ is restricted to the plasma membrane. The presence of constitutive SHIP1 phosphorylation indicates that SHIP1 is already partially activated in CLL cells. This may reflect on-going activation of these cells *in vivo*.

1.4.4 CLL and the microenvironment

The key microenvironment for CLL cell proliferation are the proliferation centres (PC), or ''Pseudo-follicles'' present within LN, and to a lesser extent the BM (Patten et al., 2008; Ghia et al., 2000). PC contain loose aggregates of proliferating CLL cells in contact with T cells, stromal cells, nurse-like cells (NLC) (Figure 1.13). Together, these interactions regulate CLL cell trafficking, survival and proliferation in a manner that is dependent on either direct cell–to-cell contact and/or soluble factors. Although there is a lack of models mimicking the complex microenvironment present in the BM or LN, *in vitro* studies using primary CLL cells have provided a better understanding of the cellular and molecular components of the microenvironment that contribute to CLL pathogenesis (Burger et al., 2011).

A

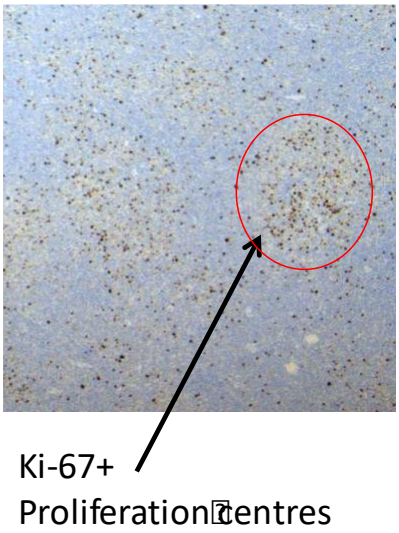

B

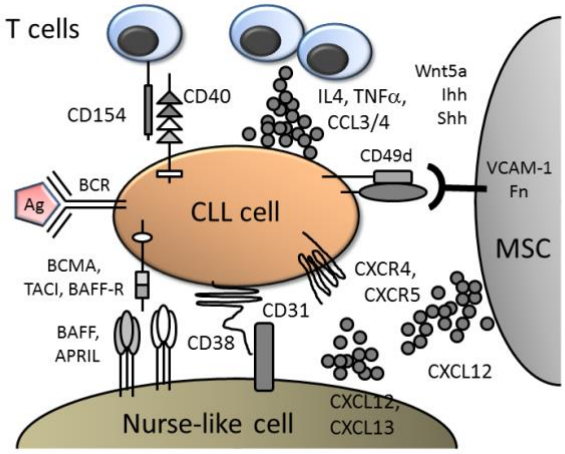

Figure 1.13. CLL cell proliferation centres

Proliferation centres are critical for providing growth and survival signals to CLL cells. (A) Immunohistochemistry image. Staining indicates Ki67+ cells. Red line identifies a proliferation centre. (B) Schematic representation of interaction of CLL cells with accessory cells, such as mesenchymal stromal cells (MSCs), nurse-like cells and T cells. Antigen (Ag) engagement of the BCR is also thought to occur within PCs. Illustration modified from Burger et al., 2009.

There are 2 main lines of evidence supporting a key role for the microenvironment in maintaining CLL. First, *in vitro* cultured CLL cells readily undergo apoptosis but are protected by co-culture with NLC (Burger et al., 2000) or BM stromal cells (Panayiotidis et al., 1996). Second, direct comparison between CLL cells from the periphery and tissue microenvironments reveal important differences. For example, circulatory CLL cells remain arrested in the G0/G1 phase of the cell cycle, whereas CLL cells from the BM or SLO have a higher fraction of proliferating cells (Andreeff et al., 1980). Direct comparison of gene expression analysis of peripheral blood, BM and LN cells by Herishanu group reported the LN as a crucial site in CLL for CLL/microenvironmental interactions due to upregulation of gene signatures linked to BCR signalling and NF-κB activation (Herishanu et al., 2011). Figure 1.14 summarises some of the key cellular and molecular interactions that occur within the CLL microenvironment and these are discussed in more detail in the following sections.

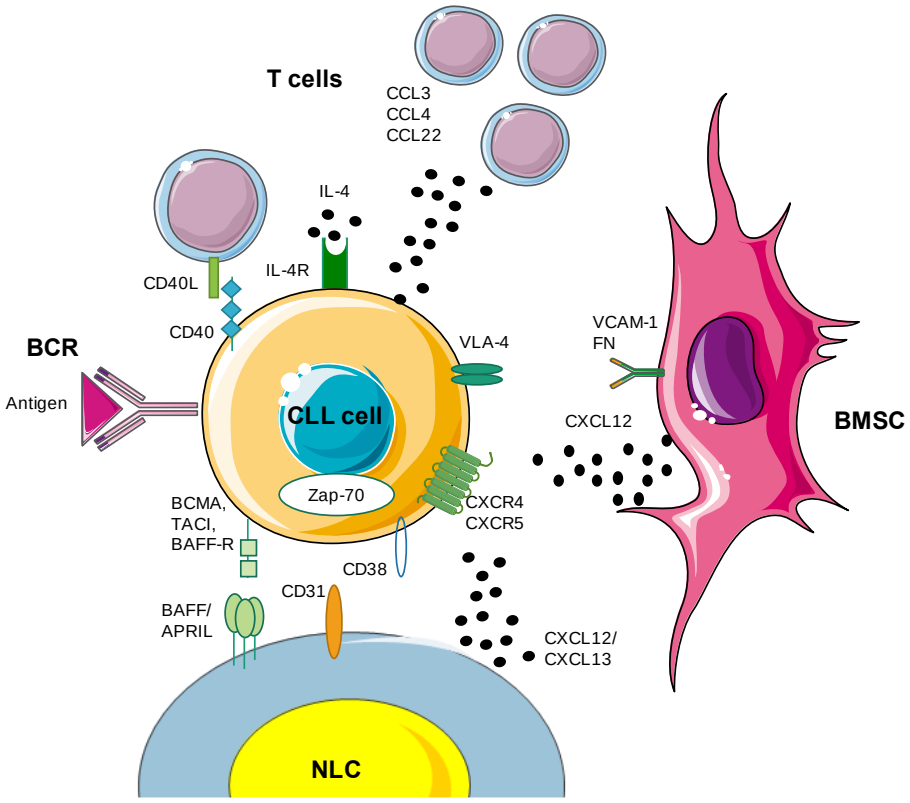

Figure 1.14. Cellular and molecular interactions within the CLL microenvironment
NLC cells produce CXCL12 and CXCL13 and BMSC primarily secrete CXCL12. Together these chemokines bind to CXCR4 and CXCR5 which are highly expressed on the surface of CLL cells to direct or retain CLL cells. Integrin receptors such as VLA-4 integrins expressed on the surface of CLL cells promote tissue retention through cell contact via the respective ligands (VCAM-1 and fibronectin) on stromal cells. CLL cells secrete the chemokines CCL3, 4 and 22 to promote T cells to move into the microenvironment. Subsequently, T cells interact with CLL cells via CD40-CD40L interaction and secretion of IL-4 to activate the IL-4R. Additional survival signals are provided by NLC via expression of the BAFF and APRIL that interact with their TNF family members receptors (BCMA, TACI, BAFF-R) present on CLL cells. CD38 expression on CLL cells may allow CLL cells to interact with its receptor CD31 which is expressed by stromal cells and NLCs. Illustration taken from Burger et al., 2009.

1.4.4.1 Nurse like cells

Initially described by Burger et al., NLC are a subset of monocyte-derived blood cells from CLL patients that spontaneously differentiate when cultured at high-density for 7–14 days (Burger et al., 2000). Specifically, they transform into fibroblast-like adherent cells and express typical stromal markers such as vimentin, STRO-1 and CXCL12. Their development has been linked to the production of High Mobility Group Box 1 (HMGB1) which may induce monocyte transformation via engagement of RAGE and TLR9 (Jia et al., 2014; Burger et al., 2000). NLC also appear to be important for development of CLL in animal models (Burger et al., 2009). CLL-NLC are characterised by a high level of expression of CD68 (Boissard et al., 2009; Tsukada, 2002) and CD163 (Boissard et al.,2015; Ysebeart & Fournie, 2011) and by a

gene expression pattern resembling that of tumour associated macrophages (Ysebeart & Fournie, 2011).

Multiple receptor systems have been implicated in mediating effects of NLC on CLL cells. For instance the secretion of chemokines such as CXCL12 (Burger et al., 2005) and CXCL13 (Bürkle et al., 2007) is thought to result in the gradient-dependent homing of CLL cells to tissue microenvironment such as the BM or SLO where they are protected from apoptosis via binding to CXCR4 and CXCR5, respectively.

Chemokine receptor activation is not limited to cell migration as stimulation of CXCR4 and CXCR5 was also reported to prolong survival of CLL cells *in vitro* by induction of extracellular signal-regulated kinase 1/2 (ERK1/2) (Burger et al., 2005) and signal transducer and activator of transcription 3 (STAT3) signalling (O'Hayre et al., 2010). Moreover, NLC also promote survival and proliferation of CLL through expression of the tumour necrosis factor super family members (TNF), B-cell activating factor of tumour necrosis factor family (BAFF) and a proliferation-inducing ligand (APRIL) (Nisho et al., 2005) which bind and activate B-cell maturation antigen (BCMA), trans-membrane activator calcium modulator and cyclophilin ligand interactor (TACI) and BAFF receptor (BAFF-R). Similarly, CD31 which is a co-stimulatory molecules expressed by NLC interacts with CD38 on CLL cells to activate alternate pro-survival pathways (Deaglio et al., 2005).

The interactions between CLL and NLCs is bidirectional and CLL cells are also able to actively recruit NLC to the microenvironment through the secretion of the chemokines CCL3/CCL4 (Burger et al., 2009).

1.4.4.2 Mesenchymal cells

MSC provide "feeder" layers for haematopoietic progenitor cells in the normal BM (Panayiotidis et al., 1996). Likewise, they are able to protect CLL cells from spontaneous and drug-induced apoptosis, an activity which is dependent on direct cell-to-cell contact (Panayiotidis et al., 1996). However, MSC are not limited to the BM as they are also present in the SLO in patients with CLL. In fact, MSC are widely dispersed throughout the microenvironmental tissue and perivascular areas (Ruan et al., 2006).

In contrast to NLC, *in vitro* analysis suggested that CLL interact differently to BM mesenchymal cells (Nisho et al., 2005). The data appears to suggest that MSC-CLL cell crosstalk is bidirectional whereby tumour cells are not only supported by stromal cells, but also are capable of activating and inducing stromal cell proliferation and secretion of cytokines (Gehrke et al., 2011), chemokines, pro-angiogenic factors, extracellular matrix components (Herishanu et al., 2011; de la Fuente et al., 1999). Similar to NLC, MSC produce CXCL12 to mediate the homing of CLL cells into the tissue microenvironments (Orimo et al., 2005). However, stromal cell secreted CXCL12 additionally promotes pseudoemperipolesis, which is basal penetration of the stromal layer by migrating cells (Burger et al., 2005). Interestingly, ZAP70+ and CD38+ expressing CLL cells migrate towards CXCL12 more readily than the non-CD38/ZAP70 expressing CLL cells (Vaisitti et al., 2010).

Extracellular matrix elements expressed by stromal cells, which are in contact with CLL, have also been associated with increased survival. Adherence of CLL cells to stromal cells through the binding of α4β1 integrin (CD49d/ VLA-4) on CLL cells to the vascular cell adhesion molecule 1 (VCAM-1) (Pittenger et al., 1999) or to the extracellular matrix component fibronectin (Wayner et al., 1989), highly expressed on the stromal cells respectively, rescues CLL cells from both spontaneous apoptosis or fludarabine-induced apoptosis (de la Fuente et al., 2002). Survival signals are transduced by PI3K/AKT signalling and BCL-XL upregulation (Herishanu et al., 2013).

Another example of MSC-CLL crosstalk includes interaction with the metalloproteinase-9 (MMP9). MMP-9 is the predominant metalloproteinase produced by CLL cells that promotes extravasation and lymphoid tissue infiltration through proteolytic degradation of basement membranes and extracellular matrix components (Munoz et al., 2006). Furthermore, MMP-9 also mediates CLL cell survival in BM-derived stromal cell co-culture (Ringhausen et al., 2004). This is through MMP9, α4β1 and CD44v binding in CLL cells which results in LYN and STAT3 activation and subsequent induction of the anti-apoptotic MCL1 (Munoz et al., 2010). Interestingly, expression of MMP9 in CLL cells is regulated through α4β1 integrin and CXCL12 (Munoz et al., 2006). In this respect, CLL cells in the BM and LN acquire and express higher levels of surface MMP-9 due to tumour cell activation in tissue microenvironment or derived from their adjacent accessory cells (Munoz et al., 2010).

1.4.4.3 T cells

Although there is extensive evidence for T-cell dysfunction in CLL (Ramsay et al., 2009), T cells have also been implicated in providing "support" to CLL cells *in vivo*. T-cell support appears to be mediated via cell-cell interactions and secreted factors. However, it remains unclear to what extent such support represents "general" T-cell support as opposed to specific cognate T cells following antigen presentation by CLL cells.

T lymphocytes may play a pivotal part in the proliferation of CLL cells, as interactions within compartmentalised tissue microenvironments are favourable to progression of disease. This is mediated predominantly by the CD4+ subset that appear to at least partially co-locate with proliferating CLL cells within PCs (Patten et al., 2008) and were required for the proliferation of CLL cells *in vivo* in a xenograft model of CLL (Bagnara et al., 2011).

The interaction of CLL cells and T cells likely mimics some aspects of that of normal B/T cells. This is through engagement of CD40R with its CD154/CD40L ligand (CD40L) and IL-4 mediated survival of CLL cells. Consistent with this, CD40L expressed by CD4+ T cells was able to overcome natural and drug induced apoptosis CLL cells via activation of the PI3K/AKT, MEK/ERK and NF-κB pathways (Herishanu et al., 2013) leading to induced expression of anti-apoptotic molecules such as MCL1, BCL-XL, BFL1 and Survivin (Hallaert et al., 2008).

Other evidence has implicated T cells in the survival and proliferation of CLL cells independent of cell-to-cell contact. For instance secretion of IL-4 (Romano et al., 1998) by T cells is able to rescue CLL cells from drug-induced or spontaneous cell death though upregulation of BCL-2 (Dancescu et al., 1992). Moreover, IL-4 enhances sIgM expression which tends to be downmodulated in CLL and further induce increased receptor signalling activity (Aguilar-hernandez et al., 2016).

1.4.5 CXCR4 function in CLL

In CLL, CXCR4 has emerged as a key receptor in the recruitment to and cross-talk between malignant B cells and their protective microenvironment (Burger et al., 2002). CXCL12 appears to have two major effects acting via CXCR4, which is expressed at 3 to 4 times higher levels on the surface of peripheral CLL cells compared to their normal counterpart (Burger et al., 1999; Möhle et al., 1999). First, it promotes actin polymerization for more efficient migration across vascular endothelium towards stromal cells resulting in pseudoemperipolesis (Burger et al., 1999). Second, CXCL12 promotes survival and rescue from spontaneous and drug induced CLL cell apoptosis (Burger & Kipps, 2002).

Elevated CXCR4 expression on CLL cells in the peripheral blood is associated with a higher degree of lymphoid organ infiltration (Calissano et al., 2009). Indeed, CLL cells expressing ZAP70 display increased chemotaxis and survival in response to CXCL12 compared with ZAP70-negative CLL cells (Richardson et al., 2006). Furthermore, $CD38^{+}$ CLL cells also display higher levels of CXCR4 mediated chemotaxis (Deaglio et al., 2007) towards CXCL12 (Vaisitti et al., 2010).

Moreover, circulating CLL cells in the PB characteristically express high levels of CXCR4 while CLL cells located in the tissue microenvironment and in close contact to CXCL12 secreting cell have lower levels of CXCR4 and high CD5 expression. This was shown as proliferating $Ki\text{-}67^{+}$ CLL cells from BM and lymphatic tissue display significantly lower levels of CXCR4 than non-proliferating CLL cells (Calissano et al., 2009). This suggests CXCR4 is down modulated as cells receive tissue based sIgM stimulation, or by cognate ligand exposure, and therefore, can be used to distinguish tissue (lymphatic and BM derived) from blood CLL cells, which express low or high CXCR4 levels, respectively (Herishanu et al., 2011; Burger et al., 1999). Collectively, low level of CXCR4 expression provides potential biomarker a fraction of cells that has recently exited the tissues into the blood. Interestingly, the natural recovery of CXCR4 on CLL cells in the circulation can be mimicked by culturing CLL cells *in vitro* where levels of CXCR4 increase rapidly within hours (Coelho et al., 2013).

1.4.6 The role of Cholesterol metabolism in cancer

It is well established that Cholesterol is an important component of cell membranes and has long been recognized to be necessary for cell growth and proliferation. Specifically early studies initially identified a relationship between novo sterol synthesis and movement through the cell cycle in lymphocytes and proliferation (Chen et al., 1975; Brown and Goldstein, 1974)

Low-density lipoproteins (LDLs) are the major carriers of cholesterol and have been studied mainly as cardiovascular risk factors but are increasingly recognized to play a role in cancer. Particularly in solid tumours high levels of LDL's are linked with increased risk of prostate cancer (Moses et al., 2009), colorectal cancer (Holtzman et al., 1987) shown to promote the survival migration and proliferation and in breast cancer cells (Nelson et al., 2013; Kitahara et al., 2011). In support of this, statins which lower LDL levels by blocking 3-hydroxy-3-methyl-glutaryl-CoA reductase (HMGCR), the rate-limiting enzyme of cholesterol synthesis have demonstrated anti-cancer properties (Gronich & Rennert, 2013). However, explanations for these results are unclear.

Overall there seems to be increasing interest and evidence suggesting that cholesterol metabolism plays a significant role in determining lymphocyte responses. A key regulator of the cholesterol biosynthetic pathway are the liver X receptors . The Liver X Receptors (LXRα and LXRβ) are part of a large Nuclear receptor super family that regulate cholesterol homeostasis in response endogenous activators such as oxysterols and intermediates of the cholesterol biosynthetic pathways (Janowski et al., 1996). LXR form dimers with RXR to activate target genes involved in cholesterol and fatty acid metabolism. Basinger et al. demonstrated LXR signalling is able to regulate sterol metabolism during proliferation of lymphocytes. The pathway suggested by the authors is that, PMA induced T cell activation promotes intracellular accumulation of cholesterol through increased cholesterol influx and biosynthesis combined with downregulation of efflux pumps (ABCA1) resulting in T cell proliferation. Negative feedback response is then regulated by oxysterols that produces as a by-products from the cholesterol biosynthesis pathway (Figure 1.15a). In support of this ,

the paper further showed that hyper activation of LXR with chemical agonists was able to inhibit proliferation of T cells during activation(Figure 1.15b). (Bensinger et al., 2008)

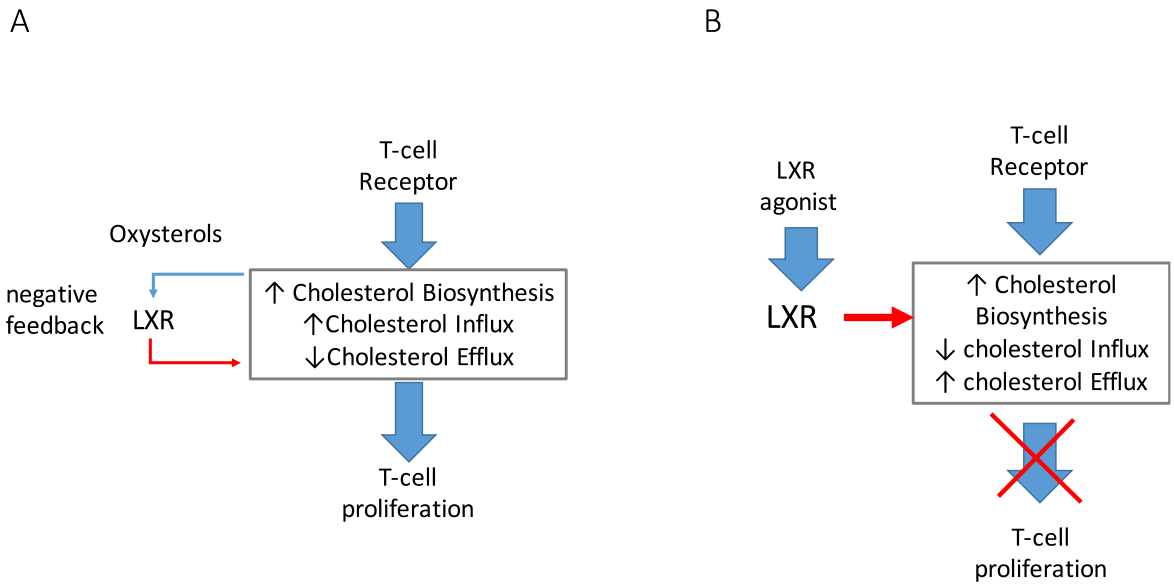

Figure 1.15 Cholesterol and LXR in normal T-cell responses

1.4.7 BCR-mediated receptor crosstalk in CLL

Similar to normal B cells, the BCR mediates cross-talk to other cell surface receptors on CLL cells, including the intergrin Very late activation antigen 4 (VLA-4) (Hoellenriegel et al., 2012) and CXCR4 (Figure 1.16). This section summarises the results on BCR→CXCR4 cross-talk in CLL cells since this is a major focus on experiments in my project.

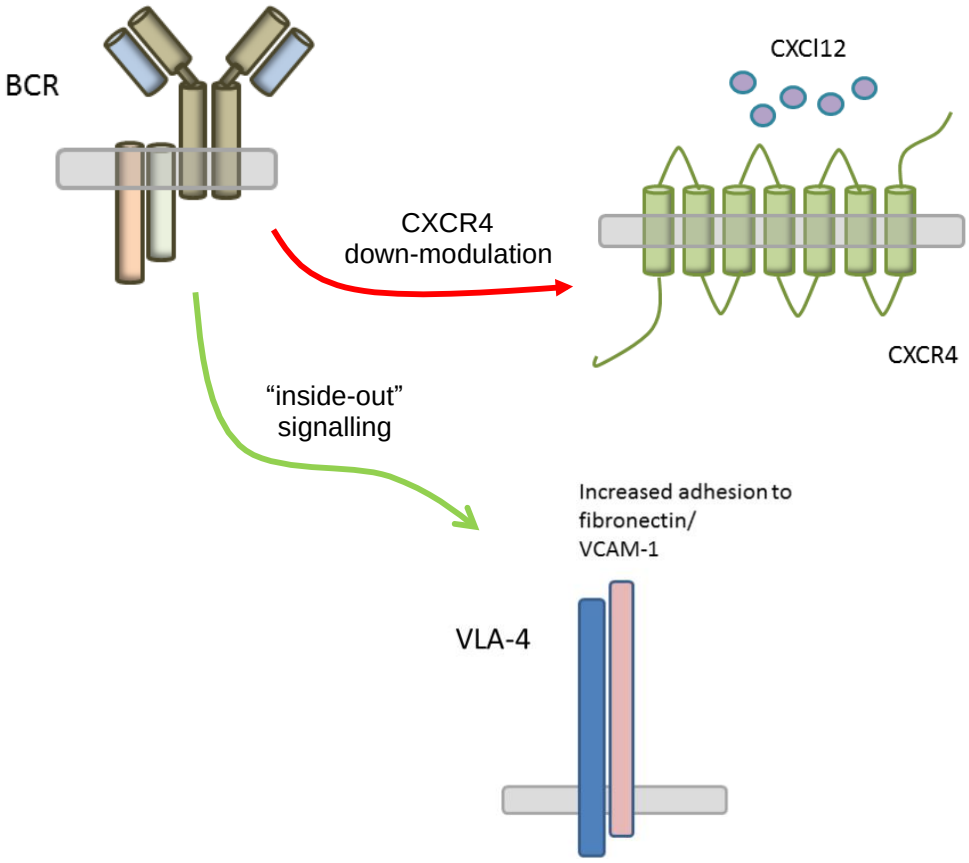

Figure 1.16. Examples of BCR-mediated cross-talk in CLL; CXCR4 and VLA-4
BCR antigen engagement leads to down-modulation of CXCR4 expression through increased endocytosis. Alternatively, BCR stimulation also can also promote increased adhesion to the fibronectin VCAM-1 via ''inside-out signalling''.

There are three major studies which have investigated CXCR4 down-modulation following BCR activation in CLL cells (Saint Georges et al., 2016; Vlad et al., 2009; Quiroga et al., 2009), CXCR4 down-modulation was due to endocytosis as it was reduced by culture in hypertonic media, which inhibits CME (Vlad et al., 2009). A more recent study by Saint Georges et al., recently demonstrated *in vitro* that BCR ligation results in concomitant down regulation of CXCR4 and CXCR5 as well as enhanced chemotaxis towards CXCL12 and CXCL13 respectively (Saint Georges et al., 2016). More specifically, the extent of down regulation of CXCR4 and CXCR5 was observed almost exclusively in high-risk cases after stimulation of the BCR with immobilised α-IgM antibodies (Saint Georges et al., 2016), although the mutational status of the IGVH and/or CD38 expression did not affect CXCR5 expression levels on the CLL cells (Haerzschel et al., 2016; Burger et al., 2007).

Unpublished experiments performed in the host laboratory has also investigated CXCR4 down-modulation by anti-IgM in CLL cells. As mentioned above, CXCR4 expression is relatively low on CLL cells following isolation from the blood and receptor expression naturally "recovers" as cells are cultured *in vitro* (Coelho *et al*., 2014). This reason for this recovery is unclear, but may reflect action of CXCR4-endocytosing ligands (e.g. CXCL12) *in vivo*. However, the natural recovery of CXCR4 expression can be effectively suppressed by anti-IgM. The extent to which anti-IgM reduced CXCR4 expression was tightly dependent on signal strength since there was a close positive correlation between CXCR4 down-modulation and anti-IgM-induced iCa^{2+} flux. Moreover, bead-bound anti-IgM (which induces stronger and longer-lasting signalling responses than soluble anti-IgM) induced a greater degree of CXCR4 down-modulation than soluble antibody.

Anti-IgM-induced CXCR4 down-modulation was inhibited by tamatinib (SYK inhibitor) or idelalisib (PI3Kδ inhibitor), but not by ibrutinib or acalabrutinib (BTK inhibitors), GO6983 (PKC inhibitor) or UO126 (MEK1/2 inhibitor). These results contrast with previous studies in DT40 cells which demonstrated that anti-IgM-induced CXCR4 endocytosis was mediated by a cascade involving SYK, BLNK, BTK and PLCγ2 which ultimately promotes PKC-dependent receptor internalisation (Guinamard et al., 1999). Thus, kinases operating in CLL cells appear to differ from those identified in other systems. Moreover, as described above (section 1.3.4.3), SHIP1 has also been implicated in BCR→CXCR4 cross-talk, especially in anergic B cells (Brauweiler et al., 2007).

1.5 Drug targeting of BCR in CLL

The recent years have seen a dramatic expansion in treatment options available for CLL, through the introduction of targeted agents (Kipps et al., 2017). This is particularly relevant to patients with p53/ATM dysfunction which are unlikely to respond to conventional chemoimmunotherapy due to defective DNA damage responses. New targeted agents include venetoclax which targets apoptosis regulating pathways in CLL cells by displacing BH3-only proteins from BCL2 resulting in induction of apoptosis (Souers et al., 2013).

A second key area of new drug approaches for CLL has been the development of inhibitors targeted against BCR-associated signalling kinases. Of these, the BTK inhibitor ibrutinib and

the PI3Kδ inhibitor idelalisib have been studied in most detailed, and are discussed further below. However, there is intense research activity in this area and other related agents are shown in Figure 1.17. This section will also introduce AQX-435, a novel small molecule SHIP1 activator, that is used widely as an experimental tool in this project and is a potential candidate for clinical development as a novel strategy to reduce BCR-signalling in malignant B cells.

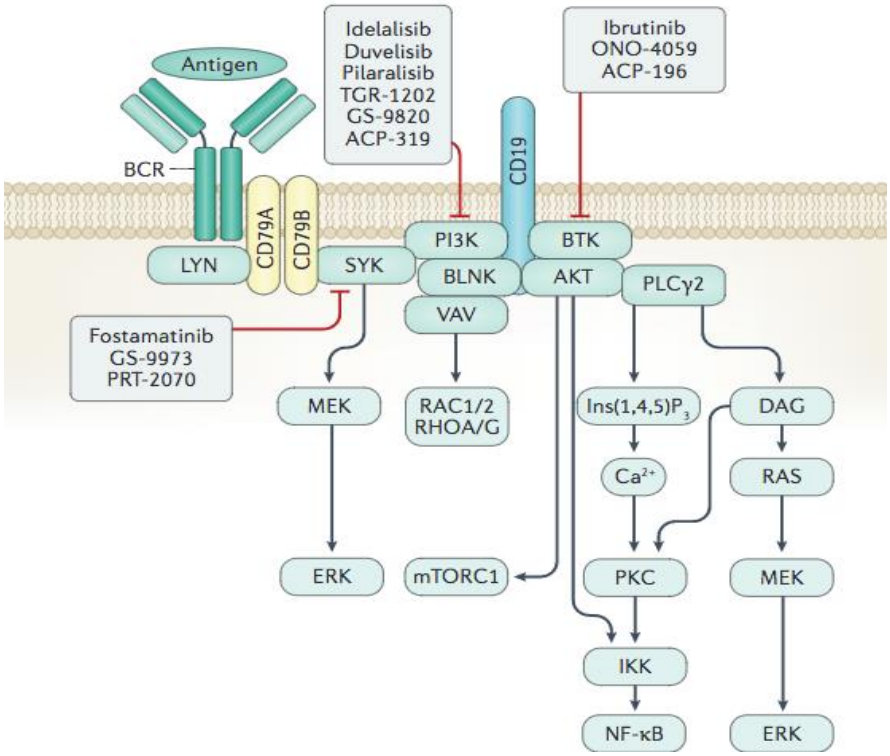

Figure 1.17. BCR signalling targeting drugs
The main pathways that lead to cell survival and proliferation downstream of the BCR are shown in along with drugs targeted against key signalling intermediates. Illustration taken from Kipps et al., 2017.

1.5.1 Ibrutinib

The BTK inhibitor ibrutinib has been approved by the FDA for treatment of CLL and mantle cell lymphoma. Ibrutinib is an irreversible inhibitor that acts by forming a covalent bond with the C^{481} residue in the BTK active site, leading to irreversible inhibition of BTK enzymatic activity and inhibition of downstream BCR signalling, including ERK/AKT phosphorylation and NF-kB DNA binding (Murray et al., 2015; Herman et al., 2011). *In vivo* studies showed that

ibrutinib delayed disease progression using an Eμ-*TCL1* adoptive transfer model (Ponader et al., 2012).

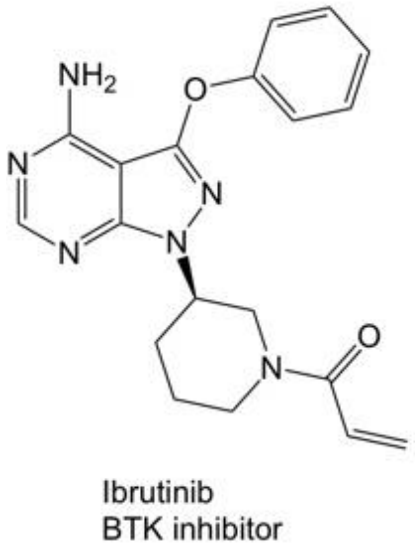

Figure 1.18 Chemical structure of Ibrutinib.

Ibrutinib has also been shown to inhibit signalling via other pathways (e.g. downstream of CXCR4) in CLL cells. Moreover, ibrutinib also inhibits cell migration and survival in a NLC co-culture assay (Ponader et al., 2012) and CD49d-mediated adhesion (Fiocari et al., 2013; de Rooij et al., 2012). Therefore, the effects of ibrutinib may not be mediated via inhibition of BCR pathways alone. Ibrutinib also has substantial off-target effects, and some of these may contribute to clinical activity. For example, Sagiv-Barfi et al., demonstrated that ibrutinib inhibits interleukin-2 inducible T-cell kinase, an enzyme that regulates the survival of Th2 $CD4^+$ cells. This study suggested that effects of ibrutinib on Th2 $CD4^+$ cells may shift the balance between Th1 and Th2 responses to enhance promote antitumor activity (Sagiv-Barfi et al., 2015).

Ibrutinib has shown improvement in overall survival (OS) and median progression free survival (PFS) compared to chlorambucil or ofatumumab. Administration of ibrutinib significantly reduces lymphadenopathy, which is associated with an initial striking increase in absolute lymphocyte count. This indicated there is induction of apoptosis in malignant cells within tissues, but also redistribution of malignant cells into the circulation. Whether

redistribution of CLL cells is through blockade of entry and/or promoting egression inside SLO release is unknown. Nevertheless, this is consistent with ibrutinib mediated effects not being exclusive to BCR and it eliciting additional activity on pathways important in tissue homing/retention.

Although initial responses to ibrutinib can be striking, resistance is becoming increasingly common. In some individuals, this is associated with mutation of BTK (at C^{481}) or PLCγ2 (Lampson & Brown, 2018). Mutant BTK retains activity but is rendered relatively resistant to inhibitory effects of ibrutinib, whereas PLCγ2 mutations are associated by by-passing signalling where PLCγ2 activation (and hence downstream iCa^{2+} release) is rendered independent of BTK (Walliser et al., 2016). Patient outcomes following development of resistance are particularly poor. There remains, therefore, a clear need for other agents to target BCR signalling in CLL cells.

1.5.2 idelalisib

The PI3Kδ inhibitor idelalisib was approved in the USA and in Europe for the treatment of relapsed CLL in combination with rituximab (Furman et al., 2014; Herman et al., 2010). *In vitro* investigations demonstrated that idelalisib displays a dual mechanism of action by reducing PI3K-dependent signalling downstream of the BCR, whilst also reducing interactions that retain CLL cells in protective tissue microenvironments (Hoellenriegel et al., 2011; Lannutti et al. 2011). Thus, idelalisib inhibits CLL cell chemotaxis toward CXCL12, CXCL13 and migration beneath stromal cells. Like ibrutinib, the direct pro-apoptotic effects of idelalisib are rather modest.

Similar to ibrutinib, patients treated with idelalisib show a marked lymphocytosis concomitant with a rapid reduction of lymphadenopathy (Furman et al., 2014). However, use of idelalisib is limited by severe toxicities (pneumonitis, colitis and transaminitis) especially in the frontline setting. These maybe linked to the known role of PI3Kδ for development and function of regulatory T cells (Chellappa et al., 2019; Okkenhaug & Vanhaesebroeck, 2003).

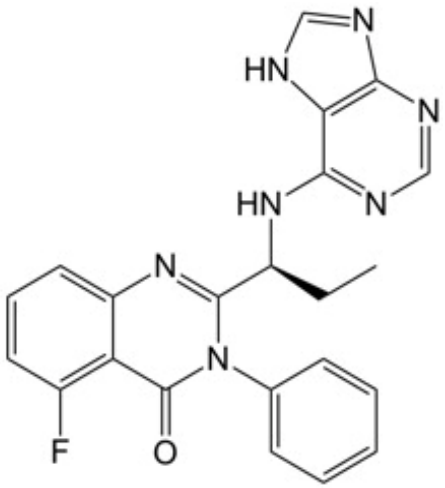

Idelalisib
PI3Kδ inhibitor

Figure 1.19 Chemical structure of Idelalisib

1.5.3 Allosteric activators of SHIP1

An novel approach to suppress inappropriate signalling in cancer cells, distinct from kinase inhibition, is to enhance activity of naturally counteracting phosphatases. Since SHIP1 naturally counters the activity of PI3K, SHIP1 activators may have clinical utility as a novel approach for treatment of various B-cell neoplasms, including CLL. My project examines this approach by using the novel SHIP1 agonist, AQX-435, and this section provides background on the development of SHIP1 activators and previous results with AQX-435.

1.5.3.1 Development of SHIP1 agonists

Early work on SHIP1 agonists was led by Andersen and colleagues who identified the sesquiterpene pelorol as a naturally occurring SHIP1 activator and prepared some initial synthetic analogues (Yang et al., 2005). Of particular relevance, this group synthesised AQX-016A and showed that it selectively activated SHIP1 *in vitro* and had *in vivo* anti-inflammatory activity in murine models of ear oedema and sepsis (Yang et al., 2005).

The presence of a metabolically unstable catechol moiety in AQX-016A drove the development of additional analogues. This led to the synthesis of AQX-MN100 which lacked the reactive hydroxyl functionality at C17 of AQX-016A. Activation of SHIP1 by AQX-MN-100 *in vitro* was shown to be dependent on the presence of the C2 domain, consistent with an allosteric mechanism of activation (Ong et al., 2007).

Biological analysis of AQX-MN100 revealed that, similar to AQX-016A, AQX-MN100 had *in vivo* anti-inflammatory activity and was well tolerated because it had no significant effects on peripheral blood cell counts, bone marrow progenitor numbers, liver function, or kidney function (Meimetis et al., 2012). Furthermore, AQX-MN100 did not reduce AKT phosphorylation in SHIP1-deficient cells.

Although studies performed to this point had focused on anti-inflammatory activity, AQX-MN100 was also shown to reduce AKT phosphorylation and induced apoptosis *in vitro* in multiple myeloma cells (Meimetis et al., 2012; Kennah et al., 2009; Ong et al., 2007). AQX-MN100 also showed synergistic effects with the proteasome inhibitor bortezomib, slowing the rate of proliferation of OPM2 multiple myeloma cells (Kennah et al., 2009). However, the development of pelorol-related compounds like AQX-MN100 was ceased due to their extremely limited aqueous solubility (Meimetis et al., 2012).

More recently, Aquinox Pharmaceuticals (Stenton et al., 2013) reported development of a new series of SHIP1 agonists designed to overcome the poor water solubility of previous agents (Shen et al., 2002). The initial focus was on development of AQX-1125 which modestly (~20%) increased catalytic activity of human recombinant SHIP1. In cells, AQX-1125 reduced AKT phosphorylation and cytokine release, and reduced the activation of mast cells and inhibited human leukocyte chemotaxis. Again, effects on SHIP1 appeared to be due to allosteric activation as effects were dependent on the presence of the SHIP1 C2 domain.

More detailed kinetic evaluation demonstrated that AQX-1125 binding promoted substrate binding (reduced Km) rather than increasing enzyme activity per se (Vmax) (Table 1.2).

Table 1.2 kinetic analysis of AQX-1125

	Control	AQX-1125
k_{cat}	3.5 ± 0.4	3.4 ± 0.3
K_M	214 ± 21	180 ± 9
V_{max}	18 ± 2	17 ± 2

K_{cat} the measure of how many substrates one enzyme can convert into a product per second. K_M represents the Michaelis constant that is defined as the substrate concentration at which half of the active sites are occupied.
V_{max} represents the rate of reaction when the enzyme is saturated with substrate is the maximum rate of reaction

In vivo studies revealed that AQX-1125 was suitable for oral dosing (>80% oral bioavailability and >5 h terminal half-life) and was taken forward for clinical evaluation in the treatment of Interstitial Cystitis Bladder Pain Syndrome (BPS/IC). Although phase 2 trial results were promising with patients reporting a greater reduction on bladder pain compared to placebo with a good tolerance to the SHIP1 activator (Nickel et al., 2016), a subsequent phase 3 trial failed to meet efficacy goals and development of AQX-1125 was suspended.

1.5.3.2 The novel SHIP1 activator AQX-435

Since AQX-1125 is a relatively weak SHIP1 activator and was developed as an anti-inflammatory agent (Stenton et al., 2013), other compounds were synthesized by Aquinox pharmaceuticals to identify a potential candidate for development as an anti-cancer agent. Over 50 compounds were screened in the host laboratory for their ability to suppress anti-IgM-induced AKT phosphorylation in malignant B cells (unpublished data), and on the basis of these results, AQX-435 was selected as both an experimental tool to probe consequences of SHIP1 activation and as a potential candidate for clinical development (Figure 1.20). This

compound lacked undesirable functionalities present in earlier compounds (Meimetis et al., 2012; Yang et al., 2005) and had much improved water solubility and other drug-like properties.

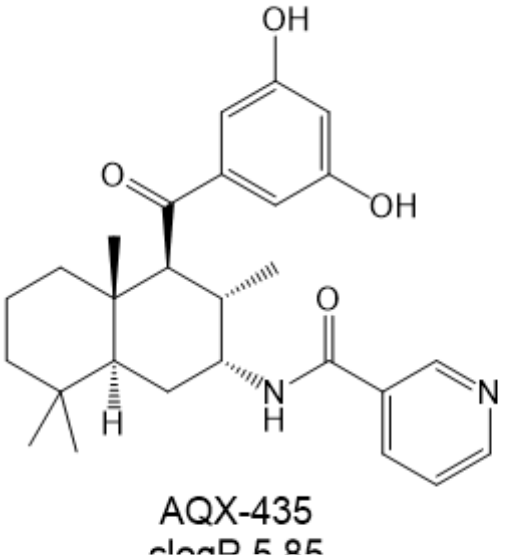

Figure 1.20 Chemical structure of AQX-435

Biological characterization of AQX-435 in *in vitro* and *in vivo* models of B-cell malignancies have been reported in abstract form (where AQX-435 was referred to as AQX-C5; Packham et al., 2018; Packham et al., 2016). Key findings are summarized below;

- AQX-435 significantly reduced anti-IgM-induced AKT phosphorylation in primary CLL cells and in established DLBCL-derived cell lines.
- AQX-435 significantly reduced induction of MYC protein expression (a downstream target for PI3K/AKT signaling) following anti-IgM stimulation of CLL cells.
- AQX-435 induced apoptosis of CLL cells. Normal B cells were significantly less sensitive to AQX-435-induced apoptosis compared to CLL cells.
- AQX-435 overcame the survival promoting effects of anti-IgM and C40L/IL4 in CLL cells.
- AQX-435 triggered down-regulation of CXCR4 on CLL cells. Again, CXCR4 expression on normal B cells was relatively unaffected by AQX-435 compared to CLL cells.

- AQX-435 significantly reduced the growth of lymphoma cells *in vivo*, including in PDX models of DLBCL.

Overall, AQX-435 is a useful tool compound to probe consequences of SHIP1 activation and a potential candidate for development as an anti-cancer agent

1.6. Hypothesis and aims

1.6.1 Hypothesis

The primary hypothesis of this project is that BCR activation and downstream signalling molecules influence expression and function of other cell surface receptors via SHIP1 and protein kinases in CLL. The secondary hypothesis is that the novel chemical SHIP1 activator, AQX-435 will characterise new pathways affected by SHIP1 activation in BCR signalling in CLL cells.

1.6.2 Aims

To investigate these hypotheses project addresses two closely inter-related areas. First, to investigate pathways of crosstalk between the BCR and other cell surface receptors which influence response to microenvironmental factors, including the role of specific kinases and the inositol lipid phosphatase SHIP1. Second, to characterise pathways regulated by the novel chemical SHIP1 activator, AQX-435.

To address the primary hypothesis the main aims of this project was to;

- Analyse regulation of CXCR4, as a target for BCR-mediated crosstalk in CLL cells as well as in established B-cell lines to determine whether pathways identified in CLL cells operated in other types of malignant B cells
- Develop a transfectable models to use RNAi to directly investigate the role of specific signalling intermediates inclduing SHIP1 in CXCR4 regulation, to complement studies performed using small molecule inhibitors/activators in CLL cells.
- To investigate the analysis of BCR cross-talk to another GPCR, EBI2, for the first time, on primary CLL cells and determine the role of SHIP1 by AQX-435.

To address the secondary hypthesis, the main aim of experiments in chapter 5 focussed on

- Compare the effects of SHIP1 activation (using AQX-435) and PI3Kδ inhibition (using idelalisib) on anti-IgM-regulated gene expression using Bioinformatical analysis on CLL.
- Investigating the effects of SHIP1 activation by AQX-35 on gene expression using RNA-Seq analysis

Chapter 2: Material and Methods

2.1 Cell culture

2.1.1 Materials

Reagent	Components
Complete RPMI-1640 (cRPMI)	RPMI-1640 (Sigma) supplemented with 10% foetal calf serum (FCS; Thermofisher Scientific), 1% penicillin/streptomycin solution (Thermofisher Scientific), 2 mM glutamine (Thermofisher Scientific)
DT40 culture medium	cRPMI-1640 supplemented with 2-mercaptoethanol (Sigma) and with 8% FCS and 2% chicken serum (Thermofisher Scientific) in place of 10% FCS
Freezing medium	90% FCS, 10% dimethyl sulfoxide (DMSO; Sigma)

2.1.2 Cell lines

This study used the following cells lines; HBL1, TMD8, OCI-LY7, RL, WSU-FSCCL, RAMOS, DT40 (see Table 3.1 for details). Human cell lines were obtained from the European Collection of Authenticated Cell Cultures (UK) or the Leibniz Institute DSMZ German Collection of Microorganisms and Cell Cultures, whereas DT40 cells were obtained from the RIKEN Institute Cell Bank (Japan). Components of the growth media used to maintain these lines is provided in Section 2.1.1. Cells were cultured at 37^{o}C in a humidified atmosphere containing 5% carbon dioxide. Identity of all human cell lines was confirmed using short tandem repeat analysis (Promega 16-plex kit) and absence of mycoplasma was confirmed by PCR analysis (ABM).

Cell line stocks were maintained by cryopreservation in freezing medium. For recovery, frozen stocks were removed from liquid nitrogen and warmed quickly to 37 ^{o}C in a water bath. Cells were then diluted in pre-warmed cRPMI. Cells were centrifuged at 350 g for 5 minutes at room temperature and the pellet was re-suspended in 10 ml of cRPMI. Cell viability was routinely determined using trypan blue exclusion.

2.1.3 Primary cells

Studies using primary cells from CLL patients and normal donors were performed following Ethics Committee approvals and in accordance with the Declaration of Helsinki.

Cryopreserved peripheral blood mononuclear cell (PBMCs) from CLL patients were obtained from the Southampton tissue bank. Diagnosis of CLL was made according to the 2008 International Workshop on CLL/National Cancer Institute (NCI) criteria and confirmed by flow cytometry (Hallek et al., 2008). Storage and characterisation of CLL samples (including mutational status of *IGHV* gene; tumour cell population percentage ($CD19^{+}CD5^{+}$); percentage of CD38 and ZAP70 expression; anti-IgM-induced calcium flux) was performed by research technicians in the tumour bank using established methods (Mockridge et al., 2007). Cryopreserved CLL samples were recovered as described for cell lines and allowed to "rest" in cRPMI for one hour before use.

Table 2.1 shows the characteristics of the CLL samples used during this project.

Table 2.1 Features of CLL samples

Sample	CD19+ CD5+ cells (%)	*IGHV* Status	sIgM expression (MFI)	Anti-IgM signalling (%)[a]	CD38 Expression (%)	ZAP70 Expression (%)
273D	85	M-IGHV	54	66	8	2
348d	98	M-IGHV	53	4	0	1
351C	97	M-IGHV	34	79	20	99
409C	73	M-IGHV	112	60	47	21
482C	94	M-IGHV	9	1	3	99
483	95	M-IGHV	49	4	3	1
498A	85	M-IGHV	16	3	1	2
498B	80	M-IGHV	15	12	1	4
511B	89	U-IGHV	29	48	24	24
513	98	U-IGHV	80	38	1	70
519B	83	M-IGHV	34	67	0	0
523C	84	M-IGHV	75	56	0	0
523F	97	M-IGHV	31	25	5	7
575E	97	M-IGHV	99	69	1	0
604C	86	M-IGHV	61	60	0	0
604F	87	M-IGHV	54	79	0	0

621B	93	M-IGHV	49	49	1	23
629C	95	U-IGHV	12	6	17	2
636B	86	M-IGHV	17	2	1	0
639	93	M-IGHV	26	6	0	10
641D	69	M-IGHV	76	77	1	9
679A	89	M-IGHV	51	13	1	13
681A	98	M-IGHV	185	31	6	2
689	97	U-IGHV	41	15	92	8
716B	88	M-IGHV	34	65	4	1
739	98	U-IGHV	99	76	81	1
774A	98	U-IGHV	40	25	15	5
780A	98	U-IGHV	81	81	62	2
780B	98	U-IGHV	47	81	98	30
802	91	U-IGHV	40	3	42	31
804	92	M-IGHV	5	3	6	1
834	93	M-IGHV	155	70	97	11
929C	83	U-IGHV	134	58	25	75

[a]Anti-IgM signalling is percentage of cells with increased iCa^{2+} following stimulation with soluble anti-IgM. CLL samples were characterised by research technicians in the CLL Bank and CLL group.

Cryopreserved "normal" PBMC's from healthy donors were obtained from blood cones from the NHS Blood and Transplant Service. Storage and characterisation of PBMCs was performed by Dr Alison Yeomans. Cryopreserved PBMC samples from normal donors were recovered as described for CLL cells and allowed to "rest" in cRPMI for one hour before use.

Table 2.2 shows the characteristics of normal PBMC samples used during this project, (% B cells, and percentage of IgM or IgG positive cells within the B cell population)

Table 2.2 Features of normal PBMC samples

Sample	$\%CD19^{+}CD5^{-}$ (B cells)	IgM+ within B cells (%)	IgG+ within B cells (%)
Donor 6	7	86.6	8
Donor 7	2.9	64.6	9.1
Donor 9	8	95.7	2.6
Donor 10	4.5	91.2	9.5

2.1.4 sIgM stimulation and chemical reagents

Human cells were stimulated via sIgM using either soluble or bead-bound goat anti-human IgM F(ab')$_2$, as previously described (Coelhlo et al., 2014; Mockridge et al., 2007). As controls, cells were treated with soluble/bead-bound control goat F(ab')$_2$. DT40 cell were stimulated with mouse anti-chicken IgM (Cambridge Bioscience). Soluble antibodies were obtained from suppliers in sodium azide-free buffers. Recombinant DC-SIGN was from R&D Systems and used as previously described (Linley et al., 2015).

The following inhibitors were used;

Inhibitor	Supplier	Target
Ibrutinib	Selleck Chemicals	BTK
Acalabrutinib	Selleck Chemicals	BTK
Idelalisib	Selleck Chemicals	PI3Kδ
Tamatinib	Selleck Chemicals	SYK
CRT006610	ABCAM Biotechnology	PKD
CRT0066051	ABCAM Biotechnology	PKD

N-acetylcysteine (NAC), ionomycin and (R)-mevalonic acid (MVA) were from Sigma. The SHIP1 activator AQX-435 was a kind gift of Aquinox Pharmaceuticals. All compounds (with the exception of the PKD inhibitors) were prepared as 10 mM stock solutions in DMSO and stored as single-use aliquots at -20 ^{o}C. NAC was prepared as 100 mM stock in H_20 and the pH was corrected to 7.0 using NaOH. 7α25-OHC was from Sigma Aldrich and was dissolved in DMSO. Appropriate solvent controls were used in all experiments.

2.1.5 siRNA transfection studies

RL cells (4x10^6 cells per transfection) were collected by centrifugation at 350 g for 5 minutes at 4 ^{o}C and re- suspended in 100 µl of Transfection Buffer (solution V and Supplement 1, Lonza). Cells were then transfected with Smartpool ON-target plus siRNAs specific for human BTK, SYK or SHIP1, or ON-target plus control siRNA pool (all Dharmacon) using a Nucleofector™ II/2b Device (Lonza) as per the manufacturer's instructions. Transfections typically contained 200 pmoles of siRNA pools. Some transfections were performed with the

addition of the green fluorescent protein (GFP) expression plasmid pmaxGFP (Lonza). Cells were allowed to recover for 24 hours before analysis/additional manipulations.

In some experiments, cells with high GFP expression were collected by FACS sorting. Cells were washed with FACS buffer (Becton Dickinson) and collected by centrifugation at 350 g for 5 minutes at 4 ^{o}C . The cell pellet was re-suspended in 200 µl of FACS buffer and "GFP^{hi}" cells collected using a FACSAria II cytometer (Becton Dickinson).

2.2 Analysis of cell surface protein expression by flow cytometry

2.2.1 Materials

Reagent	Components
Phosphate-buffered saline (PBS)	137 mM NaCl, 2.7 mM KCl, 10 mM Na_2HPO_4, 1.8 mM KH_2PO_4
FACs buffer (Becton Dickinson)	PBS supplemented with 0.01% NaN_3, 1% bovine serum albumin (BSA; Sigma), 4 mM EDTA (Sigma)
Biolegend cell staining buffer	Exact composition not provided by Biolegend but known to contain FCS and NaN_3
Staining buffer with de-lipidated BSA	PBS supplemented with 0.01% NaN_3, 1% delipidated BSA (Sigma), 4 mM EDTA

2.2.2 CXCR4 expression

Flow cytometry analysis of CXCR4 expression was performed using 1x 10^6 cells per assay. Cells were transferred to FACS tubes and re-suspended in 100 µl of Becton Dickinson FACS buffer with 2 µl of APC-conjugated mouse anti-human CXCR4 or 1 µl APC-conjugated Mouse IgG2A κ Isotype control antibody (both Biolegend). Depending on the cell type analysed, some assays were performed with the addition of 2 µl PerCPCy5.5-conjugated anti-CD5 antibody (Biolegend) and/or 1 µl pacific blue-conjugated anti-CD19 antibody (Biolegend).

Cells were incubated with antibodies for 15 min at 4°C in the dark. Cells were then washed twice with 500 µl of FACS buffer at 350 g for 5 minutes at 4 °C and re-suspended in 200 µl of FACS buffer. Fluorescence was analysed using a FACS-CANTO II (Becton Dickinson) with

10,000 events recorded per sample. Data was analysed using FlowJo (TreeStar) and CXCR4 expression on specific cell populations (e.g. $CD19^+CD5^+$ for CLL cells) was calculated by subtracting the mean fluorescent intensity (MFI) of control antibody stained cells from the MFI of anti-CXCR4 stained cells.

2.2.3 EBI2 expression

Cell surface EBI2 expression was determined as for CXCR4 using AlexaFluor647-conjugated anti-human mouse GPR183 EBI2 or control 1 μl AlexaFluor647-conjugated Mouse IgG2A κ Isotype antibodies (both Biolegend). In experiments using normal PBMCs, cells were additionally stained with PerCPCy5.5-conjugated anti-human CD27 (Biolegend) and FITC-conjugated anti-human IgG (Agilient Technologies, DAKO). EBI2 analysis was typically performed using the Biolegend cell staining buffer, although some experiments were performed to compare staining carried out using Becton Dickinson FACS buffer, Biolegend cell staining buffer or staining buffer containing de-lipidated BSA (see section 2.3.1). As for CXCR4, EBI2 expression on specific cell populations (e.g. $CD19^+CD5^+$ for CLL cells) was calculated by subtracting the mean fluorescent intensity (MFI) of control antibody stained cells from the MFI of anti-EBI2 stained cells.

2.2.4 sIgM endocytosis

Analysis of sIgM endocytosis was performed by quantifying residual expression of sIgM using either anti-IgM or anti-κ light chain antibodies (1x 10^6 cells per assay). For detection of sIgM using anti-IgM, cells were transferred to FACS tubes and washed re-suspended in 100 μl of Becton Dickinson FACS buffer with 5 μl FITC-conjugated mouse anti-human IgM or FITC-conjugated mouse IgG1, κ-light-chain control antibody (both Biolegend). For detection of sIgM using anti-κ light chain antibodies cells were re-suspended in 100 μl of FACS buffer with 5 μl PE-conjugated mouse anti-kappa light chain (kLC) antibody or PE-conjugated mouse IgG1 κ control antibody (both Biolegend). Cells were incubated for 15 min at 4 °C in the dark and then washed 500 μl of FACS buffer at 350 g for 5 minutes at 4 °C and re-suspended in 200 μl of FACS buffer. Fluorescence was analysed using a FACS-CANTO II

(Becton Dickinson) with 10,000 events recorded per sample. Data was analysed using FlowJo (TreeStar) and sIgM expression was calculated by subtracting the MFI of control antibody stained cells from the MFI of anti-KLC or anti-IgM stained cells.

2.3 Analysis of intracellular calcium flux and cell viability using flow cytometry

2.3.1 Calcium flux analysis

Analysis of intracellular Ca^{2+} was performed using $2.5x10^6$ cells per assay. Cells were incubated at 37°C for 30 minutes in 2 ml of cRPMI containing 2 µl of 10% pluronic F-127 (Sigma) and 0.8 µl of Fluro3-AM (50 µg/ml; Life Technologies). Cells were then collected by centrifugation at 350 g for 5 minutes, re-suspended in 500 µl cRPMI and kept at room temperature in the dark before analysis. Before acquisition, each tube was pre-warmed in a water bath at 37°C for approximately 5 minutes. The samples were then vortexed gently and placed on the flow cytometer (FACSCanto II flow cytometer, BD Biosciences). Data was collected for 30 seconds to establish a baseline before addition of stimuli (e.g. anti-IgM). Events were then recorded for a further 270 seconds. Data was analysed using the kinetics function on FlowJo (v9.9.5 or v10.5.5) and the percentage of responding CLL cells was calculated as previously described (Mockridge et al., 2007).

2.3.2 Annexin V/propidium iodide staining

Cell viability was analysed using annexin-V/propidium iodide (PI) staining. Annexin-V binds with high affinity to phosphatidylserine (PS) which, in viable cells, is located on the cytoplasmic face of the plasma membrane. By contrast, during apoptosis, PS is translocated to the outer leaflet of the plasma membrane where it is accessible to annexin-V. PI fluoresces following intercalation into DNA and is excluded from cells with an intact plasma membrane. PI is therefore used to identify cells with a permeable plasma membrane in which annexin V may bind to intracellular PS.

CLL cells (1 x10^6 per assay) were washed with 500 µl of Becton Dickinson FACS buffer and then re-suspended in 300 µl of Annexin-V staining buffer (10 mM HEPES pH 7.4, 0.14 M NaCl, 2.5 mM $CaCl_2$) supplement with 2.5 µg/ml of Annexin-V-FITC (kindly provided by the Protein Core Facility, University of Southampton) and 12.5 µM PI (Invitrogen, Molecular Probes, California, USA). Cells were and incubated at 4 ^oC for 15 minutes in the dark before analysis using a FACS-CANTO II flow cytometer (Becton Dickinson). 10,000 events were recorded per sample and data was analysed using FlowJo (v9.9.5 or v10.5.5). For analysis, the proportion of Annexin V^-/PI^- cells was calculated as a measure of cell viability.

2.4 Immunoblotting

2.4.1 Materials

Reagent	Components
RIPA Buffer	0.15 M NaCl, 1% NP40, 0.5% sodium deoxycholate, 1% sodium dodecyl sulfate (SDS) , 0.05 M Tris-HCl pH 8.0
SDS sample buffer	12.5mM Tris-HCl pH 6.8, 1.4% SDS, 4% Sucrose , 0.002% Bromophenol Blue
10x Running buffer	250 mM Tris base, 1900 mM glycine, 1% SDS
Transfer Buffer	500 ml of ethanol, 200 ml 10x running buffer, to 2000 ml with deionised H_2O
TBS/Tween	20 mM Tris-HCl pH 7.5, 150 mM NaCl, 0.1% Tween-20
Milk-TBS/Tween	TBS/Tween supplemented with 5% milk powder
BSA-TBS/Tween	TBS/Tween supplemented with 5% BSA

2.4.2. Cell lysates

Cells were collected by centrifugation at 350 g for 10 minutes at 4°C, washed in ice-cold PBS and re-suspended in RIPA Buffer, supplemented with phosphatase and protease inhibitor cocktails (Sigma, each 1:100). Cells were incubated on ice for 30 minutes before centrifugation at 16,100 g at 4°C for 10 minutes. Supernatants containing protein lysates

were collected and stored at -20°C. Protein concentration of the cell lysate was determined using the Bio-Rad protein assay (Sigma) according to the manufacturer's instructions. Immunoblotting was performed using equal amounts of protein for each sample.

2.4.3 SDS-poly acrylamide electrophoresis (PAGE)

Equal amounts cell lysates (typically 20 – 40 µg) were diluted in SDS sample buffer which had been freshly supplemented with diothiothreitol (DTT) (1/30 dilution of 30x DTT reducing agent; Cell Signalling Technology). Samples were heated at 95°C for 5 minutes and then stored on ice.

Proteins samples were resolved using SDS-PAGE using standard gel stacking and resolving gels as described in Molecular Cloning: a Laboratory Manual (Sambrook, 1989). Protein standards (PageRuler plus protein ladder; Thermofisher Scientific) were run on each gel to allow estimation of molecular weights and confirm transfer of proteins to nitrocellulose. Electrophoresis was carried out in 1X running buffer at 120 V for 1 hour using a BIO-Rad Mini-Protean Tetra vertical electrophoresis tank. Proteins were then transferred to a nitrocellulose membrane using transfer buffer at 100 V for 1 hour.

2.4.4 Antibody incubations and imaging

Following transfer, membranes were washed twice in TBS/Tween before blocking of non-specific binding sites using BSA-TBS/Tween or Milk-TBS/Tween for 1 hour. Membranes were then incubated at 4^{o}C overnight in primary antibody diluted in BSA-TBS/Tween or Milk-TBS/Tween (Table 2.3).

Table 2.3 Primary antibodies used in Western blotting

Antibody	Species	Dilution	Supplier
Anti-β-actin	Rabbit	1:1000	Cell Signalling Technologies
Anti-HSC70	Rabbit	1:1000	Cell Signalling Technologies
Anti-GAPDH	Rabbit	1:1000	Cell Signalling Technologies
Anti-ERK1/2	Rabbit	1:100	Cell Signalling Technologies
Anti-phospho ERK1/2 (p42/42)	Rabbit	1:1000	Cell Signalling Technologies
Anti-AKT	Rabbit	1:1000	Cell Signalling Technologies
Anti-phospho AKT (S^{473})	Rabbit	1:1000	Cell Signalling Technologies
Anti-SYK	Rabbit	1:1000	Cell Signalling Technologies
Anti-BTK	Rabbit	1:1000	Cell Signalling Technologies
Anti-phospho PKD (S^{916})	Rabbit	1:1000	CellSignalling Technologies
Anti-SHIP1	rabbit	1:1000	Cell Signalling Technologies
Anti-SREBP1	rabbit	1:1000	Abcam
Anti-ABCA1	rabbit	1:1000	Abcam

Following incubation with primary antibodies, membrane were washed 3 times with TBS/Tween for 5 minutes and then incubated with appropriate secondary antibodies (horse radish peroxidase-conjugated goat anti-mouse Ig or goat anti-rabbit Ig; both from Agilent Technologies) diluted 1:2000 in BSA-TBS/Tween or Milk-TBS/Tween for 1 hour at room temperature. The membranes were then washed 3 times with TBS/Tween and incubated with 600 ul of Supersignal West Pico Chemiluminescent light and dark (1:1) (ThermoFisher Scientific) according to the manufacturer's instructions. Images were collected using the Bio-Spectrum Imaging System and quantified using Image J (www.ImageJ.nih.gov). For quantitation, protein expression was normalised to an appropriate loading control (β-actin, GAPDH or HSC-70) except for phospho-proteins where signals were normalised to the appropriate total protein.

2.5 RNA expression analysis

2.5.1 RNA extraction and complimentary DNA (cDNA) synthesis

Total RNA was extracted and purified from collected cell lysates using the ReliaPrep™ RNA Cell Miniprep System according to the manufacturer's (Promega) instructions. RNA was eluted into deionised water and stored at –70 °C. RNA concentration was determined using a Thermo Nanodrop 1000 (ThermoFisher Scientific)

cDNA was synthesised using 500 µg of total RNA and 1 µl of oligo-dT (Promega) in a total volume of 14 µl RNase-free H_2O water. The samples were heated to 70°C for 5 minutes and then cooled to 4°C. cDNA synthesis was performed in a total volume of 25 µl using mouse moloney leukaemia virus (MMLV) reverse transcriptase (RT), 1.25 µl of dNTPs (each 10 mM), 5 µl 5x MMLV RT buffer and 1 µl of RNAsin ribonuclease inhibitor (all reagents from Promega). The reaction was incubated at 42°C for 60 minutes and then samples were heated to 95°C for 5 minutes to inactivate RT. cDNA was diluted to a final volume of 100 µl by addition of nuclease-free H_2O and stored at -20°C.

2.5.2 Quantitative polymerase chain reaction (Q-PCR)

Taqman Q-PCR (Applied Bioscience) was performed to quantify RNA expression. Reactions contained 5 µl of cDNA, 5 µl primer mix (1µl primer and 4µl H_20) and 10 µl of Q-PCR master mix (both Applied Biosystems). Amplification was performed using an Applied Biosystems 7500 Real Time PCR system and using the following probe sets; EBI2 (Hs00270639_s1), SREBF1 (hs01088679_g1), MYC (Hs00153408_m1), ABCA1 (Hs01059137_m1), SCD (Mm00772290_m1), SQLE (Hs01123768_m1), HMGR1 (Ce02448890_g1) and controls B2M(HS00187842_m1) and Nuclease free water (Promega) ΔCt values were generated and differential expression determined using the ΔΔCt method.

2.6 Data analysis and statistics

Data processing and statistical analyses were conducted using Graphpad Prism (v6.0). The statistical significance between different groups of values was analysed using Student's t-tests. The Pearson rank correlation coefficient was calculated to determine the strength of association between various parameters.

Pathway analysis for RNA-seq data (see Chapter 5) was performed using Ingenuity Pathway Analysis (IPA; Qiagen).

Chapter 3: Characterisation of mechanisms of cross-talk between BCR signalling pathways, SHIP1 and CXCR4

3.1 Introduction

Crosstalk-between the BCR and other cell surface receptors plays a central role in the co-ordination of immune responses and is also likely to modulate behaviour of malignant B cells (Becker et al., 2017; Calpe et al., 2011; Burger et al., 2002). One key target for receptor cross-talk is the GPCR CXCR4. In common with many other GPCRs, CXCR4 is rapidly internalised following binding of ligand (CXCL12) via CME (Marchese, 2014). However, CXCR4 endocytosis is also triggered following engagement of the BCR in both normal B cells and various types of malignant B cells. For example, in CLL, anti-IgM reduced CXCR4 cell surface expression in signal responsive samples (Vlad et al., 2009; Quiroga et al., 2009). CXCR4 down-modulation was due to endocytosis as it was reduced by culture in hypertonic media, which inhibits CME (Vlad et al., 2009). In normal B cells, BCR-induced CXCR4 endocytosis is thought to be important for correct positioning of antigen-engaged B cells and movement within lymph nodes during an effective immune response (Gatto et al., 2013).

Given the potential importance of BCR→CXCR4 crosstalk there is a clear need to understand the nature of the communicating pathways. Previous studies in DT40 cells (derived from a chicken bursal lymphoma and a common model for investigating B-cell signalling pathways), demonstrated that anti-IgM-induced CXCR4 endocytosis is mediated by a cascade involving SYK, BLNK, BTK and PLCγ2 which ultimately promotes PKC-dependent receptor internalisation (Guinamard et al., 1999). By contrast, in normal immature B cells, SHIP1 may drive CXCR4 down-modulation following BCR engagement, since deletion of *Inpp5d* (encoding SHIP1) significantly reduced the extent of antigen-induced CXCR4 down-modulation (Brauweiler et al., 2007). Therefore, previous work has implicated both kinases and phosphatases (SHIP1) as mediators of BCR→CXCR4 cross-talk.

Unpublished experiments performed in the host laboratory have begun to unravel the nature of the signalling pathways that mediate anti-IgM-induced CXCR4 down-modulation

in CLL cells (summarised in Figure 3.1). CXCR4 expression is relatively low on CLL cells following isolation from the blood and receptor expression naturally "recovers" as cells are cultured *in vitro* (Coelho et al., 2014). This reason for this recovery is unclear, but may reflect action of CXCR4-endocytosing ligands (e.g. CXCL12) *in vivo*. However, the natural recovery of CXCR4 expression can be effectively suppressed by anti-IgM. Importantly, anti-IgM-induced CXCR4 down-modulation was inhibited by tamatinib (SYK inhibitor) or idelalisib (PI3Kδ inhibitor), but not by ibrutinib or acalabrutinib (BTK inhibitors), GO6983 (PKC inhibitor) or UO126 (MEK1/2 inhibitor). Thus, kinases operating in CLL cells appear to differ from those identified previously in DT40 cells which indicated a key role for BTK and PKC (Guinamard et al., 1999).

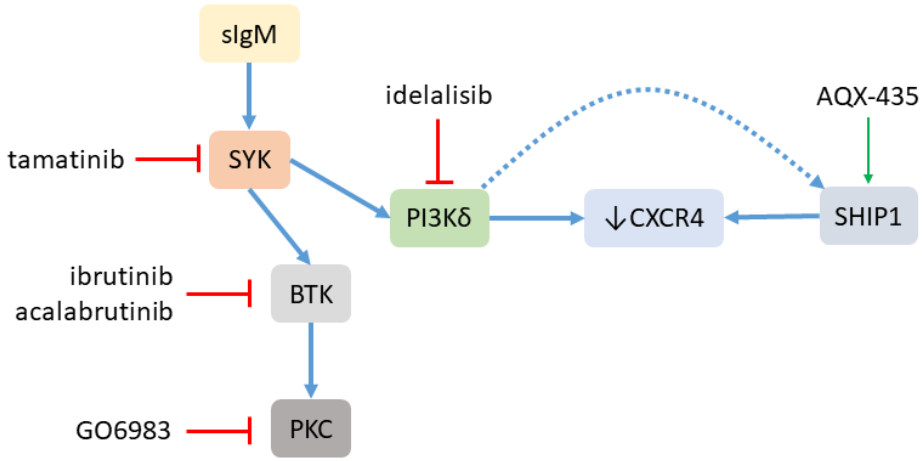

Figure 3.1. Summary of signalling pathways involved in down-modulation of CXCR4 cell surface expression in primary CLL cells.
Diagram is based on unpublished results from the host laboratory and is illustrative, not showing all intermediate signalling connections. Anti-IgM-induced CXCR4 down-modulation is inhibited by tamatinib or idelalisib, but not ibrutinib, acalabrutinib or GO6983. CXCR4 is also down-modulated by the SHIP1 agonist AQX-435. It is not clear whether these are distinct pathways each capable of independently down-regulating CXCR4 or whether (as shown by the dotted line) that SHIP1 acts downstream of PI3Kδ.

In addition to these results obtained using kinase inhibitors, the host laboratory has also demonstrated that the SHIP1 agonist, AQX-435, is sufficient to trigger CXCR4 endocytosis by ~50% (Packham et al., 2016). Interestingly, AQX-435 was a much more effective inducer of CXCR4 down-modulation in CLL cells, compared to normal B cells. How accumulation of $PI(3,4)P_2$ following SHIP1 activation might trigger CXCR4 endocytosis is not clear, but it is interesting to note that phosphoinostides are recognised as important regulators of CME (Marchese, 2014).

Taken together, these findings indicate roles for both kinases and phosphatases in CXCR4 down-modulation in CLL cells. At present, it is now known whether SYK/PI3Kδ and SHIP1 act in a single pathway. For example, the requirement for SYK/PI3Kδ may be to generate $PI(3,4,5)P_3$, which then acts as a substrate for SHIP1, and accumulation of $PI(3,4)P_2$ may then drive CXCR4 internalisation (Figure 3.1). Alternately, SYK/PI3Kδ and SHIP1 may represent distinct pathways which are both capable of independently down-modulating CXCR4 expression.

3.2 Hypothesis

The signalling intermediates that function in the pathway to allow crosstalk between CXCR4 and BCR are also operational in B cell maliganies other than CLL.

3.2.2 Aims and Objectives

The overall goal of the experiments in this chapter was to extend analysis of BCR→CXCR4 cross-talk to established B-lymphoma cell lines. This was to determine whether similar pathways operated in other types of malignant B cells, including the role of specific kinases and response to activation of SHIP1 using AQX-435. However, analysis of established B-lymphoma cell lines was also important since it would potentially enable the use of RNAi to directly investigate the role of specific signalling intermediates in CXCR4 regulation, to complement studies performed using small molecule inhibitors/activators in CLL cells where transfection is much more technically demanding.

There were four specific aims;

1. To characterise the effect of anti-IgM and AQX-435 on CXCR4 expression in a panel of B-lymphoma cell lines.
2. To investigate the effects of AQX-435 on sIgM endocytosis.
3. To analyse the effects of kinase inhibitors on anti-IgM→CXCR4 cross-talk in a B-lymphoma cell line.
4. To perform siRNA knockdown to directly investigate the role of specific kinases in anti-IgM-induced CXCR4 down-modulation.

3.3 Effects of anti-IgM or AQX-435 on CXCR4 expression on B-lymphoma cell lines

3.3.1 Selection of cell lines

I selected a panel of sIgM positive B-lymphoma cell lines to analyse effects of anti-IgM or AQX-435 on CXCR4 expression (Table 3.1). The cell lines represented examples of both the activated B cell-like (ABC) and germinal centre B cell-like (GCB) subtypes of diffuse large B-cell lymphoma (DLBCL), and Burkitt's lymphoma (BL). I also selected chicken DT40 lymphoma cells as these were used for initial characterisation of pathways of anti-IgM-induced CXCR4 down-regulation (Guinamard et al., 1999). Anti-IgM signal responsiveness of the lines was confirmed for WSU-FSCCL and RL cells in subsequent experiments in this chapter (see below Figures 3.9 and 3.14) and for TMD8, OCI-LY7 and HBL1, as part of other studies in the host laboratory (unpublished). Immunoblot analysis also confirmed that all cell lines expressed SHIP1 (Appendix A1).

Table 3.1. Details of selected B-cell lymphoma cell lines

Cell line	Species	Disease classification	References
HBL1	Human	ABC-DLBCL[a]	Abe et al., 1988
TMD8	Human	ABC-DLBCL	Shuji et al., 2006
OCI-LY7	Human	GCB-DLBCL[b]	Tweeddale et al., 1987
RL	Human	GCB-DLBCL	Beckwith et al., 1990
WSU-FSCCL	Human	tFL[c] (GCB-like)	Mohammad et al., 1993
Ramos	Human	BL[d]	Benjamin et al., 1983
DT40	Chicken	Bursal lymphoma	Baba et al., 1985

[a]Activated B cell-like diffuse large B-cell lymphoma; [b]Germinal centre B cell-like diffuse large B-cell lymphoma; [c]Transformed follicular lymphoma; [d]Burkitt's lymphoma.

Although relatively infrequent, *CXCR4* and *INPP5D* mutations have been described in B-cell malignancies (Schmidt et al., 2015). In particular, nonsense and frameshift *CXCR4* mutations in Waldenstrom's macroglobulinaemia reduce CXCR4 endocytosis (Poulain et al., 2016). It was important, therefore, to consider whether any of the selected lines might carry these mutations. I analysed the COSMIC database (https://cancer.sanger.ac.uk/cell_lines/cbrowse/all) which includes exome sequencing data for OCI-LY7, RL and Ramos cells, and results from the Klijn et al., study which included RNA sequencing data for WSU-FSCCL, TMD8, OCI-LY7 and Ramos (Klijn et al., 2015). However, there was no evidence for *CXCR4* or *INPP5D* mutations in any of the lines.

3.3.2 Characterisation of basal CXCR4 expression

Cell surface CXCR4 expression on the B-cell lines was quantified using flow cytometry. A representative experiment using RL cells and showing the gating and histogram plots is presented in Figure 3.2.

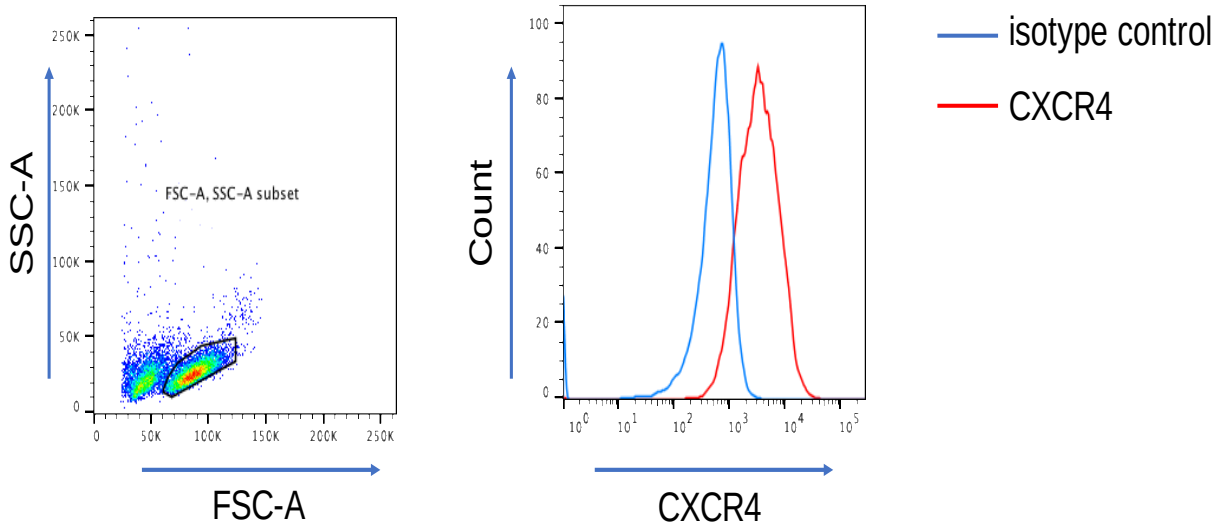

Figure 3.2. Representative flow cytometric analysis for quantitation of CXCR4
RL cells were incubated with APC-conjugated anti-CXCR4 or control antibody and expression of CXCR4 was analysed by flow cytometry. (Left) Gating on viable cells on FSC/SSC dot plot. (Right) Histogram plot showing results of staining with anti-CXCR4 or control antibody on gated, viable cells. For quantitation, CXCR4 mean fluorescence intensity (MFI) was calculated by subtracting MFI value obtained from control antibody-stained cells from the MFI value obtained from anti-CXCR4 stained cells.

I next characterised basal CXCR4 expression on the panel of human B-lymphoma cell lines. DT40 cells were not included in this analysis since distinct antibodies were required to detect human and chicken CXCR4 precluding any meaningful cross-comparison of MFI values between species. All of the tested lines expressed CXCR4, although there was marked variation in basal expression between individual lines (Figure 3.3). The number of lines analysed is too small to draw firm conclusions but there was no indication that this variation was related to the different origin of the cell lines.

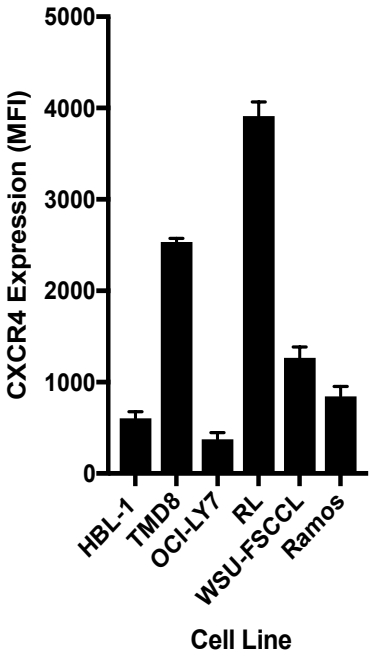

Figure 3.3. CXCR4 expression on B-lymphoma cell lines
Expression of basal CXCR4 (mean MFI ±SD) was quantified by flow cytometry. Data is derived from two independent experiments each performed in duplicate.

3.3.3 Effect of anti-IgM or AQX-435 on CXCR4 expression

The next experiment was to investigate the effect of anti-IgM or AQX-435 on CXCR4 expression. Before analysing the B-lymphoma lines, I performed a validation experiment in primary CLL cells to ensure that results were comparable to those obtained previously in the host laboratory. Compared to B-cell lines, primary CLL cells express relatively low levels of sIgM and, in line with these previous experiments, I used a bead-bound form of anti-IgM which induces stronger and longer-lasting signalling (Krysov et al., 2014) and more effective CXCR4 down-modulation (Packham et al., 2016) compared to soluble anti-IgM. The

experiments were performed with CLL samples selected on the basis of retained anti-IgM-induced Ca^{2+} mobilisation (ICa^{2+} >10%) since this correlates tightly with the extent of anti-IgM-induced CXCR4 down-modulation. AQX-435 was used at 30 µM, based on previous experiments performed in the laboratory and CXCR4 expression was analysed after 6 hours to minimise potentially confounding effects due to spontaneous apoptosis of CLL cells in culture. Cells were additionally stained with anti-CD19 and anti-CD5 antibodies to specifically quantify CXCR4 expression on the malignant cells. Consistent with previously results, both anti-IgM and AQX-435 caused a substantial reduction in CXCR4 expression (Figure 3.4).

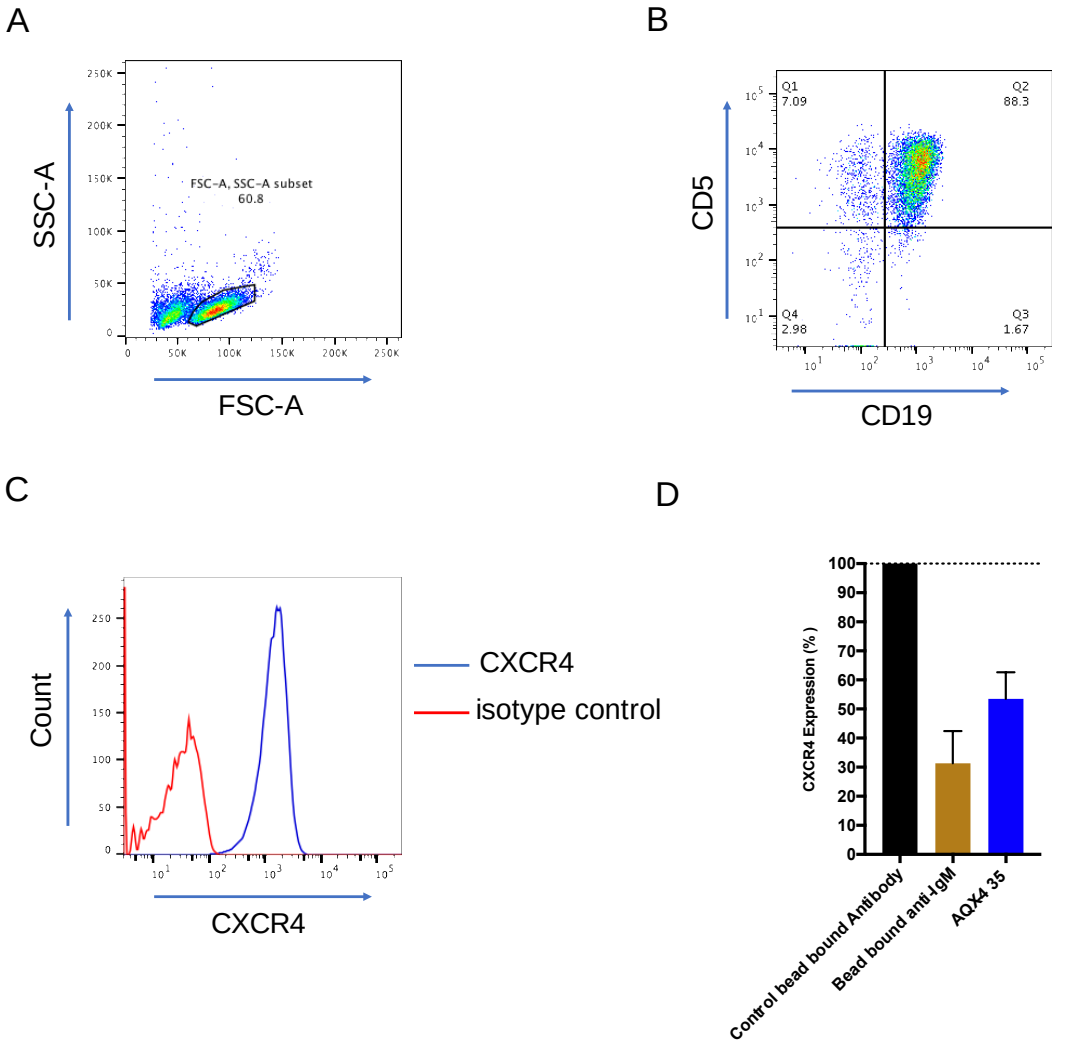

Figure 3.4. Effect of anti-IgM or AQX-435 on CXCR4 expression in primary CLL cells
CLL samples (n=3) were treated in duplicate with bead-bound anti-IgM, bead-bound control antibody or AQX-435 (30 µM). After 6 hours, cells were stained with pacific blue-conjugated-anti-CD19, PerCP-Cy5.5-conjugated anti-CD5, and APC-conjugated anti-CXCR4 or control antibody. Expression of CXCR4 was analysed by flow cytometry. Representative plots for (A) gating for viable cells on FSC/SSC dot plot, (B) gating on $CD5^+/CD19^+$ cells and (C) histogram showing control CLL cells stained with APC-conjugated control or anti-CXCR4 antibodies. (D) Quantitation of CXCR4 expression (mean ±SD) showing relative CXCR4 expression with values for control cells set to 100%.

I next analysed the effect of anti-IgM or AQX-435 on CXCR4 expression on the human B-lymphoma cell lines. The experiment was performed using soluble anti-IgM (which is sufficient to induce strong signal responses in cell lines) and CXCR4 expression was analysed at 24 hours (since spontaneous cell death was not an issue in these experiments).

Anti-IgM reduced CXCR4 expression (by >10%) in all of the cell lines (Figure 3.5). The strongest responses were observed in HBL1 and RL cells (~40% reduction), whereas responses were very modest but still statistically significant in OCI-LY7 cells. The reason for the modest effect of anti-IgM in OCI-LY7 cells is not clear but may reflect the previous finding that the basal expression of CXCR4 in this cell line was the lowest amongst the various cell lines analysed (Figure 3.3), perhaps precluding further down-modulation. In contrast to CLL cells, AQX-435 only significantly reduced CXCR4 expression in TMD8 cells (~20% decrease). In the other lines, CXCR4 was either not significantly differently expressed between AQX-435 and control cells (Ramos) or was actually significantly increased following AQX-435 treatment. This effect was very substantial in OCI-LY7 cells. Although I did not directly quantify cell death in these experiments (e.g. using Annexin V/PI staining), analysis of FSC/SSC plots did not reveal substantial levels of cell killing following treatment with anti-IgM or AQX-435 at this time point.

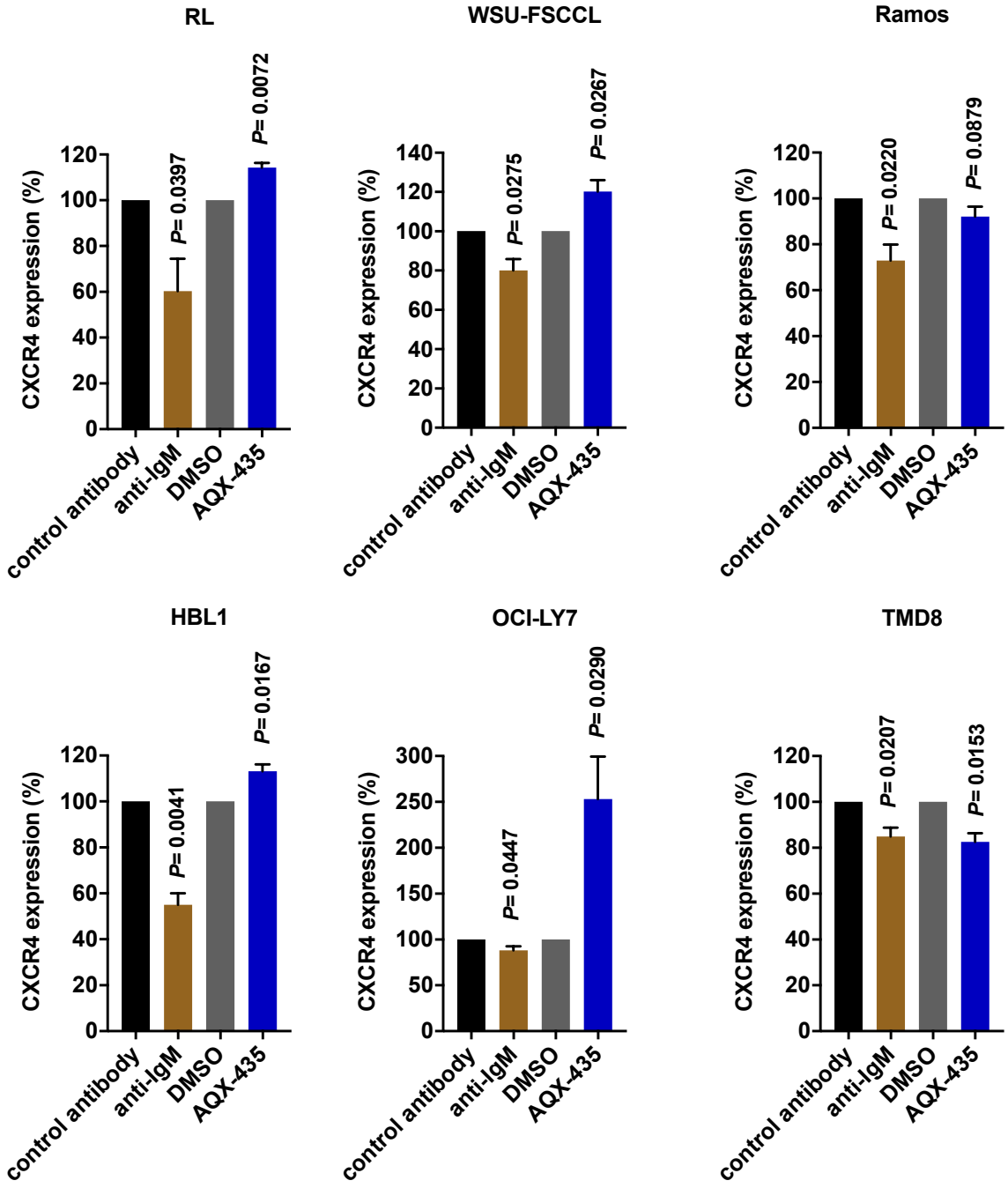

Figure 3.5. Effect of anti-IgM or AQX-435 on CXCR4 expression on human B-cell lines

Cell lines were treated with soluble control antibody or anti-IgM, or with AQX-435 (30 µM) or DMSO (solvent control) for 24 hours. Expression of CXCR4 was quantified by flow cytometry. Graph shows relative mean (±SD) CXCR4 expression for each cell line derived from three independent experiments each performed in duplicate and with values for control antibody or DMSO-treated cells set to 100%. The statistical significance of the differences between control antibody/anti-IgM and DMSO/AQX-435-treated cells are shown (paired Student's t-test).

Similar experiments were performed using DT40 cells. Here, cells were stimulated with the M4 anti-chicken IgM antibody and chicken CXCR4 was detected using an indirect labelling approach (incubation with mouse anti-chicken CXCR4 followed by FITC-conjugated goat anti-mouse IgG). Titration experiments were performed to identify the optimal concentration of primary antibody for detection of CXCR4 (data not shown). Due to the high cost of the antibody required, these experiments were only performed twice. Consistent with previous studies (Guinamard et al., 1999) anti-IgM substantially reduced CXCR4 expression on DT40 cells (Figure 3.6). Results with AQX-435 were more variable (no effect or an increase in CXCR4 expression in the two experiments), but, similar to the human lymphoma cell lines, there was no convincing evidence that AQX-435 down-regulated CXCR4 expression.

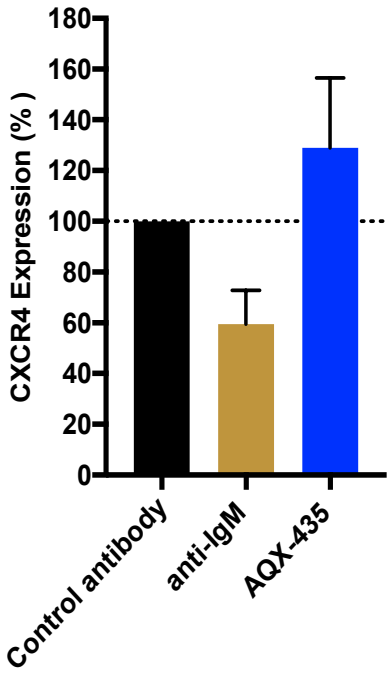

Figure 3.6. Effect of anti-IgM or AQX-435 on CXCR4 expression on chicken DT40 lymphoma cells.
DT40 cells were treated with control antibody or anti-IgM (M4), or with AQX-435 (30 µM) for 24 hours. Expression of CXCR4 was quantified by flow cytometry. Graph shows relative mean (±SD) CXCR4 expression derived from two independent experiments each performed in duplicate, and with values for control antibody treated cells set to 100%.

3.3.4 Effect of soluble and bead-bound anti-IgM on CXCR4 expression on RL cells

In CLL cells, bead-bound anti-IgM induces stronger CXCR4 down-regulation compared to soluble anti-IgM (L Smith et al., unpublished). Although soluble anti-IgM was capable of inducing CXCR4 downregulation in most B-cell lines, it was important to compare the effectiveness of soluble and bead-bound anti-IgM before moving onto more detailed experiments. Therefore, RL cells were treated with soluble or bead-bound anti-IgM/control antibody and CXCR4 expression was quantified by flow cytometry. CXCR4 expression was analysed at 6 hours, to avoid long-term exposure of cells to the beads. Consistent with previous experiments (Figure 3.4), soluble anti-IgM reduced CXCR4 expression by ~40% (Figure 3.7). Although bead-bound anti-IgM also significantly reduced CXCR4 expression, the extent of downregulation was much less (~10%). Parallel experiments in CLL samples selected on the basis of retained anti-IgM-induced Ca^{2+} mobilisation (iCa^{2+}>10%). confirmed that bead-bound anti-IgM was more effective than soluble anti-IgM at down-modulating CXCR4 expression in these cells (Figure 3.8).

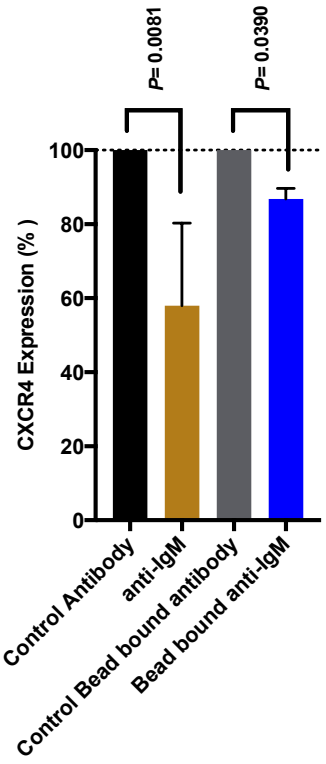

Figure 3.7. Effect of soluble or bead-bound anti-IgM on CXCR4 expression on RL cells
RL cells were treated for 6 hours with soluble or bead-bound anti-IgM or control antibody and expression of CXCR4 was quantified using flow cytometry. Graph shows mean (±SD) CXCR4 expression with values for control antibody-treated cells set to 100%. Data are derived from four independent experiments each performed in duplicate. The statistical significance of the indicated differences are shown (paired Student's t-test).

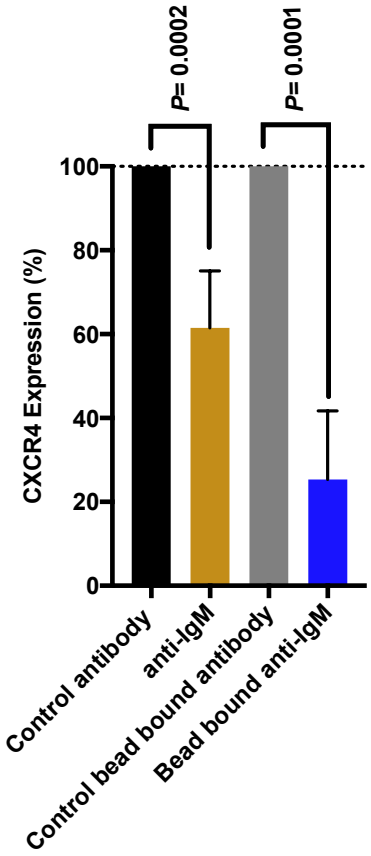

Figure 3.8. Effect of soluble or bead-bound anti-IgM on CXCR4 expression on CLL cells
CLL samples (n=3) cells were treated in duplicate with soluble or bead bound anti-IgM or control antibody. After 6 hours, expression of CXCR4 was quantified in viable $CD19^{+}CD5^{+}$ cells using flow cytometry. Graph shows mean (±SD) CXCR4 expression with data for control antibody-treated cells set to 100%. The statistical significance of the indicated differences are shown (paired Student's t-test).

Overall, these results demonstrate substantial variation in the response of lymphoma lines in terms of the effects of anti-IgM or AQX-435 on CXCR4 expression. Similar to CLL, anti-IgM reduced CXCR4 expression in the lymphoma lines. Interestingly, AQX-435 failed to down-modulate CXCR4 expression in most cell lines, and in fact often appeared to increase CXCR4 levels. Interestingly, soluble anti-IgM induced stronger CXCR4 down-modulation compared to bead-bound anti-IgM.

3.4 Effect of AQX-435 on sIgM endocytosis

Although effects of AQX-435 on BCR-induced signalling have been investigated in various models, it is not known whether AQX-435 might also influence BCR endocytosis. My next aim was, therefore, to analyse the effects of AQX-435 on sIgM endocytosis. I selected the WSU-FSCCL cell line for these studies since it was derived from a transformed follicular lymphoma (FL), and like the majority of FL cases, carries *N*-linked glycosylation sites within the variable regions of Ig introduced by SHM. These sites carry high-mannose sugars which allow binding to the lectin DC-SIGN (Coelho et al., 2011). Whereas anti-IgM induces downstream signalling and sIgM endocytosis, DC-SIGN engagement is distinct, since it triggers signalling without sIgM endocytosis (Linley et al., 2015). This is thought to be important in FL, since engagement of malignant cells by microenvironmental lectins *in vivo* would result in protracted growth-promoting signal responses. Therefore, WSU-FSCCL cells were selected as a model to investigate whether AQX-435 would (i) promote sIgM endocytosis alone, (ii) inhibit anti-IgM-induced sIgM endocytosis and/or (iii) promote DC-SIGN-induced sIgM endocytosis.

3.4.1 Effect of AQX-435 on anti-IgM-induced signalling in WSU-FSCCL cells

Prior to analysis of endocytosis, I investigated the effect of anti-IgM and AQX-435, alone and in combination, on anti-IgM-signalling in WSU-FSCCL cells. Cells were pre-treated with AQX-435 or DMSO for one hour and then incubated with control antibody or anti-IgM. Signalling was quantified using immunoblot analysis of AKT phosphorylation (Figure 3.9). The experiment demonstrated that AQX-435 substantially reduced anti-IgM AKT phosphorylation.

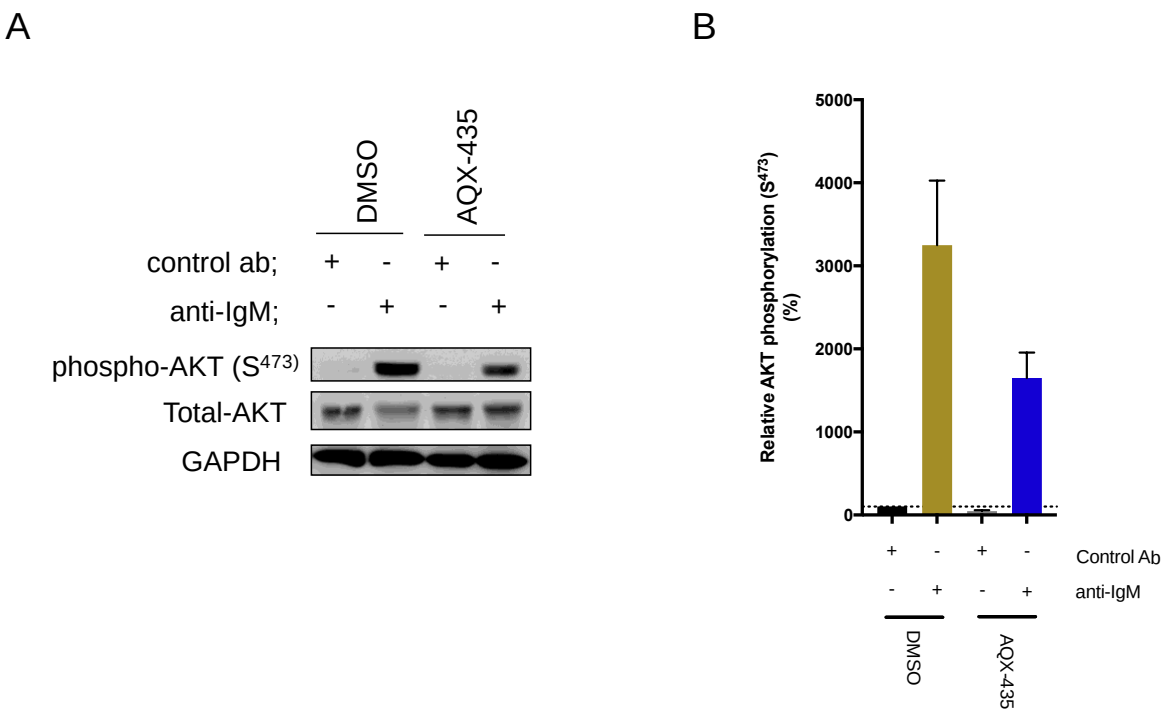

Figure 3.9. Effect of AQX-435 on anti-IgM-induced AKT phosphorylation in WSU-FSCCL cells
WSU-FSCCL cells were pre-treated with AQX-435 (30 µM) or DMSO as a control for 1 hour and then incubated with soluble anti-IgM or control antibody for 15 minutes. Expression of total and phospho-AKT (S^{473}) was analyzed by immunoblotting. (A) Representative results. (B) Graph shows mean (±SD) phospho-AKT (S^{473}) expression from two independent experiments with values for control antibody/DMSO treated cells set to 100 %.

3.4.2 Effect of AQX-435 on sIgM endocytosis

Having established that, consistent with activation of SHIP1, AQX-435 reduced anti-IgM-induced AKT phosphorylation, I investigated whether AQX-435 altered sIgM endocytosis. I first investigated if AQX-435 alone was sufficient to reduce sIgM expression. WSU-FSCCL cells were treated with a range of concentrations of AQX-435 (10, 20 or 30 µM) and expression of sIgM was quantified by flow cytometry. There was a modest increase in sIgM expression in cells treated with AQX-435 (maximum ~10%) and, overall, the experiment demonstrated that AQX-435 alone did not reduce sIgM expression, even after relatively protracted exposure (Figure 3.10).

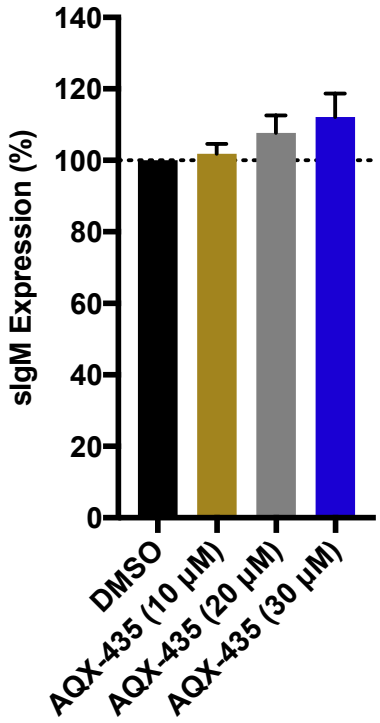

Figure 3.10. Effect of AQX-435 on sIgM expression
WSU-FSCCL cells were treated with indicated concentrations of AQX-435 or DMSO as a control for 6 hours. sIgM was detected by staining with FITC-anti-IgM antibody (BD Pharmingen) and quantified by flow cytometry. Graph shows mean (±SD) percentage sIgM expression derived from three independent experiments, each performed in duplicate with values for control cells set to 100%.

The next experiments investigated the effects of AQX-435 on anti-IgM-induced endocytosis. This required an alternate approach to quantify sIgM expression since binding of anti-IgM to trigger endocytosis would prevent (or block) subsequent engagement of any residual sIgM by a second, detecting antibody. I, therefore, used an anti-light chain antibody (anti-κLC) to quantify residual sIgM expression following incubation with AQX-435 and/or anti-IgM. WSU-FSCCL cells express very little sIgD (data not shown) so the signal detected with anti-kappa light chain (κLC) is largely a measure of sIgM expression.

Although the anti-IgM and anti-κLC antibodies were raised against distinct immunogens, it is still possible that binding of the anti-IgM antibody might sterically hinder subsequent binding of anti-κLC. It was necessary, therefore, to control for any such "blocking" in these experiments. To do this experiments were performed at both 37 ^{o}C and 4^{o}C, at which energy-dependent endocytosis is prevented (Métézeau et al., 1984). Thus, any reduction in anti-κLC binding by anti-IgM at 4^{o}C is due to steric hindrance. To correct for any blocking, the

reduction in anti-κLC binding by anti-IgM (±AQX-435) at 4°C was subtracted from the relevant values obtained at 37°C. For AQX-435-only treated cells (where anti-IgM-induced blocking is not an issue), the reduction in anti-κLC binding in AQX-435-treated cells at 37°C was calculated as a percentage of anti-κLC binding in untreated cells at 37°C.

As expected, anti-IgM triggered strong sIgM endocytosis with an ~70% reduction in corrected anti-κLC staining after 10 minutes at 37°C (Figure 3.11). AQX-435 alone did not down-modulate sIgM expression, or alter the extent of anti-IgM-induced sIgM endocytosis.

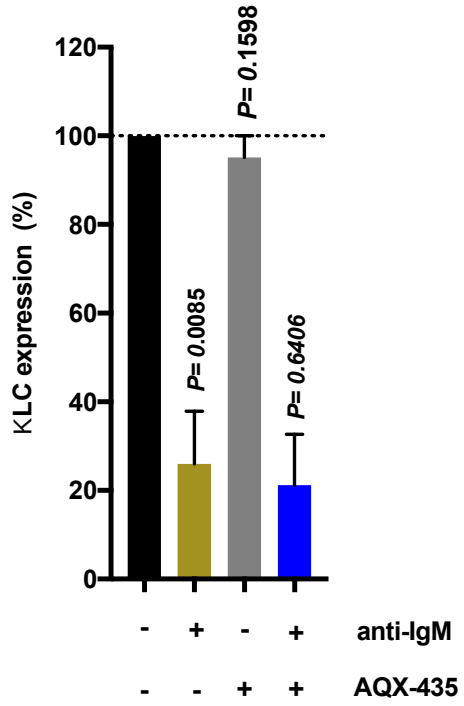

Figure 3.11. Effect of AQX-435 on sIgM endocytosis
WSU-FSCCL cells were pre-treated with AQX-435 (30 μM) or left untreated as a control for 1 hour and then incubated with soluble anti-IgM or with no added antibody for 30 minutes at 4 °C, or for 20 minutes at 4 °C followed by 10 minutes at 37 °C. Cells were washed with ice-cold media and remaining sIgM was detected by staining with PE-conjugated anti-κLC antibody and flow cytometry. Graph shows mean (±SD) percentage κLC expression derived from three independent experiments, each performed in duplicate, and with values for control cells set to 100%. The statistical significance of differences between anti-IgM (±AQX-435)-treated and control cells are indicated (paired Student's t-test).

Finally, I investigated whether AQX-435 promoted sIgM endocytosis in WSU-FSCCL following binding of DC-SIGN to the mannosylated BCR. sIgM was quantified using an anti-κLC antibody as described above. As expected, DC-SIGN alone did not trigger sIgM endocytosis.

Moreover, AQX-435 did not promote sIgM endocytosis in the presence of DC-SIGN (Figure 3.12)

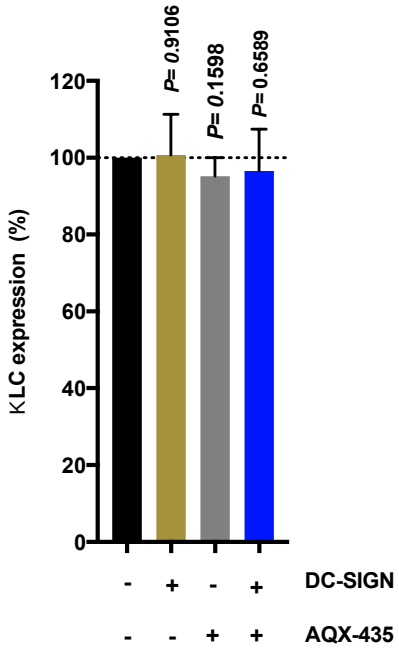

Figure 3.12. Effect of AQX-435 and DC-SIGN on sIgM endocytosis
WSU-FSCCL cells were pre-treated with AQX-435 (30 μM) or left untreated as a control for 1 hour and then incubated with DC-SIGN or with no added reagent for 30 minutes at 4 °C, or for 20 minutes at 4 °C followed by 10 minutes at 37 °C. Cells were washed with ice-cold media and remaining sIgM was detected by staining with PE-conjugated anti-κLC antibody and flow cytometry. Graph shows mean (±SD) percentage κLC expression derived from three independent experiments, each performed in duplicate, and with values for control cells set to 100%. The statistical significance of differences between DC-SIGN (±AQX-435)-treated and control cells are indicated (Student's t-test).

Taken together, these results obtained using the WSU-FSCCL cell line, confirm that activation of SHIP1 using AQX-435 reduces anti-IgM-induced PI3K activity, but has no effect on sIgM endocytosis, alone, or in the presence of sIgM ligands (anti-IgM, DC-SIGN).

3.5 Analysis of the effects of kinase inhibitors on BCR→CXCR4 cross-talk in a B-lymphoma cell line

Previous studies in the host laboratory used kinase inhibitors to characterise the signalling pathways that leads to CXCR4 down-modulation following anti-IgM treatment of CLL cells. The results indicate that anti-IgM-induced CXCR4 down-modulation is dependent on SYK

and PI3K, but not BTK or PKC. However, results with kinase inhibitors need to be treated with caution since activities of these agents might be mediated by off-target effects. RNAi-mediated depletion of kinases would provide a more definitive approach to determine the role of intermediate signalling molecules, including specific kinases and SHIP1, but is extremely challenging in primary CLL cells where transfection efficiencies are very low. Although not trivial, RNAi has been used in established B-cell lines.

Therefore, the aim of these experiments was to use kinase inhibitors to determine whether similar or distinct pathways operated in CLL cells and B-cell lines, as an essential preliminary to the application of RNAi. Analysis focused on current clinically used drugs (idelalisib, ibrutinib, acalabrutinib) or against relevant targets (tamatinib, a SYK inhibitor). RL cells were selected for these studies since (i) they expressed relatively high levels of CXCR4 (Figure 3.4) and (ii) CXCR4 was downregulated by anti-IgM to approximately the same extent as in CLL cells (Figure 3.5). Moreover, RL cells have been used previously for transfection studies (Chen et al., 2013). Experiments were performed using soluble anti-IgM (which down-modulated CXCR4 to a greater extent than bead-bound anti-IgM in this cell line – Figure 3.7) and at 6 hours, to minimise potential effects of drug-induced apoptosis.

3.5.1. Effect of SYK or PI3Kδ inhibition on anti-IgM-induced CXCR4 down-modulation in RL cells

I first investigated the effect of SYK or PI3Kδ inhibition on anti-IgM-induced CXCR4 down-modulation. The compounds selected, tamatinib and idelalisib, were tested over a range of concentrations (0.5 μM – 10 μM) that had already been investigated in CLL cells. In this series of experiments, CXCR4 expression was down-modulated by ~50% following treatment with anti-IgM in the absence of any drug (Figure 3.13). The extent of down-modulation was significantly reduced by tamatinib and idelalisib at 10, 3 or 1 μM. Thus, similar to CLL cells, anti-IgM-induced CXCR4 down-modulation is mediated via SYK and PI3Kδ.

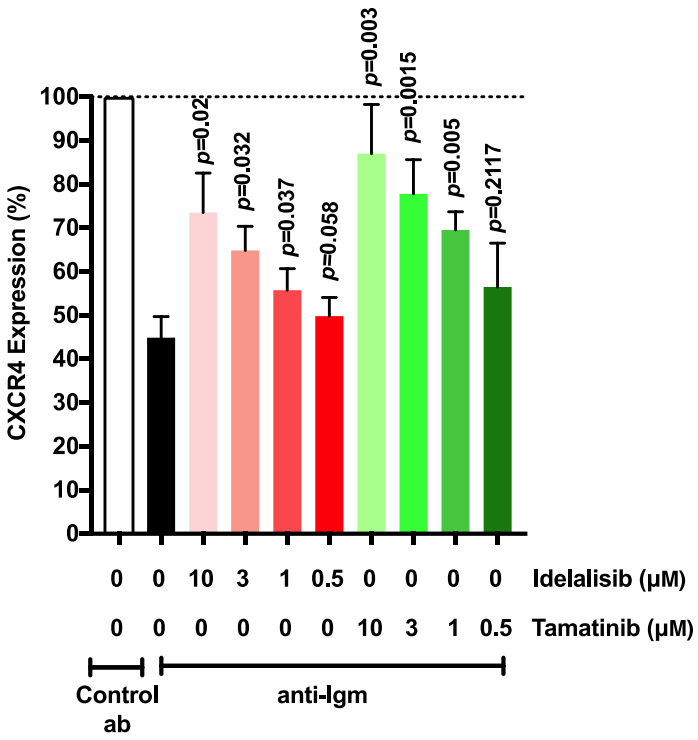

Figure 3.13. Effect of tamatinib or idelalisib on anti-IgM-induced CXCR4 down-modulation in RL cells. RL cells were pre-treated with the indicated concentrations of tamatinib or idelalisib, or DMSO as a control for 1 hour prior to stimulation with soluble anti-IgM. Control cells were treated with soluble control antibody. After 6 hours, CXCR4 expression was quantified by flow cytometry. Graph shows mean (±SD) CXCR4 expression with values for control antibody-treated cells set to 100%. Data are derived from four independent experiments each performed in duplicate. The statistical significance of the differences between drug-treated and relevant DMSO-treated control are shown (paired Student's t-test).

I performed parallel immunoblot analysis to confirm the inhibitory effects of tamatinib and idelalisib on anti-IgM-induced signalling. AKT phosphorylation was used as a readout for signalling since it is downstream of both SYK and PI3K. Anti-IgM-induced AKT phosphorylation was inhibited by both tamatinib and idelalisib (Figure 3.14). Responses to drugs seemed to be concentration dependent and matched quite closely the concentration-dependent effects of tamatinib and idelalisib on CXCR4 down-modulation (Appendix A2). Similar results were observed for analysis of ERK1/2 phosphorylation (data not shown).

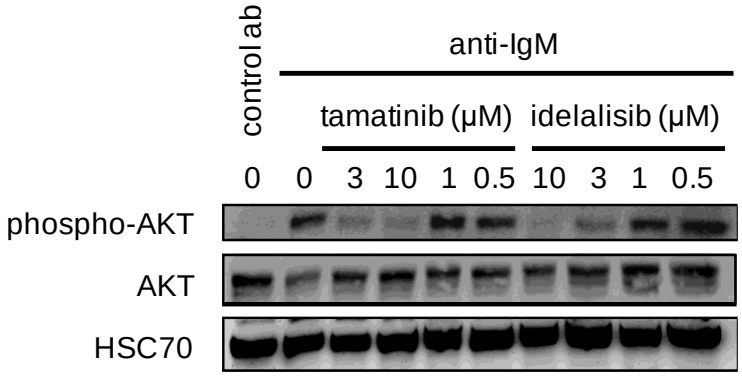

Figure 3.14 Effect of tamatinib and idelalisib on anti-IgM AKT phophoryation in RL cells.
RL cells were pre-treated with the indicated concentrations of tamatinib or idelalisib, or DMSO as a control for 1 hour prior to stimulation with soluble anti-IgM. Control cells were treated with a soluble control antibody. After 6 hours, cells were collected and analysed by immunoblotting. Representative immunoblot of 3 experiments demonstrating total and phosphorylated AKT (S^{473}), and HSC70.

3.5.2. Effect of BTK inhibition on anti-IgM-induced CXCR4 down-modulation in RL cells

In contrast to SYK and PI3Kδ, BTK does not appear to play a substantial role in anti-IgM-induced CXCR4 down-modulation in CLL cells. Thus, ibrutinib only inhibits anti-IgM response at 10 μM (likely due to off-target effects), and the more selective BTK inhibitor acalabrutinib had no effect at any concentration tested (maximum 10 μM). I, therefore, investigated the effects of various concentrations of ibrutinib and acalabrutinib on anti-IgM-induced CXCR4 down-modulation in RL cells (Figure 3.15). Both drugs significantly reduced anti-IgM-induced CXCR4 down-modulation at some of the tested concentrations, but, overall effects were very modest (generally only inducing ~10% reversal of down-modulation). The ability of the drugs to effectively block BTK activity in B-cell lines was confirmed by analysis of BTK autophosphorylation which was completely blocked at concentrations of ibrutinib or acalabrutinib >100 nM (pers. comm. R Arthur). Therefore, similar to CLL, BTK does not appear to play a substantial role in CXCR4 down-modulation in RL cells.

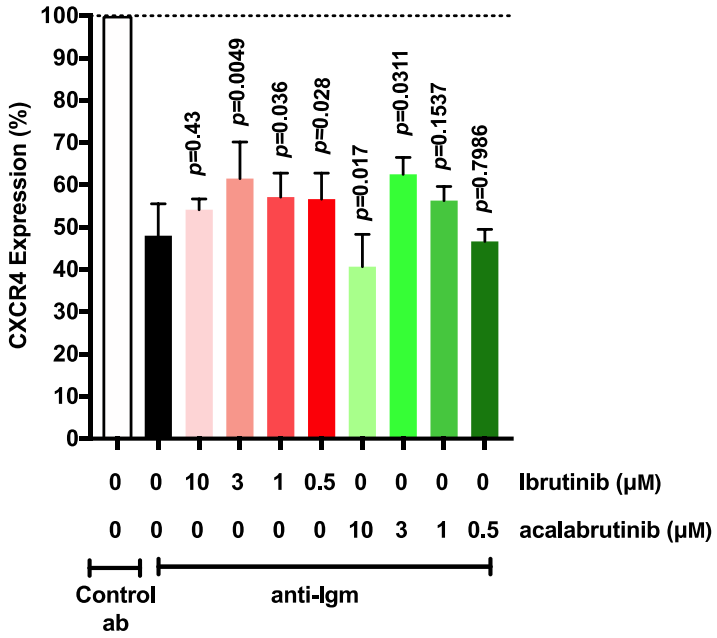

Figure 3.15. Effect of ibrutinib or acalabrutinib on anti-IgM-induced CXCR4 down-modulation in RL cells

RL cells were pre-treated with the indicated concentrations of ibrutinib or acalabrutinib, or DMSO as a control for 1 hour prior to stimulation with soluble anti-IgM. Control cells were treated with a soluble control antibody. After 6 hours, CXCR4 expression was quantified by flow cytometry. Graph shows mean (±SD) CXCR4 expression with values for control antibody-treated cells set to 100%. Data are derived from three independent experiments each performed in duplicate. The statistical significance of the differences between drug-treated and DMSO-treated control are shown (paired Student's t-test).

Overall, these results demonstrate importantly similarities in the kinases involved in the pathways that mediate anti-IgM-induced CXCR4 down-modulation between RL and primary CLL cells, and validate RL cells as a suitable model for the subsequent RNAi experiments.

3.6 Investigating the role of protein kinase D (PKD) in anti-IgM-induced CXCR4 down-modulation in CLL cells

Whilst these experiments were underway, Saint-Georges et al., published a paper demonstrating that cross-talk between sIgM and CXCR4 involved protein kinase D (PKD) since the PKD inhibitor CID755673 effectively interfered with anti-IgM-induced CXCR4

down-modulation in CLL cells (Saint-Georges et al., 2016). This was surprising since PKD generally acts downstream of PKC and BCR→CXCR4 crosstalk does not appear to require PKC activity (Saint-Georges et al., 2016; our unpublished data with PKC inhibitor GO6983). I, therefore, performed experiments to further investigate the role of PKD. These experiments were performed using primary CLL cells, to match previous studies in the laboratory and the work of Saint-Georges et al., (Saint-Georges et al., 2016).

Experiments reported by Saint-Georges et al., were performed using the PKD inhibitor CID755673 (Sharlow et al., 2008), the specificity of which has been questioned in other studies (Rozengurt et al., 2010). I, therefore, selected two other CRT0066051 (CRT5) and inhibitors CCRT066106 (CRT6) that have been shown to be relatively selective PKD inhibitors when tested *in vitro* for inhibitory activity against a large panel of recombinant enzymes (pers. comm., Dr S Matthews. Dundee). The experiments were performed with CLL samples selected on the basis of retained anti-IgM-induced Ca^{2+} mobilisation (iCA^{2+} >10%). CLL samples were pre-treated with either CRT6, CRT5 or solvent controls for 1 hour and then incubated with bead immobilised anti-IgM for 6 hours. Flow cytometry was used to quantify CXCR4 expression on $CD19^{+}CD5^{+}$ cells. basal CXCR4 expression was also analysed at start of the experiment. Given CLL is a heterogeneous disease and basal expression of CXCR4 as well as extent of anti-IgM down-modulation varies between each sample, the effect of CRT5 and CRT6 was normalised such that (DMSO/H_2O-only treated) at 24 hours were set to 100% and then effect of anti-IgM down-modulation was set to 0%. In addition, to confirm the inhibitors were functional, I analysed auto-phosphorylation of PKD at S^{916} by western blotting.

Western blotting demonstrated that anti-IgM activated PKD in primary CLL cells and that this response was effectively inhibited by either of the compounds (Figure 3.16B). However, the down-modulation of CXCR4 by anti-IgM was essentially unaffected (Figure 3.16A). Thus, in contrast to the conclusions of Saint-Georges et al., BCR→CXCR4 crosstalk does not appear to involve PKD in CLL. Since PKD did not appear to play an important role in cross-talk in CLL cells, I did not further evaluate its function in B-cell lines.

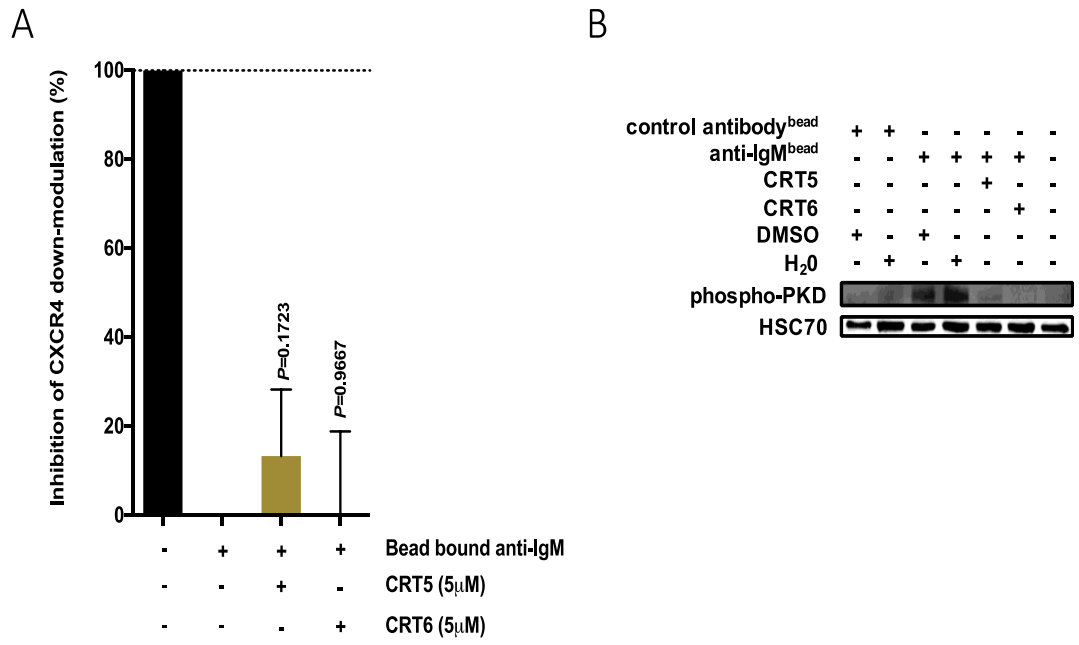

Figure 3.16. Effect of PKD inhibition on anti-IgM induced CXCR4 down-modulation in CLL cells
CLL samples (n=3) were pre-treated in duplicate for one hour with either DMSO, H20, CRT6 or CRT5. Cells were then treated with bead bound anti-IgM or control antibody. After 6 hours CLL cells were stained with pacific blue conjugated-anti-CD19, PerCP-Cy5-conjugated anti-CD5 and APC-conjugated anti-CXCR4 or isotype control antibody. CXCR4 expression was quantified on CD19+CD5+ cells by flow. (A) Graph shows mean (±SD) CXCR4 expression with values for control antibody-treated cells and anti-IgM treated cells (set to 100% and 0%, respectively). The statistical significance of the indicated differences are shown (paired Student's t-test). (B) Expression of phospho-PKD (S916) and HSC70 was analyzed by immunoblotting after 6 hours. Figure shows representative results. Note, I was unable to monitor expression of total PKD due to absence of suitable antibodies.

3.7. siRNA knockdown to directly investigate the role of kinase in anti-IgM-induced CXCR4 down regulation

The final aim of the experiments described in this chapter was to develop siRNA transfections to test directly the role of individual kinases signalling intermediate in anti-IgM-induced CXCR4 downregulation in RL cells. The initial targets selected were SYK and BTK. Based on inhibitor studies I would expect siRNA-mediated knock down of these targets to interfere or have no effect on anti-IgM-induced CXCR4 down-modulation, respectively. Although it would have been interesting to extend the analysis to PI3K or AKT, these are comprised of families of kinase isoforms encoded by different genes (PI3Kα, β, γ and δ, and AKT1-3) and may, therefore, have required multiple siRNAs to ablate activity. Some later experiments were also performed using SHIP1-targeted siRNA as I also hoped to use this approach to directly evaluate the role of SHIP1 responses to AQX-435.

Pilot experiments (not shown) were performed to investigate the effect of different amounts of siRNA on target expression at 24 hours post-transfection. The siRNAs were either pools targeted against SYK or BTK with a ON-TARGETplus modifications (Dharmacon SMART-pools) which have been designed and validated to reduce off target when compared to unmodified siRNA (Jackson et al., 2006). Non-targeted pools were used as controls. In duplicate experiments, maximal knockdown for both BTK and SYK (~50%) was observed in cells transfected with 100 or 200 pmol of siRNAs. Higher amounts of siRNAs (300 pmol) actually reduced effectiveness of target knock-down; this may reflect saturation and non-specific inhibition of RNAi mechanisms. Based on these results, I used both siRNAs at 200 pmol in follow-on experiments.

3.7.1 Effect of siRNA-mediated BTK or SYK knockdown on anti-IgM-induced CXCR4 down-modulation

I first investigated the effects of BTK knock-down on anti-IgM-induced CXCR4 down-modulation. RL cells were electroporated with BTK-targeted or control siRNAs for 24 hours.

Cells were then treated with anti-IgM for 6 hours and CXCR4 expression was quantified by flow cytometry. Control siRNA-transfected cells were treated in parallel with control antibody. I also analysed expression of cells that were transfected with control or BTK siRNAs and then pre-treated with either ibrutinib or acalabrutinib for 1 hour prior to anti-IgM stimulation for 6 hours.

Similar to previous studies in transfected RL cells, anti-IgM reduced CXCR4 expression in control siRNA transfected cells, illustrating that the transfection procedure *per se* does not substantially alter BCR→CXCR4 cross-talk (Figure 3.17). Knockdown of BTK did not significantly alter anti-IgM-induced down-modulation. CXCR4 down-modulation was also not effected by ibrutinib or acalabrutinib, in either control or BTK siRNA transfected cells. Immunoblot analysis further confirmed knockdown of BTK in these experiments (by ~40%). Overall, results with BTK siRNA transfections are consistent with the idea that sIgM→CXCR4 cross-talk is independent of BTK.

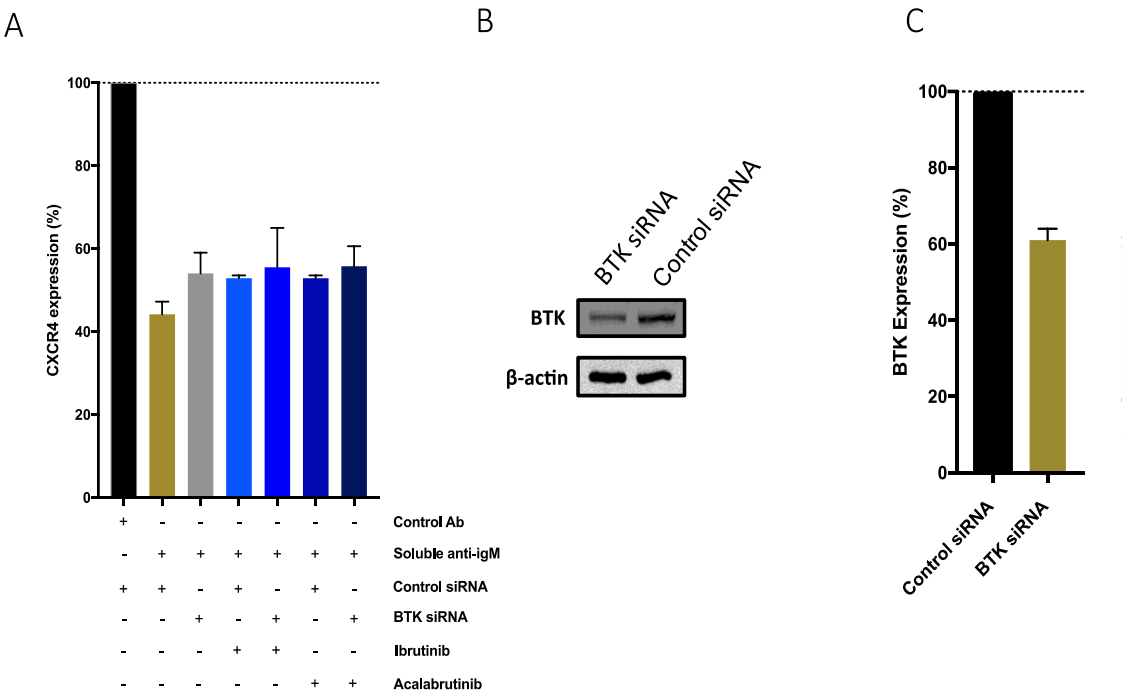

Figure 3.17 Effect of BTK siRNA on anti-IgM induced CXCR4 down-modulation
RL cells were transfected with 200 pmol of BTK-targeted siRNAs or control siRNAs using a Nucleofector. After 24 hours, cells were pre-treated for 1 hour with either 10 µM of ibrutinib or acalabrutinib, or DMSO as a control and cells were then treated with soluble anti-IgM for 6 hours. (A) Expression of CXCR4 quantified by flow cytometry. Graph shows mean (±SD) CXCR4 expression with values for control antibody/control siRNA cells set to 100%. Data are derived from three independent experiments each performed in duplicate. (B,C) Expression of BTK and β-actin was analysed by immunoblotting. Graph shows mean (±SD) BTK expression with values for control siRNA transfected cells set to 100%. Data are derived from three independent experiments each performed in duplicates.

Similar experiments were performed to investigate the effect of SYK knockdown on CXCR4 regulation (Figure 3.18). Again, anti-IgM induced effective CXCR4 down-regulation in control transfected cells. SYK knock-down was effective (~80% reduction), but this only very modestly reduced anti-IgM-induced CXCR4 down-modulation. This was unexpected considering that the SYK inhibitor tamatinib reduced anti-IgM-induced CXCR4 down-modulation much more substantially than ibrutinib/acalabrutinib in these cells (Figure 3.13).

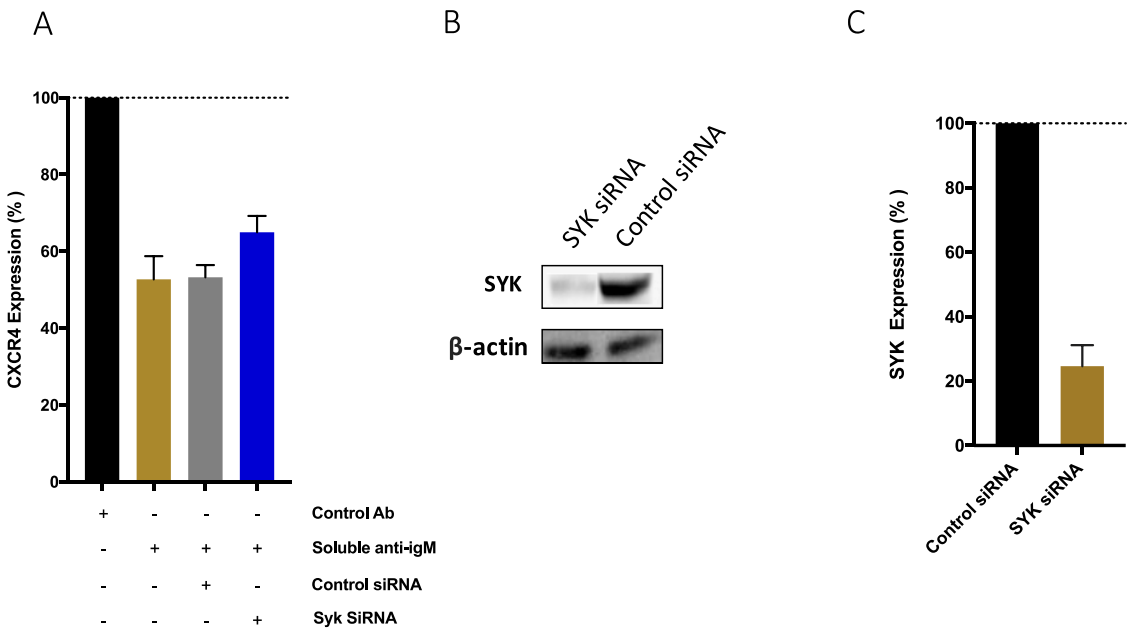

Figure 3.18. Effect of SYK siRNA on anti-IgM-induced CXCR4 down-modulation
RL cells were transfected with 200 pmol of SYK-targeted siRNAs or control siRNAs using a Nucleofector. After 24 hours, cells were treated with soluble anti-IgM or control antibody for an additional 6 hours. (A) Expression of CXCR4 quantified by flow cytometry. Graph shows mean (±SD) CXCR4 expression with values for control antibody/control siRNA cells set to 100%. Data are derived from three independent experiments each performed in duplicate. (B,C) Expression of SYK and β-actin was analysed by immunoblotting. Graph shows mean (±SD) SYK expression with values for control siRNA transfected cells set to 100%. Data are derived from two independent experiments each performed in duplicate.

3.7.2 Using GFP as a marker to identify transfected cells in siRNA knock-down experiments

The failure of SYK siRNA knockdown to decrease anti-IgM-induced CXCR4 down-modulation, despite sensitivity of this pathway to tamatinib, suggested that even a ~80% reduction of expression was not sufficient to effectively counter SYK function in these experiments. Therefore, it was important to try to improve the effectiveness of target knock-down.

I considered various approaches to improve the efficacy of siRNA-mediated knockdown. One option would be to extend the time between transfection and analysis to extend the duration for knock-down. This might be effective for relatively long-lived proteins. However, I decided not to explore this because of the risk of increased cell death at protracted time points following transfection. Another option would be to further optimise the concentration of siRNA used. However, my pilot studies indicated that the effectiveness of knock-down was similar (50%) over several amounts (100 and 200 pmol) and larger amounts of siRNA (300 pmol) actually led to reduced knock-down.

As an alternate approach to increase knock-down efficiency, I opted for a strategy utilising co-expression of siRNAs and a GFP expression plasmid, as previously used for RL cells (Chen et al., 2013). In this approach, the goal is to select or gate on cells with the highest GFP fluorescence as these cells are also likely to have been most effectively transfected with siRNAs, hopefully leading to enhanced knock-down in this cell fraction.

To select an optimal amount of GFP expression plasmid for these experiments, I first electroporated RL cells with 200 pmol of control or SHIP1-specific siRNA and various amounts of the GFP expression plasmid, pmaxGFP. SHIP1-targeted siRNAs were used in these experiments as BTK and SYK siRNAs were not available at this time and I also hoped to use siRNA to assess the role of this phosphatase in response to AQX-435 and anti-IgM. Flow cytometry was performed to quantify GFP expression under the different transfection conditions. There was a clear increase in GFP expression with increasing amounts of pmaxGFP in cells transfected with either control or SHIP1 siRNA (Figure 3.19).

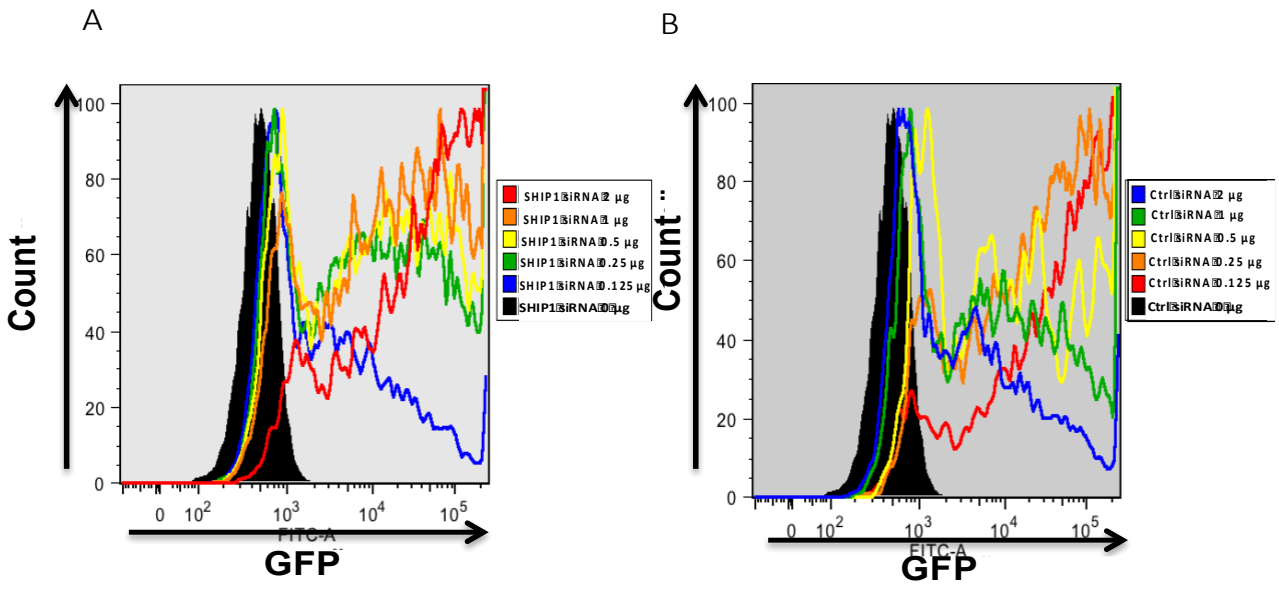

Figure 3.19. Expression of GFP in cells transfected with siRNAs and different amounts of pmaxGFP
RL Cells were electroporated with 200 pmol of SHIP1-targeted siRNA or control siRNAs and with the indicated amounts of pmaxGFP using a Nucleofector. After 24 hours, GFP expression was analysed by flow cytomtery. Graphs show histogram plots of a GFP fluorescence in cells transfected with (A) SHIP1-targeted or (B) control siRNAs. The experiment was performed once.

Based on these results, I decided to proceed using 200 pmol siRNA and 1 µg pmaxGFP. RL cells were co-transfected with pmaxGFP and control or SHIP1-targeted siRNA and a subpopulation of cells with the highest expression of GFP (GFP^{hi}) were collected by flow sorting (Figure 3.20).

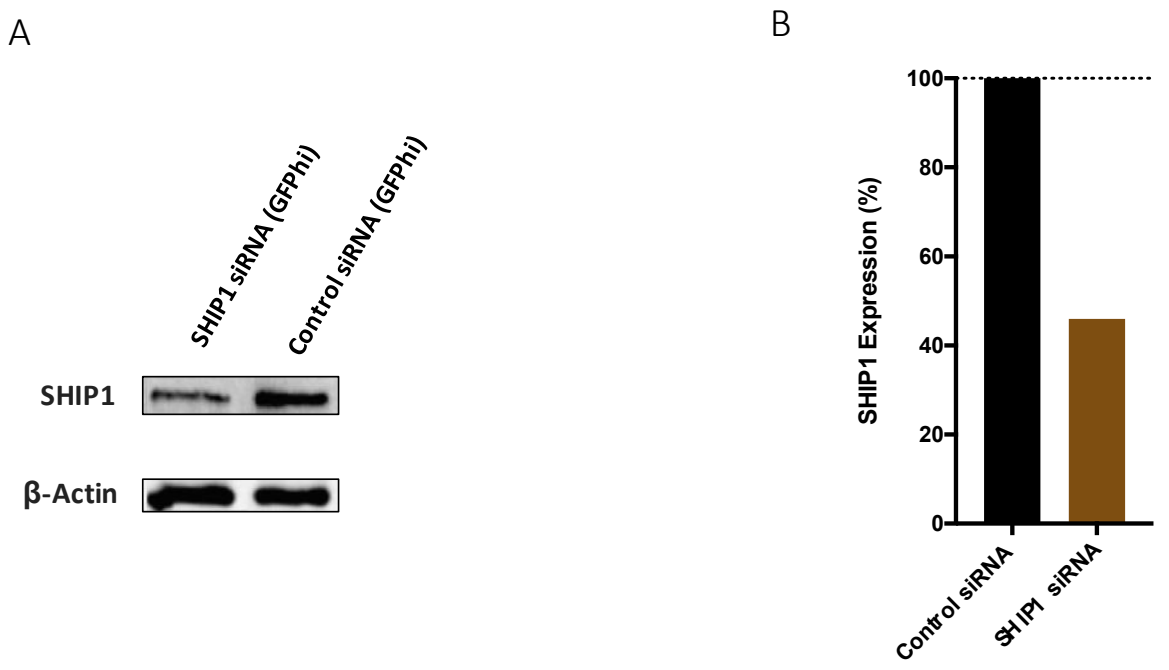

Figure 3.20 SHIP1 knockdown in sorted GFP^{hi} cells

RL cells were electroporated with 200 pmol of SHIP1-targeted or control siRNAs and 1 µg of pmaxGFP using a Nucleofector. After 24 hours, GFP expression was analysed by flow cytometry and populations of SHIP1-targeted siRNA and control siRNA transfected cells expressing GFP^{Hi} were collected by FACS sorting. (A) Expression of SHIP1 and β-actin were analysed and quanitifed by immunoblotting. (B) Graph shows mean (±SD) SHIP1 expression with values for control siRNA transfected cells set to 100%. Data are derived from two independent experiments each performed in duplicate.

SHIP1 and β-actin expression were quantified in the GFP^{hi} subpopulations using immunoblotting (Figure 3.20). However, quantification of the results demonstrated that even selection of high-GFP expressing cells did not improve target knock-down beyond ~56% in this experiment. Given these technical challenges, further siRNA analyses were not performed.

3.8 Summary of key findings

The overall goal of the experiments in this chapter was to extend analysis of BCR→CXCR4 cross-talk to established B-lymphoma cell lines. This was to determine whether similar pathways operated in other types of malignant B cells and to establish model systems for use of RNAi to directly investigate the role of specific signalling intermediates in CXCR4 regulation.

The key findings from the experiments described in this chapter were;

1. In a panel of established B-cell lines, anti-IgM was generally an effective down-modulator of CXCR4 expression, whereas the SHIP1 activator, AQX-435, did not down-modulate expression of cell surface CXCR4.
2. In RL cells, soluble anti-IgM was a more effective down-modulator of CXCR4 than bead-bound anti-IgM.
3. AQX-435 did not affect sIgM endocytosis in WSU-FSCCL cells.
4. Anti-IgM-induced CXCR4 down-modulation in RL cells is dependent on SYK and PI3Kδ activity, but relatively unaffected by the BTK inhibitors ibrutinib or acalabrutinib.
5. Anti-IgM-induced CXCR4 down-modulation in primary CLL cells was unaffected by inhibition of PKD.
6. Consistent with results using BTK inhibitors, anti-IgM-induced CXCR4 down-modulation was unaffected by BTK siRNA. However, CXCR4 down-modulation was also relatively unaffected by SYK siRNA suggesting that the degree of knock-down achieved in these experiments was not sufficient to effectively interfere with signalling events

Overall, these results shed new light of mechanisms of cross-talk to CXCR4. In particular, B-cell lines were generally sensitive to anti-IgM-induced CXCR4 down-modulation, whereas, in contrast to CLL cells, AQX-435 did not reduce CXCR4 expression. The effects of inhibitors of SYK, PI3Kδ and BTK on anti-IgM-induced down-modulation were similar in CLL cells and the RL cell line, indicating that similar mechanisms of BCR→CXCR4 cross-talk operate in these different cell types. However, development of siRNA transfection methods proved technical challenging and it was unfortunately not possible to achieve sufficient target knock-down to

use this approach to reliably characterise the role of individual signalling intermediates in BCR→CXCR4 cross-talk.

3.9 Discussion

3.9.1 Regulation of CXCR4 by anti-IgM or AQX-435 in B-cell lines

Previous studies in CLL cells have shown that CXCR4 expression recovers following culture *in vitro*, and that this can be reduced or reversed by engagement of sIgM (Saint-Georges et al., 2016; Coelho et al., 2014 ; Quiroga et al., 2009; Vlad et al., 2009; L Smith unpublished). In addition, treatment of cells with the SHIP1 agonist, AQX-435, is sufficient to down-modulate CXCR4. By contrast, in normal B cells, anti-IgM retained the ability to down-modulate CXCR4 expression, whereas AQX-435 had relatively little effect, pointing to differences in the way different B cells may respond to these stimuli. Experiments presented in this chapter investigated the relative effectiveness of anti-IgM and AQX-435 for CXCR4 down-modulation in a panel of established B-cell lines. Anti-IgM trigged CXCR4 down-modulation in all of the cell lines tested, whereas AQX-435 did not induce substantial CXCR4 down-modulation in any of the cell lines tested. In fact, AQX-435 modestly increased CXCR4 expression in most cell lines tested. These results support the idea that anti-IgM is a general modulator of CXCR4 expression across various types of B cells, whereas down-modulatory effects of AQX-435 are more cell-type specific, and perhaps selective for CLL cells.

One exception to this general pattern of regulation was the OCI-LY7 cell line where anti-IgM only very modestly triggered CXCR4 down-modulation. The reason for this is not clear since anti-IgM was able to induce initial signalling responses in this cell line. Moreover, OCI-LY7 cells did not appear to have not mutations effecting either CXCR4 or SHIP1. However, basal CXCR4 expression was relatively low in OCI-LY7 cells and this may preclude further down-modulation.

While the anti-IgM-induced CXCR4 down-modulation appears to operate broadly across various B-cell types, down-modulatory responses to AQX-435 were largely restricted to CLL cells. The reason why AQX-435 is capable of effectively down-regulating CXCR4 expression

in CLL cells, but not on the other B-cell types tested is not clear. All of these cell types tested expressed SHIP1, so the difference is not simply due to lack of target expression. Indeed, AQX-435 was able to decrease AKT phosphorylation following anti-IgM treatment in WSU-FSCCL cells and similar inhibitory effects of AQX-435 have been shown for anti-IgM-induced AKT phosphorylation in TMD8 cells (Dr E Lemm, unpublished; see also Chapter 5 below). One possibility is that CLL cells are somehow "primed" to respond to AQX-435 and this may be linked to on-going antigen engagement of CLL BCRs by (auto)antigen *in vivo*. Therefore, antigen engagement may lead to a partial activation of SHIP1, such that AQX-435 alone is sufficient to engage CXCR4 down-modulating pathways. By contrast, B-cell lines may only reveal effects of AQX-435 following anti-IgM stimulation *in vitro*.

Finally, these studies of cell lines shed potential light on the mechanism by which anti-IgM reduces CXCR4 expression in CLL cells. The natural recovery of CXCR4 on CLL cells cultured *in vitro* is likely to be due to re-expression of CXCR4 at the cell surface, either from previously endocytosed and then recycled receptors, or following *de novo* expression. Thus, it was not clear whether anti-IgM interfered with re-expression of CXCR4 at the cell surface and/or enhanced CXCR4 endocytosis, either of which would result in reduced cell surface CXCR4 expression. Previous studies have shown that anti-IgM-induced CXCR4 down-modulation in CLL cells is reduced in hypotonic media, which inhibits CME, indicating that anti-IgM actively triggers CXCR4 endocytosis (Vlad et al*.,* 2009). However, hypotonic media is a relatively non-specific approach to block endocytosis and likely has additional effects. My results showing that anti-IgM down-modulates CXCR4 in B-cell lines, where CXCR4 expression is stable and not recovering, indicates that anti-IgM can act in systems in the absence of on-going recovery, presumably by directly inducing internalisation of CXCR4 from the cell surface.

3.9.2 Comparison of effects of soluble and bead-bound anti-IgM

It was also interesting to note that soluble anti-IgM induced more effective down-modulation of CXCR4 expression than bead-bound anti-IgM in RL cells, whereas the opposite is observed in CLL cells. CLL cells have low expression of sIgM and the bead-bound form of anti-IgM was developed as an approach to trigger more robust signalling responses in these cells. Binding of anti-IgM to beads may be expected to enhance the extent of sIgM cross-linking and/or decrease endocytosis, thereby sustaining signal responses. Consistent with this, bead-bound anti-IgM induces stronger and longer lasting activation of AKT and ERK, compared to soluble anti-IgM (Krysov et al., 2013). Downstream responses, including activation of mRNA translation and the unfolded protein responses, are also more prominent in cells exposed to bead-bound anti-IgM (Yeomans et al., 2016; Krysov et al., 2012). In contrast to CLL cells, the B-cell lines have relatively high sIgM expression, and show strong signal responses following treatment with soluble anti-IgM, including CXCR4 down-modulation. The reason why bead-bound anti-IgM is a less effective down-modulator of CXCR4 expression in B-cell lines is not clear, but a similar observation has been made for anti-IgM-induced mRNA translation in normal B cells, where the response was greater for soluble anti-IgM compared to bead-bound anti-IgM (Yeomans et al., 2016). Thus, immobilisation of anti-IgM to beads compensates for the low BCR expression of CLL cells, triggering stronger signalling responses. However, in normal B cells and B-cell lines, with relatively high BCR expression, hyper-activation of the BCR is not required to elicit effective signalling responses and may actually reduce the overall response.

3.9.3 Lack of effect of AQX-435 on sIgM endocytosis in WSU cells

In addition to signalling, antigen engagement triggers BCR endocytosis and I performed a series of experiments to investigate potential effects of AQX-435 on sIgM expression. These studies were performed using WSU-FSCCL, allowing me to compare effects of AQX-435 following engagement of sIgM by two distinct ligands, anti-IgM and DC-SIGN, which do and do not induce sIgM endocytosis, respectively. In these studies, AQX-435 alone did not down-modulate sIgM. Furthermore, AQX-435 did not interfere with anti-IgM-induced endocytosis,

or promote endocytosis following binding of DC-SIGN. Thus, sIgM endocytosis appears to be unaffected by AQX-435-mediated SHIP1 activation. The ability of AQX-435 to inhibit anti-IgM-induced AKT phosphorylation but not sIgM endocytosis is consistent with the idea that BCR internalisation may be independent of signalling, at least for soluble ligands.

3.9.4 Effect of kinase inhibitors on anti-IgM-induced CXCR4 down-modulation

I tested the effects of inhibitors of SYK (tamatinib), PI3Kδ (idelalisib) and BTK (ibrutinib, acalabrutinib) on anti-IgM-induced CXCR4 down-modulation in RL cells. Overall the results were similar to those obtained using CLL cells, since CXCR4 down-modulation was reduced by tamatinib and idelalisib, but not by the BTK inhibitors. Thus, at least as probed by this small panel of inhibitors, the kinases that act downstream of the BCR to mediate sIgM → CXCR4 cross-talk seem to be similar.

Whilst this work was underway, Saint-Georges et al., published results of experiments showing that the PKD inhibitor CID755673 decreased anti-IgM-induced CXCR4 down-modulation by ~60% in CLL cells (Saint-Georges et al*.,* 2016). This was surprising since PKD is generally activated downstream of PKC, but both our own studies and those of Saint-Georges et al., agreed that anti-IgM → CXCR4 cross-talk was unaffected by inhibitors of PKC. Notably, my review of the literature revealed that previous studies have identified "off-target" effects of CID755673, limiting its use as a tool to probe PKD function (Sharlow et al*.,* 2008). Using two structurally distinct inhibitors that the University of Dundee Protein Kinase Unit have shown to be quite selective for PKD (pers. comm. S Matthews), I demonstrated that neither compound affected CXCR4 down-modulation (although they did inhibit anti-IgM-induced PKD autophosphorylation). Thus, BCR→CXCR4 cross-talk in CLL cells appears to be independent of both PKC and PKD, and results obtained with CID755673 (Sharlow et al*.,* 2008) may be due to off-target effects.

3.9.5 siRNA studies

My studies of established cell lines provide some important new insight into the regulation of CXCR4 by anti-IgM or AQX-435. However, a major goal of these studies was to select models suitable for genetic manipulation via siRNA transfections, to directly address the role of specific signalling intermediates in CXCR4 regulation. RL cells were selected for these studies since they showed a similar pattern of sensitivity to primary CLL cells in terms of the ability of various kinase inhibitors to interfere with anti-IgM-induced CXCR4 down-modulation.

Following a series of pilot experiments, initial results with BTK siRNA were promising. Thus, BTK siRNA reduced BTK expression, but did not affect anti-IgM-induced CXCR4 down-modulation, seemingly confirming that this response is independent of BTK. However, SYK siRNAs also did not substantially reduce the effects of anti-IgM, although anti-IgM-induced CXCR4 down-modulation was substantially blocked by tamatinib. Thus, it seems likely that the reduction in target expression obtained in the transfections may not be sufficient to effective decrease function. SYK and BTK function as part of a signalosome which forms at activated BCRs and only a small fraction of the total protein expression in the cell may be required to form these complexes. Thus, although the pool of kinase is substantially reduced, there is likely to be ample residual protein left to be recruited to the BCR and form a fully active signalosome. Unfortunately, efforts to improve the effectiveness of siRNA through selection of GFP^{hi} cells as a marker of efficient transfection did not increase the percentage reduction of target (SHIP1) expression.

An alternate method to address the role of specific signalling intermediates would be CRISP-Cas9 to genetically ablate target genes. However, this was not addressed due to (i) likely difficulties with toxicity associated with full depletion of for e.g. SYK in long-term experiments and (ii) the extensive time required to generate CRISPR-Cas9-edited clones. Moreover, the observation that AQX-435 did not down-regulate CXCR4 in any B-cell line tested, including RL cells, reduced the overall value of this approach. Therefore, I did not pursue CRISPR-Cas9, or other potential approaches to increase the effectiveness of siRNA

Chapter 4: Expression and regulation of EBI2 in CLL cells

4.1 Introduction

Antigen engagement of the B-cell receptor (BCR) on chronic lymphocytic leukaemia (CLL) engages pro-proliferation and survival pathways that result in accumulation of malignant cells. For example, BCR stimulation of CLL cells decreases expression of the chemokine receptor CXCR4 (Chapter 3) and enhances adhesion to VCAM-1 via increased expression of the α4β1 integrin subunit CD49d (Majid et al., 2011). Given that CXCR4 and CD49d are subject to cross-talk downstream of BCR in order to mediate cell migration and/or adhesion which are likely to be important not just for disease pathogenesis, but also for response to treatment it is, therefore, important to investigate possible interfaces between the BCR and other cell surface receptors. The main goal of the experiments described in this chapter was to extend analysis of cross-talk in CLL cells to a second GPCR, EBI2. EBI2 was selected as the target for these studies as several lines of evidence suggested it was a potential target for BCR-mediated cross-talk in normal B cells, and may play an important role in CLL;

(i) EBI2 plays an important role in normal B cell responses by controlling movement of B cells to inter- and outer-follicular areas within secondary lymphoid organs (Kelly et al., 2011).
(ii) EBI2 RNA (GPR183) is subject to BCR crosstalk in normal B cells (Gatto et al., 2013; Kelly et al., 2011; Glynne et al., 2000).
(iii) Overexpression of EBI2 in the B-cell compartment of mice results in development of a CLL-like disease (Arfelt et al., 2017)
(iv) Expression of EBI2 at the protein level is higher in memory B cells compared to naive B cells (Clottu et al., 2017).

Despite these findings, no reported studies have investigated expression of EBI2 at the protein level in CLL cells, and whether it is a target for cross-talk.

4.2.1 Hypothesis

BCR crosstalk with the GPCR EBI2 similar to CXCR4 plays an in important role in CLL's response to microenviromental factors and is regulated by SHIP1 in CLL.

4.2.2 Aims and Objectives

The overall goal of the experiments in this chapter was to characterise expression of EBI2 on CLL cells and determine whether, like CXCR4, it was a target for modulation following stimulation of sIgM or activation of SHIP1 using AQX-435 in these cells.

There were four specific aims;

1. To develop methods to quantify EBI2 cell surface expression by flow cytometry
2. To analyse EBI2 expression on CLL cells and compare expression between disease subsets and with normal B-cells
3. To investigate the effect of anti-IgM and AQX-435 on EBI2 expression in CLL
4. To investigate the effect of the EBI2 ligand 7α25-OHC on signalling and CLL cells survival

4.3 Flow cytometric detection of EBI2 expression on normal B cells

I first developed a flow cytometry analysis for quantification of cell surface EBI2 expression. Initial experiments were performed using PBMCs from healthy donors, to allow comparison with the recent study by Clottu et al., which characterized, for the first time, the expression of EBI2 on human lymphocytes using flow cytometry. PBMCs were incubated with anti-CD19 and anti-EBI2 antibodies, before analysis of EBI2 and CD19 expression by flow cytometry (Figure 4.1). In contrast to Clottu et al., who detected relatively abundant expression of EBI2

on both B and T cells (especially memory cells), the staining for EBI2 was not substantially different from cells stained with the control antibody.

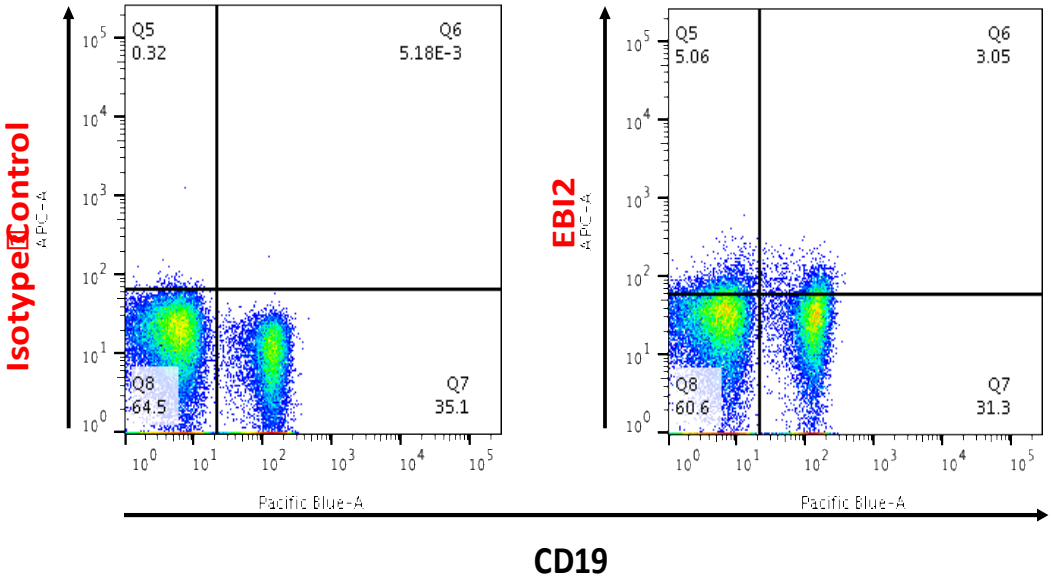

Figure 4.1.

Expression of EBI2 on normal B cells

PBMCs from healthy donors were stained with Pacific Blue-conjugated anti-CD19 and Alexafluor647-conjugated anti-EBI2 or control antibody in FACS buffer, before analysis by flow cytometry. Viable cells were gated on a FSC/SSC dot plot and histograms show staining with anti-CD19 (x-axes) either control antibody (left) or anti-EBI2 (right) (y-axes).

Protocol			
	Host laboratory	Clottu et al.,	Biolegend
Initial wash/treatment	FACs buffer (PBS, 1% (w/v) BSA, 0.01% NaN_3)	Fix in 37% formaldehyde	Proprietary cell staining buffer (not defined but contains BSA)
Staining buffer	FACs buffer	PBS, 1% (w/v) BSA	Proprietary cell staining buffer supplemented with FCS and NaN_3
Post-stain wash	FACs buffer	PhosFlow fixation buffer	Proprietary cell staining buffer

Table 4.1. Comparison of EBI2 staining protocols

Evaluation of the Clottu et al., study revealed two potential factors that were considered as potential explanations for the differences in results shown here and described in their paper. First, Clottu et al., used a non-commercial antibody produced at Novartis. Second, their staining was performed using fixed cells (see Table 4.1 for comparison of protocols).

I also noted that the datasheet for the EBI2 antibody used in our experiments (Biolegend) showed abundant EBI2 expression in normal lymphocytes. In contrast to our protocol which used BSA as a blocking agent, the Biolegend protocol used FCS. Since BSA is known to bind 25-OHC (Lin & Morel, 1995), we speculated that EBI2-ligands bound to albumin in our staining buffer were triggering receptor endocytosis leading to low apparent surface expression. Therefore, I compared directly detection of EBI2 in normal lymphocytes using BSA- or FCS-containing buffers. As an additional control, I compared EBI2 detection using staining buffers containing BSA or de-lipidated BSA. I did not examine the effect of cell fixation, since with this approach it would not be possible to discriminate cell surface versus intracellular EBI2.

The best staining results were obtained with the FCS-containing staining buffer (Figure 4.2). EBI2 was detected on essentially all $CD19^+$ B cells and on a majority of the $CD19^-$ cells. Within the B cells it was possible to identify two sub-populations which are presumably naïve and memory B cells, since memory B cells have been shown to express increased EBI2 than naïve B cells (Clottu et al., 2017). Consistent with initial experiments (Figure 4.1), very few cells appeared to express EBI2 when cells were stained in buffer containing BSA. Use of de-lipidated BSA did appear to increase EBI2 detection, but under these conditions, the proportion of cells that were considered $EBI2^+$ was still quite low. Based on these results, the FCS-containing buffer was selected for further studies. Although it is possible that eliminating FCS/BSA completely from the staining buffers might further increase staining, I felt that it was important to retain some protein blocking capacity to minimize background staining which could be particularly problematic in planned time course experiments where the proportion of dead cells may be high.

Another variable between our experiments and those of Clottu et al., was the choice of antibody. However, staining of PBMCs from healthy donors using the commercial Biolegend antibody and the Novartis EBI2 antibody (a kind gift of Dr Andreas Sailer) yielded very similar results with FCS-containing buffers (data not shown) and further studies were performed using the Biolegend antibody.

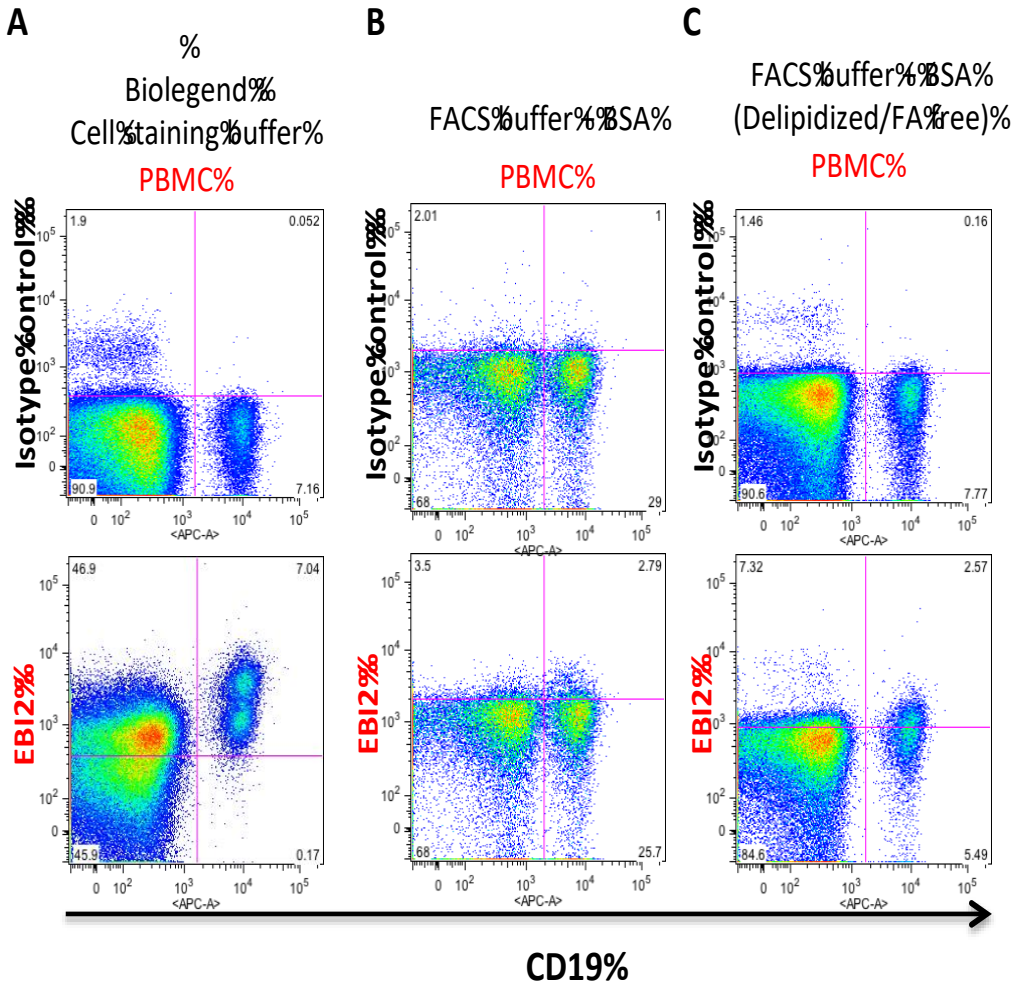

Figure 4.2. Effect of different staining buffers on EBI2 staining on normal PBMCs
PBMC from healthy donors were stained with APC-conjugated anti-CD19 and Alexafluor647-conjugated anti-EBI2 (bottom) or control antibody (top) using the indicated staining buffers (see Table 4.1). Expression of EBI2 was analysed on viable cells using flow cytometry.

Having established the FCS-based staining protocol for EBI2 detection, I analysed basal expression of EBI2 on B cells from 4 different healthy donors. In addition to the anti-EBI2 and anti-CD19 antibodies used before, I also included anti-CD27 and anti-IgG antibodies in the staining step and separately analysed EBI2 expression on $CD19^{+}CD27^{-}IgG^{-}$ (naive B cells) and $CD19^{+}CD27^{+}IgG^{-}$ (largely non-switched memory B cells). Consistent with the literature (Clottu et al., 2017), EBI2 was detected in both cell populations, but was expressed more highly on memory B cells (Figure 4.3).

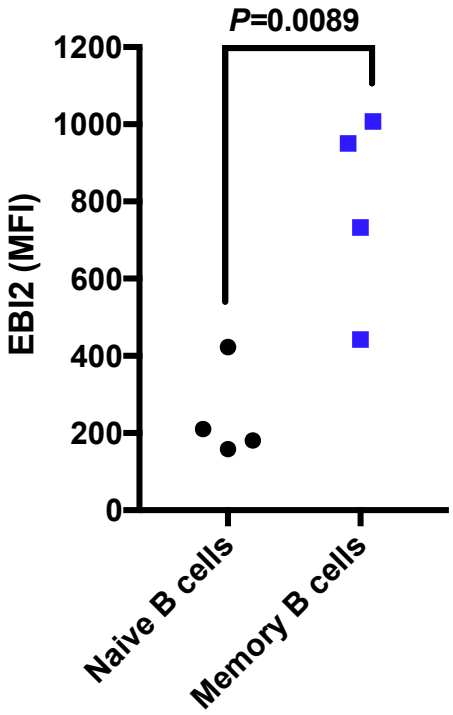

Figure 4.3. EBI2 expression on normal B lymphocytes
PBMC from healthy donors (n=4) were stained in duplicate with pacific blue-conjugated anti-CD19, PerCP-Cy5-conjugated anti-CD27, FITC- conjugated anti-human IgG and Alexafluor647-conjugated anti-EBI2 or control antibody in FCS-containing staining buffer. Graph shows EBI2 expression in naive and memory B cells and the statistical significance of the difference (Student's t-test).

4.4 EBI2 expression on primary CLL cells

I next analysed expression of EBI2 on unstimulated CLL cells. Anti-CD19 and anti-CD5 antibodies were included in the staining allowing me to analyse EBI2 expression specifically on CLL cells. Analysis was performed using a total of 25 samples, comprising examples of both U-CLL and M-CLL, and I compared expression values for CLL cells with those obtained from normal B cells obtained in the previous experiments using an identical staining protocol (Figure 4.3). There was considerable variation in EBI2 expression between individual CLL samples (MFI range 9 - 405) (Figure 4.4). Overall, EBI2 expression was relatively low on CLL samples, even compared to naive B cells (mean MFI of ~100 for CLL cells and ~250 for naive B cells).

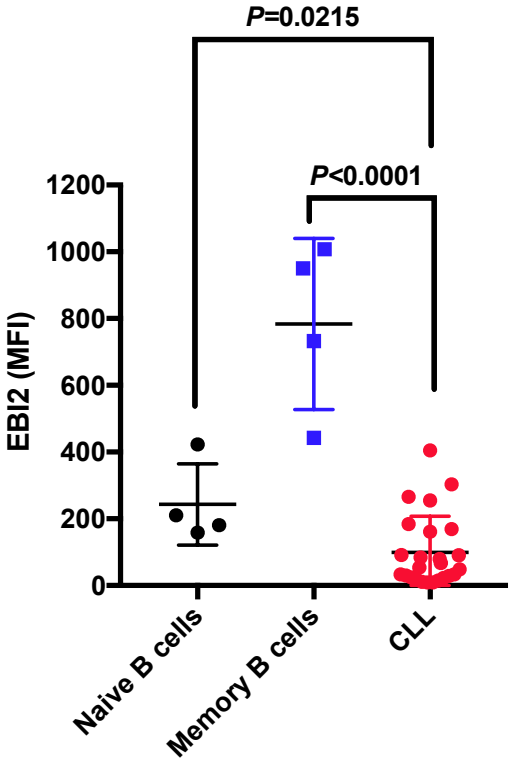

Figure 4.4. Expression of EBI2 on CLL cells
Primary CLL samples (n=25) were stained in duplicate with PerCP-Cy5-conjugated anti-CD5, APC-conjugated anti-CD19 and Alexafluor647-conjugated anti-EBI2 or control antibodies. Expression of EBI2 was quantified on viable $CD19^{+}CD5^{+}$ cells using flow cytometry. Graph shows individual data points (mean of duplicate determinations) for EBI2 expression in each CLL sample (as well as mean ±SD of the entire cohort) alongside values for normal naive and memory B cells (see Figure 4.3), and the statistical significance of the indicated differences (Student's t-test).

Since EBI2 expression differs between naive and memory B cells, it was important to determine whether the variable expression of EBI2 on CLL cells reflected differing cell-of-origin (pre-GC for U-CLL and post-GC for M-CLL). I, therefore, determined whether EBI2 expression was correlated with *IGHV* mutational status (Figure 4.5). Although the mean EBI2 expression of M-CLL samples was slightly higher than that of U-CLL samples, the difference between these disease subsets was not statistically significant. Therefore, CLL cells typically express low levels of EBI2 (compared to normal B cells) independent of *IGHV* mutation status.

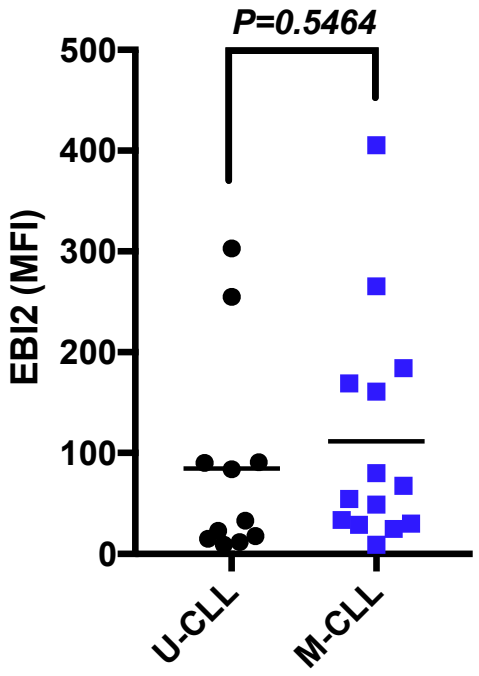

Figure 4.5. Expression of EBI2 on U-CLL and M-CLL samples
Graph shows mean (±SD) EBI2 expression (as well as data for individual samples) on U-CLL (n=11) and M-CLL (n=14) samples. The statistical significance of the differences is shown (Student's t-test).

I also investigated whether variation in EBI2 expression on CLL cells correlated with other clinical/biological markers, including sIgM expression and signalling capacity (iCa^{2+} mobilisation) and expression of ZAP70 and CD38. However, similar to *IGHV* mutations status, variation in EBI2 expression was unrelated to any of these markers (Figure 4.6). The two anomalies which demonstrated an EBI2 MFI over 300 were retrospectively traced back to patients sample to if these could be associated expression of basal SHIP1 , but no correlation was found (data not shown)

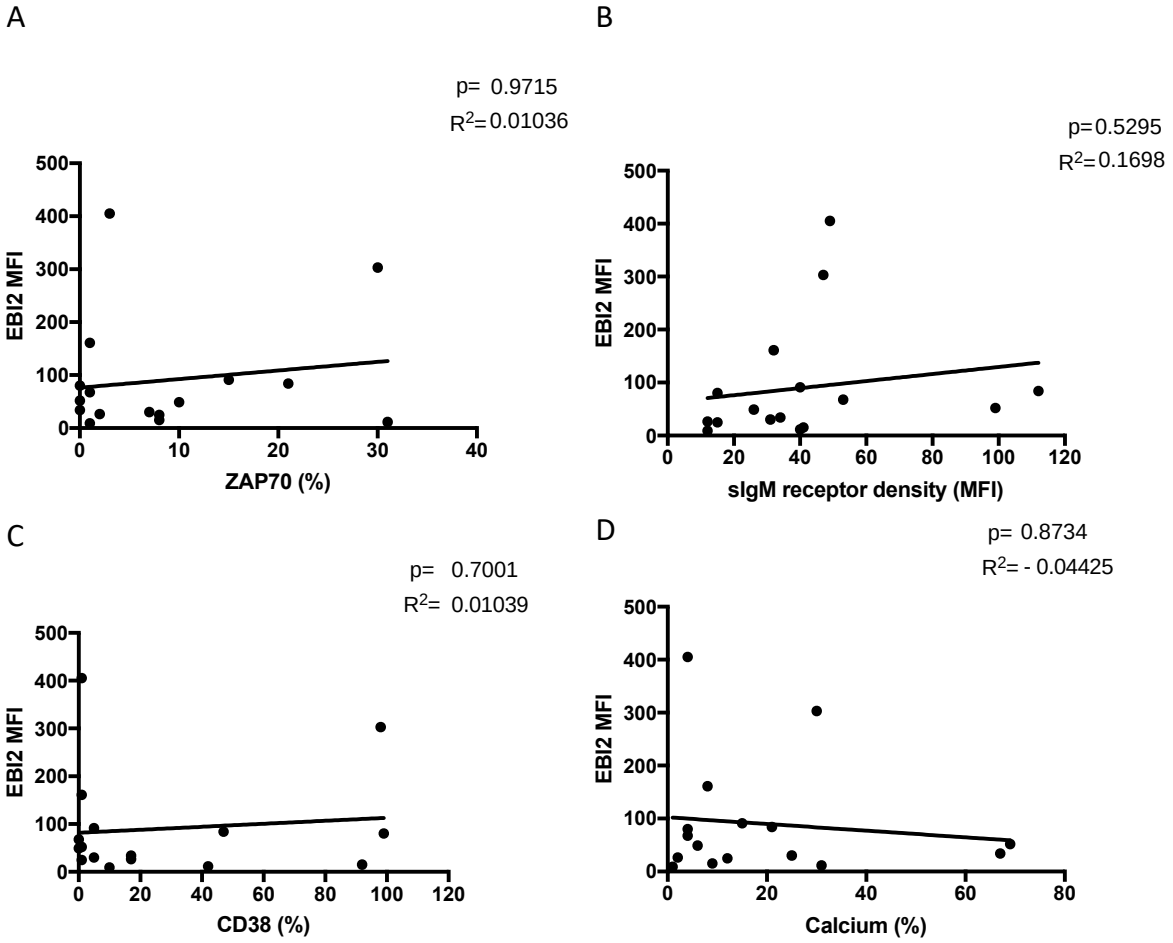

Figure 4.6. Correlations between clinical/biological markers and basal expression of EBI2 on CLL cells. Correlation between EBI2 expression on 25 CLL samples and (A) anti-IgM-induced iCa^{2+} flux, (B) ZAP-70 expression, (C) CD38 expression and (D) sIgM expression. Graphs show results of linear regression and statistical significance was calculated using Spearman's rank correlation coefficient.

4.5 Analysis of EBI2 signalling response in CLL cells

Since CLL cells expressed EBI2 (albeit at relatively low levels compared to normal B cells), I next investigated the potential function of the receptor. Treatment of $EBI2^{+}$ breast cancer cells with the EBI2 ligand 7α25-OHC has been shown to induce phosphorylation of ERK and AKT after 10 minutes (Jensen et al., 2013). I, therefore, investigated phosphorylation of

these markers following treatment of CLL cells with 7α25-OHC. The experiments were performed with CLL samples (575E, 409C, 780A) selected on the basis of strong anti-IgM-induced iCa^{2+} mobilisation (iCa^{2+}>30%) and relatively high expression of $EBI2^{+}$ (MFI >100). 7α25-OHC was used at a range of concentrations (up to 10^4 nM) in line with previous studies (Rutkowska et al., 2016; Daugvilaite et al., 2014). I also stimulated CLL cells with soluble anti-IgM as a positive control (Figure 4.7)

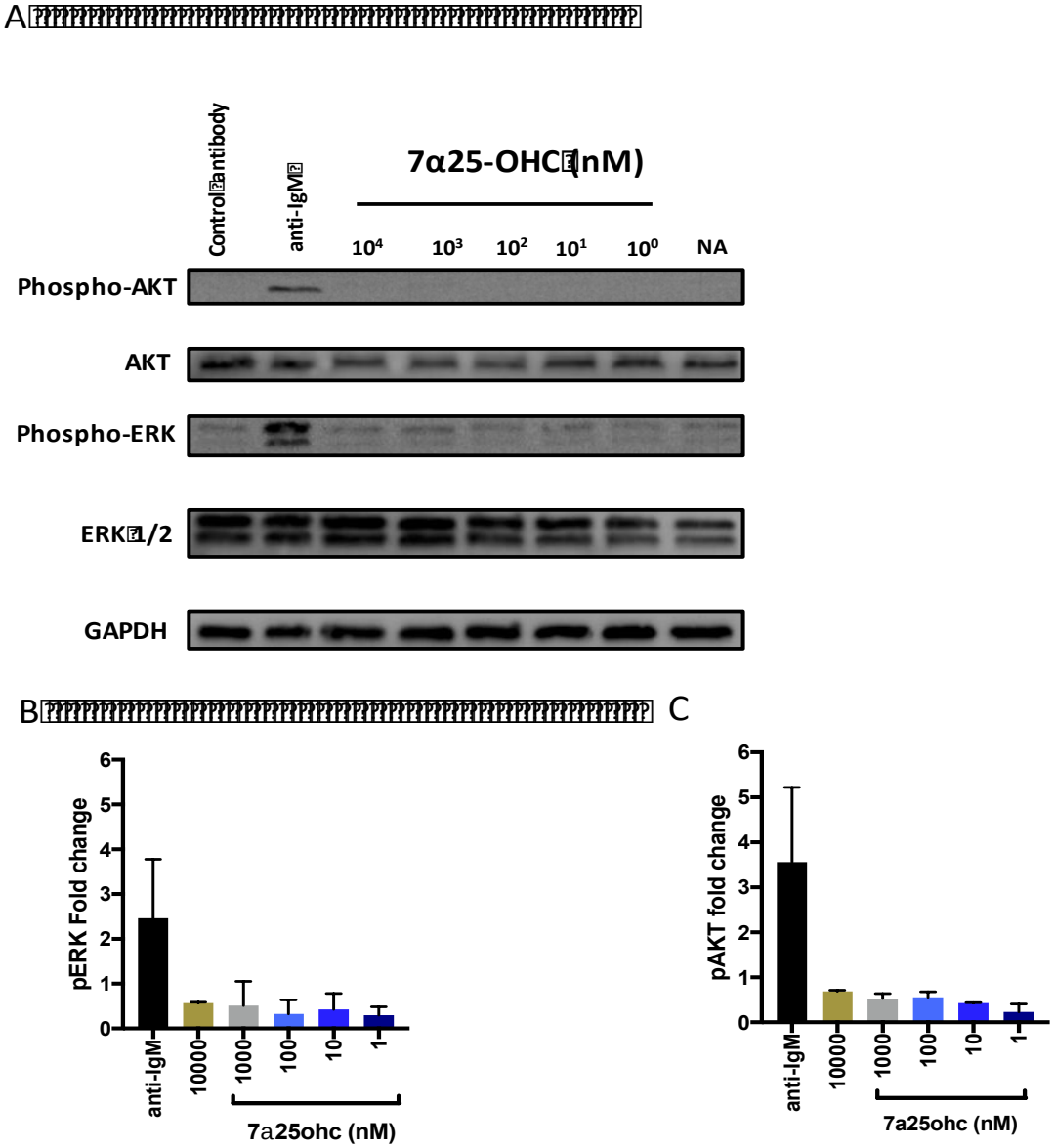

Figure 4.7. Effect of 7α25-OHC on ERK and AKT phosphorylation in CLL cells

CLL samples (n=3) cells were treated with soluble anti-IgM/control antibody, or various concentrations of 7α25-OHC for 10 minutes. Expression of total and phosphorylated ERK1/2 and AKT, and GAPDH (loading control) was analysed by immunoblotting. (A) Representative immunoblots. Graphs show mean (±SD) of (B) ERK phosphorylation or (C) AKT with values for control cells set to 1.0.

As expected, anti-IgM treated induced strong phosphorylation of both ERK and AKT (~3-fold increase). By contrast, there was no evidence for increased ERK/AKT phosphorylation in 7α25-OHC-treated cells.

I next investigated whether 7α25-OHC was capable of inducing iCa^{2+} flux in CLL cells (Figure 4.8) using the same samples selected for analysis of ERK/AKT phosphorylation. As expected, anti-IgM, but not control antibody, induced a significant increase in iCa^{2+} in CLL cells, although the extent of response varied between samples. The Ca^{2+} ionophore ionomycin also induced a strong increase in iCa^{2+} in all samples, confirming the ability of the cells to release iCa^{2+}. By contrast, iCa^{2+} was only very modestly increased (~10%) in CLL cells following treatment with 7α25-OHC.

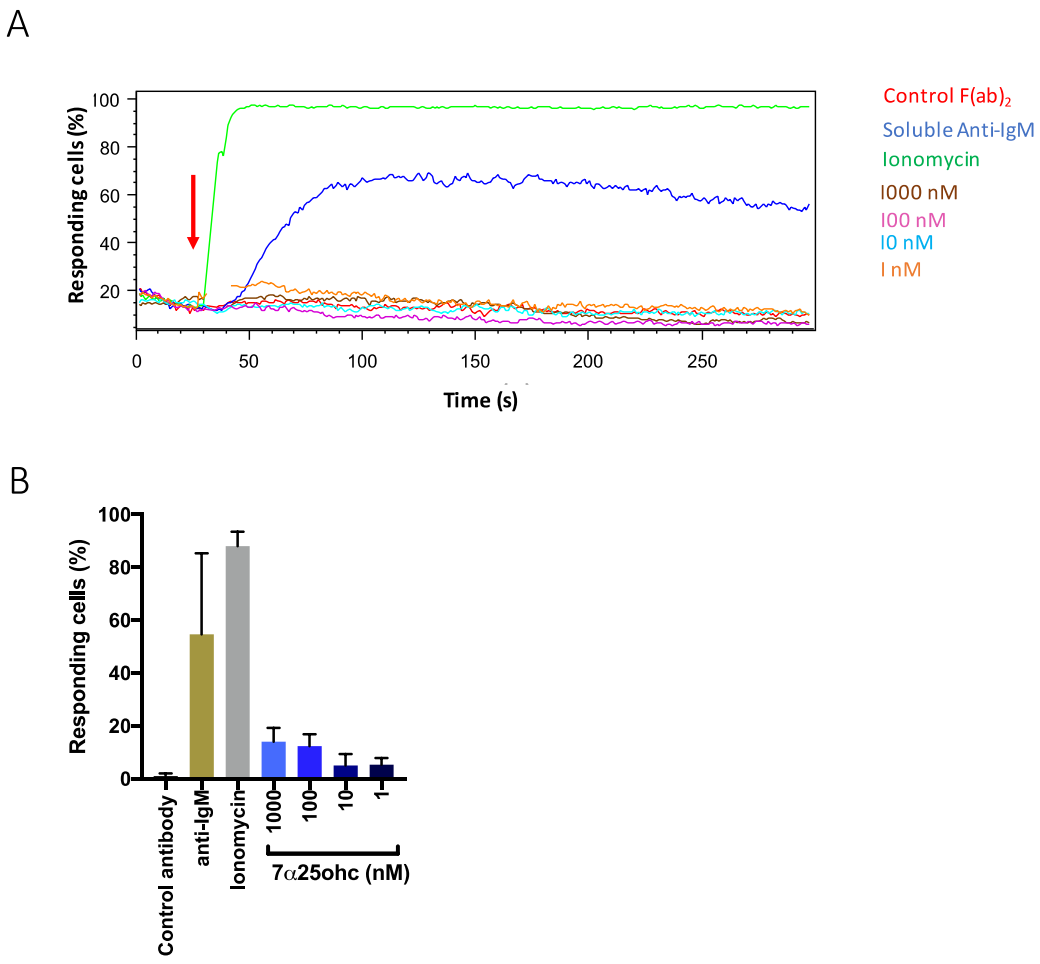

Figure 4.8. Effect of 7α25-OHC on iCa2+ in CLL cells
Analysis of iCa2+ flux in CLL samples (n=3) following treatment with ionomycin, soluble anti-IgM/control antibodies or the indicated concentrations of 7α25-OHC. (A) Representative results of percentage of cells responding to point of addition of reagents indicated by the red arrow (B) Graph shows percent responding cells for all samples analysed (mean ±SD).

Finally, I investigated if stimulation of the EBI2 receptor with 7α25-OHC would promote CLL cell survival. Cells were treated with a range of concentrations of 7α25-OHC and cell viability was analysed after 24 and 48 hours using annexinV/PI staining (Figure 4.9). The experiments were performed with CLL samples (575E, 409C, 780A) selected on the basis of strong anti-IgM-induced iCa^{2+} mobilisation (iCa^{2+}>30%) and relatively high expression of $EBI2^{+}$ (MFI>100). As expected, there was a significant drop in viability of control cells during the experiment, due to spontaneous apoptosis. However, cell death was not substantially affected by addition of 7α25-OHC at any concentration.

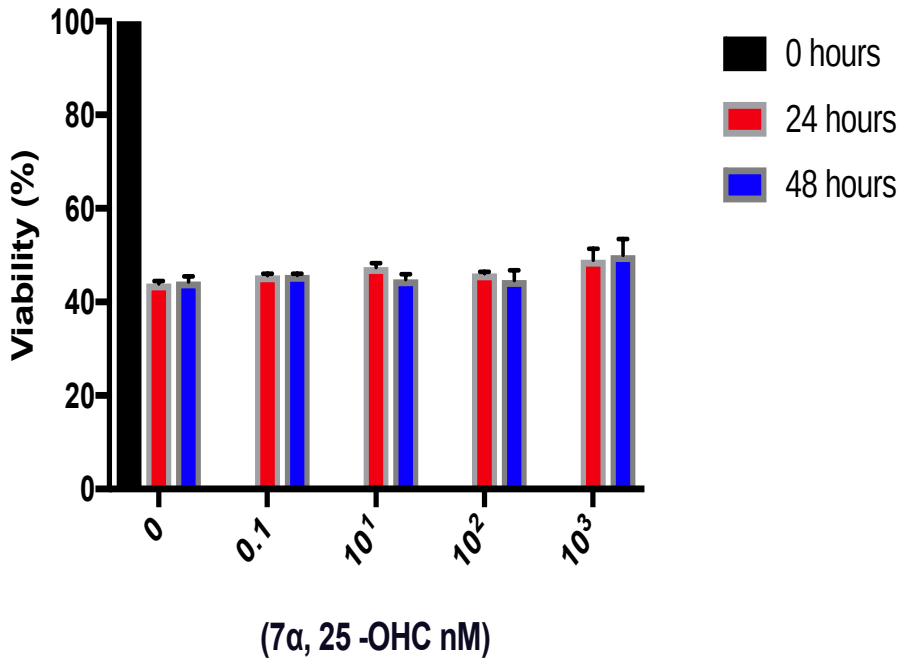

Figure 4.9. Effect of 7α25-OHC on CLL cell survival
CLL samples (n=4) were treated with indicated concentration of 7α25-OHC for 24 or 48 hours. Cells were collected and viability analysed using AnnexinV/PI. Cell viability was also measured at the start of the experiment. Graph shows mean (±SD) relative proportion of viable (AnnexinV-/PI-) cells with values for cells at the start of the experiment set to 100%.

Overall, these experiments failed to demonstrate a response of CLL cells to 7α25-OHC in terms of either signalling (ERK/AKT phosphorylation, iCa^{2+} flux) or viability. One possibility is that the lack of responsiveness of CLL cells reflects the low level of expression of EBI2 stimulation on these cells compared to normal B cells.

4.6 Regulation of EBI2 expression

The next goal was to investigate the effect of anti-IgM and AQX-435 on EBI2 expression to determine whether EBI2 was a target for cross-talk with BCR-associated signaling pathways. However, before performing these experiments it was important to investigate whether, like CXCR4, expression of EBI2 was modulated during culture of CLL cells *in vitro*.

CLL samples were recovered and expression of EBI2 was analysed by flow cytometry at various times points up to 24 hours. Results for a representative sample shown in Figure 4.10. Interestingly, there was an initial increase in EBI2 expression (at 2 hours post-recovery), but after that EBI2 expression rapidly declined. Similar results were observed in an additional 2 samples (not shown). Although the decline in EBI2 expression with time was of potential interest, I was concerned that this was a technical artefact, driven by endocytosis of EBI2 due to ligands (e.g. oxysterols) present in the culture medium. It was not possible to perform experiments in the absence of serum over this time course, as CLL cells very readily undergo apoptosis under these conditions (Dos Santos et al., 2017). Therefore, additional experiments were performed for up to a maximum of either four or five hours post-recovery.

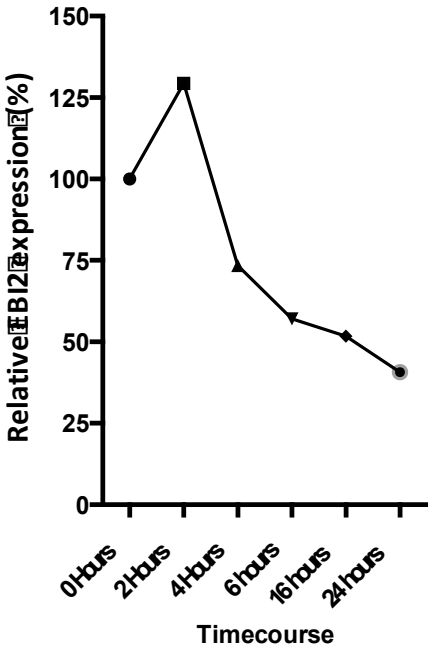

Figure 4.10. EBI2 expression following recovery of CLL cells
CLL samples (n=2) were cultured for up to 24 hours before staining with pacific blue-conjugated-anti-CD19, PerCP-Cy5-conjugated anti-CD5 and Alexafluor647-conjugated anti-EBI2 or control antibodies. EBI2 expression was quantified on CD19+CD5+ cells using flow cytometry. Data points are means of duplicate determinations with values for EBI2 expression at the start of the experiment set to 100%.

4.6.1 Effect of anti-IgM on *EBI2* mRNA expression in CLL cells

To investigate the effect of anti-IgM on EBI2, I first examined expression of EBI2 RNA, since any regulation at this level would be expected to be independent of effects of culture components on receptor endocytosis. For initial analysis, I analysed publicly available data from a study which used gene expression microarrays to investigate the effect of soluble anti-IgM on mRNA expression in CLL samples and normal peripheral blood B cells at times up to 390 minutes post-stimulation (Vallat et al., 2013). Data for EBI2 RNA was extracted using the NCBI GEO microarray database portal and plotted to show EBI2 RNA expression (relative to control cells at the same time point) in CLL samples and normal B cells (Figure 4.11).

This analysis indicated that anti-IgM stimulation significantly increased EBI2 expression in CLL samples with the maximal response at 3.5 hours. However, there was substantial inter-sample variation in the extent of EBI2 RNA induction. By contrast, there was only a very small increase in EBI2 RNA in normal B cells.

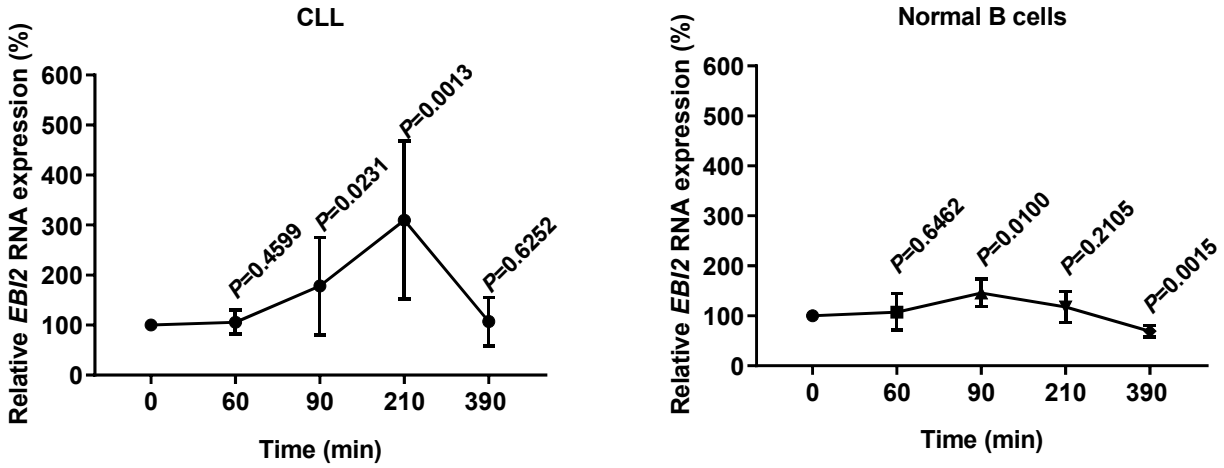

Figure 4.11. Effect of anti-IgM on *EBI2* RNA expression in CLL and normal B cells
Expression data for EBI2 (GPR183) from the Vallat et al., study was accessed via the NCBI GEO portal (accession GSE39411). Graphs show mean (±SD) EBI2 RNA expression following stimulation with soluble anti-IgM with values for control antibody-treated cells set to 100% for each time point for CLL samples (n=11) and normal B cell samples (n=6). The statistical significance of the differences between anti-IgM and control cells is shown for each time point (Student's t-test).

4.6.2 Effect of anti-IgM on EBI2 protein expression on CLL cells

I next performed a series of experiments to investigate the effect of anti-IgM on EBI2 expression at the protein level on CLL samples. An initial pilot experiment was performed to compare effects of soluble and bead-bound anti-IgM (data not shown). This experiment revealed substantial technical difficulties in analysing EBI2 expression on cells stimulated with bead-bound anti-IgM. Thus, there was considerable auto-fluorescence from the bound beads into the channel used to detect binding of the alexafluor647-conjugated anti-EBI2 and control antibodies. This dramatic auto-fluorescence has been observed in previous experiments (Coehlo et al., 2016). Autofluorescence was also observed in experiments analysing effects of bead-bound anti-IgM on CXCR4 expression in CLL cells but this was readily easy to compensate due to the relatively strong expression of CXCR4. However, the fluorescent signal for EBI2 expression was substantially lower than for CXCR4, and, in this situation, it was not possible to adequately compensate bead auto-fluorescence and retain sensitivity for EBI2 detection. Therefore, additional experiments were performed using soluble anti-IgM only.

I investigated the effect of soluble anti-IgM on EBI2 expression at time points up to 4 hours post-stimulation using a total of 11 samples. The cohort comprised examples of U-CLL and M-CLL and a range of signalling responses (percentage range of responding cells in iCa^{2+} flux assay was 3 - 69%). Overall, there was no consistent effect of anti-IgM on relative EBI2 expression (Figure 4.12). Similar results were obtained when the cohort was divided into M-CLL and U-CLL samples. There was also no clear correlation between the extent of EBI2 induction by anti-IgM and iCa^{2+} (not shown), although it was notable that EBI2 expression was maximally increased (by ~30%) in the sample with the highest signalling capacity (575E).

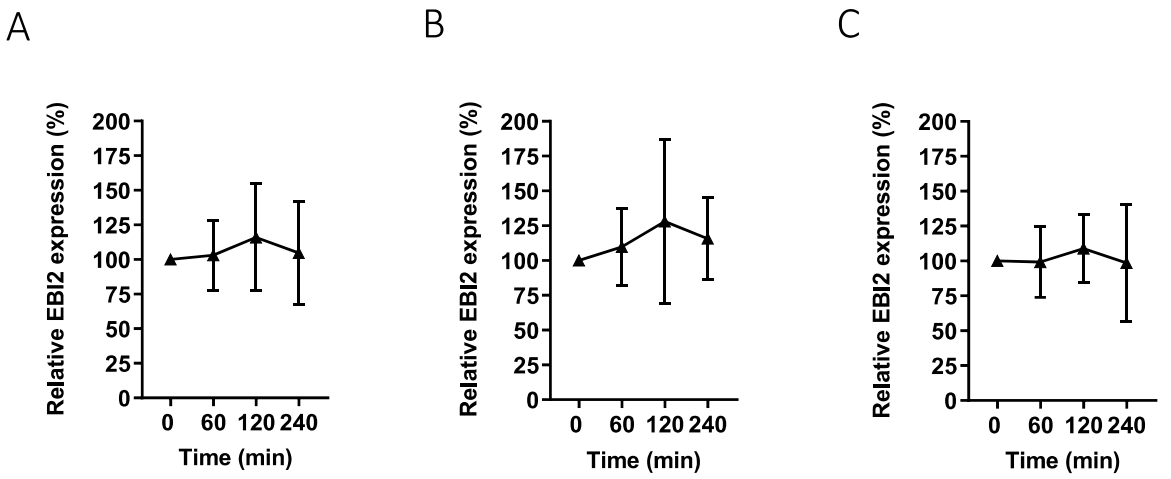

Figure 4.12. Effect of anti-IgM on expression of EBI2 on CLL cells
Primary CLL samples (n=11) were treated in duplicate with soluble anti-IgM or control antibody for the indicated times. Cells were then stained with PerCP-Cy5-conjugated anti-CD5, pacific blue-conjugated anti-CD19 and Alexafluor647-conjugated anti-EBI2 or control antibodies and EBI2 expression on $CD19^{+}CD5^{+}$ cells was quantified by flow cytometry. Graph shows mean (±SD) EBI2 expression with values for control antibody treated cells set to 100% at each time point for (A) all samples, (B) U-CLL and (n=4) (C) M-CLL (n=7).

4.6.3 Parallel analysis of anti-IgM EBI2 RNA and protein

Together, these analyses indicate a potentially modest and variable induction of *EBI2* RNA, but not protein expression, in anti-IgM stimulated cells. However, since I compared public datasets for RNA expression versus in-house data for EBI2 protein, this difference could be due to variation in stimulation and/or sample selection. I, therefore, performed a small experiment using three samples to analyse in parallel the effect of anti-IgM on *EBI2* RNA and protein expression, using Q-PCR and flow cytometry, respectively (Figure 4.13).

Similar to previous analysis (Figure 4.11), there was some indication for an increase in *EBI2* RNA expression in anti-IgM-treated cells (Figure 4.13). There was also an apparent peak in EBI2 protein at 60 minutes post-stimulation for one of the samples. However, both of these responses were highly variable between samples. It was perhaps notable that sample 511A (red) showed an increase in both EBI2 RNA (~4-fold higher expression in anti-IgM-treated cells) and protein expression (~2.5-fold higher expression in anti-IgM-treated cells).

However, samples 636B also showed a substantial increase in RNA (~2.5-fold) without a matching increase in EBI2 protein expression. It was also somewhat surprising that the apparent increase in EBI2 protein expression in 511A(red) cells peaked at 60 minutes, thereby preceding the apparent increase in RNA.

Overall, these studies do not demonstrate a consistent pattern of regulation of EBI2 following anti-IgM treatment of CLL cells.

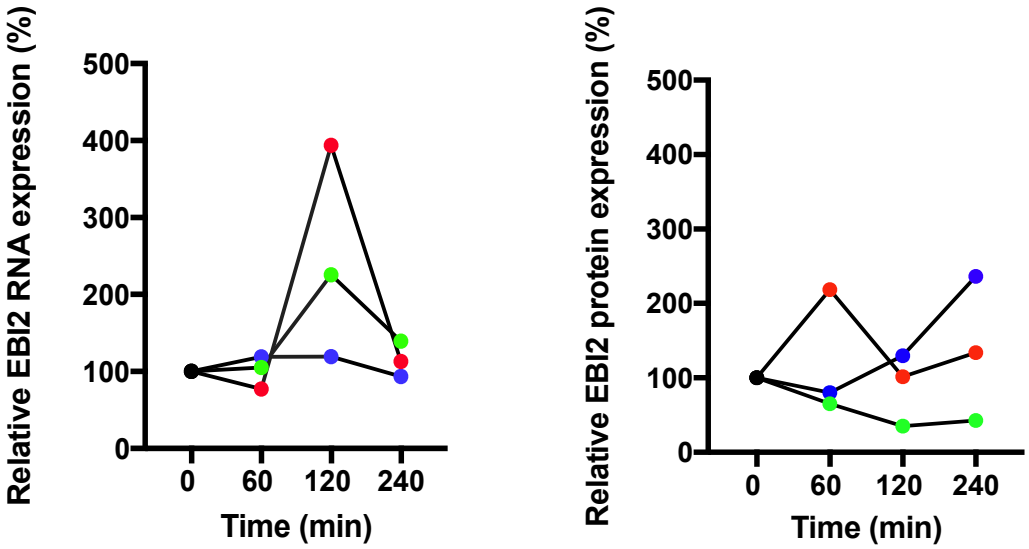

Figure 4.13. Parallel analysis of effect of anti-IgM on EBI2 RNA and protein expression
Primary CLL samples (n=3) were treated in duplicate with soluble anti-IgM or control antibody for the indicated times. EBI2 expression was then analysed by Q-PCR and flow cytometry (as described for Figure 4.12). Graphs show values of parallel EBI2 RNA (left) and protein (right) expression for 3 individual samples (Green/red/blue) with values for control antibody treated cells set to 100% at each time point.

4.6.4 Effect of AQX-435 on EBI2 expression

Finally, I investigated the effect of AQX-435 on EBI2 expression to determine whether as for CXCR4, AQX-435 altered expression in CLL cells. AQX-435 was tested at 30 μM, a concentration that is sufficient to trigger down-modulation of CXCR4 (Figure 3.4) and expression was analysed at time points up to 5 hours after addition of drug. However, there was no effect of AQX-435 on EBI2 expression at any time point (Figure 4.14).

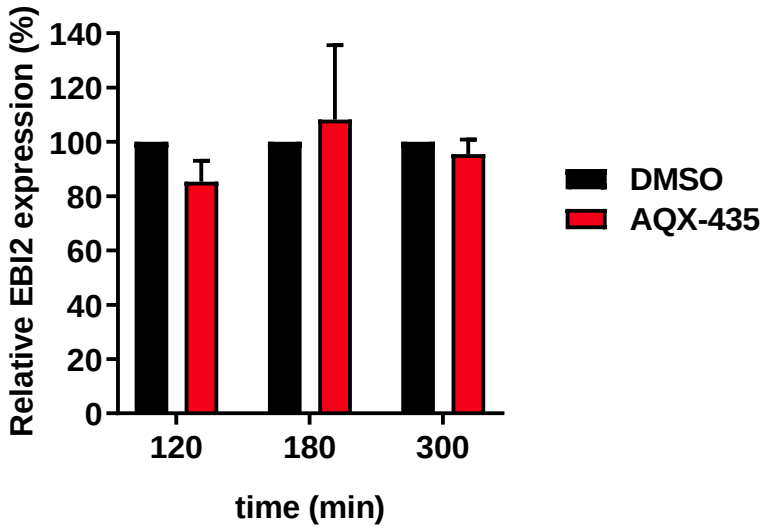

Figure 4.14. Effect of AQX-435 on EBI2 expression
Primary CLL samples (n=3) were treated in duplicate with AQX-435 (30 µM) or DMSO for 2, 3 or 5 hours. Cells were then stained with PerCP-Cy5-conjugated anti-CD5, pacific blue-conjugated-anti-CD19 and Alexafluor647-conjugated anti-EBI2 or control antibody. EBI2 expression on CD19+CD5+ was quantified using flow cytometry. Graph shows mean (±SD) EBI2 expression with values for control cells set to 100%. The difference in EBI2 expression between DMSO and AQX-435-treated cells was not significant (P>0.05; Student's t-test) at any time point.

4.7 Summary of main findings

The overall goal of the experiments in this chapter was characterise expression of EBI2 on CLL cells and determine whether, like CXCR4, it was a target for modulation following stimulation of sIgM or activation of SHIP1 using AQX-435 in these cells.

The key findings from the experiments described in this chapter were;

1. EBI2 expression is generally low on CLL cells and is not clearly different between U-CLL and M-CLL (or subsets identified by other markers) despite variable expression of EBI2 between normal naive and memory B cells.
2. The EBI2 ligand 7α25-OHC did not induce signalling or alter viability of CLL cells

3. Anti-IgM may increase expression of *EBI2* RNA in CLL cells, but overall effects were modest and variable between samples, and were not accompanied by a clear increase in EBI2 protein expression.
4. AQX-435 did not alter EBI2 protein expression.

Overall, the results provide little evidence that sIgM-induced signalling or SHIP1 activation using AQX-435 leads to modulation of EBI2 expression in CLL cells. However, there were considerable technical challenges in analysis of EBI2 which complicated analysis, especially related to the overall low level expression of EBI2 on CLL cells and the modulatory potential effect of EBI2 ligands.

4.8 Discussion

4.8.1 Potential relevance of EBI2 in CLL

During an antigen-driven, T-cell dependent antibody response the GPCR EBi2 plays and vital role in both early and late phase B cell responses. During the early EBI2 is expressed constitutively in mature naive B cells and engagement of the BCR by antigen results in a substantial (5-fold) and rapid (within one hour) increase of *EBI2* mRNA expression (Gatto et al., 2013; Kelly et al., 2011; Glynne et al., 2000) which is known to be critical to direct movement which activated B cells to inter- and outer-follicular areas of the LN (Kelly et al., 2011) in response to its ligand 7α,25-OHC (Hannedouche et al., 2011).

Additionally, EBI2 plays a key role in late phase immune response because it influences whether B cells commit to an early plasma blast response by retaining EBI2 expression or become GC B cells by acquiring a major transcriptional change such as the expression of the EBI2 suppressor, BCL6 (Gatto et al., 2013). Although at the start of the study, there were no experiments describing expression of EBI2 at the protein level in either human or mouse cells, Clottu et al., recently reported memory B cells have been shown to express increased EBI2 compared to naïve B cells (Clottu et al., 2017)

Despite the important role EBI2 plays in both early phase B cell response, there has only been one related studies in CLL. Arfelt et al., reported that that overexpression of EBI2 in the B-cell compartment of mice results in development of a CLL-like disease. More importantly, the study demonstrated that *EBI2* RNA expression is downregulated in CLL cells compared to normal B cells (Arfelt et al., 2017).

Evidently, EBI2 expression and function is a target for BCR crosstalk in normal B cells but it's regulation in malignant B cells has not been studied. Given the function and regulation of CXCR4 plays an important role in malignant B cell, I, therefore, characterised expression of EBI2 on primary CLL cells and its potential regulation by sIgM.

4.8.2 Flow cytometric detection of EBI2

It is notable that very few studies have investigated EBI2 protein expression, in either human and mouse cells. Overall, my attempts to develop a flow cytometry assay to detect EBI2 expression on normal B cells and CLL cells revealed substantial technical challenges. Specifically, it seemed that ligands present in staining buffers, most notably with BSA, were driving endocytosis resulting in lack of detectable expression of EBI2. One possibility is that BSA is bound to oxysterols (Lin & Morel, 1995) which then promote EBI2 endocytosis leading to reduced surface receptor expression.

It was remarkable that this occurred even in the presence of sodium azide (NaN_3) and with incubation at low temperature both of which would be expected to minimise endocytosis (Penheiter et al., 2002). However, it should be noted that a rise in sample temperature is unavoidable in these experiments, as the sample was put in an incubator. Secondly, NaN_3 blocks mitochondria ATP production, but might not fully deprive cells of ATP especially in malignant cells which may have increased dependency on glycolysis.

To reduce these influences, assays were performed in presence of FCS. However, there may still be an influence of ligands present in the serum in these experiments as it was not possible to fully eliminate BSA/FCS due to the need to have blocking activity in the antibody binding steps.

Delipidation did somewhat improve detection compared to standard BSA, but was still less effective compared to FCS. However, the effectiveness of delipidation in removing oxysterols is not known. Clearly the potential influences of ligand identified in these experiments raises the additional possibility that EBI2 surface expression is also modulated in tissue culture, during the 1 hour recovery and over longer incubations periods. Indeed, in recovery experiments there was an initial increase in surface EBI2 expression (at 2 hours), that was followed by a substantial and protracted decline. It was considered likely that this decline could be driven by culture factors. To prevent any potential artefact on EBI2 expression as a consequence of the oxysterol ligand supplement in the tissue culture medium, I performed performing the experiments in serum-free conditions, but this resulted in extensive cell death within just 4 hours and, therefore, prevented me from adopting this as a potential approach (data not shown). Therefore, I had to limit the time period over which experiments looking at modulation by anti-IgM or AQX-435 were performed.

Despite difficulties, I was able to confirm EBI2 is expressed at higher levels in memory B cells than naïve as previously (Clottu et al., 2017). For CLL cells, EBI2 expression was generally lower and demonstrated intersample variability. Strikingly, in some samples EBI2 expression did not obviously exceed background staining. Importantly, variation in EBI2 expression was not different between subsets, especially U-CLL and M-CLL suggesting variation in CLL is not simply a feature of differing cell-of-origin. The low level expression of cell surface EBI2 in CLL cells is consistent with analysis of EBI2 RNA in a previous study (Arfelt et al., 2017).

4.8.3. EBI2 Signalling

Given EBI2 like CXCR4 is part of the GPCR, I investigated potential function of the receptor in CLL cells. Previous studies have shown stimulation of EBI2 with 7α,25-OHC induces ERK and AKT phosphorylation (Jensen et al, 2013). However, treatment of CLL cells with 7α,25-OHC did not result in detectable changes in downstream signalling or cell survival. Due to the lack of observed responses, it would have been beneficial to have a positive control in

these experiments. Normal B cells could have been used, however, there is no comparator data in the literature to describe effects of ligand in these cells because of the limited studies conducted on EBI2.

4.8.4. BCR Modulation of EBI2

Overall, the challenges described above made analysis of EBI2 modulation by anti-IgM or AQX-435 challenging, and restricted incubations to relatively short periods. Moreover, I encountered substantial technical difficulties in analysing regulation of EBI2 by anti-IgM as the use of bead bound anti-IgM caused strong auto-fluorescence. Despite compensation, this fluorescence appeared to "bleed-through" into the APC channel used for EBI2 detection. Control beads do not provide an adequate control since they do not bind to CLL cells. This issue has been reported before (Coehlo et al., 2016) and, therefore, only soluble anti-IgM stimulation was used in my experiments.

Analysis of public datasets provided some evidence for *EBI2* RNA modulation with anti-IgM, although this was very variable between samples (Vallat et al., 2013). The modest increase in *EBI2* RNA observed was consistent with data obtained from mouse models, where *EBI2* RNA is induced 5-fold at 2 hours following BCR stimulation *in vivo* (Gatto & Brink, 2013). Interestingly, the induction of *EBI2* RNA by anti-IgM was substantially less in normal human B cells compared to CLL cells, although It is important to bear in mind that not all peripheral blood B cells will express sIgM and this might explain the apparent reduced response.

Parallel analysis of regulation of *EBI2* RNA and protein by anti-IgM indicated a potentially modest and variable induction of *EBI2* RNA, but not EBI2 protein expression. Similarly (and in contrast to effects on CXCR4), AQX-435 did not alter EBI2 expression in presence or absence of anti-IgM. The fact that the increase in EBI2 RNA expression in anti-IgM-treated cells was not evident at the protein level perhaps suggests any *EBI2* RNA induction is suppressed by artefactual down-modulation of cell surface expression in culture conditions.

In summary, the overall picture is that EBI2 is expressed at low levels on CLL cells and this may not be adequate to trigger functional/signalling responses. Moreover, results

demonstrate minimal evidence for cross-talk since there was no change in EBI2 expression after with AQX-435 and highly variable effects anti-IgM. However, it is important to consider technical challenges that arose, which complicated analysis and limit the conclusions that can be drawn.

Chapter 5: Gene expression profiling reveals a role for cholesterol efflux in AQX-435-induced apoptosis of CLL cells

5.1 Introduction

Antigen engagement of BCR on CLL cells engages pro-proliferation and survival pathways that result in accumulation of malignant cells. A common event in various subtypes of B-cell cancers is the downstream activation of PI3K-dependent cascades which activate onco-proteins such as MYC to ensure malignant B-cell survival and proliferation. This can be driven by either mutations within the PI3K pathway, or inappropriate activation of signalling pathways (e.g. via the BCR). Currently, the PI3Kδ isoform specific inhibitor Idelalisib is approved for treatment of CLL and follicular lymphoma. Idelalisib interferes with B-cell signalling by preventing the PI3K-dependent conversion of the plasma membrane inositol lipid $PI(4,5)P_2$ to $PI(3,4,5)P_3$. This, in turn, decreases the membrane recruitment and subsequent activation of key downstream mediators such as BTK and PLCγ2.

In this chapter, I have explored an alternate pharmaceutical strategy to target PI3K signalling in malignant B cells via activation of SHIP1 (INPP5D), an inositol lipid phosphatase which catalyses the conversion of $PI(3,4,5)P_3$ to $PI(3,4)P_2$ (Scharenberg et al., 1998). Like PI3K inhibition, SHIP1 activation reduces the accumulation of $PI(3,4,5)P_3$ and thereby suppresses downstream pro-tumour signalling. However, SHIP1 is also thought to impose direct "inhibition" on B cells via $PI(3,4)P_2$ accumulation which has distinct inhibitory second messenger properties (Landego et al., 2012). Therefore, I used gene expression profiling to characterise the effects of AQX-435 on CLL cells.

5.2.1 Hypothesis

The chemical activator AQX-435 will characterise novel pathways affected by SHIP1 activation during BCR signalling in CLL cells.

5.2.2 Goals and Aims

The overall goal of the experiments in this chapter was to use RNA-Seq to investigate the effect of AQX-435 on mRNA expression in CLL cells, and to then probe the functional significance of these responses.

There were three specific aims;

1. Determine effects of AQX-435 and idelalisib on anti-IgM-induced gene expression
2. Identify AQX-435-specific effects on gene expression
3. To investigate functional consequences of AQX-435-induced gene expression changes in CLL cells

5.3 Analysis of effects of AQX-435 on anti-IgM-induced signalling in CLL cells

The main goal of the experiments described in this chapter was to use RNA-Seq data to gain insight into the effects of AQX-435 on CLL cells. However, before this analysis was performed, I carried out experiments to confirm the inhibitory effects of AQX-435 on anti-IgM-induced signalling by analysis of AKT phosphorylation, previously shown to be inhibited by AQX-435 in CLL cells (Packham et al., 2016 ASH abstract, unpublished). In addition, I analysed auto-phosphorylation of SYK on Y525/Y526. This is because SYK activation lies upstream of PI3K and would, therefore, not be expected to be affected by either idelalisib or AQX-435.

CLL cells were pre-treated with AQX-435 or idelalisib for 1 hour and then stimulated with bead-bound anti-IgM. The concentrations of AQX-435 and idelalisib (30 μM and 10 μM, respectively) were selected based on previous experiments in the host laboratory (Packham et al., 2016 ASH abstract, unpublished) and, for idelalisib, ensured effective target inhibition (Figure 3.14). Cells were analysed by immunoblotting at 2 or 15 minutes following stimulation for analysis of phosphorylation of SYK and AKT, respectively. For AKT, I analysed phosphorylation at the Ser^{473} site because modification at this site is more readily detected using AKT signalling-specific antibodies. However, previous experiments in the host laboratory have shown that inhibition of Ser^{473} phosphorylation by AQX-435 is accompanied by concurrent inhibition of Thr^{308} phosphorylation (Packham et al., 2016 ASH abstract, unpublished). The experiment was performed using three separate CLL samples, all of which were considered as anti-IgM signal responsive based on analysis of iCa^{2+} mobilisation. However, there was still variation in the extent of anti-IgM-induced phosphorylation between samples. Therefore, following quantitation, the extent of phosphorylation in anti-IgM/DMSO-treated cells was set to 1.0, allowing direct comparison of inhibitor effect between samples.

Immunoblot analysis (Figure 5.1), confirmed that AQX-435 and idelalisib effectively decreased induction of AKT phosphorylation, consistent with reduced accumulation of $PI(3,4,5)P_3$. Importantly, neither compound inhibited the proximal auto-phosphorylation of SYK. Thus, the selected concentrations of compounds are sufficient to reduce $PI(3,4,5)P_3$-mediated signalling. Moreover, analysis of SYK confirms that AQX-435 does not act to suppresses anti-IgM signalling per se, but acts downstream of SYK.

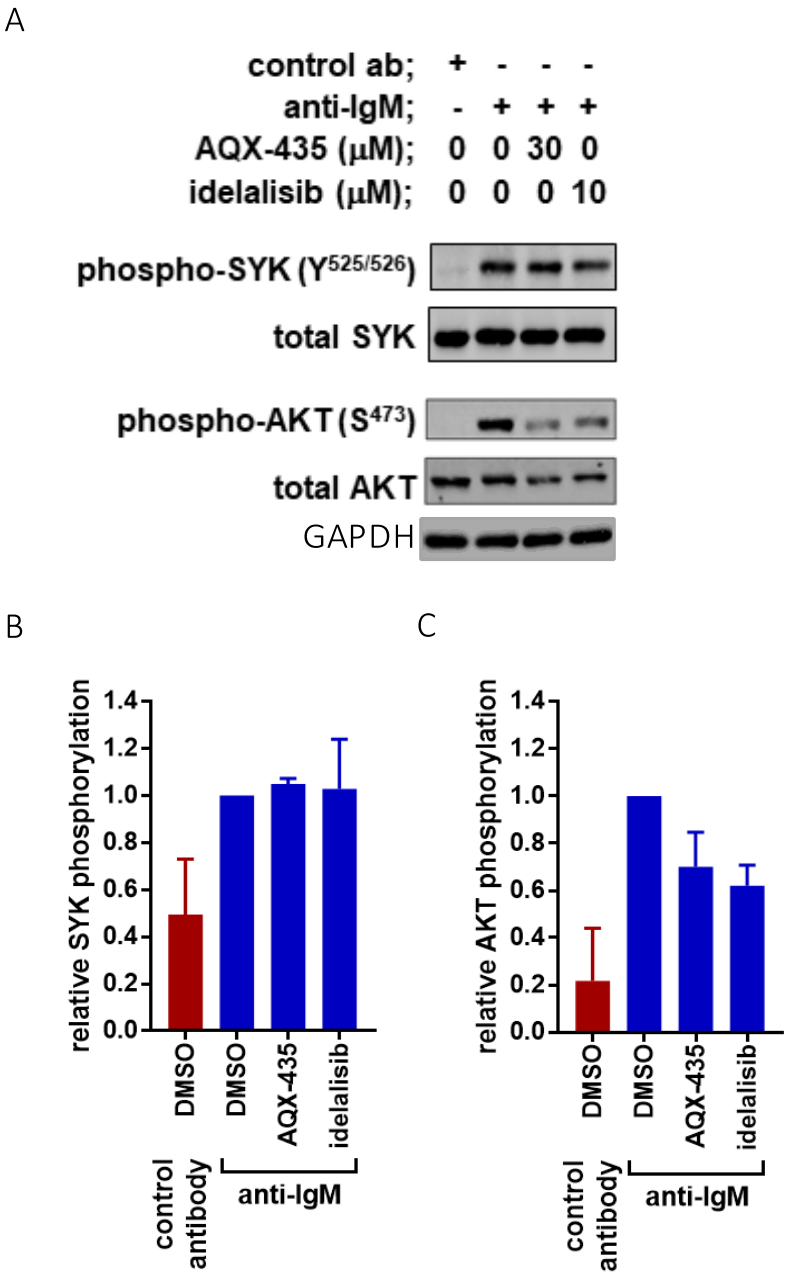

Figure 5.1. Effect of AQX-435 on anti-IgM-signalling in CLL samples

CLL samples (n=3) were pre-treated with AQX-435 (30 μM), idelalisib (10 μM) or DMSO as a control for 1 hour and then stimulated with bead-bound anti-IgM or control antibody. Cells were collected for immunoblot analysis after 2 (SYK) or 15 (AKT) minutes. Figure show (A) representative immunoblot analysis and (B, C) quantitation for all samples analyzed. Graphs show mean (±SD) phosphorylation with values for anti-IgM/DMSO-treated cells set to 1.0.

5.4. RNA-Seq analysis of CLL samples

5.4.1. Experimental overview and initial bioinformatical analysis

To investigate regulation of gene expression in CLL cells, I performed bioinformatical analysis of RNA-Seq data generated by Dr Elizabeth Lemm. The experiment used six CLL samples all of which were considered as anti-IgM signal responsive (Table 5.1). Each sample was pre-treated with AQX-435 (30 μM), idelalisib (10 μM) or DMSO for 1 hour, and then incubated with bead-bound anti-IgM or control antibody for a further 6 hours. Total RNA was prepared and RNA-Seq analysis was performed by the Oxford Genomics Centre using an Illumina sequencing platform.

Table 5.1 Details of samples used for RNA-Seq

Sample	*IGHV* mutation status[a]	*IGHV* gene usage	$CD5^+/CD19^+$ cells (%)	sIgM (MFI)	Anti-IgM signal capacity (%)[b]
351C	M	IGHV3-66*01 F, or IGHV3-66*04 F	97	34	79
563C	M	IGHV3-30-3*01 F	88	45	81
621B	M	IGHV1-3*01	93	49	49
781A	M	IGHV1-8*01 F	87	43	53
805	U	IGHV1-69*06	87	126	49
882	U	IGHV1-8*01 F	85	96	34

[a]M, mutated; U, unmutated. [b]Percent responding cells by iCa^{2+} analysis (Mockridge et al., 2014). Data was provided by the Southampton Tumour Bank.

Initial quality control, mapping of reads and identification of differentially expressed genes was performed by Dr Dean Bryant, an experienced bioinformatician within the group, as outlined in Appendix B. Dr Bryant also performed principal component analysis (PCA) and prepared some heat maps for initial visualisation of the data. I interpreted the data using these outputs before moving on to perform more detailed bioinformatical analysis using Ingenuity Pathway Analysis (IPA).

PCA was used to reduce dimensionality of the data and analyse the overall effects of the different conditions on gene expression (Figure 5.2). Control antibody treated samples

clustered relatively tightly independent of treatment indicating that either drug alone had relatively modest effects on gene expression. By contrast, there was clear separation between anti-IgM/DMSO-treated and control antibody-treated (with DMSO, AQX-435 or idelalisib) suggesting that the main determinant of differential gene expression in this experiment was anti-IgM stimulation. Anti-IgM/AQX-435- and anti-IgM/idelalisib-treated samples were intermediate between control antibody and anti-IgM-treated samples, indicating that both agents attenuate, but do not fully suppress, anti-IgM-induced gene expression changes.

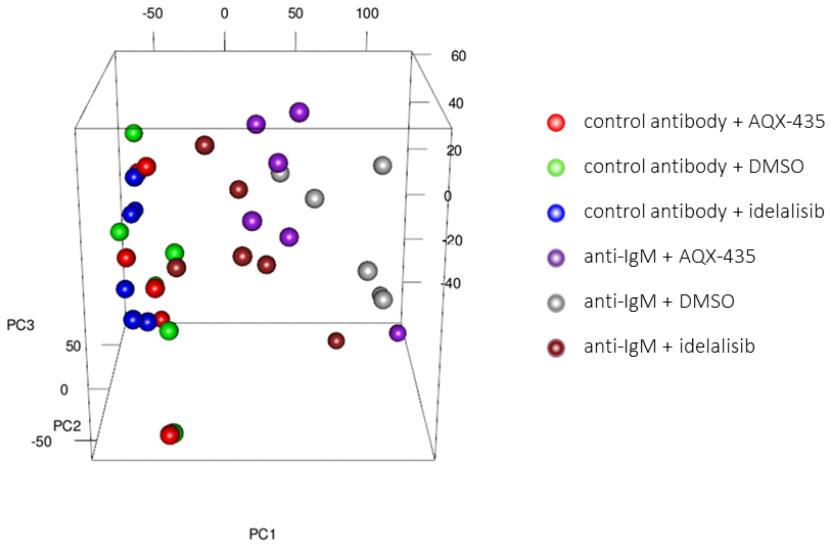

Figure 5.2. Principal component analysis
PCA was performed by Dr Dean Bryant in R using the prcomp() function. A 3D plot was produced using a custom R code based on the RGL package and is represented here in 2 dimensions with principal component 1 (PC1) as the x-axis. Each dot represents a separate gene expression dataset, colour-coded according to condition.

A heatmap showing supervised hierarchical clustering for the 2000 most differentially expressed genes is shown in Figure 5.3. Visual examination confirms that the strongest influence on gene expression was anti-IgM stimulation with clear evidence for both up-regulatory (coloured blue) and down-regulatory (coloured red) effects. Consistent with the PCA, anti-IgM-induced gene expression changes appeared to be partially reduced, but not completely blocked, by idelalisib or AQX-435. This effect was clearest for idelalisib.

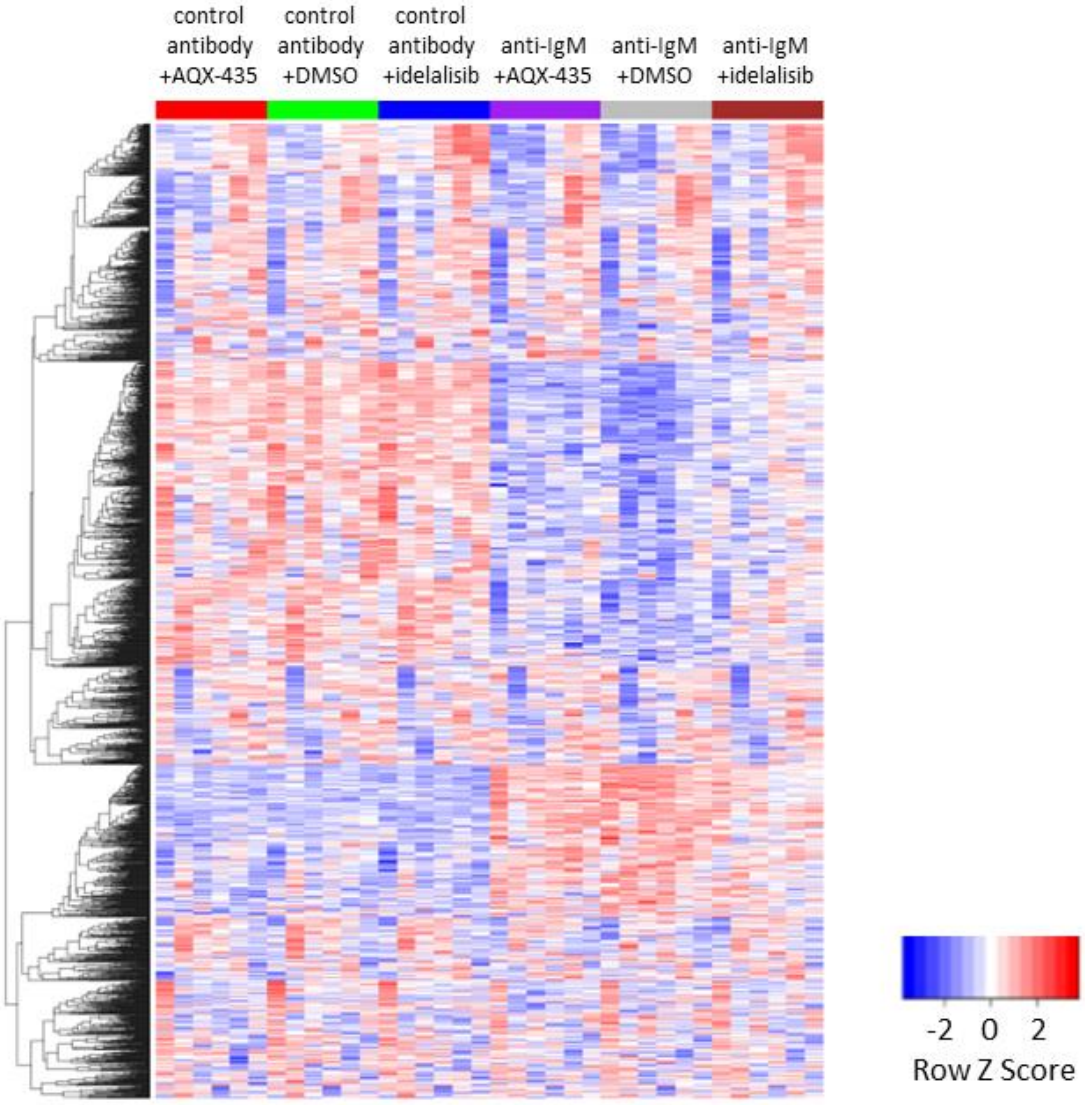

Figure 5.3. Heatmap of transcriptomics data for the 2000 most differentially expressed genes
The heatmap was prepared by Dr D Bryant using a custom code based on the ggplot2 package in R.

5.4.2. Anti-IgM-induced gene expression

I first investigated regulation of gene expression by anti-IgM by analysing genes that were differentially expressed between samples treated with control antibody/DMSO and anti-IgM/DMSO. Anti-IgM had a substantial effect on the gene expression profile of CLL cells. Using cut-offs of $\log_2$FC <-1.0/>1.0 and FDR <0.05, there were 1663 and 2187 genes that were upregulated or downregulated, respectively, in anti-IgM-treated cells (Figure 5.4).

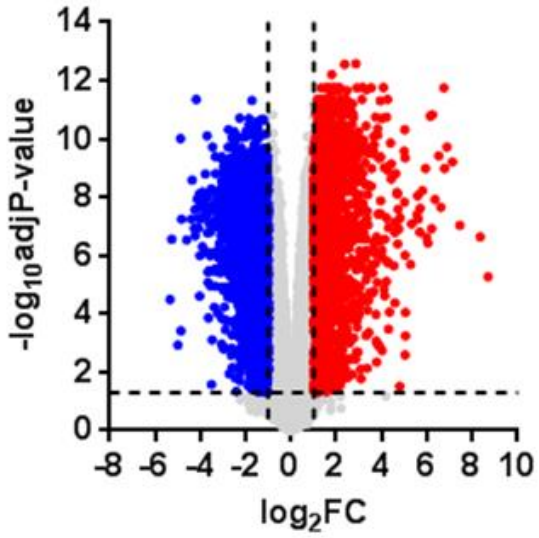

Figure 5.4. Volcano plot showing the effect of anti-IgM on gene expression in CLL samples
Each data point represents an individual gene and is coloured red if significantly upregulated (log_2FC >1.0; FDR <0.05) or blue if significantly downregulated (log_2FC <-1.0; FDR <0.05). All other data points are coloured grey.

I used IPA to probe the nature of the genes that were regulated anti-IgM. Because of the large number of regulated genes, I considered the upregulated and downregulated genes as separate gene sets. For the upregulated genes, the top 3 canonical pathways were "tRNA charging", "sirtuin 136 signalling pathway" and "unfolded protein response" (Table 5.2). Other canonical pathways of note included "protein ubiquitination pathway", "antigen presentation pathway", "purine nucleotides de novo biosynthesis II", "Nur77 [NR4A1] signalling in T-lymphocytes", and "superpathway of cholesterol biosynthesis".

Table 5.2. Selected IPA canonical pathways enriched in the anti-IgM-induced gene expression signature

Ingenuity Canonical Pathway[a]	Rank	p-value	Ratio	z-score[b]
tRNA charging	1	2.74×10^{-14}	0.513	4.472
Sirtuin Signaling Pathway	2	6.17×10^{-11}	0.175	1.095
Unfolded protein response	3	1.09×10^{-10}	0.357	NaN
Protein Ubiquitination Pathway	4	1.88×10^{-8}	0.162	NaN
Antigen Presentation Pathway	5	4.37×10^{-8}	0.368	NaN
Purine Nucleotides De Novo Biosynthesis II	8	1.18×10^{-6}	0.636	2.646
Nur77 Signaling in T Lymphocytes	18	7.66×10^{-5}	0.220	NaN
Superpathway of Cholesterol Biosynthesis	45	1.61×10^{-3}	0.250	2.646

[a]IPA canonical pathway analysis was performed using genes that were significantly up-regulated (log_2FC >1.0; FDR<0.05) in anti-IgM-treated cells. Of the 1663 significantly up-regulated genes, 1508

were included in the IPA analysis. [b]NaN, no activity pattern predicted. A full list of significant pathways is provided in Appendix B.

The pathways "tRNA charging", "sirtuin signalling pathway", "purine nucleotides de novo biosynthesis II" and "superpathway of cholesterol biosynthesis" were assigned positive z-scores and, therefore, predicted to be upregulated with anti-IgM stimulation. IPA analysis did not assign a predicted activity pattern for the pathways "unfolded protein response", "protein ubiquitination pathway", "antigen presentation pathway" and "Nur77 [NR4A1] signalling in T-lymphocytes".

IPA Upstream Regulator analysis predicted that the strongest driver of anti-IgM-induced gene expression was MYC ($P=7.25 \times 10^{-38}$).

For the downregulated genes, the top 3 canonical pathways were "B cell receptor signalling", "phospholipase C signalling" and "PI3K signalling in B lymphocytes" (Table 5.3). Other canonical pathways of interest included "sphingosine-1-phosphate signalling", "cAMP-mediated signalling", "p70S6K signalling", "ERK/MAPK signalling", "calcium signalling" and "CXCR4 signalling". All of these pathways had negative z-scores and were, therefore, predicted to be down-regulated in anti-IgM-treated cells.

Table 5.3. Selected IPA canonical pathways enriched in the anti-IgM-down-regulated gene expression signature

Ingenuity Canonical Pathway[a]	Rank	p-value	Ratio	z-score
B Cell Receptor Signalling	1	3.16×10^{-8}	0.196	-3.657
Phospholipase C Signalling	2	2.75×10^{-7}	0.172	-4.902
PI3K Signalling in B Lymphocytes	3	7.20×10^{-6}	0.191	-4.082
Sphingosine-1-phosphate Signalling	7	4.48×10^{-5}	0.184	-3.411
cAMP-mediated signalling	16	3.89×10^{-4}	0.140	-3.772
p70S6K Signalling	24	5.45×10^{-4}	0.159	-2.985
ERK/MAPK Signalling	42	2.53×10^{-3}	0.132	-3.657
Calcium Signalling	59	5.69×10^{-3}	0.126	-3.357
CXCR4 Signalling	69	8.36×10^{-3}	0.129	-3.300

[a]IPA canonical pathway analysis was performed using genes that were significantly down-regulated ($log_2FC < 1.0$; FDR<0.05) in anti-IgM-treated cells. Of the 2187 significantly down-regulated genes, 1845 were included in the IPA analysis. A full list of significant pathways is provided in Appendix B.

Overall, anti-IgM triggered a profound reprogramming of gene expression in CLL cells. Consistent with previous studies, the induced gene expression signature was characterised by activation of pathways linked to mRNA translation (Yeomans et al., 2016) and the unfolded protein response (Krysov et al., 2015). There was also evidence for increased metabolism, including mitochondrial metabolism (e.g. the "Sirtuin signalling pathway" which comprises multiple mitochondrial components), purine nucleotide and cholesterol biosynthesis (McCaw et al., 2017; Pallasch et al., 2008). The main predicted driver was MYC, consistent with previous studied from the host group showing induction of MYC *in vitro* following anti-IgM stimulation of CLL cells, and expression of MYC *in vivo* in CLL LN PCs (Krysov et al., 2014). The downregulated signature was dominated by reduced expression of signalling pathways, perhaps indicative of feedback inhibition of BCR signalling as a mechanism to curtail responses.

5.4.3. Effect of AQX-435 or idelalisib on anti-IgM-induced gene expression

I investigated the effect of AQX-435 or idelalisib on anti-IgM-regulated gene expression by comparing the fold change for the 3850 genes that were significantly up- or down-regulated by anti-IgM in the presence of DMSO with the fold change in expression for the same genes in the presence of anti-IgM and AQX-435 or idelalisib. Considering cut-offs of $\log_2$FC >1 and FDR<0.05, of the 1663 genes that were significantly induced by anti-IgM alone, 513 and 851 were no longer significantly induced in the presence of AQX-435 or Idelalisib, respectively. Similarly, of the 2187 genes that were significantly repressed by anti-IgM ($\log_2$FC <-1, FDR<0.05), 933 and 1535 were no longer significantly repressed in the presence of AQX-435 or idelalisib, respectively.

To further investigate the effect of idelalisib/AQX-435 on anti-IgM-regulated gene expression, I plotted x/y graphs showing the fold change in gene expression for anti-IgM alone versus anti-IgM with idelalisib or AQX-435 for each of the 3850 genes that were significantly up- or down-regulated by anti-IgM ($\log_2$FC>1/<-1, FDR<0.05) (Figure 5.5). Data points for genes that were no longer significantly differently expressed (FDR>0.05) in the

presence of AQX-435/idelalisib were coloured grey. Genes that were significantly induced ($log_2FC>1$, FDR<0.05) by anti-IgM alone that remained significantly regulated in the presence of AQX-435/idelalisib independent of log_2FC (i.e. any log_2FC, FDR<0.05) were coloured red whereas genes that were significantly repressed (i.e. $log_2FC<-1$, FDR<0.05) by anti-IgM alone that remained significantly regulated in the presence of AQX-435/idelalisib independent of log_2FC (i.e. any log_2FC, FDR<0.05) were coloured blue. I also plotted the line of equality (i.e. x=y) and the line-of-best fit from linear regression analysis.

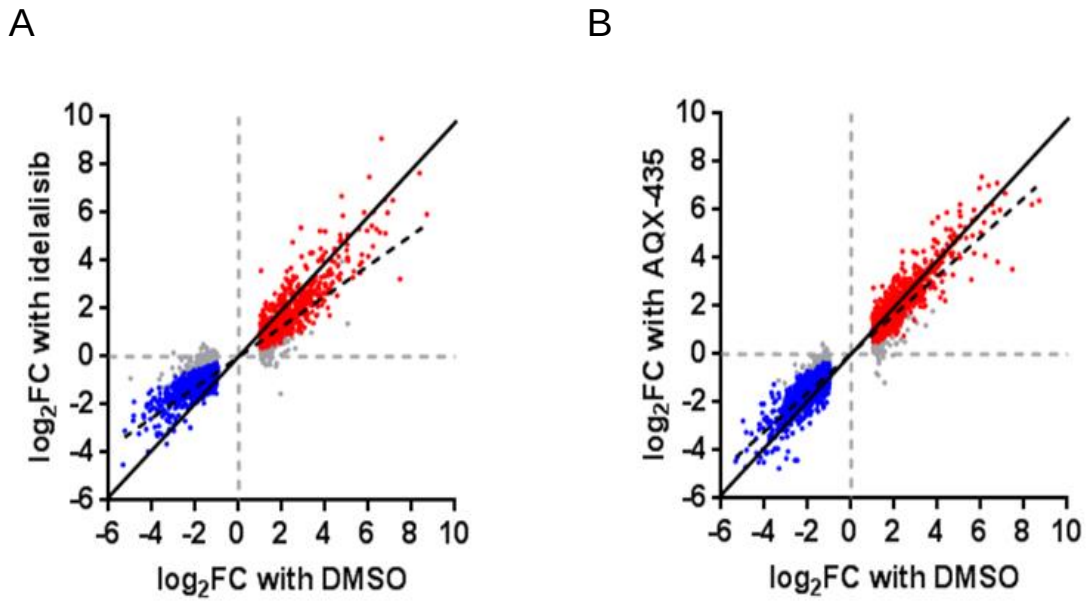

Figure 5.5. Effects of idelalisib or AQX-435 on anti-IgM-regulated gene expression
Graphs show fold difference in gene expression (log_2FC) for the 3850 genes that were differentially expressed (log_2FC <-1/>1, FDR<0.05) between control antibody (+DMSO) and anti-IgM (+DMSO) treated cells, for DMSO (x-axes) versus (A) idelalisib or (B) AQX-435 (y-axes). The line of equality (solid) and line-of-best fit (dotted) are also shown. Genes that were still significantly regulated (FDR<0.05) in the presence of idelalisib/AQX-435 were coloured red or blue (for anti-IgM induced or repressed genes, respectively) whereas genes that were no longer significantly regulated in the presence of idelalisib/AQX-435 were coloured grey.

This analysis revealed that the regulation (up or down) of the majority of genes by anti-IgM was reduced in the presence of idelalisib such that the line-of-best fit had a gradient <1.0 (Figure 5.5A). Thus, idelalisib partially attenuates the majority of the anti-IgM-induced gene expression signature. A similar result was observed for AQX-435, but the difference between the line of equality and the line-of-best fit was smaller, indicating a more modest effect overall (Figure 5.5B).

To quantify the overall effect of idelalisib/AQX-435, I compared the fold induction for all 1663 anti-IgM-induced genes and the fold repression for the all 2187 anti-IgM-repressed genes in the presence or absence of each drug (Figure 5.6). Overall, idelalisib reduced the extent of induction of gene expression by 30% and the extent of repression of gene expression by 48%. AQX-435 reduced the induction of gene expression by 13% and the repression of gene expression by 26%. The differences between the fold induction/repression in the presence or absence of either drug were highly statistically significant (P<0.0001, paired Student's t-test).

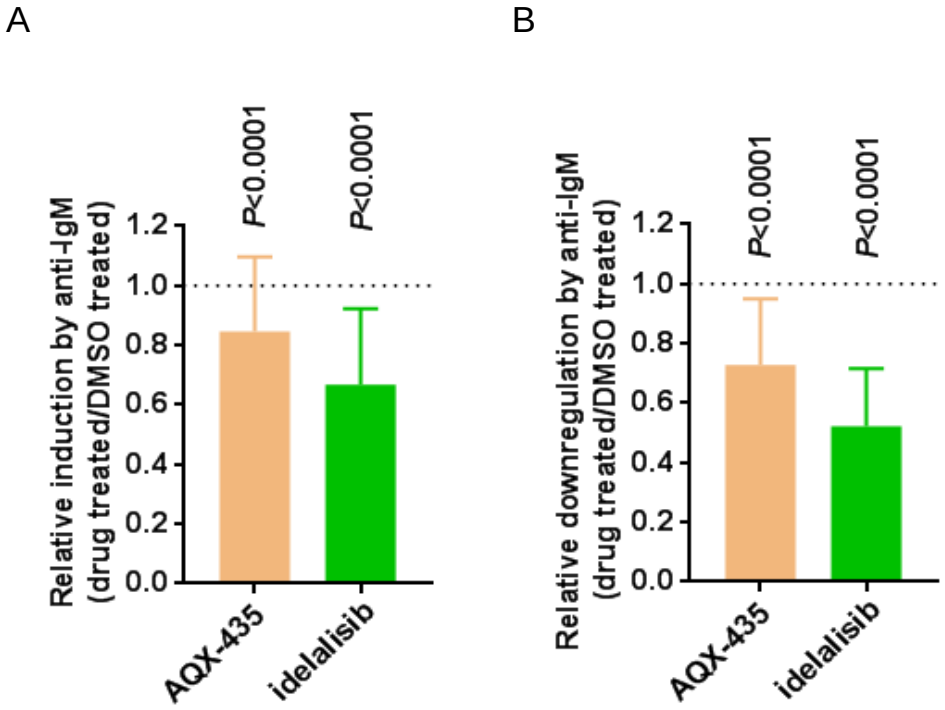

Figure 5.6. Effect of AQX-435 or idelalisib on anti-IgM-regulated gene expression
Graphs show the mean (±) relative fold induction (A) or repression (B) of gene expression in the presence of AQX-435 or idelalisib with values for each of the 1663 anti-IgM-induced or 2187 anti-IgM-repressed genes set to 1.0 for anti-IgM/DMSO-treated samples. The statistical significance of the difference in expression between control and AQX-435/idelalisib-treated cells was determined using Student's t-tests.

In summary, idelalisib and AQX-435 share the ability to reduce both induction and repression of gene expression by anti-IgM. Rather than ablating regulation a subset of the anti-IgM-regulated genes, both drugs attenuate the majority of the anti-IgM-regulated gene

expression signature. Effects were observed for both compounds, but were more dramatic for idelalisib.

5.4.4. Identification of an AQX-435-specific gene expression signature

The next step was to identify potential specific effects of AQX-435 on transcription in the absence of anti-IgM. Dr Bryant performed differential gene expression analysis to identify genes that were significantly differently expressed between control antibody/DMSO and control antibody/AQX-435 treated samples. A heatmap showing supervised hierarchical clustering for the top 100 differentially expressed genes is shown in Figure 5.7 and a volcano plot showing data for all genes is shown in Figure 5.8.

Visual examination shows that these differentially expressed genes were predominantly induced in the presence of AQX-435. Importantly, these AQX-435-regulated genes were not affected by idelalisib and, therefore, appear to represent an AQX-435-specific response. Using previously established cut-offs (log_2FC <-1/>1, FDR<0.05), AQX-435 significantly increased expression of 36 genes and reduced expression of 36 genes (Figure 5.8).

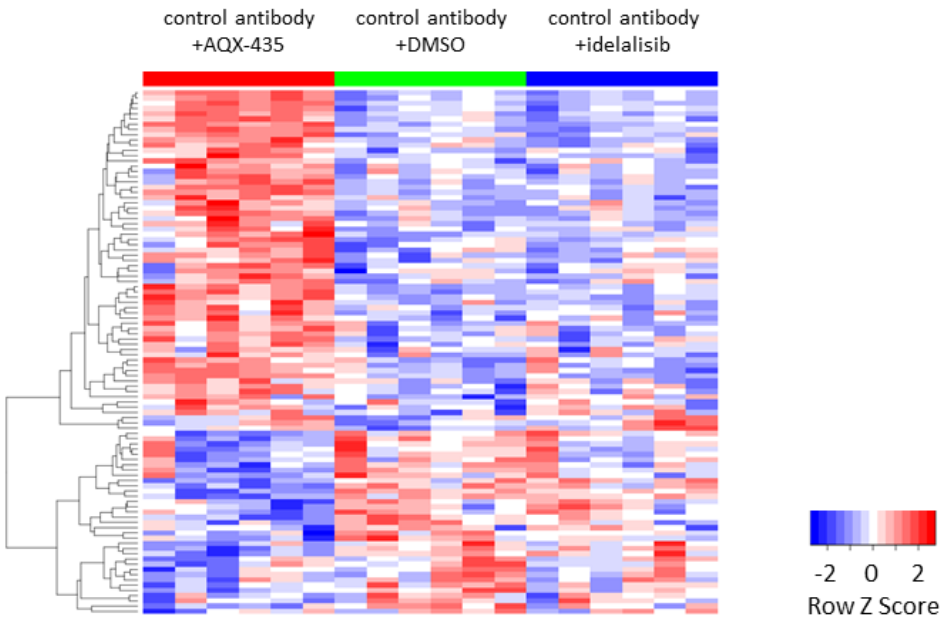

Figure 5.7. Heatmap showing expression of the 100 most differentially expressed genes in response to AQX-435.
The heatmap was prepared by Dr D Bryant using a custom code based on the ggplot2 package in R.

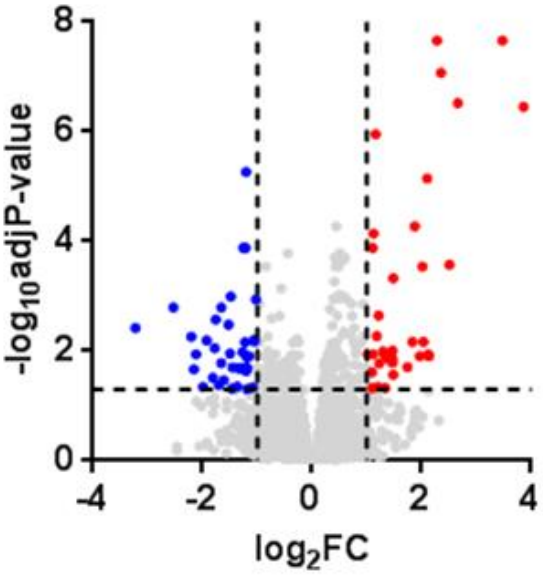

Figure 5.8. Volcano plots showing the effect of AQX-435 on gene expression in the absence of anti-IgM

Each data point represents an individual gene and is coloured red if significantly upregulated (log_2FC >1.0; FDR <0.05) or blue if significantly downregulated (log_2FC <-1.0; FDR <0.05). All other data points are coloured grey.

I used IPA to probe the nature of the genes that were selectively regulated by AQX-435. When the entire gene-set (both up and downregulated) was analysed, there was a striking association with the "LXR/RXR activation" canonical pathway (P=3.36 $x10^{-11}$ versus 1.16 x 10^{-3} for the second ranked pathway) (Table 5.4). The positive z-scored indicated activation.

Table 5.4. IPA canonical pathways enriched in the AQX-435-regulated gene expression signature.

Ingenuity Canonical Pathway[a]	Rank	p-value	Ratio	z-score[b]
LXR/RXR Activation	1	3.36 $x10^{-11}$	0.074	0.816
Chemokine signalling	2	1.16 $x10^{-3}$	0.039	NaN
Granulocyte Adhesion and Diapedesis	3	1.38 $x10^{-3}$	0.022	NaN
Agranulocyte Adhesion and Diapedesis	4	1.75 x 10^{-3}	0.021	NaN
Cholecystokinin/Gastrin-mediated Signaling	5	2.97 $x10^{-3}$	0.028	NaN

[a]IPA canonical pathway analysis was performed using genes that were significantly differentially expressed (log_2FC <-1/>1; FDR<0.05) in AQX-435-treated cells. Of the 64 significantly regulated genes, 64 were included in the IPA analysis. [b]NaN, no activity pattern predicted.

The "LXR/RXR activation" canonical pathway relates to transcription targets of the liver X receptor (LXR) which acts a heterodimeric partner for RXR and modulates expression of

genes involved in fatty acid metabolism and cholesterol homeostasis (Janowski et al., 1996; Tontonoz and Mangelsdorf, 2003). Consistent with identification of LXR activation as the top-ranked canonical pathway, the top predicted upstream regulators included LXRα ("NRIH3"), a synthetic LXR agonist ("GW3965"), and natural LXR ligands ("24-hydroxycholesterol" and "25-hydroxycholesterol") (Table 5.5).

Table 5.5. IPA upstream regulators enriched in the AQX-435-regulated gene expression signature.

Upstream Regulator[a]	Rank	p-value of overlap
NR1H3	1	1.14×10^{-9}
GW3965	2	1.59×10^{-9}
Cholesterol	3	8.18×10^{-9}
DUB	4	1.92×10^{-8}
LSS	5	1.92×10^{-8}
25-hydroxycholesterol	6	2.08×10^{-8}
24-hydroxycholesterol	8	6.61×10^{-8}

[a]IPA upstream regulator analysis was performed using genes that were significantly differentially expressed (log_2FC <-1/>1; FDR<0.05) in AQX-435 –treated cells. Of the 64 significantly regulated genes, 64 were included in the IPA analysis.

In summary, this gene expression analysis indicates that, in addition to a shared ability of AQX-435 and idelalisib to attenuate anti-IgM-induced gene expression (via decreased PI(3,4,5)P3-mediated signalling-pi3k signaling), AQX-435 drives a specific gene expression signature related to LXR activation that is not observed with idelalisib (Figure 5.8.1). Pathway analysis suggests that this response may be mediated, at least in part, by activation of LXR-dependent transcription. Furthermore idelalisb seems to drive downregulation of pathways predominantly of cholesterol biosynthesis and the ''Unfolded protein response'' which maintain protein homeostasis vital for tumorigenesis. I have outlined the genes that are affected by idelalisb and AQX-435 that are relevant and critical to this project in a venn diagram below (Figure 5.8.1).

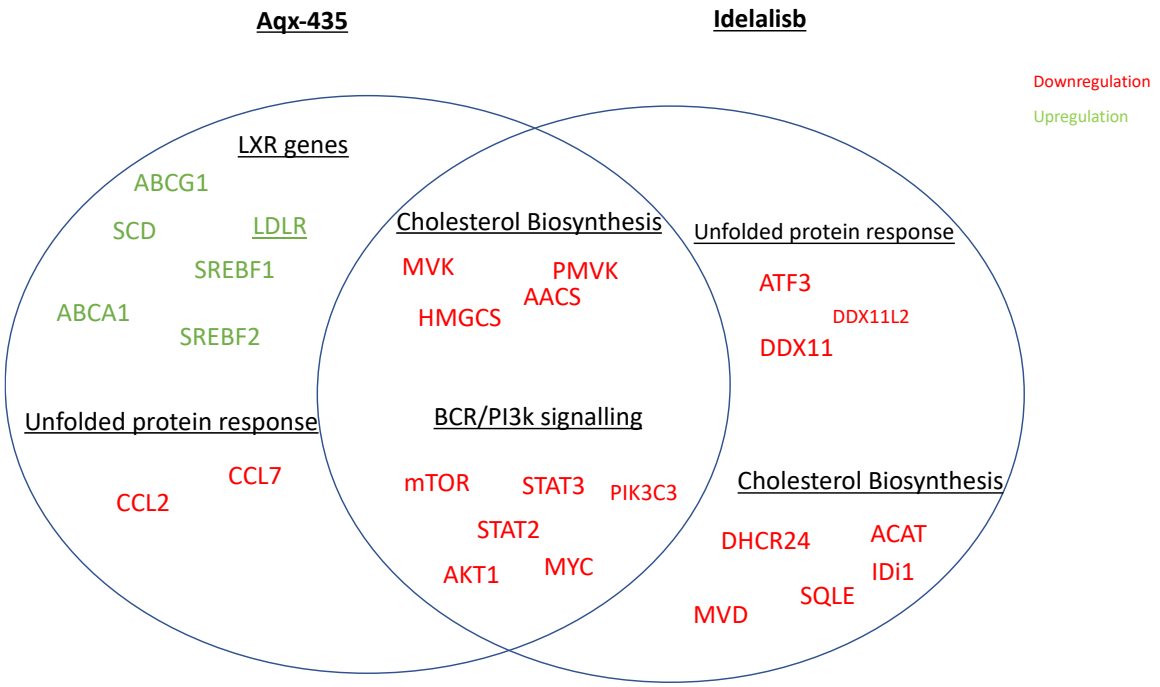

Figure 5.8.1 Venn diagram representing critical gene expression changes with Aqx-435 and idelalisb

5.4.5 Effect of anti-IgM and AQX-435 on LXR target genes and cholesterol biosynthesis

I next analysed the effect of anti-IgM and AQX-435 on the expression of specific LXR target genes. A major function of LXR is to control cellular levels of cholesterol and I, therefore, focused on analysis of LXR target genes involved in cholesterol homeostasis. This included *ABCA1* and *ABCG1* which encode membrane transporters which promote cholesterol efflux (reverse cholesterol transport) and *MYLIP* which encodes for the E3 ubiquitin ligase MYLIP/IDOL that induces degradation of the low density lipoprotein receptor LDLR and thereby reduces cellular uptake of cholesterol (Figure 5.9 A,B) (Hong et al., 2010). I also analysed expression of the LXR-target genes *SREBF1* and *SCD* (Bensinger et al., 2008). *SREBF1* is a transcription factor and acts as a master regulator of de novo lipogenesis, whereas *SCD* catalyses the rate-limiting step in the formation of monounsaturated fatty acids. Increased lipogenesis is also important for cholesterol homeostasis since it provides substrates to counter excess cholesterol via storage of cholesterol esters. Finally, I analysed

expression of genes encoding *CCL2* and *CCL7*, chemokines that are downregulated by LXR (Castrillo et al., 2003).

Figure 5.9. Regulation of cholesterol efflux/influx by LXR
LXR activation leads to a net efflux of cholesterol by (A) increasing expression of ABCA1 and ABCG1 which export cholesterol to high density lipoprotein (HDL). (B) LXR also induces expression of MYLIP/IDOL, an ubiquitin E3-ligase which targets the low density lipoprotein (LDL) receptor (LDLR) for degradation and thereby reduces cholesterol uptake.

Given the key role of LXR in regulation of cholesterol homeostasis, it was interesting to note that the "Superpathway of Cholesterol Biosynthesis" was identified as a canonical pathway

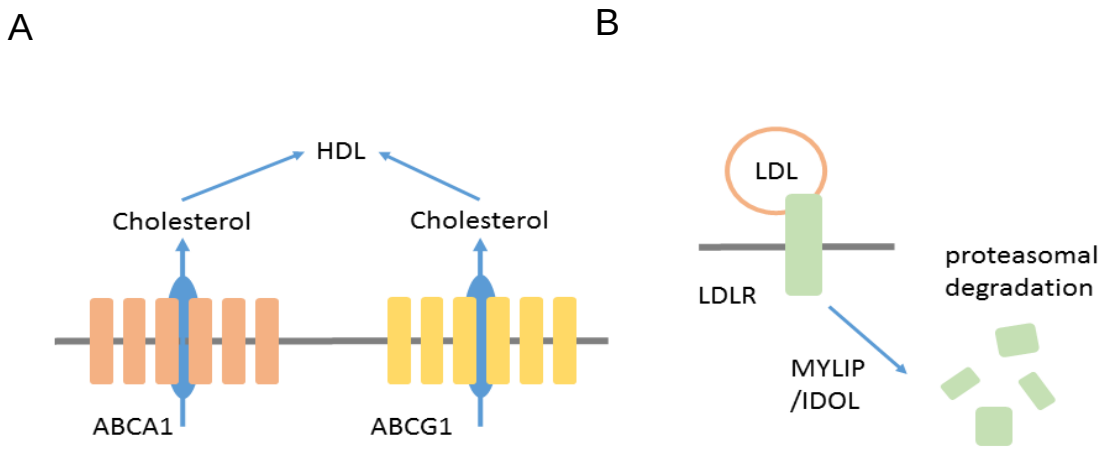

in IPA analysis of the anti-IgM-induced gene expression signature (Table 5.2). This suggested that, in addition to effects of AQX-435 on cholesterol homeostasis in the absence of stimulation, AQX-435 may also influence modulation of cholesterol-related pathways downstream of the BCR. Therefore, in addition to LXR target genes, I analysed expression of genes encoding all enzymes in the cholesterol biosynthetic pathway (Figure 5.10). Finally, I also analysed expression of *SREBP2* (which encodes a master regulator of cholesterol biosynthesis that is closely related to *SREBP1*) and two other genes involved in fatty acid synthesis (*ACACA* and *FASN*).

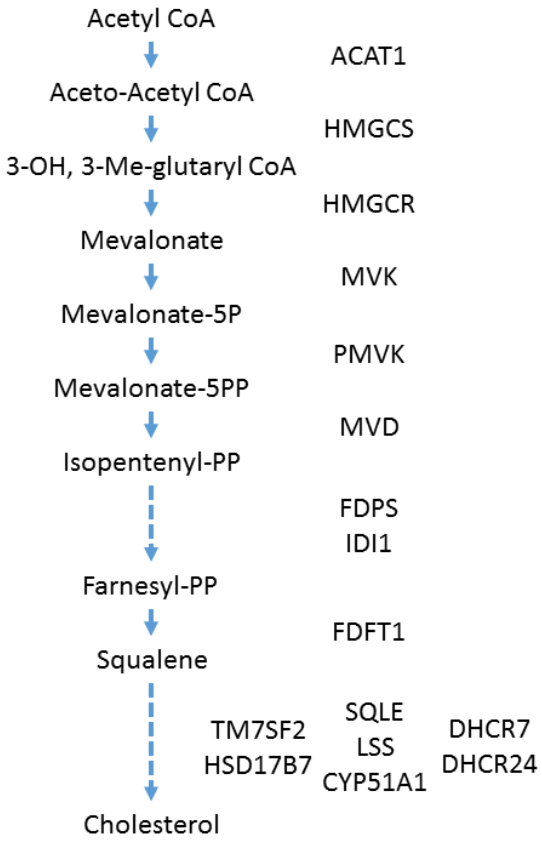

Figure 5.10. Cholesterol biosynthetic pathway
Dotted lines represent steps with multiple intermediates. 3-Hydroxy-3-Methylglutaryl-CoA Reductase (HMGCR) catalyses the synthesis of mevalonate and is rate-limiting for cholesterol biosynthesis whereas squalene epoxidase (SQLE) catalyses conversion of squalene to squalene epoxide which is the first synthetic intermediate committed for cholesterol biosynthesis.

To visualise changes in gene expression for each condition, fold differences were calculated and presented as heat maps. The specific comparisons were between (i) control antibody/DMSO and control antibody/AQX-435 or idelalisib-treated cells to show the effects of compounds alone; (ii) control antibody/DMSO and anti-IgM/DMSO-treated cells to show the effect of anti-IgM; and (iii) anti-IgM/DMSO and anti-IgM/AQX-435 or idelalisib-treated cells to show the effect of compounds on response to anti-IgM (Figure 5.11).

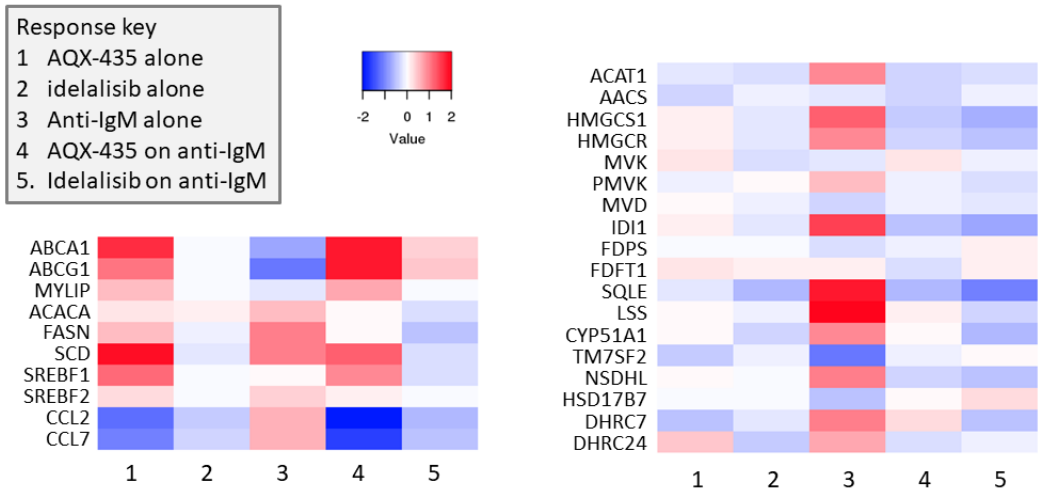

Figure 5.11. Heat maps summarising effects of anti-IgM and/or AQX-435/idelalisib on gene expression in CLL samples

Heatmaps showing differences in gene expression between cells treated with (1) control antibody/DMSO and control antibody/AQX-435, (2) control antibody/DMSO and control antibody/idelalisib, (3) control antibody/DMSO and anti-IgM/DMSO, (4) anti-IgM/DMSO and anti-IgM/AQX-435 and (5) anti-IgM/DMSO and anti-IgM/idelalisib. Each cell is coloured according to log_2FC values. Images were prepared using Heatmapper (http://www.heatmapper.ca/).

Consistent with IPA analysis, the heatmaps revealed strong activation of biosynthetic pathways following sIgM activation (see column 3 in Figure 5.11). In particular, there was clear activation of the cholesterol and fatty acid biosynthetic pathways. Anti-IgM increased expression of *SREBP2* (master regulator of cholesterol biosynthesis) and expression of more than half of enzymes involved in cholesterol biosynthesis were increased by >50%. These changes in gene expression were decreased by both AQX-435 and idelalisib (with the exception of *SCD*) suggesting that this biosynthetic signature is largely mediated via PI(3,4,5)P3 -dependent signalling (columns 4 and 5). In addition to increased cholesterol biosynthesis, anti-IgM also decreased expression of *ABCA1, ABCG1* and *MYLIP*, indicating further adaption to accumulate/retain intracellular cholesterol.

In cells treated with AQX-435 alone (column 1), there was strong evidence for regulation of LXR-target genes, including induction of *ABCA1, ABCG1, MYLIP, SCD* and *SREBP1*. These changes in gene expression were not observed in cells treated with idelalisib (column 2), confirming that LXR-activation in specific for AQX-435. Importantly, *ABCA1* and *ABCG1* were still induced in cells treated with anti-IgM and AQX-435, indicating a dominant effect of AQX-435. Similar results were obtained for the LXR-repressed target genes, *CCL2* and *CCL7*.

Taken together, these analyses reveal that anti-IgM stimulation results in PI(3,4,5)P3 -mediated activation of cholesterol biosynthesis and inhibition of cholesterol efflux. This is consistent with the known requirement for PI3K to drive synthesis of cholesterol to support cell division (Porstmann et al., 2008; Du et al., 2006; Horton et al., 2006). AQX-435 appears to counter accumulation of cholesterol by (i) suppressing PI(3,4,5)P3 -mediated activation of cholesterol biosynthesis and (ii) driving LXR-dependent cholesterol efflux via *ABCA1/ABCG1.*

5.5. Confirmation of LXR activation by AQX-435

I performed Q-PCR to confirm activation of LXR-dependent gene expression, initially focusing on expression of *SREBF1* in 7 CLL samples, 1 of which had been included in the RNA-seq experiment (351C). *SREBF1* RNA was induced following 6 hours of treatment with AQX-435 by >33% in 6/7 of the samples (Figure 5.12A). The median fold induction was ~2-fold but the extent of induction varied greatly between responding samples (0.36-fold to 63-fold increase). Using a non-parametric Wilcoxon test, the expression of *SREBF1* RNA between control and drug treated cells was significantly different (P=0.0156).

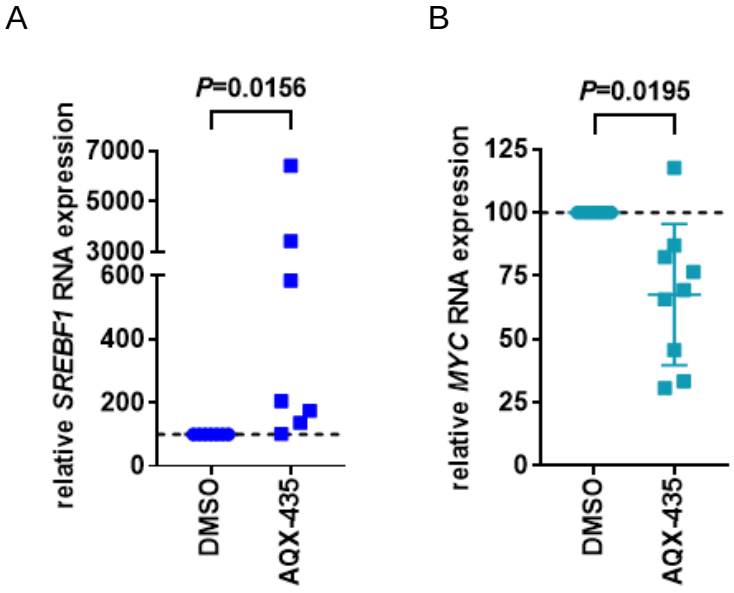

Figure 5.12. Effect of AQX-435 on *SREBF1* and *MYC* RNA expression in CLL samples
CLL samples (n=7 for SREBF1 and n=9 for MYC) were treated with AQX-435 (30 µM) or DMSO for 6 hours before expression of (A) SREBP1 and (B) MYC was analysed using Q-PCR. Graphs show relative RNA expression with values for DMSO-treated cells set to 100 for each individual sample, as well as mean and SD. The statistical significance of the difference in expression between DMSO and AQX-435-treated samples is shown (Wilcoxon sign rank test).

As an additional control, I also analysed expression of *MYC* RNA which would not be expected to be induced by treatment by AQX-435 alone. In contrast to *SREBF1*, AQX-435 significantly reduced expression of MYC RNA (Figure 5.12B).

Parallel studies performed by Dr Lemm in the group confirmed that AQX-435 also increased expression of other LXR target genes (*ABCA1* and *SCD1*) in primary CLL samples (unpublished data). Taken together, these Q-PCR studies confirmed that AQX-435 increased expression of LXR-dependent gene expression in CLL samples.

I next performed time course experiments to explore the kinetics of AQX-435-induced LXR activation. These experiments were performed using the TMD8 cell line (derived from ABC-DLBCL) and, therefore, also served to determine whether this effect of AQX-435 was specific for CLL cells or was observed in other cell models. TMD8 cells were treated with AQX-435 at 30 µM for up to 24 hours and expression of the LXR targets; *ABCA1, SCD* and *SREBF1* were analysed by Q-PCR. I also analysed expression of *HMGR1* and *SQLE* (cholesterol biosynthesis) and *MYC* as additional controls.

Q-PCR analysis demonstrated that AQX-435 increased expression of all three LXR target genes in TMD8 cells (Figure 5.13 A-C). The response was first detected at 3 hours following addition of AQX-435 and peaked at 3-6 hours. RNA levels declined thereafter. Therefore, AQX-435 induces a rapid, but transient activation of LXR-dependent gene expression. Moreover, the response is not specific for CLL cells but is also observed in the TMD8 lymphoma-derived cell line.

In contrast to the LXR-target genes, expression of cholesterol biosynthetic genes was not substantially increased by AQX-435 and levels declined below the starting point at later time points (Figure 5.13 D, E). Expression of MYC was also rapidly downregulated in AQX-435-treated cells (Figure 5.13 F)

Overall, these results confirm that AQX-435 activates LXR-dependent transcription.

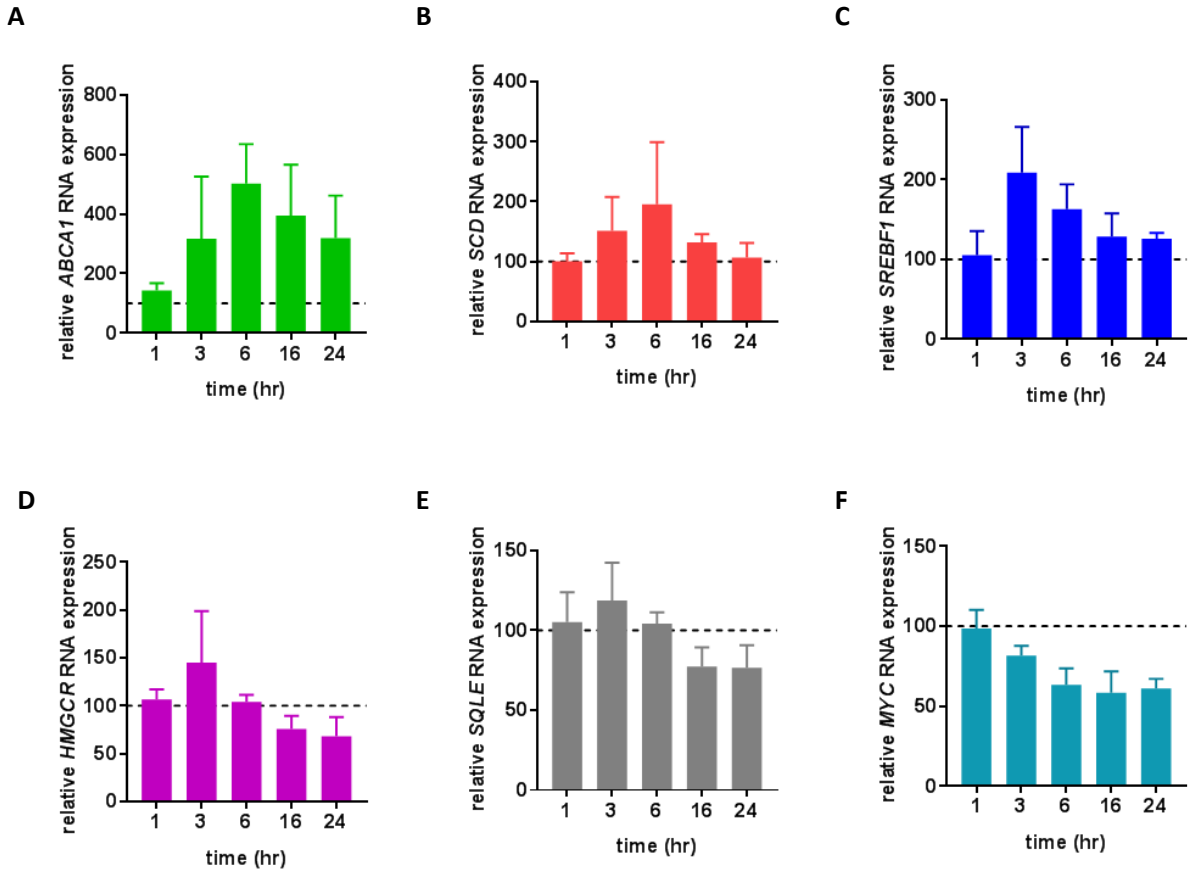

Figure 5.13. Effect of AQX-435 on gene expression in TMD8 cells
TMD8 cells were treated with AQX-435 (30 µM) or DMSO for up to 24 hours before analysis of expression of the indicated genes using Q-PCR. Graphs show mean gene expression (±SD) derived from three independent experiments with values for DMSO-treated cells set to 100 for each time point.

5.6 Effect of mevalonic acid on AQX-435-induced apoptosis

LXR activation leads to depletion of cellular cholesterol (via induction of cholesterol efflux pumps, ABCA1 and ABCG1) and in other cell systems, LXR-induced apoptosis can be reversed by supplementing cells with mevalonic acid (MVA), a key intermediate in the cholesterol biosynthesis pathway (Figure 5.10) (Yeganeh et al., 2014). To investigate the functional significance of LXR activation in CLL cells, I, therefore, analysed the effect of MVA on spontaneous and AQX-435-induced apoptosis.

I first investigated the effect of MVA on spontaneous apoptosis. MVA was tested at several concentrations (500 uM, 1 mM, 5mM). As expected, culturing of CLL cells for 24 hours was accompanied by spontaneous cell death (relative reduction in viability of ~40% to 50% compared to cells at the start of the experiment) which was unaffected by DMSO (control). MVA reduced apoptosis at all concentrations tested in all patients samples (Figure 5.14). However, the differences in viability between control and MVA treated in all patient samples cells were overall modest (~15% improvement in relative viability). Thus, spontaneous apoptosis of CLL cells is only modestly affected by MVA. Based on these results, a concentration of 5 mM was selected for the next series of experiments investigating effects of MVA on AQX-435-induced CLL cell apoptosis.

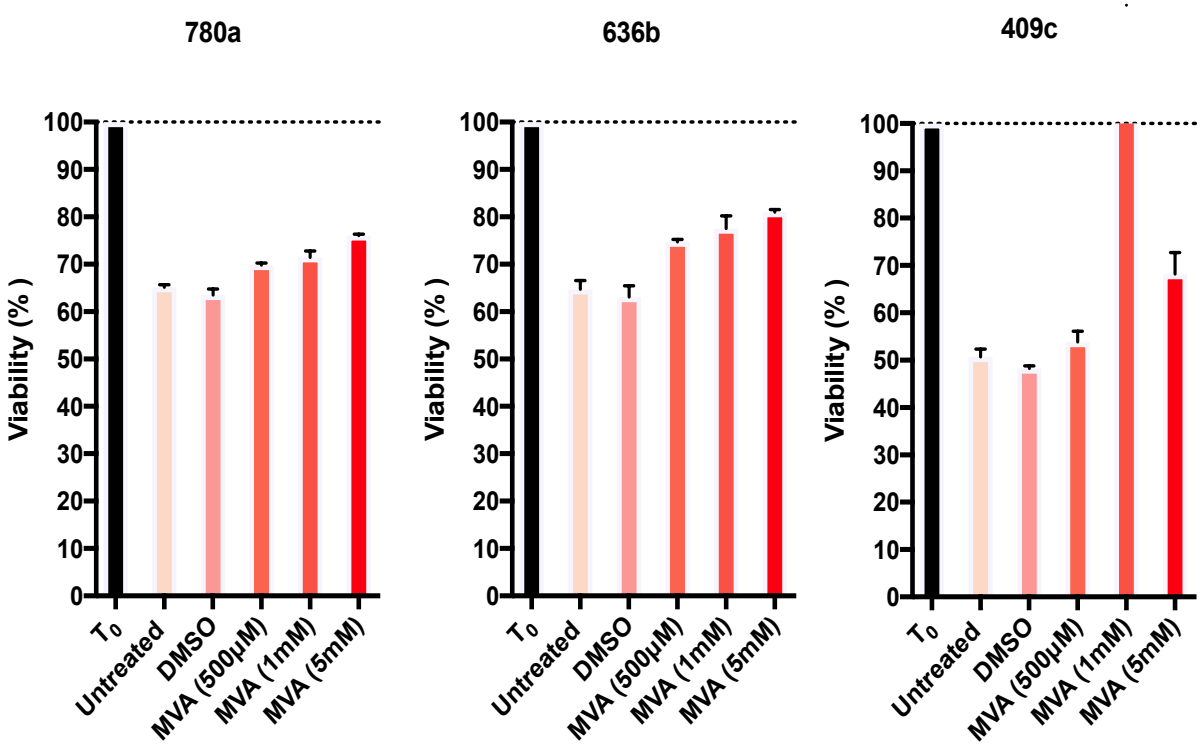

Figure 5.14 Effect of MVA on CLL cell viability
CLL samples (n=3) were treated with the indicated concentrations of MVA, DMSO or left untreated in duplicates. After 24 hours, cell viability was measured using Annexin-V/PI staining. Cell viability was also analysed at the start of the experiment (0 hours). Graph shows mean (±SD) relative viability ($AnnexinV^-/PI^-$ cells) with values for cells at the start of the experiment (T_0) set to 100 %.

To investigate the effect of MVA on AQX-435-induced apoptosis, CLL cells were treated with AQX-435 (10, 20, 30 µM) alone or in the presence of MVA (5 mM) for 24 hours. Cell viability was quantified using AnnexinV/PI staining. Both the extent of spontaneous and AQX-435-induced apoptosis varied between each sample and are shown in Appendix C. Interestingly,

overall MVA substantially reduced AQX-435-induced apoptosis (up to 30µM inhibition) in the majority of patient samples (Figure 5.15). However, MVA significantly reduced AQX-435-induced apoptosis at higher concentrations (20 and 30 µM) where AQX-435 induces greater levels of apoptosis. Thus, depletion of intracellular cholesterol by LXR activation appears to play a substantial role in AQX-435-induced apoptosis of CLL cells.

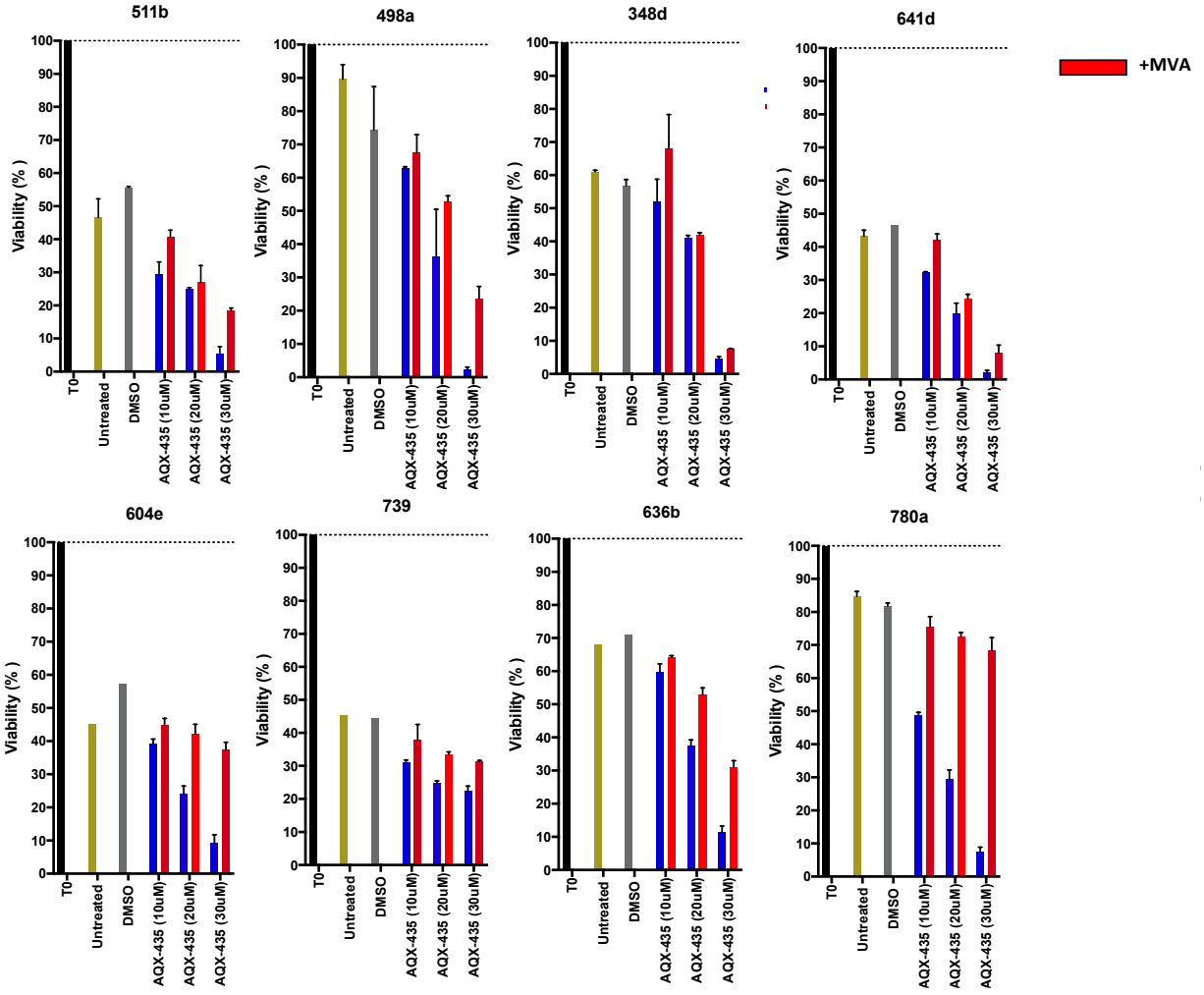

Figure 5.15. Effect of mevalonic acid on CLL cell apoptosis

CLL samples (n=8) were treated in duplicate with the indicated concentrations of AQX-435 in the presence or absence of MVA (5 mM), or left untreated as control. After 24 hours, cell viability was measured using Annexin-V/PI staining. Cell viability was also analysed at the start of the experiment (0 hours). Graph shows mean (±SD) relative viability (percentage $AnnexinV^-/PI^-$ cells) with values for cells at the start of the experiment set to 100%.

5.7 Effect of the anti-oxidant N-acetylcystein (NAC) on AQX-435-induced apoptosis

The natural ligands for LXR are oxysterols (Schulman, 2017) and I, therefore, speculated that AQX-435 may induce LXR activation via cholesterol oxidation. To address this, I compared the effects of MVA and the anti-oxidant N-acetylcysteine (NAC; a precursor for glutathione biosynthesis) on AQX-435-induced apoptosis. However, I first tested the effect of NAC on spontaneous apoptosis at 1mM or 5 mM. Similar to MVA, NAC induced a modest improvement in relative liability (~15%) at 5 mM, although a minimal or no effect was seen at 1 mM (Figure 5.16). Based on these results, a concentration of 5 mM was selected for the next series of experiments. This concentration is consistent with previous studies performed using CLL cells (Vaisitti et al., 2017)

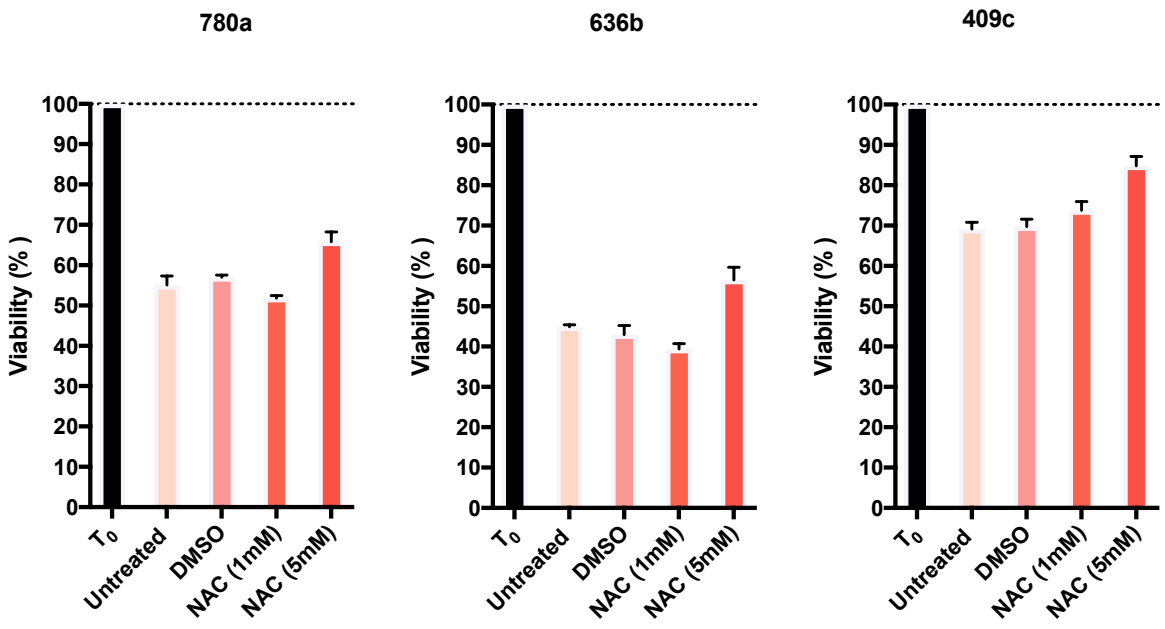

Figure 5.16 Effect of NAC on CLL cell viability
CLL samples (n=3) were treated with the indicated concentrations of NAC, DMSO or left untreated. After 24 hours, cell viability was measured using Annexin-V/PI staining. Cell viability was also analysed at the start of the experiment (0 hours). Graph shows mean (±SD) relative viability ($AnnexinV^-/PI^-$ cells) with values for cells at the start of the experiment (T_0) set to 100 %.

Next I compared the effects of MVA and the anti-oxidant NAC on AQX-435-induced apoptosis. Consistent with the experiment above, MVA significantly reduced AQX-435-

induced apoptosis, most dramatically in cells of most (7/8) patient samples treated at all concentration of compound (Figure 5.17). Interestingly, NAC suppressed apoptosis to further extent than MVA consistently at all concentration of AQX-435. Given that NAC is an antioxidant, Inhibition of AQX-435-induced apoptosis by NAC is consistent with the idea that AQX-435 may drive oxidation of cholesterol to generate oxysterols.

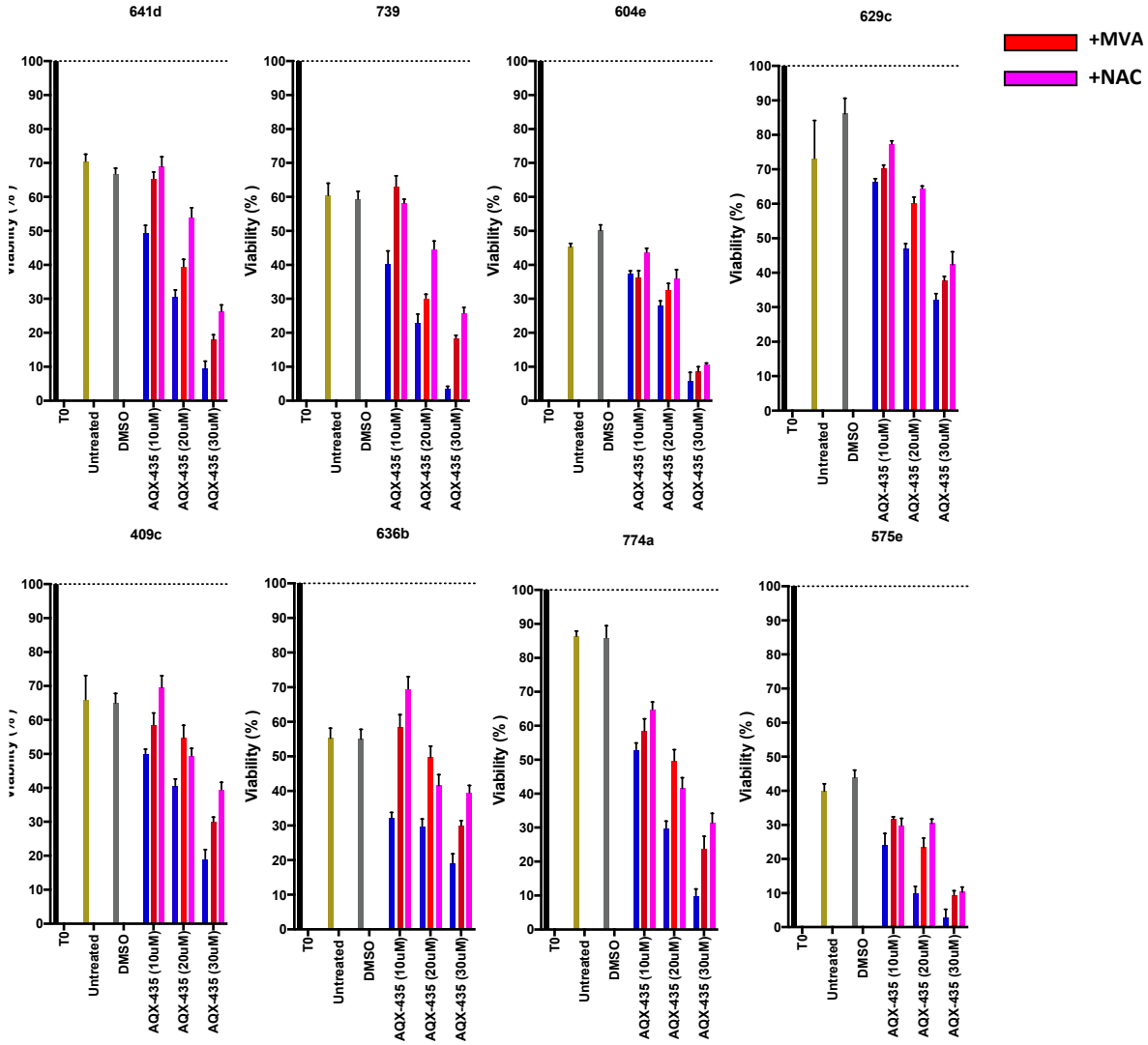

Figure 5.17. Effect of MVA and NAC on AQX-435 induced CLL apoptosis.
CLL samples (n=8) were treated in duplicate with the indicated concentrations of AQX-435 in the presence or absence of MVA or NAC (both 5 mM), or left untreated as control. After 24 hours, cell viability was measured using Annexin-V/PI staining. Cell viability was also analysed at the start of the experiment (0 hours). Graph shows mean (±SD) relative viability (percentage $AnnexinV^-/PI^-$ cells) with values for cells at the start of the experiment set to 100%.

5.8 Effect of MVA and NAC on AQX-435-induced LXR activity

Finally, I investigated the effect of MVA and NAC on AQX-435-induced LXR activation, by both analysis of RNA and protein.

5.8.1 RNA analysis

To investigate effects of MVA/NAC on LXR-dependent transcription, CLL cells were treated with AQX-435 in the presence of MVA or NAC for 6 hours and expression for *ABCA1* and *SREBF1* RNA quantified using Q-PCR (Figure 5.18). Consistent with previous results, AQX-435 increased expression of ABCA1 and SREBF1 RNA expression in a dose-dependent manner. Both MVA and NAC reduced the induction of ABCA1/SREBF1 RNAs in AQX-435-treated cells.

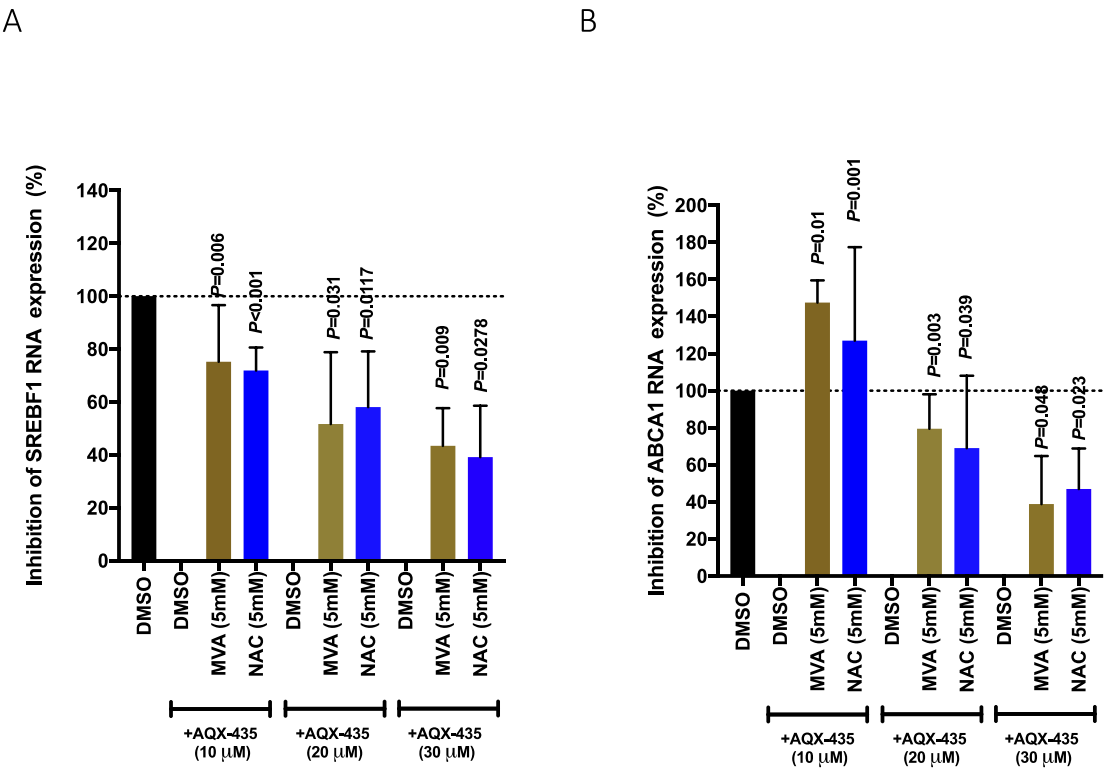

Figure 5.18. Effect of MVA and NAC on AQX-435-induced *SREBF1* and *ABCA1* RNA expression in CLL samples

CLL samples (n=5) were treated with the indicated concentrations of AQX-435, alone or in the presence of MVA or NAC for 6 hours. Expression of (A) SREBF1 and (B) ABCA1 RNA was analysed using Q-PCR. Graphs show relative RNA expression (mean ±SD) with values for untreated cells set to 100 for each individual sample. The statistical significance of the differences between AQX-435 induced SREBF1/ABCA1 expression (LXR activation) and AQX-435 +MVA/NAC are shown (paired Student's t-test).

5.8.2 Protein analysis

Similar experiments were performed to investigate the effects of MVA or NAC on AQX-435-induced expression of SREBF1 and ABCA1 at the protein level (Figure 5.19, 5.20). Although the extent of induction was quite variable between the different samples, western blotting demonstrated substantial increase in expression of both SREBF1 and ABCA1 proteins in cells treated with AQX-435. This is an important result, since it extends previous Q-PCR analysis and confirms that changes in LXR target mRNAs are also associated with increased protein expression. Similar to RNA analysis (Figure 5.18), both MVA and NAC reduced induction of ABCA1 and SREBF1 protein expression in AQX-435-treated cells.

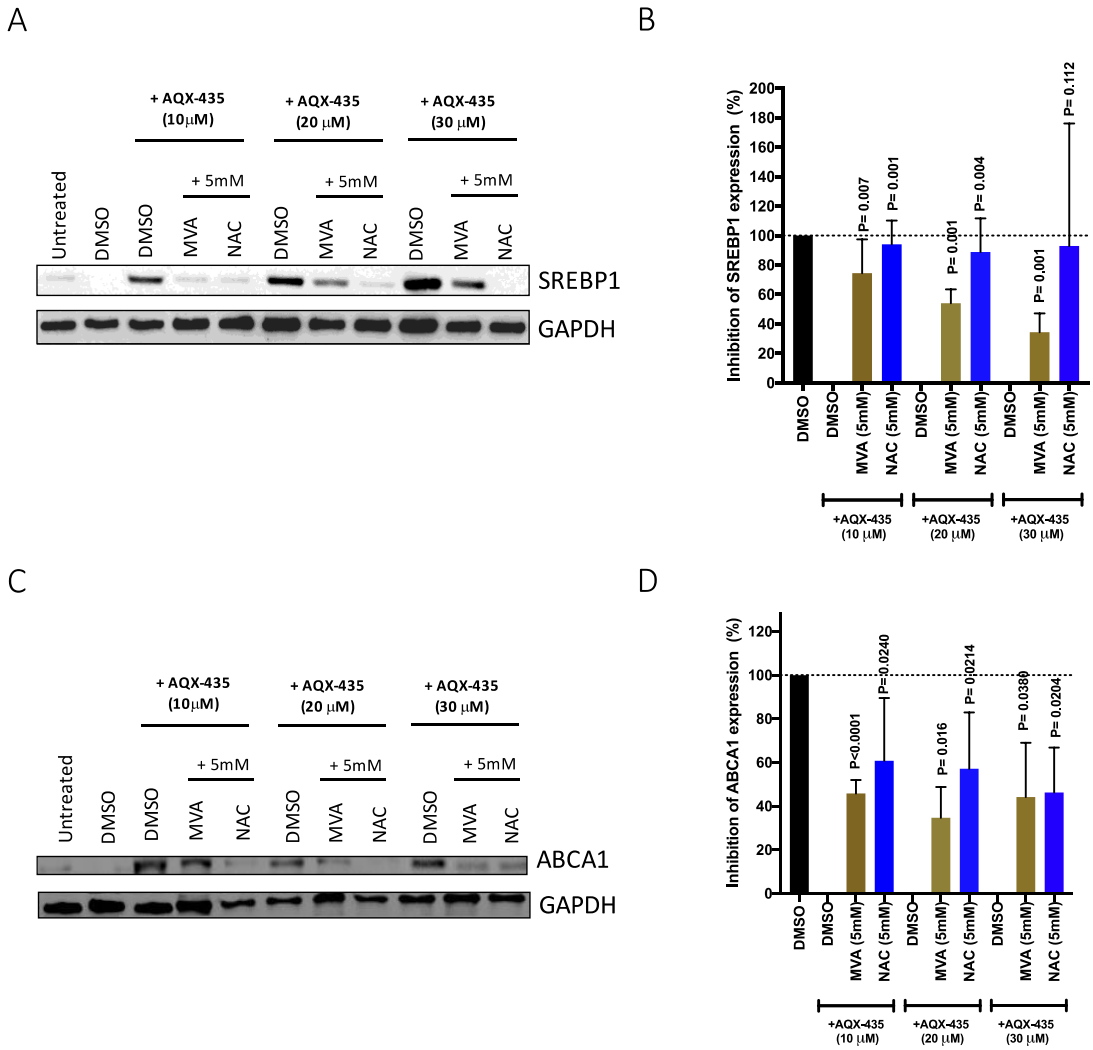

Figure 5.19. Effect of MVA on AQX-435-induced SREBF1 and ABCA1 protein expression in CLL samples.

CLL samples (n=4) were treated with the indicated concentrations of AQX-435, alone or in the presence of MVA or NAC for 6 hours. Expression of SREBP1, ABCA1 and GAPDH (loading control) was analysed by immunoblotting. Graphs show relative protein expression (mean ±SD) with values for DMSO-only treated cells set to 100 for each individual sample. The statistical significance of the differences between AQX-435 induced SREBP1/ABCA1 expression (LXR activation) and AQX-435 +MVA/NAC are shown (paired Student's t-test).

5.9 Summary of key findings

The key findings from the experiments described in this chapter were;

- AQX-435 reduces phosphorylation of AKT, but not SYK, following anti-IgM stimulation of CLL cells
- RNA-seq analysis demonstrates that idelalisib and AQX-435 share the ability to partial inhibit anti-IgM-induced changes in gene expression in CLL cells
- AQX-435 alone induces a distinct gene expression programme, not shared with idelalisib, that is linked to activation of LXR
- Supplementation of cholesterol using mevalonate reduces AQX-435-induced LXR activation and apoptosis
- The anti-oxidant, NAC, reduces AQX-435-induced LXR activation and apoptosis

5.10 Discussion

5.10.1 Effects of AQX-435 on anti-IgM signalling in CLL cells

I have explored an alternate pharmaceutical strategy to target PI3K signalling in malignant B cells via activation of SHIP1, an inositol lipid phosphatase which catalyses the conversion of PI(3,4,5)P3 to PI(3,4)P2. Similar to direct PI3Kδ inhibition by idelalisib, SHIP1 activation reduced the induction of AKT phosphorylation, consistent with the idea that these agents share the ability to reduce accumulation of $PI(3,4,5)P_3$, albeit via distinct mechanisms. Importantly, neither agent affected anti-IgM-induced phosphorylation of SYK. This was the expected result since SYK lies upstream of PI3K. However, it provides important support for the selectivity of AQX-435 and demonstrates that AQX-435 does not block sIgM signalling

capacity per se. Overall, AQX-435 has been shown to reduce anti-IgM-induced AKT phosphorylation without effects on sIgM expression (Figure 3.11), SYK phosphorylation (Figure 5.2) or iCa^{2+} mobilisation (Packham et al., 2016 - ASH Abstract).

It was interesting to note that idelalisib was somewhat more effective for inhibition of AKT phosphorylation compared to AQX-435. This difference was modest in my experiments, but has been observed in larger series of experiments performed in the laboratory where AQX-435 (30 µM) and idelalisib (10 µM) reduced anti-IgM-induced AKT phosphorylation by ~60% and ~95%, respectively (Packham et al., 2016- ASH Abstract) Both agents were used at relatively high concentrations so this difference likely reflects differences in mechanisms of action, rather than being a result of sub-optimal dosing. Differences in potency/efficacy of AQX-435 and idelalisib are likely to be multifactorial, but may reflect, at least in part, the differing modes of action of these agents. Thus, increasing idelalisib concentrations will ultimately lead to full PI3K blockade once all of the kinase active sites have been occupied. By contrast, the inhibitory effects of AQX-435 are limited by the availability of SHIP1; once the available SHIP1 is fully activated addition of further compound will not enhance inhibitory effects. It is also important to consider that, in contrast to PI3Ki, SHIP1 does not block production of $PI(3,4,5)P_3$, but accelerates its breakdown. Thus, even when SHIP1 is fully activated, there remains a transient "window" in which $PI(3,4,5)P_3$ may engage downstream effectors prior to its breakdown.

5.10.2 The transcriptional response to anti-IgM and its modulation by idelalisib and AQX-435

The overall anti-IgM response was broad with induction or repression of a large number of RNAs. This likely reflects ability of sIgM to activate multiple transcription factors, and also the use of bead-bound anti-IgM in these experiments, which gives strong and protracted signal responses. BCR-induced gene signature genes have been relatively well studied and I identified good concordance with the genes regulated in this experiment with known BCR-responsive pathways. This included many growth promoting pathways, including confirmation of pathways previously identified in CLL cells, including activation of the UPR (Krysov et al., 2015), mRNA translation (Yeomans et al., 2016) and metabolism (Vangapandu

et al., 2017). Further analysis using IPA predicted that MYC was the strongest driver of these anti-IgM-induced gene expression. This is consistent with the known activation of MYC following sIgM activation of CLL cells and its expression within a subset of cells in the PCs of CLL LNs (Krysov et al., 2013). MYC is a major driver of many growth promoting pathways (RNA translation, metabolism etc.) and is known to be a rather promiscuous factor, with potentially 1000s of transcriptional targets (McMahon, 2010).

In contrast to induction, down-modulation of gene expression following BCR stimulation has been relatively little studied. However, it was striking that, in these experiments, anti-IgM repressed more genes than were induced, indicating that down-modulation of gene expression is likely to be important in determining biological responses. It was interesting that the downregulated signature was dominated by pathways which were themselves directly linked to BCR signalling. One possibility is that this regulation reflects a negative feedback to curtail responses following activation. Thus, feedback inhibition acting on the BCR may be short-term (e.g. via pre-existing phosphatases) and long-term (via transcriptional reprogramming).

Consistent with the PCA, anti-IgM-induced gene expression changes appeared to be partially reduced, but not completely blocked by idelalisib or AQX-435. A similar picture was apparent for anti-IgM down-regulated genes. Importantly, either drug tended to reduce the whole signature, rather than fully inhibit regulation of a subset of RNAs. Similar to the effect of the drugs on AKT phosphorylation, inhibitory effects of idelalisib were somewhat greater than AQX-435. Given that AQX-435 and idelalisib shared the ability to counter both up- and down-regulation anti-IgM-induced gene expression, it seems likely that both responses are at least partially driven by PI(3,4,5)P3 -dependent activation of downstream effector pathways.

The explanation for the broad, yet partial, effect of AQX-435 and idelalisib is not entirely clear. One possibility is that the multiple signalling pathways that are activated downstream of sIgM in CLL cells, including PI(3,4,5)P3 -dependent pathways, converge on multiple downstream transcription factors. Thus, a reduction in PI(3,4,5)P3 levels (by PI3K inhibition or SHIP1 activation) would reduce the extent of regulation of many downstream target genes, especially when acting via promiscuous transcription factors such as MYC. However,

parallel pathways remain intact so effects of targeting PI(3,4,5)P3 are partial. An example of such as parallel pathway might be increased iCa^{2+} which is not inhibited by idelalisib or AQX-435 in CLL cells and leads to activation of multiple transcription factors, including NF-κB and NFAT. Such redundancy in signalling pathways is observed in many systems and provides mechanisms by which tumour cells can circumvent targeted inhibition of individual signalling pathways.

5.10.3 Bioinformatics analysis reveals an AQX-435-specific gene expression programme linked to LXR activation

Analysis of AQX-435-specific effects on gene expression identified a relatively small set of RNAs with increased or decreased expression in AQX-435-only treated cells. This signature was not observed with idelalisib and is, therefore, specific for AQX-435. One possibility is that this gene expression signature is driven by accumulation of $PI(3,4)P_2$ which would occur in cells treated with AQX-435 but not idelalisib. IPA indicated that this AQX-453 associated response was driven by activation of the LXR canonical pathway.

Importantly, IPA revealed a very strong association between the AQX-435-specific gene expression signature and known LXR target genes, including both upregulated (*ABCA1, ABCG1, MYLIP, SCD* and *SREBP1*) and downregulated genes (*CCL7, CCL2*). Moreover, the strongest predicted drivers of the AQX-435-specific signature were known LXR ligands, including both natural (oxysterols) and synthetic (GW3965) ligands. Thus, IPA analysis suggested that a substantial proportion of the AQX-435-specifc gene expression was a consequence of LXR activation.

I performed a series of experiments to confirm and extend the results from RNA-seq indicating that AQX-435 led to activation of LXR. Overall, the experiments presented in this chapter validate IPA analysis as AQX-435 induces RNA and protein expression of the LXR target genes *SREBP1* and *ABCA1* in CLL cells. Furthermore, AQX-435 induced transient

induction of multiple LXR target genes (*ABCA1, SCD* and *SREBF1*) in TMD8 cells. Together, these experiments confirm that AQX-435 induces LXR target expression at both the RNA and protein level in CLL cells. Moreover, the response is not specific for CLL cells, but also observed in lymphoma derived TMD8 cells.

5.10.4 Effect of MVA and NAC on AQX-435-induced apoptosis

I performed a series of experiments to investigate the functional significance of LXR for responses of CLL cells to AQX-435. AQX-435 has been shown to induce apoptosis of CLL samples (Packham et al., 2016-ASH Abstract) with relative selectivity towards CLL cells compared to normal B cells. Moreover AQX-435 induces higher levels of apoptosis of CLL cells than idelalisib, suggesting that this response is independent of reduced levels of PI(3,4,5)P3 . However, the mechanisms by which AQX-435 induce CLL cell apoptosis are not known.

I first hypothesised that depletion of cellular cholesterol as a result of increased cholesterol efflux following LXR activation might contribute to AQX-435 induced apoptosis. Indeed, in other systems, LXR-induced apoptosis has been shown to be rescued by MVA to restore intracellular cholesterol levels (Bensinger et al., 2008). Moreover, a previous study showed that activation of LXR in CLL cells with synthetic ligand sufficient to induce apoptosis (Geyeregger et al., 2009). Thus, I determined if pre-treatment of with MVA would suppress AQX-435-induced apoptosis.

Overall, MVA was quite effective, reducing AQX-435-induced apoptosis by up to 60%. MVA effects were most dramatic when cells were exposed to AQX-435 at 10 µM where the induction of apoptosis by AQX-435 is moderate. However, protective effects of MVA were also observed in cells treated with higher concentrations of AQX-435 which induce more substantial levels of apoptosis. By contrast, spontaneous apoptosis of CLL cells was only modestly affected by MVA (~15%). It was notable that there was substantial intersample variation in the ability of MVA to rescue CLL cells from AQX-435 induced apoptosis. However, analysis using the Spearman's rank correlations test (data not shown) failed to demonstrate

any correlation between extent of protection by MVA and extent of AQX-435-induced death or any of several molecular prognostic markers (*IGHV* mutation status, CD38, ZAP70, iCa^{2+}).

Since the natural ligands for LXR are oxysterols, I speculated that AQX-435 may somehow be driving oxidation of cholesterol to generate oxysterols. I, therefore, also investigated the effects of the glutathione precursor NAC in these experiments. Consistent with the idea that NAC is an anti-oxidant and may prevent conversion of cholesterol to oxysterol to activate LXR, NAC also reduced AQX-435 induced apoptosis. Taken together, these results suggest that AQX-435-induced apoptosis of CLL cells involves both pro-oxidant pathways (potentially driving accumulation of oxysterols) and cholesterol depletion via LXR (potentially a consequence of oxysterol accumulation). However, the relationship between these steps requires further study

5.10.5 Effect of MVA and NAC on LXR activation

Next, I Investigated the effect MVA and NAC on LXR activation, by analysis of AQX-435 induced LXR target (*SREBF1, ABCA1*) RNA and protein (ABCA1, SREBP1) expression. Both agents reduced LXR activation.

The mechanistic reduction of LXR targets by NAC is perhaps easy to understand. By acting as an antioxidant, NAC may reduce oxysterol production and, therefore, reduces LXR activity. More importantly, it provides a mechanistic link between pro-oxidative activity and activation of LXR by AQX-435. By contrast, it is interesting to think why MVA would reduce LXR activation since increasing cholesterol (via MVA addition) would not be expected to reduce oxysterols *per se*. However, given that multiple feedback mechanisms link cholesterol homeostasis, and specifically dysregulation in negative feedback mechanism have previously been reported in cancer cells, these alterations may prevent or even shift oxysterol metabolism from anabolic toward catabolic to ensure cholesterol accumulation (Bovenga et al., 2015). Interestingly, similar effects have been observed in T cells, where

supplementation with mevalonate after treatment with an LXR agonist also induced an inhibitory effect on LXR-dependent gene expression (Bensinger et al., 2008).

5.10.6 Dual effects of AQX-435 on cholesterol homeostasis

In addition to the AQX-435 specific effect on cholesterol efflux, it was notable that AQX-435 also modulated expression of cholesterol biosynthetic gene expression in anti-IgM treated cells. Thus, anti-IgM induced most of the biosynthetic pathway. Anti-IgM also downregulated efflux pumps (ABCG1, ABCA1), indicating there is a strong drive to accumulate cholesterol. This is consistent with the known requirement for cholesterol, the most abundant membrane component, to support cell growth following BCR stimulation. Importantly, in addition to its ability to promote efflux (which would counter effects of BCR stimulation), AQX-435 reduced anti-IgM induced cholesterol biosynthesis. This activity was shared with idelalisib so is likely to be mediated via reduced $PI(3,4,5)P_3$ and is consistent with known activity of mTORC1 in driving cell growth and survival. Thus, AQX-435 appears to exert dual effects on cholesterol. Firstly, via reducing PI(3,4,5)P3, it interferes with activation of biosynthesis following BCR stimulation. Secondly, it induces efflux and reduces influx. This second function appears independent of PI(3,4,5)P3 .

Results from a previous study demonstrated that T-cell receptor crosslinking promoted cholesterol accumulation by supressed LXR target genes encoding the sterol transporters ABCA1 and ABCG1, and that this could be reversed by the addition of an LXR agonist. A more definitive link to sterol metabolism was established in this study by the observation that the inhibitory effect of LXR on T-cell proliferation is completely blocked if lymphocytes are supplemented with MVA (Bensinger et al., 2008). Thus, it seems that the similar mechanistic interactions may operate in B cells and T cells.

Overall, a key finding in this chapter is identification of LXR activation as potential mode of action for AQX-435 in addition to inhibition of PI3K signalling by preventing accumulation of PI(3,4,5)P3. However, the critical question that remains is whether this is mediated via

$PI(3,4)P_2$ and it is important to consider that effects of AQX-435 on LXR may be off-target effects. Regardless, there is substantial interest in LXR agonist in their own right as anti-cancer drugs. For example, T0901317 has been shown to induce modulation of LXR signalling as a prevention and therapy for colon cancer (Chuu, 2011). It would be interesting to determine whether the combination of a PI3K inhibitor (such as idelalisib) and an LXR agonist recapitulates the effects of AQX-435.

Chapter 6: Final Discussion

6.1 Overview of findings

At the beginning of this thesis the primary hypothesis of this project is that BCR activation and downstream signalling molecules influence expression and function of other cell surface receptors via SHIP1 and protein kinases in CLL. The secondary hypothesis is that the novel chemical SHIP1 activator, AQX-435 will characterise new pathways affected by SHIP1 activation in BCR signalling in CLL cells.

In order to investigate these hypotheses the project addressed two closely inter-related areas , (i) to investigate pathways of cross-talk between the BCR and other cell surface receptors which influence response to microenvironmental factors (CXCR4 and EBI2), including the role of specific kinases and the inositol lipid phosphatase SHIP1 and (ii) to characterise pathways regulated by the novel chemical SHIP1 activator, AQX-435.

I have outlined the three specific aims this along with the key findings and summaries below;

Aim: To Investigate signal transduction pathway in BCR→CXCR4 cross-talk in malignant B and extend analysis to established B-lymphoma cell lines.

The key findings from the experiments described in Chapter 3 were;

- In a panel of established B-cell lines, anti-IgM was generally an effective down-modulator of CXCR4 expression, whereas the SHIP1 activator, AQX-435, did not down-modulate expression of cell surface CXCR4.
- In RL cells, soluble anti-IgM was a more effective down-modulator of CXCR4 than bead-bound anti-IgM.
- AQX-435 did not affect sIgM endocytosis in WSU-FSCCL cells.

- Anti-IgM-induced CXCR4 down-modulation in RL cells is dependent on SYK and PI3Kδ activity, but relatively unaffected by the BTK inhibitors ibrutinib or acalabrutinib.
- Anti-IgM-induced CXCR4 down-modulation in primary CLL cells was unaffected by inhibition of PKD.
- Consistent with results using BTK inhibitors, anti-IgM-induced CXCR4 down-modulation was unaffected by BTK siRNA. However, CXCR4 down-modulation was also relatively unaffected by SYK siRNA suggesting that the degree of knock-down achieved in these experiments was not sufficient to effectively interfere with signalling events

Experiments investigating the regulation of CXCR4 were presented in Chapter 3. Regulation of CXCR4 has been relatively well studied in CLL cells, and the main focus of experiments in chapter 3 were to extend analysis of BCR→CXCR4 cross-talk to established B-lymphoma cell lines. This was to determine whether similar pathways operated in other types of malignant B cells (focusing on the role of specific kinases and response to activation of SHIP1 using AQX-435) but also to use B-cell lines as a transfectable model system to use RNAi to directly investigate the role of specific signalling intermediates in CXCR4 regulation. The main findings were that anti-IgM was generally an effective down-modulator of CXCR4 expression in B-cell lines, whereas the SHIP1 activator, AQX-435, did not substantially down-modulate cell surface CXCR4 expression. This contrasts clearly with results obtained with CLL cells where both anti-IgM (in signal responsive samples) and AQX-435 trigger CXCR4 down-modulation. Overall the results from inhibitor experiments in this chapter support my primary hypothesis demonstrated that anti-IgM-induced CXCR4 endocytosis (BCR-CXCR4 crosstalk) is mediated consistently by a cascade involving SYK and PI3Kδ, which are signalling pathway axis operated in both CLL cells and B-cell lines since. Although I was able to achieve target knock-down in transfected cells, the degree of knock-down did not seem to be sufficient to use RNAi as a reliable tool to directly investigate the role of specific signalling intermediates.

AIM: To investigate whether the GPCR EBI2, a key BCR-regulated receptor that is critical for coordination of normal B-cell responses, is also subject to BCR-mediated cross-talk in CLL cells.

The key findings from the experiments described in Chapter 4 were;

- EBI2 expression is generally low on CLL cells and is not clearly different between U-CLL and M-CLL (or subsets identified by other markers) despite variable expression of EBI2 between normal naive and memory B cells.
- The EBI2 ligand 7α25-OHC did not induce signalling or alter viability of CLL cells
- Anti-IgM may increase expression of EBI2 RNA in CLL cells, but overall effects were modest and variable between samples, and were not accompanied by a clear increase in EBI2 protein expression.
- AQX-435 did not alter EBI2 protein expression.

Results described in Chapter 4 were aimed at extending analysis of cross-talk to another GPCR, EBI2. Although regulation of EBI2 expression following antigen engagement of the BCR is known to be critical for effective immune responses, via effects on positioning of B cells (Kelly et al., 2011), EBI2 expression and function has not been investigated in any detail in CLL cells. However, the observation that overexpression of EBI2 in the B-cell compartment of mice results in development of a CLL-like disease (Arfelt et al., 2017), indicates that this receptor may play an important role in human disease. Therefore, experiments focused on analysing, for the first time, EBI2 expression on primary CLL cells and investigating whether, like CXCR4, EBI2 expression was modulated in response to sIgM engagement or activation of SHIP1 by AQX-435. The main findings were that EBI2 expression was generally low on CLL cells compared to normal B cells, and was not clearly different between U-CLL and M-CLL (or subsets identified by other markers) despite variable expression of EBI2 between normal naive and memory B cells. Moreover, the EBI2 ligand 7α25-OHC did not induce signalling or alter viability of CLL cells, which may reflect the low expression of EBI2 on these cells. Finally, the was some evidence that EBI2 RNA was increased by anti-IgM (but not AQX-435) in a

subset of samples, but that analysis of cell surface protein expression may have been complicated by effects of ligands in the culture medium. Overall, the results in this chapter do not provide suffient evidence to support my hypothesis that there that sIgM-induced signalling or SHIP1 activation using AQX-435 leads to modulation of EBI2 expression in CLL cells (BCR-EBI2 crosstalk). However, the study uncovered considerable technical challenges in examination of EBI2 which complicated analysis, especially related to the overall low level expression of EBI2 on CLL cells and the potential modulatory effect of EBI2 ligands.

Aim To probe the effects of AQX-435 on CLL cells by using RNA SEQ data CLL cells in comparison to idelalisib and anti-IgM-induced.

The key findings from the experiments described in this Chapter 5 were;

- AQX-435 reduces phosphorylation of AKT, but not SYK, following anti-IgM stimulation of CLL cells
- RNA-seq analysis demonstrates that idelalisib and AQX-435 share the ability to partial inhibit anti-IgM-induced changes in gene expression in CLL cells
- AQX-435 alone induces a distinct gene expression programme, not shared with idelalisib, that is linked to activation of LXR
- Supplementation of cholesterol using mevalonate reduces AQX-435-induced LXR activation and apoptosis
- The anti-oxidant, NAC, reduces AQX-435-induced LXR activation and apoptosis

Experiments described in the final results chapter (Chapter 5) focused on a detailed characterisation of the effects of AQX-435 in CLL cells by using RNA-seq analysis to probe the potential effects of SHIP1 activation on gene expression. An important aim of the gene expression profiling was to compare the effects of AQX-435 and the PI3Kδ inhibitor idelalisib on gene expression, in the presence or absence of sIgM stimulation, to uncover AQX-435 responses that may be driven by reduced $PI(3,4,5)P_3$ levels (shared with idelalisib) versus increased $PI(3,4)P_2$ (AQX-435-independent).

Bioinformatical analysis demonstrated that idelalisib and AQX-435 shared the ability to partially reduce a large proportion of the 3850 of genes that were induced or repressed in anti-IgM-treated cells, including induction of cholesterol biosynthetic pathways. Indeed, this chapter results supported my secondary hypothesis as bioinformatical analyses revealed an AQX-435-specific signature that appeared to be linked to altered cholesterol influx/efflux via activation of LXR. The functional relevance of this pathway was further confirmed by experiments showing that supplementation of cellular cholesterol using mevalonic acid substantially reduced AQX-435-induced apoptosis. This study provides important new insight into cellular effects of AQX-435.

6.2 Receptor cross-talk

Crosstalk-between the BCR and other cell surface receptors plays a central role in the co-ordination of immune responses and is also likely to modulate behaviour of malignant B cells (Becker et al., 2017; Calpe et al., 2011; Burger et al., 2002). This is supported by the fact that kinase inhibitors such as ibrutinib and idelalisib which block BTK and PI3K activity in treated patients results in a striking redistribution of malignant cells from the tissues to the circulation (lymphocytosis). Therefore, the interface between the BCR and receptors that mediate cell migration and/or adhesion is likely to be important not just for disease pathogenesis, but also for response to treatment and there is a clear need to understand the which impact on expression of regulated receptors such as CXCR4, and to identify over receptors which are targets for cross-talk.

CXCR4 has been relatively well studied as a target for cross-talk in CLL cells in previous studies (Saint-Georges et al., 2016; Haerzschel et al., 2016; Vlad et al., 2009; Quiroga et al., 2009). In order to elucidate BCR → CXCR4 crosstalk early studies using the DT40 cells demonstrated that anti-IgM-induced CXCR4 endocytosis is mediated by a cascade involving SYK, BLNK, BTK and PLGγ2 which ultimately promotes PKC-dependent internalisation (Guinamard et al. 1999). Other studies in mouse pre-B-cells have demonstrated that BCR-induced inhibition of CXCR4 was dependent on the phosphotase SHIP1 (Brauweiler et al.,

2007). This paper concluded that SHIP1 was required for inhibition of CXCR4 signalling, but did not directly address the potential effects of SHIP1 on CXCR4 receptor expression per se. Furthermore, the host laboratory interestinlgy demosntrated that in CLL cells only a subset of canonical signalling kinases activated downstream of the BCR are required to mediate sIgM→CXCR4 cross-talk. Analysis focused on current clinically used drugs (idelalisib, ibrutinib, acalabrutinib) or against relevant targets (SYK inhibitor tamatinib) Also, activation of SHIP1 using small chemical compound agonists was sufficient to down-modulate CXCR4 on CLL cells (unpublished data).

To extend this study, the first goal of my project was to extend these studies to established B-cell lines in order to determine whether similar pathways operated in other types of malignant B cells. In terms of the comparison between CLL and B-cell lines, the major difference was that AQX-435 did not trigger CXCR4 down-modulation in any of the lines tested, whereas anti-IgM-induced CXCR4 down-modulation was observed for at least a subset. The reason why AQX-435 did not down-modulate CXCR4 expression in B-cell lines is not clear, since all cell lines studied expressed SHIP1. One possibility is that SHIP1 is partially activated in CLL cells, such that these cells are "primed" to respond to AQX-435. This may be related to activation of anergy-associated features in CLL cells, since SHIP1 is activated in normal anergic B cells (O'Neill et al., 2011; Merrel et al., 2006). Unfortunately, and as discussed above, it was not possible to perform RNAi experiments to investigate directly the role of specific molecues in CXCR4 regulation. Thus, it remains unclear as to whether SHIP1 mediates the PI3Kδ-dependent pathway downstream of sIgM that drives CXCR4 down-regulation, or whether sIgM→ PI3Kδ signalling and SHIP1 activation are two independent pathways, each capable to driving CXCR4 down-modulation. It is also not clear whether the effects of AQX-435 on CXCR4 are truly mediated via SHIP1, or reflect an off-target effects of the drug.

As part of the my studies, I did perform some experiments investigating anti-IgM-induced CXCR4 down-modulation in CLL cells. First, these showed that cross-talk was not mediated via PKD. This was perhaps an expected result, since PKD is classically activated downstream of PKC, which did not appear to play a role in cross-talk. However, they did conflict with the results of Saint-Georges et al., which did indicated a role for PKD (Saint-Georges et al., 2016), although they were obtained with a different PKD inhibitor with known off-target activity

(Rozengurt et al., 2010). These observations underline the potential impact of off-target effects in studies of chemical inhibitors/activators and the importance of using genetic experiments to definitively demonstrate the role of specific proteins in cross-talk pathways. Second, analysis of the GEP data sets demonstrated that anti-IgM, but not AQX-435, downregulated *CXCR4* RNA expression. Thus, effects of BCR signalling on CXCR4 are likely to be bi-phasic with an early down-modulatory phase triggered by receptor endocytosis, followed by a later transcriptional effect.

The migration and homing of B cells is dependent on complex interactions between the activity of multiple cell surface receptors, many of which are modulated following antigen engagement of the BCR. This underscores the importance of investigating other potential targets for BCR cross-talk in CLL cells. For example, in addition to CXCR4, anti-IgM has also be shown to regulated expression and/or function of other cell surface receptors, including CXCR5 (Saint-Georges et al., 2016; Haerzschel et al., 2016), SIP1R (Till et al., 2015), CD49-VLA4 (De Gorter et al., 2007) and VCAM-11(Majid et al., 2011).

Results in Chapter 4 addressed whether a regulatory role for SHIP1 extends to other receptors subject to BCR-mediated cross-talk in CLL cells such as the expression and regulation of EBI2 in CLL cells. While EBI2 is not a chemokine receptor, it is part of the wider family of GPCR and that plays an important role in order to position B cells inside the follicles of the lymph nodes in response to its ligand 7α,25-dihydroxycholesterol (7α,25-OHC) in collaboration with CCR7 and CXCR5 during a humoral response.

At the start of the my experiments there were no papers describing characterisation of EBI2 expression at the protein level in mouse cells or human cells; previous studies were restricted largely to analysis of EBI2 RNA and consequences of gene knock-out. Although limited in scope, these studies revealed a key role for EBI2 as a BCR target that is required for optimal B-cell responses. Furthermore, there were no studies that investigated regulation of EBI2 expression in CLL cells in any detail, despite evidence showing that (i) it is required for B-cell responses in mice, (ii) it is a target for BCR-mediated cross-talk and (iii) overexpression of EBI2 in the B-cell compartment of mice results in development of a CLL-like disease (Arfelt et al., 2017).

Here, for the first time I characterised the expression of EBI2 receptor expression in CLL cells. EBI2 expression on CLL cells was substantially lower than normal B cells and variation in expression of EBI2 was not clearly related to the differing cell-of-origin or the established molecular prognostic markers. Although I was able to develop a method to quantify EBI2 on CLL cells, there was no solid evidence that it was a target for modulation in CLL cells, either in response to anti-IgM or AQX-435.

Nevertheless, my experiments demonstrate that different GPCRs (CXCR4 vs EBI2) may be subject to distinct patterns of regulation in CLL cells. Despite the development of a CLL-like disease following enforced expression of EBI2 in the B-cell compartment of mice (Artfelt et al., 2017), the low expression of EBI2 and absence of detectable 7α,25-OHC-induced signalling response argues against a critical role for this receptor in CLL. However, this may reflect the challenging staining procedure to optimally detect EBI2 due to of BSA-bound oxysterol that is present in our staining buffer may trigger receptor endocytosis, and therefore, it remains possible that EBI2 does exert an important influence on malignant cells within tissue microenvironments. Thus the role of EBI2 in human CLL, if any, remains unclear.

6.3 Potential future studies on receptor cross-talk

Receptor cross-talk has now been heavily studied in CLL cells, but I think there are a couple of interesting areas that could be pursued in future studies. First, it is now evident that multiple receptors are involved in determining migration/homing activity and many of these could be subject to modulation. Thus, rather than single receptor studies, it would be more powerful to compare multiple receptors in future studies. Proteomics approaches (Li et al., 2017) especially using plasma membrane enriched fractions to increase sensitivity for low abundance proteins, would be a good way forward. This would provide a more "global" view of how anti-IgM (and potentially other agents such as AQX-435) modulate the capacity of CLL cells to respond to extracellular cues, and how these responses differ between distinct disease subsets and in response to drug manipulation. Since it is an unbiased approach, it would have the capacity to identify new targets for cross-talk.

Furthermore, the fact that the signalling pathway which connect BCR and CXCR4 crosstalk are similar in CLL and other lymphoma cell line mandates further investigation of the role of SHIP1 in primary lymphoma cells. This could provide further insight in the role of SHIP1 in tumorigenesis in cells of different origin and other B cell malignancies.

Finally, although there is an increasing understanding of the kinases which mediate sIgM→CXCR4 cross-talk, the precise mechanisms responsible for induced CXCR4 internalisation are not known. In other systems, CXCR4 endocytosis has been linked to phosphorylation of the intracellular domains of CXCR4 (Wang et al., 2001) and it would be interesting to determine whether similar pathways contribute to internalisation of CXCR4 in anti-IgM (or AQX-435) treated CLL cells.

6.4 Analysis of AQX-435

The second major goal was characterisation of effects of AQX-435. Previous studies demonstrated that AQX-435 reduced anti-IgM-induced AKT phosphorylation, and also induced apoptosis and CXCR4 down-modulation. Although AQX-435 and idelalisib shared the ability to inhibit AKT phosphorylation, AQX-435 was substantially more effective than idelalisib for effects on apoptosis and CXCR4. Thus some responses to AQX-435 may be mediated via reduced $PI(3,4,5)P_3$ (shared with idelalisib), and other via accumulation of $PI(3,4)P_2$ (specific for AQX-435). Moreover, AQX-435-induced CXCR4 down-modulation and apoptosis has been shown to be more dramatic in CLL cells compared to normal B cells, suggesting some degree of SHIP1 "priming" in CLL cells (as discussed in Chapter 3). Thus, AQX-435 is an interesting chemical tool to probe consequences of SHIP1 activation and may be a candidate for clinical trials.

My studies have added some important new insight into activity of AQX-435. First, AQX-435 inhibitory effects on AKT phosphorylation were not accompanied by effects on upstream SYK phosphorylation or sIgM expression endocytosis. These findings lend further weight to the idea that AQX-435 reduces BCR signalling via effects on SHIP1. Moreover, gene expression analysis reveal a new effect on LXR activation which is not shared with idelalisib and is important for AQX-435-induced apoptosis.

A summary of the effects of AQX-435 on signalling, CXCR4 expression, LXR activation and apoptosis is shown in Figure 6.1.

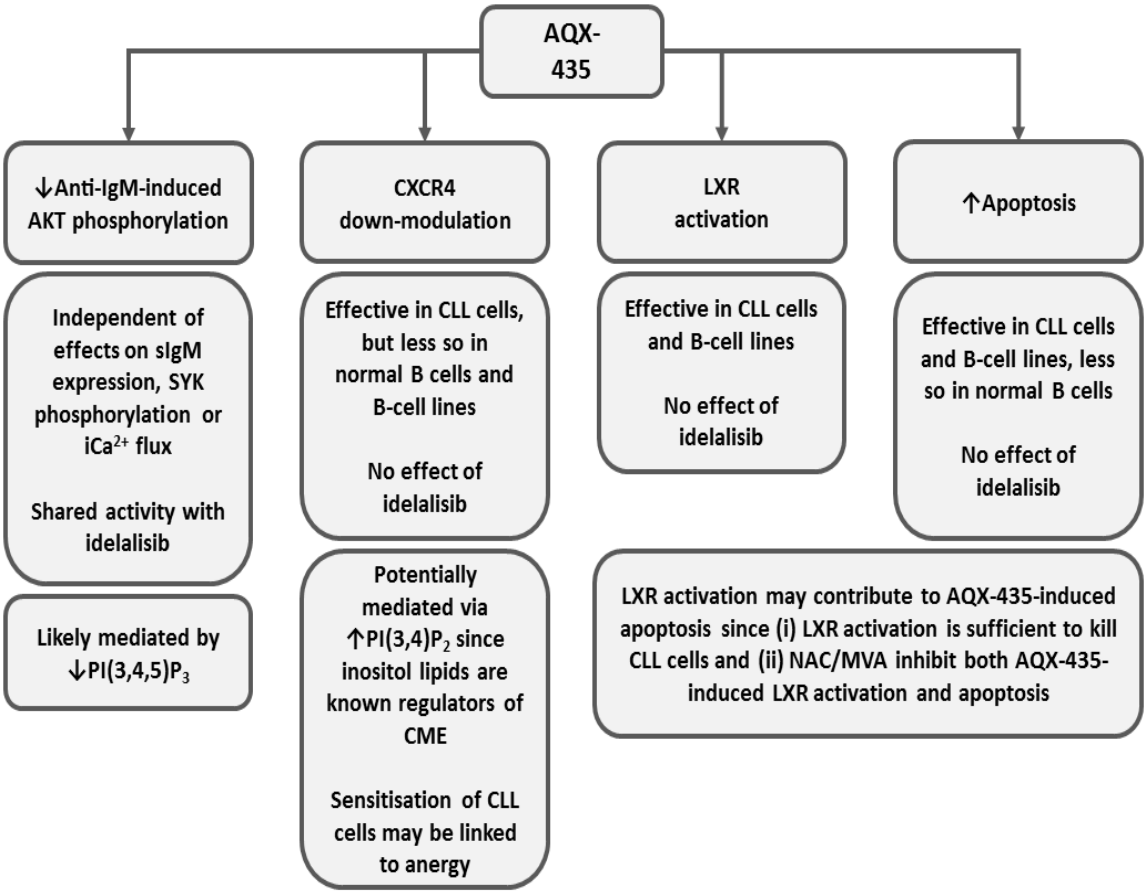

Figure 6.1 A summary of the effects of AQX-435 on anti-IgM-induced AKT phosphorylation, CXCR4 down-modulation, LXR activation and apoptosis.
Information is derived from results performed in this project and other studies in the host laboratory.

Based on these observations, I speculate that;

1. Inhibition of AKT phosphorylation is mediated via SHIP1's ability to reduce levels of $PI(3,4,5)P_3$.
2. Down-modulation of CXCR4 may be mediated via SHIP1's ability to increase levels of $PI(3,4)P_2$, since $PI(3,4)P_2$ has been linked to receptor CME (Marchese, 2014; Landego et al., 2012; Brauweiler et al., 2007)
3. LXR activation may not be a consequence of SHIP1 activation since I was unable to find any literature that provided a no clear mechanistic data linking alterations in $PI(3,4)P_2$ and LXR activation. However, it is possible linking pathways exist but have not yet been described. Alternatively, LXR activation may be mediated by increased

reactive oxygen species driving accumulation of oxysterols since it was reduced by NAC. This could represent an off-target effect of AQX-435.

4. Activation of LXR may contribute to AQX-435 induced apoptosis. since activation of LXRis sufficient to induce apoptosis of CLL cells (Geyeregger et al., 2009). Moreover, both MVA and NAC reduced both activation of LXR and induction of apoptosis, consistent with some mechanistic linkage between these responses.
5. CXCR4 down-modulated is not likely to be mediated via LXR since AQX-435 did not down-modulate CXCR4 expression in B-cell lines, despite activation of LXR in these cells.

6.5 Potential future studies on AQX-435

These observations suggest a series of experiments to investigate the linkage between AQX-435, ROS, SHIP1 and LXR and its biological effects, including signalling inhibition, apoptosis and receptor cross-talk. These could be addressed using further inhibitor experiments to investigate their inter-relationship, and should also, as discussed in Chapter 3, involve careful dissection of normal B-cell subsets to probe potential mechanisms for cell-type selective responses. However, it will be critical to resolve which functions represent on- and off-target effects. I was not able to establish effective RNAi for knock-down, so the next logical step would be to use CRISPR-cas9, for example to determine whether deletion of SHIP1 ablates responses to AQX-435. CRISPR-cas9 is well established for B-cell lines, but it would be important to carefully select models which replicate the features of the effects of AQX-435 in CLL cells. For example, analysis of CXCR4 down-modulation would be challenging because, to date, I have not identified any B-cell lines which show this response.

It is worth considering the potential clinical development of AQX-435. Use of idelalisib is limited by toxicity so it would be useful to determine if the more modest inhibition of PI3K signalling seen in AQX-435 treated cells is associated with less toxicity, in particular, via effects on Treg cells (Compagno et al., 2017). Experiments from the host laboratory and collaborators have shown that AQX-435 has significant anti-tumour activity in xenograft models, using either the TMD8 cell line, or patient derived DLBCL patient derived Xenografts

(PDXs). It also combined effectively with ibrutinib to boost *in vivo* responses. However, future *in vivo* studies should focus on analysis of syngeneic models to test effects of AQX-435 in the presence of an effective host immune system.

Finally, the effect of AQX-435 on LXR may be beneficial in an anti-cancer drug, regardless of whether it is mediated via SHIP1-dependent or independent effects. In CLL, McCaw et al. recently demonstrated there is a high incidence of elevated low-density lipoprotein (LDL) levels in CLL patients and interestingly there was a survival benefit from taking cholesterol-lowering statin (Chow et al., 2016) (McCaw et al., 2017). The study further implied the long-chain fatty acids and free cholesterol components of LDL may enhance proliferative responses of CLL cells to inflammatory signals by potentiating cytokine-induced STAT3 phosphorylation independent of BCR stimulation. Finally, the authors found an indirect link between the extent of LDL-potentiated STAT3 phosphorylation and HMGCoA reductase expression. Given that HMGCoA reductase is the rate limiting step in cholesterol synthesis highlights the importance of the cholesterol biosynthesis pathway. Thus, malignant B cells, including CLL cells, are particularly sensitive to induction of apoptosis by LXR agonists. Moreover, activation of LXR may be an attractive approach to counter altered cholesterol metabolism that has been shown to operate in a subset of lymphoma DLBCL (Shipp et al., 2013). This is supported by the fact that statins which lower LDL levels by blocking 3-hydroxy-3-methyl-glutaryl-CoA reductase (HMGCR), the rate-limiting enzyme of cholesterol synthesis demonstrate anti-cancer properties similar results published by Gronich et al. (Gronich et al., 2013). Overall, a combined SHIP1/LXR activator may provide a unique therapeutic agent via its dual ability to interfere with PI3K-mediated signalling and perturb cholesterol homeostasis.

List of References

- AGUILAR-HERNANDEZ, M.M., BLUNT, M.D., DOBSON, R. 2016. IL-4 enhances expression and function of surface IgM in CLL cells. Blood 127(24):3015-3025.
- AKERLUND, J., GETAHUN, A., CAMBIER, J.C. 2007. B cell expression of the SH2-containing inositol 5-phosphatase (SHIP1) is required to establish anergy to high affinity, proteinacious autoantigens. *Journal of autoimmunity*. 62:45-54.
- AMREIN, P.C., ATTAR, E.C., TAKVORIAN, T. 2011. Phase II study of dasatinib in relapsed or refractory chronic lymphocytic leukeamia. *Clin Cancer Res*, 17(9):2977-2986.
- ANDREEFF, M., DARZYNKIEWICZ, Z., SHARPLESS TK, CLARKSON BD, MELAMED MR. 1980. Discrimination of human leukeamia subtypes by flow cytometric analysis of cellular DNA and RNA. *Blood* 55: 282-293.
- ANDRITSOS L. A., BYRD, J. C., HEWS, B., KIPPS, T. J., JOHNS, D. & BURGER, J. A. 2010. Preliminary results from a phase I/II dose escalation study to determine the maximum tolerated dose of plerixafor in combination with rituximab in patients with relapsed chronic lymphocytic. *leukeamia*, 95, Abstract 772.
- ANSEL, K. M., HARRIS, R. B. & CYSTER, J. G. 2002. CXCL13 is required for B1 cell homing, natural antibody production, and body cavity immunity. *Immunity*, 16, 67-76.
- ARMITAGE, R. J., FANSLOW, W. C., STROCKBINE, L. 1992. Molecular and biological characterization of a murine ligand for CD40. Nature. 357: 80–82.
- BAGNARA, D. 2011. A novel adoptive transfer model of chronic lymphocytic leukeamia suggests a key role for T lymphocytes in the disease. *Blood*, 117, 20, 5463–72.
- BAUDOT, A.D., JEANDEL, P.Y., MOUSKA, X. 2009. The tyrosine kinase SYK regulates the survival of chronic lymphocytic leukeamia B cells through PKCdelta and proteasome-dependent regulation of Mcl-1 expression. *Oncogene*. Sep 17; 28(37):3261-73.
- BECKER M.,HOBEIKA E., JUMAA H., RETH M, . MAITY P.C. 2017. CXCR4 signaling in mature B cell requires IgD–BCR. 2017. *Proceedings of the National Academy of Sciences* , 114 (20) 5231-5236;
- BECKWITH, M. 1990. Phorbol ester-induced, cell-cycle-specific, growth inhibition of human B-lymphoma cell lines. *J. Natl. Cancer Inst* 82: 501-509.
- BENSCHOP, R.J., AVISZUS, K., ZHANG, X., MANSER, T., CAMBIER, J.C. & WYSOCKI, L.J. 2001. Activation and anergy in bone marrow B cells of a novel immunoglobulin transgenic mouse that is both hapten specific and autoreactive. *Immunity*, 14,1, 33–43.
- BENSINGER, S. J., BRADLEY, M. N., JOSEPH, S. B., ZELCER, N., JANSSEN, E. M., HAUSNER, M. A., TONTONOZ, P. 2008. LXR signaling couples sterol metabolism to proliferation in the acquired immune response. *Cell,* 134(1), 97–111. doi:10.1016/j.cell.2008.04.052

- BEVERLY, A., SIMON, P. 2010. CXCL12 (SDF-1)/CXCR4 *Pathway in Cancer Clin Cancer Res*, (16) (11) 2927-2931.
- BIANCOTTO, A. 2012. Phenotypic complexity of T regulatory subsets in patients with B-chronic lymphocytic leukeamia. *Mod Pathol*, 25, 2, 246–59.
- BINDER, M., MULLER, F., JACKST, A., LECHENNE, B., PANTIC, M., BACHER, U., ZU, E.C., VEELKEN, H., MERTELSMANN, R., PASQUALINI, R. 2011. B-cell receptor epitope recognition correlates with the clinical course of chronic lymphocytic leukeamia. *Cancer.* p 117(9):1891–900.
- BINET, J.L., AUQUIER, A., DIGHIERO, G. 1981. A new prognostic classification of chronic lymphocytic leukeamia derived from a multivariate survival analysis *Cancer*, 48pp. 198–206
- BLUM KA, ADVANI A, FERNANDEZ L. 2009. Phase II study of the histone deacetylase inhibitor MGCD0103 in patients with previously treated chronic lymphocytic leukaemia. *Br J Haematol*.147(4):507-514.
- BLUNT, M. D., & STEELE, A. J. 2016. Releasing the brakes on BTK-targeting miRNA. *Blood,* 128(26), 3023-3024.
- BOTTONI, A., RIZZOTTO, L., LAI, T., LIU, C., SMITH, L. L., MANTEL, R., REIFF, S., EL-GAMAL, D., LARKIN, K., JOHNSON, A. J., LAPALOMBELLA, R., LEHMAN, A., PLUNKETT, W., BYRD, J. C., BLACHLY, J. S., WOYACH, J. A., & SAMPATH, D. 2016. Targeting BTK through microRNA in chronic lymphocytic leukeamia. *Blood*, 128(26), 3101-3112.
- BRAUWEILER, A., MERRELL, K. & GAULD, S.B. 2007. Cutting edge: acute and chronic exposure of immature B cells to antigen leads to impaired homing and SHIP1-dependent reduction in stromal cell-derived factor-1 responsiveness. Journal of *Immunology,* 178, 6, 3353–3357.
- BROWNE, C.D., DEL NAGRO, C.J, CATO, M.H., DENGLER, H.S.& RICKERT, R.C. 2009. Suppression of Phosphatidylinositol 3,4,5-Trisphosphate Production Is a Key Determinant of B Cell Anergy. *Immunity*, 31, 749–60.
- BUCHNER, M., FUCHS, S., PRINZ, G., PFEIFER, D., BARTHOLOMÉ, K., BURGER, M., CHEVALIER, N., VALLAT, L., TIMMER, J., GRIBBEN, J.G., JUMAA, H., VEELKEN, H., DIERKS, C., ZIRLIK, K. 2009. Spleen tyrosine kinase is overexpressed and represents a potential therapeutic target in chronic lymphocytic leukeamia. *Cancer Res* 69(13):5424-32.
- BUECHELE, C., BAESSLER, T., SCHMIEDEL, B.J., SCHUMACHER, C.E., GROSSE-HOVEST, L., RITTIG, K. 2012. 4-1BB ligand modulates direct and Rituximab-induced NK-cell reactivity in chronic lymphocytic leukeamia. *European Journal of Immunology,* 42, 737-748.
- BURGER J.A., BURGER M., KIPPS T.J. 1999. Chronic lymphocytic leukemia B cells express functional CXCR4 chemokine receptors that mediate spontaneous migration beneath bone marrow stromal cells. *Blood*. 1;94(11):3658-67.
- BURGER, J. A. & KIPPS, T. J. 2002. Chemokine receptors and stromal cells in the homing and homeostasis of chronic lymphocytic leukemia B cells. *Leuk Lymphoma,* 43, 461-6.
- BURGER, J. A. & KIPPS, T. J. 2006. CXCR4: a key receptor in the crosstalk between tumor cells and their microenvironment. *Blood*, 107, 1761-7.
- BURGER, J. A. & PELED, A. 2009. CXCR4 antagonists: targeting the microenvironment in leukemia and other cancers. *Leukemia*, 23, 43-52.
- BURGER, J. A., QUIROGA, M. P., HARTMANN, E., BURKLE, A., WIERDA, W. G., KEATING, M. J. & ROSENWALD, A. 2009b. High-level expression of the T-cell

chemokines CCL3 and CCL4 by chronic lymphocytic leukemia B cells in nurselike cell cocultures and after BCR stimulation. *Blood*, 113, 3050-8.

- BURGER, J. A., TSUKADA, N., BURGER, M., ZVAIFLER, N. J., DELL'AQUILA, M. & KIPPS, T. J. 2000. Blood-derived nurse-like cells protect chronic lymphocytic leukemia B cells from spontaneous apoptosis through stromal cell-derived factor-1. *Blood*, 96, 2655-63.
- BURGER, M., HARTMANN, T., KROME, M., RAWLUK, J., TAMAMURA, H., FUJII, N., KIPPS, T. J. & BURGER, J. A. 2005. Small peptide inhibitors of the CXCR4 chemokine receptor (CD184) antagonize the activation, migration, and antiapoptotic responses of CXCL12 in chronic lymphocytic leukemia B cells. *Blood*, 106, 1824-30.
- BURGER, J.A,, TSUKADA, N., BURGER, M., ZVAIFLER, N.J,, DELL'AQUILA, M., KIPPS, T.J., 2000. Blood-derived nurse-like cells protect chronic lymphocytic leukeamia B cells from spontaneous apoptosis through stromal cell-derived factor-1. *Blood*. 96: 2655-2663.
- BURGER, J.A. 2011. Nurture versus nature: the microenvironment in chronic lymphocytic leukeamia. *Hematology Am Soc Hematol Educ* Program: 96–103.
- BURGER, M., HARTMANN, T., KROME, M., RAWLUK, J., TAMAMURA, H. & FUJII, N. 2005. Small peptide inhibitors of the CXCR4 chemokine receptor (CD184) antagonize the activation, migration, and antiapoptotic responses of CXCL12 in chronic lymphocytic leukeamia B cells. *Blood*, 106, 1824–1830.
- BUTCHER, E. C. & PICKER, L. J. 1996. Lymphocyte homing and homeostasis. *Science,* 272, 60-66.
- C.D. HELGASON, C.D., C.P. KALBERER, C.P., J.E. DAMEN, J.E., S.M. CHAPPEL, S.M., N. PINEAULT, N. & G. KRYSTAL, G. 2000. A dual role for Src homology 2 domain-containing inositol-5-phosphatase (SHIP) in immunity: aberrant development and enhanced function of b lymphocytes in ship –/– mice. *J Exp Med*, 191, 781–794.
- CALANDRA, G., BRIDGER, G. & FRICKER, S. 2010. CXCR4 in clinical hematology. *Current Topics in Microbiology and Immunology*, 341, 173–191.
- CALIGARIS-CAPPIO, F., BERTILACCIO, M.T. & SCIELZO, C. 2014. How the microenvironment wires the natural history of chronic lymphocytic leukeamia. *Semin Cancer Biol*, 24, 43-48.
- CALIN, M., FERRACIN, A., CIMMINO, C,. 2005. A microRNA signature associated with prognosis and progression in chronic lymphocytic leukeamia. *The New England Journal of Medicine,* vol. 353, no. 17, pp. 1793–1801.
- CALISSANO, C., DAMLE, R. N., HAYES, G., MURPHY, E. J., HELLERSTEIN, M. K. & MORENO, C. 2009. In vivo intraclonal and interclonal kinetic heterogeneity in B-cell chronic lymphocytic leukeamia. *Blood*, 114, 4832-4842.
- CALPE, E., CODONY, C., BAPTISTA, MJ., ABRISQUETA, P., CARPIO, C., PURROY, N., BOSCH, F. & CRESPO, M. 2011. ZAP-70 enhances migration of malignant B lymphocytes towards CCL21 by inducing CCR7 expression via IgM-ERK1/2 activation. *Blood*, 118, 4401–10.
- CAMBIER. J.C., PLEIMAN, C.M., CLARK, M.R,. 1994. Signal transduction by the B cell antigen receptor and its coreceptors. Annu Rev Immunol; 12:457–86. *Cancer Res* July 15 2006 (66) (14) 7158-7166;
- CAO, Y., HUNTER, Z.R., LIU, X., XU, L., YANG, G., CHEN, J. 2014 . CXCR4 WHIM-like frameshift and nonsense mutations promote ibrutinib resistance but do not supplant MYD88 -directed survival signalling in Waldenstrom macroglobulinaemia cells. *Br J Haematol*; 168: 701–707.

- CAPLAN, A.I. 1991. Mesenchymal stem cells. J Orthop Res, 9, 641–650.
- CASTRILLO A, JOSEPH S..B., MARATHE C., MANGELSDORF D.J., TONTONOZ P. 2003 .*J Biol Chem*. Mar 21; 278(12):10443-9.
- CHEN L., MONTI S., JUSZCZYNSKI P., OUYANG J., CHAPUY B., NEUBERG D., DOENCH J.G., BOGUSZ A.M., HABERMANN T.M., DOGAN A., WITZIG T.E., KUTOK J.L., RODIG S.J., GOLUB T., 2013. SHIPP M.A. SYK Inhibition Modulates Distinct PI3K/AKT-Dependent Survival Pathways and Cholesterol Biosynthesis in Diffuse Large B Cell Lymphomas. *Cancer cell.* ;23(6):826–38.
- CHEN, L., HUYNH, L. & APGAR, J, 2008. ZAP-70 enhances IgM signaling independent of its kinase activity in chronic lymphocytic leukeamia. Blood. 111, 5, 2685–2692.
- CHEN, L., WIDHOPF, G. & HUYNH, L. 2002. Expression of ZAP-70 is associated with increased B-cell receptor signaling in chronic lymphocytic leukeamia. *Blood*, 100,3, 4609–4614.
- CHEN, S-SS., CHANG, B.Y., CHANG, S., TONG, T., HAM, S., SHERRY, B., BURGER, J.A., RAI, K.R. & CHIORAZZI. N. 2016. BTK inhibition results in impaired CXCR4 chemokine receptor surface expression, signaling and function in chronic lymphocytic *leukeamia*, 30, 833–843;
- CHILOSI, M. 1983. Routine immunofluorescent and histochemical analysis of bone marrow involvement of lymphoma/leukaemia: the use of cryostat sections. *Br J Cancer*, 48, 6, 763–775.
- CHILOSI, M. 1985. Immunohistochemical demonstration of follicular dendritic cells in bone marrow involvement of B-cell chronic lymphocytic leukeamia. *Cancer*, 56, 2, 328–32.
- CINAMON, G., ZACHARIAH, M. A., LAM, O. M., FOSS JR., F. W. & CYSTER, J. G. 2008. Follicular shuttling of marginal zone B cells facilitates antigen transport. *Nature Immunology*, 9, 54-62.
- CIRAOLO, E., MORELLO, F., HIRSCH, E. 2011. Present and future of PI3K pathway inhibition in cancer: perspectives and limitations. *Curr Med Chem*. ;18:2674–2685
- CLARKE P.A, WORKMAN P. Phosphatidylinositide-3-kinase inhibitors: addressing questions of isoform selectivity and pharmacodynamic/predictive biomarkers in early clinical trials. *J Clin Oncol.* 2012;30:331–333
- CLAYTON E., BARDI G., BELL S.E., CHANTRY D., DOWNES C.P., GRAY A., HUMPHRIES L.A., RAWLINGS D., REYNOLDS H., VIGORITO E., TURNER M. 2002. A Crucial Role for the p110δ Subunit of Phosphatidylinositol 3-Kinase in B Cell Development and Activation. *J Exp Med*.196:753–763.
- COFFMAN, R. L., LEBMAN, D. A. AND ROTHMAN, P.. 1993. Mechanism and regulation of immunoglobulin isotype switching. *Adv. Immunol*. 54: 229–270.
- CONTRI, A., BRUNATI , A.M., TRENTIN, L., CABRELLE, A., MIORIN, M., CESARO, L. 2005. Chronic lymphocytic leukeamia B cells contain anomalous LYN tyrosine kinase, a putative contribution to defective apoptosis. *J Clin Invest*, 115(2):369–78
- COUGHLIN S., NOVISKI M., MUELLER J.L., CHUWONPAD A., RASCHKE W.C., WEISS A., ZIKHERMAN J 2015.. An extracatalytic function of CD45 in B cells is mediated by CD22. *PNAS* ; 112 (47) E6515-E6524
- CUESTA-MATEOS, C., LÓPEZ-GIRAL, S., ALFONSO-PÉREZ, M., DE SORIA, V. G., LOSCERTALES, J., GUASCH-VIDAL, S., BELTRÁN, A. E., ZAPATA, J. M. & MUÑOZ-CALLEJA, C. 2010. Analysis of migratory and prosurvival pathways induced by the homeostatic chemokines CCL19 and CCL21 in B-cell chronic lymphocytic leukeamia. *Exp Hematol*, 38, 756–64, 764 e1-4.

- CUNÍ, S., PÉREZ-ACIEGO, P., PÉREZ-CHACÓN, G., VARGAS J.A., SÁNCHEZ A., MARTÍN-SAAVEDRA F.M., BALLESTER S., GARCÍA-MARCO J., JORDÁ J., DURÁNTEZ, A. 2004. A sustained activation of PI3K/NF-kappaB pathway is critical for the survival of chronic lymphocytic leukeamia B cells. *Leukeamia*. 18:1391–1400 10.1038/sj.leu.2403398
- CYSTER, J.G. & ANSEL, K.M., REIF, K. 2000. Follicular stromal cells and lymphocyte homing to follicles. *Immunol Rev,* 176,181–93.
- DAL BO, M. 2010. Microenvironmental interactions in chronic lymphocytic leukeamia: hints for pathogenesis and identification of targets for rational therapy. *Curr Pharm Des*, 18(23):3323–34.
- DAL PORTO, J.M., GAULD, S.B., MERRELL, K.T, MILLS D., PUGH-BERNARD A.E., Cambier J. B cell antigen receptor signaling 101. Mol. Immunol. 41(6-7), 599–613. (2004)
- DANCESCU, M. 1992. Interleukin 4 protects chronic lymphocytic leukemic B cells from death by apoptosis and upregulates Bcl-2 expression. *J Exp Med,* 176, 5, 1319–26.
- DAUGVILAITE, VIKTORIJA et al. "Oxysterol-EBI2 signaling in immune regulation and viral infection." *European journal of immunology* vol. 44,7 (2014): 1904-12. doi:10.1002/eji.201444493
- DE GORTER, D. J., BEULING, E. A. & KERSSEBOOM, R. 2007. Bruton's tyrosine kinase and phospholipase Cgamma2 mediate chemokine-controlled B cell migration and homing. Immunity, 26, 1, 93–104.
- DE LA FUENTE, M.T., CASANOVA, B., GARCIA-GILA, M., SILVA, A. & GARCIA-PARDO, A. 1999. Fibronectin interaction with alpha4beta1 integrin prevents apoptosis in B cell chronic lymphocytic leukeamia: correlation with Bcl-2 and Bax. *Leukeamia*, 13, 266-274.
- DE NIGRIS, F., SCHIANO, C., INFANTE, T. & NAPOLI, C. 2012. CXCR4 inhibitors: tumor vasculature and therapeutic challenges. *Recent Patents on Anticancer Drug Discovery,* 7, 251–264.
- DEAGLIO, S., AYDIN, S., GRAND, M. M., VAISITTI, T., BERGUI, L., D'ARENA, G., CHIORINO, G. & MALAVASI, F. 2010. CD38/CD31 interactions activate genetic pathways leading to proliferation and migration in chronic lymphocytic leukeamia cells. *Mol Med,* 16, 87-91.
- DEAGLIO, S., VAISITTI, T. & AYDIN, S. 2007. CD38 and ZAP-70 are functionally linked and mark CLL cells with high migratory potential. *Blood110*, 12, 4012–4021.
- DEAGLIO, S., VAISITTI, T., BERGUI, L., BONELLO, L, HORENSTEIN, A.L. & TAMAGNONE, L. 2005. CD38 and CD100 lead a network of surface receptors relaying positive signals for B-CLL growth and survival Blood, 105, 3042–3050.
- DEGLESNE, P.A., CHEVALLIER N., LETESTU R., BARAN-MARSZAK F., BEITAR T, SALANOUBAT C., SANHES L., NATAF J., ROGER C., VARIN-BLANK N., AJCHENBAUM-CYMBALISTA F. 2006. Survival response to B-cell receptor ligation is restricted to progressive chronic lymphocytic leukeamia cells irrespective of Zap70 expression. Cancer Res.: Jul 15;66(14):7158-66.
- DI CRISTOFANO, A., KOTSI P., PENG Y.F., CORDON-CARDO C, ELKON K.B., PANDOLFI P.P. 1999 Impaired Fas response and autoimmunity in Pten+/– mice. *Science.*;285:2122–2125.
- DU X., KRISTIANA I., WONG J., BROWN A.J. 2006 Involvement of Akt in ER-to-Golgi transport of SCAP/SREBP: a link between a key cell proliferative pathway and membrane synthesis. *Mol Biol Cell* 17: 2735–2745.

- DUDA, D.G., KOZIN, S.V., KIRKPATRICK, N.D., XU, L., FUKUMURA, D. & JAIN, R.K. 2011. CXCL12 (SDF1alpha)-CXCR4/CXCR7 pathway inhibition: an emerging sensitizer for anticancer therapies?*Clinical Cancer Research*, 17, 2074–2080.
- DÜRIG, J., SCHMÜCKER, U. & DÜHRSEN, U. 2001. Differential expression of chemokine receptors in B cell malignancies. *Leukeamia*, 15, 752–756.
- ENDE, Z., HUANBIN X., LIN W., ILONA K., WU K., YU, H., WAN, G AND WEIPING Z. 2012. 2012 Bone marrow and the control of immunity. *Cellular & Molecular Immunology*, 11–19
- ENDERS, A., BOUILLET, P., PUTHALAKATH, H., XU Y., TARLINTON, D.M., STRASSER A. 2003. Loss of the pro-apoptotic BH3-only Bcl-2 family member Bim inhibits BCR stimulation-induced apoptosis and deletion of autoreactive B cells. *J Exp Med*;198(7):1119–26
- FAYAD, L., KEATING, M.J., REUBEN, J.M., O'BRIEN, S., LEE, BN., LERNER, S., KURZROCK R. 2010. Interleukin-6 and interleukin-10 levels in chronic lymphocytic leukeamia: correlation with phenotypic characteristics and outcome. *Blood*, 97: 256-263.
- FLINN, I.W., O'BRIEN, S., KAHL B., PATEL, M., OKI Y., FOSS, F.F, et al. 2018. Duvelisib, a novel oral dual inhibitor of PI3K-delta,gamma, is clinically active in advanced hematologic malignancies. *Blood* ;131(8):877-87.
- FÖRSTER, R., DAVALOS-MISSLITZ, A. C. & ROT, A. 2008. CCR7 and its ligands: balancing immunity and tolerance. *Nat Rev Immunol*, 8, 362–71.
- FORSTER, R., MATTIS, A. E., KREMMER, E., WOLF, E., BREM, G. & LIPP, M. 2003. A putative chemokine receptor, BLR1, directs B cell migration to defined lymphoid organs and specific anatomic compartments of the spleen. *Cel*l, 87, 1037-1047.
- FRIEDMAN, D. R. (2017). Lipids and Their Effects in Chronic Lymphocytic Leukeamia. EBioMedicine, 15, 2–3. doi:10.1016/j.ebiom.2016.12.001
- FRUMAN, DA. 2004. Phosphoinositide 3-kinase and its targets in B-cell and T-cell signaling. *Curr Opin Immunol* 16:314–20.
- FURMAN, R.R., ASGARY, Z., MASCARENHAS, J.O. 2000. Modulation of NF-kappa B activity and apoptosis in chronic lymphocytic leukeamia B cells. *J Immunol*. Feb 15; 164(4):2200-6.
- GATTEI, V, BULIAN, P, DEL PRINCIPE, MI, ZUCCHETTO, A, MAURILLO, L, BUCCISANO, F, BOMBEN, R, DAL-BO M, LUCIANO F, ROSSI, F.M, DEGAN, M, AMADORI, S, DEL POETA, G. 2008. Relevance of CD49d protein expression as overall survival and progressive disease prognosticator in chronic lymphocytic leukeamia. *Blood* p111(2):865–873.
- GEHRKE, I., GANDHIRAJAN, R. K., POLL-WOLBECK, S.J., HALLEK, M. & KREUZER, K.A. 2011. Bone marrow stromal cell-derived vascular endothelial growth factor (VEGF) rather than chronic lymphocytic leukeamia (CLL) cell-derived VEGF is essential for the apoptotic resistance of cultured CLL cells. *Mol Med*, 17, 619-627.
- GEYEREGGER, R., SHEHATA, M., ZEYDA, M., KIEFER F.W., STUHLMEIER, K.M., PORPACZY, E., ZLABINGER G.J., JÄGER U., STULNIG, T.,M 2009. Liver X receptors interfere with cytokine-induced proliferation and cell survival in normal and leukemic lymphocytes. *J Leukoc Biol*. 2009 Nov; 86(5):1039-48.
- GOODNOW, C.C., BRINK, R. & ADAMS, E. 1991. Breakdown of self-tolerance in anergic B lymphocytes. Nature, 352, 6335, 532–6.
- GORGUN, G., HOLDERRIED, T.A, ZAHRIEH, D., NEUBERG, D. & GRIBBEN, J.G. 2005. Chronic lymphocytic leukeamia cells induce changes in gene expression of CD4 and CD8T cells. *The Journal of Clinical Investigation,* 115, 1797-1805.

- GURVINDER, K. & DUFOUR, J.M. 2016. Cell Lines: Valuable Tools or Useless Artifacts. *Spermatogenesis,* 2.1, 1–5.
- HAAS, K. M. (2015). B-1 lymphocytes in mice and nonhuman primates. Annals of the New York Academy of Sciences, 1362(1), 98–109. doi:10.1111/nyas.12760
- HALLAERT, D. Y. 2008. c-Abl kinase inhibitors overcome CD40-mediated drug resistance in CLL; Implications for therapeutic targeting of chemoresistant niches. *Blood*. 352, 6335, 532–6
- HARRIS, N.L., JAFFE, E.S., DIEBOLD, J., FLANDRIN, G., MULLER-HERMELINK, H.K., VARDIMAN, J., LISTER, T.A., BLOOMFIELD, C.D. 1997. World Health Organization classification of neoplastic diseases of the hematopoietic and lymphoid tissues: report of the Clinical Advisory Committee meeting-Airlie House, Virginia. *J Clin Oncol*. (12):3835-49.
- HARWOOD, N.E. & BATISTA, F.D. 2008. New insights into the early molecular events underlying B cell activation*. Immunity*, 28, 5, 609–19.
- HASBOLD, J., LYONS, A. B., KEHRY, M. R. AND HODGKIN, P. D. 1998. Cell division number regulates IgG1 and IgE switching of B cells following stimulation by CD40 ligand and IL-4. *Eur. J. Immunol*. 28: 1040–1051.
- HASHIMOTO, A, OKADA, H., JIANG, A. 1998. Involvement of guanosine triphosphatases and phospholipase C-gamma2 in extracellular signal-regulated kinase, c-Jun NH2-terminal kinase, and p38 mitogen-activated protein kinase activation by the B cell antigen receptor. *J Exp Med,* 188(7):1287–1295.
- HERISHANU, Y., GIBELLINI, F., NJUGUNA, N., HAZAN-HALEVY, I., FAROOQUI, M. & BERN, S. 2011. Activation of CD44, a receptor for extracellular matrix components, protects chronic lymphocytic leukeamia cells from spontaneous and drug induced apoptosis through MCL-1. *Leuk Lymphoma*, 52, 1758-1769.
- HERISHANU, Y., KATZ, B.Z., LIPSKY, A. & WIESTNER, A. 2013. Biology of Chronic Lymphocytic Leukeamia in Different Microenvironments: Clinical and Therapeutic Implications. *Hematology/oncology clinics of North America*, 27,2,173-206.
- HERISHANU, Y., PÉREZ-GALÁN, P., LIU, D., 2011. The lymph node microenvironment promotes B-cell receptor signaling, NF-kappaB activation, and tumor proliferation in chronic lymphocytic leukeamia. *Blood*, 117(2):563–574.
- HERMAN, S.E., GORDON, A.L., HERTLEIN, E. 2011. Bruton tyrosine kinase represents a promising therapeutic target for treatment of chronic lymphocytic leukeamia and is effectively targeted by PCI-32765. *Blood*. Jun 9; 117(23):6287-96.
- HERMAN, S.E., GORDON, A.L., WAGNER, A. 2010 . Phosphatidylinositol 3-kinase-δ inhibitor CAL-101 shows promising preclinical activity in chronic lymphocytic leukeamia by antagonizing intrinsic and extrinsic cellular survival signals. *Blood*, Sep 23; 116(12):2078-88.
- HEWAMANA, S., ALGHAZAL, S., LIN, T.T. 2008. The NF-kappaB subunit Rel A is associated with in vitro survival and clinical disease progression in chronic lymphocytic leukeamia and represents a promising therapeutic target. *Blood*, May 1; 111(9):4681-9
- HODGKIN, P. D., GO, N. F., CUPP, J. E. AND HOWARD, M. 1991. Interleukin-4 enhances anti-IgM stimulation of B cells by improving cell viability and by increasing the sensitivity of B cells to the anti-IgM signal. Cell. Immunol. 134: 14–30.
- HODGKIN, P. D., YAMASHITA, L. C., COFFMAN, R. L. AND KEHRY, M. R.,1990. Separation of events mediating B cell proliferation and Ig production by using T cell membranes and lymphokines. *J. Immunol*. 45: 2025–2034.

- HONG, C., DUIT, S., JALONEN, P., OUT, R., SCHEER, L., SORRENTINO, V., ZELCER, N. (2010). The E3 ubiquitin ligase IDOL induces the degradation of the low density lipoprotein receptor family members VLDLR and ApoER2. *The Journal of biological chemistry,* 285(26), 19720–19726. doi:10.1074/jbc.M110.123729
- HORTON J.D., SHAH N.A., WARRINGTON J.A., ANDERSON N.N., PARK S.W, et al. (2003) Combined analysis of oligonucleotide microarray data from transgenic and knockout mice identifies direct SREBP target genes. *Proc Natl Acad Sci* USA 100: 12027–12032.
- HUDAK, S. A., GOLLNICK, S. O., CONRAD, D. H. AND KEHRY, M. R. 1987. Murine B cell stimulatory factor 1 (interleukin 4) increases expression of the Fc receptor for IgE on mouse B cells. *Proc. Natl. Acad. Sci.* USA 84: 4606–4610.
- JAIN, P., JAVDAN, M., FEGER, F.K., CHIU, P.Y., SISON, C. & DAMLE, R.N. 2012. Th17 and non-Th17 interleukin-17-expressing cells in chronic lymphocytic leukeamia: delineation, distribution, and clinical relevance *Haematologica*, 97, 599–607.
- JIA, L., CLEAR, A., LIU, F.T., MATTHEWS, J., UDDIN, N., MCCARTHY, A. 2014. Extracellular HMGB1 promotes differentiation of nurse-like cells in chronic lymphocytic leukeamia. *Blood,* 123,1709–1719.
- RAI, K.R., SAWITSKY, A., CRONKITE, E.P., CHANANA, A.D., LEVY, R.N., PASTERNACK, B.S. 1975. Clinical staging of chronic lymphocytic leukeamia Blood, 46 pp. 219–234
- KAMINSKI, D.A., WEI, C., QIAN, Y., ROSENBERG, A.F. & SANZ, I. 2012. Advances in Human B Cell Phenotypic Profiling. *Frontiers in Immunology*, 3, 302.
- KATER, A.P., SPIERING. M, LIU, R.D. 2014. Dasatinib in combination with fludarabine in patients with refractory chronic lymphocytic leukaemia: a multicenter phase 2 study. *LeukRes* ;38(1):34-41.
- KATRINAKIS, G., KYRIAKOU, D., PAPADAKI, H., KALOKYRI, I., MARKIDOU, F. & ELIOPOULOS. G.D. 1996. Defective natural killer cell activity in B-cell chronic lymphocytic leukaemia is associated with impaired release of natural killer cytotoxic factor(s) but not of tumour necrosis factor-alpha. Acta Haematologica, 96, 16-23.
- KAY, N.E & ZARLING, J. 1987. Restoration of impaired natural killer cell activity of B-chronic lymphocytic leukeamia patients by recombinant interleukin-2. *American Journal of Hematology,* 24, 161-167.
- KAY, N.E & ZARLING, J.M. 1984. Impaired natural killer activity in patients with chronic lymphocytic leukeamia is associated with a deficiency of azurophilic cytoplasmic granules in putative NK cells. *Blood,* 63:305-309.
- KEAM, S.J. 2011. Dasatinib: a review of its use in the treatment of chronic myeloid leukaemia and Philadelphia chromosome-positive acute lymphoblastic leukaemia. *Drugs,* 71(13):1771-1795.
- KENNAH M, YAU T.Y., NODWELL M., KRYSTAL G., ANDERSON R..J, ONG C.J., MUI A.L.. 2009. Activation of SHIP via a small molecule agonist kills multiple myeloma cells. *Exp Hematol*. ;37:1274–1283.
- KENT C.W., LANDAY A. “Liver X receptor alpha (LXRalpha) as a therapeutic target in chronic lymphocytic leukeamia (CLL).” Journal of leukocyte biology vol. 86,5 (2009): 1019-21.
- KINDT, T., GOLDSBY, R., OSBORNE, B., KUBY, J. AND KUBY, J. (2007). Kuby immunology. New York: W.H. Freeman.
- KLYUSHNENKOVA, E., MOSCA, J.D., ZERNETKINA, V., MAJUMDAR, M.K., BEGGS, K.J. & SIMONETTI, D.W. 2005. T cell responses to allogeneic human mesenchymal stem cells: immunogenicity, tolerance, and suppression. *J Biomed Sci*, 12, 47–57.

- KRAUSE G., HASSENRUCK F., HALLEK M. Copanlisib for treatment of B-cell malignancies: the development of a PI3K inhibitor with considerable differences to idelalisib. *Drug Des Devel Ther* 2018;12:2577-90.
- KRYSOV, S., DIAS, S., PATERSON, A., MOCKRIDGE, C. I., POTTER, K. N., SMITH, K. A., ASHTON-KEY, M., STEVENSON, F. K. & PACKHAM, G. 2012. Surface IgM stimulation induces MEK1/2-dependent MYC expression in chronic lymphocytic leukemia cells. *Blood*, 119, 170-9.
- KRYSOV, S., STEELE, A. J., COELHO, V., LINLEY, A., SANCHEZ HIDALGO, M., CARTER, M., POTTER, K. N., KENNEDY, B., DUNCOMBE, A. S., ASHTON-KEY, M., FORCONI, F., STEVENSON, F. K. & PACKHAM, G. 2014. Stimulation of surface IgM of chronic lymphocytic leukemia cells induces an unfolded protein response dependent on BTK and SYK. *Blood,* 124, 3101-9.
- KUROSAKI T., SHINOHARA H., BABA Y. 2010. B cell signaling and fate decision. *Annu. Rev Immunol.* 28, 21–55.\
- LAGNEAUX, L., DELFORGE, A., DE BRUYN, C., BERNIER, M., BRON, D. 1999. Adhesion to bone marrow stroma inhibits apoptosis of chronic lymphocytic leukeamia cells. *Leukeamia Lymphoma*, 35: 445-453.
- LAMPSON B.L., BROWN J.R. 2018. Are BTK and PLCG2 mutations necessary and sufficient for ibrutinib resistance in chronic lymphocytic leukeamia*?. Expert Rev Hematol* ;11(3):185–194. doi:10.1080/17474086.2018.1435268
- LANEMO, M.A., HELLQVIST, E., SIDOROVA, E., SODERBERG, A., BAXENDALE, H., DAHLE, C., WILLANDER, K., TOBIN, G., BACKMAN, E., SODERBERG, O. 2011. A new perspective: molecular motifs on oxidized LDL, apoptotic cells, and bacteria are targets for chronic lymphocytic leukeamia antibodies. *Blood.* p111(7):3838–48.
- LANHAM, S., HAMBLIN, T., OSCIER, D., IBBOTSON, R., STEVENSON, F. & PACKHAM G. 2003. Differential signaling via surface IgM is associated with VH gene mutational status and CD38 expression in chronic lymphocytic leukeamia. *Blood*, 101, 1087-1093.
- LEBIEN, T.W & TEDDER, T.F. 2008. B lymphocytes: how they develop and function. *Blood*, 112, 5, 1570–80.
- LEE, Y.K. 2005. VEGF receptor phosphorylation status and apoptosis is modulated by a green tea component, epigallocatechin-3-gallate (EGCG), in B-cell chronic lymphocytic leukeamia. *Blood,* 104,3,788–94.
- LEUNG, W-H., TARASENKO, T., BIESOVA, Z., KOLE, H., WALSH, E.R. & BOLLAND, S. Aberrant antibody affinity selection in SHIP-deficient B cells. *European Journal of Immunology*, 43, 371–81.
- LI, S., HE, Y., LIN, Z., XU, S.,ZHOU, R., LIANG, F., WANG, J,. YANG, H., LIU, S., AND REN Y. 2017. Digging More Missing Proteins Using an Enrichment Approach with *ProteoMiner* Journal of Proteome Research 16 (12), 4330-4339
- LI, F. 1998. Control of apoptosis and mitotic spindle checkpoint db survivin. *Nature,* 396, 6711, 580–4.
- LIOUBIN, M.N., ALGATE, P.A., CARLBERG, K., BOWTELL, D., ROHRSCHNEIDER, L.R. 1996. P150-Ship, a signal transduction molecule with inositol polyphosphate-5-phosphatase activity. *Genes Dev*, 10:1084-95
- LIU, Q., OLIVEIRA-DOS-SANTOS, A.J., MARIATHASAN, S., BOUCHARD, D., JONES, J., R. SARAO, R. 1998. The inositol polyphosphate 5-phosphatase ship is a crucial negative regulator of B cell antigen receptor signalling *J Exp Med,* 188pp. 1333–1342

- LJUNGSTROM, V. et al 2016. Whole-exome sequencing in relapsing chronic lymphocytic leukeamia: clinical impact of recurrent RPS15 mutations. *Blood* 127, 1007–1016
- LÓPEZ-GIRAL, S., QUINTANA, N. E. & CABRERIZO, M. 2004. Chemokine receptors that mediate B cell homing to secondary lymphoid tissues are highly expressed in B cell chronic lymphocytic leukeamia and non-Hodgkin lymphomas with widespread nodular dissemination. *J Leukocyte Biol* 76, 2, 462-471.
- MA, Q., JONES, D. & BORGHESANI, P. R. 1998. Impaired B-lymphopoiesis, myelopoiesis, and derailed cerebellar neuron migration in CXCR4- and SDF-1-deficient mice. *Proceedings of the National Academy of Sciences of the United States of America,* 95, 16, 9448-9453.
- MAKI, G., HAYES, G.M., NAJI, A., TYLER, T., CAROSELLA, E.D., ROUAS-FREISS, N. 2008. NK resistance of tumor cells from multiple myeloma and chronic lymphocytic leukeamia patients: implication of HLA-G. *Leukeamia*, 22, 998-1006.
- MALCOVATI, L., PAPAEMMANUIL, E., BOWEN, D.T., BOULTWOOD, J., DELLA-PORTA, M.G., PASCUTTO, C., et al 2011. Chronic Myeloid Disorders Working Group of the International Cancer Genome Consortium and of the Associazione Italiana per la Ricerca sul Cancro Gruppo Italiano Malattie Mieloproliferative. Clinical significance of SF3B1 mutations in myelodysplastic syndromes and myelodysplastic/myeloproliferative neoplasms. *Blood*.;118(24):6239–46.
- MALISZEWSKI, C. R., GRABSTEIN, K., FANSLOW, W. C., ARMITAGE, R., SPRIGGS, M. K. AND SATO, T. A. 1993. Recombinant CD40 ligand stimulation of murine B cell growth and differentiation: cooperative effects of cytokines. *Eur. J. Immunol.* 23: 1044–1049.
- MCCARTHY, D. J., CHEN, Y., & SMYTH, G. K. (2012). Differential expression analysis of multifactor RNA-Seq experiments with respect to biological variation. *Nucleic acids research,* 40(10), 4288–4297. doi:10.1093/nar/gks042
- MCCAW, L., SHI, Y., WANG, G., LI, Y. J., & SPANER, D. E. (2017). Low Density Lipoproteins Amplify Cytokine-signaling in Chronic Lymphocytic Leukeamia Cells. *EBioMedicine*, 15, 24–35. doi:10.1016/j.ebiom.2016.11.033
- MEIMETIS L., NODWELL M., YANG L., WANG X., WU J., HARWIG C. 2012. Synthesis of SHIP1-activating analogs of the sponge meroterpenoid pelorol. European Journal of Organic Chemistry; (27):5195 - 207.
- MÉTÉZEAU, P., ELGUINDI, I., & GOLDBERG, M. E. (1984). Endocytosis of the membrane immunoglobulins of mouse spleen B-cells: a quantitative study of its rate, amount and sensitivity to physiological, physical and cross-linking agents. *The EMBO journal*, 3(10), 2235–2242.
- MILETIC, A.V., ANZELON-MILLS, A.N, MILLS, D.M. 2010. Coordinate suppression of B cell lymphoma by PTEN and SHIP phosphatases. *The Journal of Experimental Medicine,* 207(11):2407-2420.
- MINGES-WOLS, H.A., UNDERHILL, G.H., KANSAS, G.S. & WITTE, P.L. 2002. The role of bone marrow-derived stromal cells in the maintenance of plasma cell longevity. *J Immunol,* 169, 4213–4221.
- MITTAL A.K, CHATURVEDI, N.K, RAI, K.J. 2014 .Chronic Lymphocytic Leukeamia Cells in a Lymph Node Microenvironment Depict Molecular Signature Associated with an Aggressive Disease. *Molecular Medicine* p20(1):290-301.

- MOODY J.L, PEREIRA C.G, MAGIL A., FRITZLER M.J, JIRIK F.R. 2003. Loss of a single allele of SHIP exacerbates the immunopathology of Pten heterozygous mice. *Genes Immun;*4:60–66.
- MOTTA, M., RASSENTI, L., SHELVIN, B.J., LERNER, S., KIPPS, T.J. & KEATING, M.J. 2005. Increased expression of CD152 (CTLA-4) by normal T lymphocytes in untreated patients with B-cell chronic lymphocytic leukeamia. *Leukeamia,* 19, 1788–1793.
- MRAZ, M. & KIPPS, T.J. 2013. MicroRNAs and B cell receptor signaling in chronic lymphocytic leukeamia. Leukeamia and Lymphoma, 54, 8, 1836–1839.
- MUELLNER, M.K., URAS, I.Z., GAPP, B.V., KERZENDORFER. C., SMIDA, M., LECHTERMANN, H., CRAIG-MUELLER, N., COLINGE, J., DUERNBERGER, G., NIJMAN, S.M. 2011. A chemical-genetic screen reveals a mechanism of resistance to PI3K inhibitors in cancer. *Nat Chem Biol*. Sep 25; 7(11):787-93.
- MURRAY, M.Y., ZAITSEVA, L., AUGER, M.J, et al. 2015. Ibrutinib inhibits BTK-driven NF-κB p65 activity to overcome bortezomib-resistance in multiple myeloma. Cell Cycle. ;14(14):2367–2375. doi:10.1080/15384101.2014.998067
- NABHAN, C. & ROSEN, S.T. 2014. Chronic Lymphocytic Leukeamia: *A Clinical Review*. JAMA, 312, 21, 2265-2276.
- NADKARNI, J.J., PERAMBAKAM, S.M., RATHORE, V.B., AMIN, K.M., PARIKH, P.M., NARESH, K.N. & ADVANI, S.H. 1998. Expression of adhesion molecules in B-cell chronic lymphocytic leukaemia: an analysis in lymphoid compartments–peripheral Blood, bone marrow and lymph node. *Cancer Biotherapy & Radiopharmaceuticals,* 13, 269–274.
- NAGASAWA, T., KIKUTANI, H., KISHIMOTO, T. 1994. Molecular cloning and structure of a pre-B-cell growth-stimulating factor. *Proceedings of the National Academy of Sciences of the United States of America,* 91(6):2305-2309.
- NAYIOTIDIS, P., JONES, D., GANESHAGURU, K., FORONI, L/, HOFFBRAND. AV. 1996. Human bone marrow stromal cells prevent apoptosis and support the survival of chronic lymphocytic leukaemia cells in vitro. *Br J Haematol*, 92: 97-103.
- NICKEL, J.C., EGERDIE, B., DAVIS, E., EVANS, R., MACKENZIE, L., SHREWSBURY, S.B. 2016. A Phase II Study of the Efficacy and Safety of the Novel Oral SHIP1 Activator AQX-1125 in Subjects with Moderate to Severe Interstitial Cystitis/Bladder Pain Syndrome. *J Urol*. J196(3):747-54.
- NIEDERMEIER, M., HENNESSY, B.T,, KNIGHT, Z.A., HENNEBERG, M., HU, J., KURTOVA, A.V., WIERDA, W.G., KEATING. M.J, SHOKAT, K.M., BURGER, J.A. 2009. Isoform-selective phosphoinositide 3'-kinase inhibitors inhibit CXCR4 signaling and overcome stromal cell-mediated drug resistance in chronic lymphocytic leukeamia: a novel therapeutic approach. Blood. 113(22):5549-57.
- NIEMANN, C.U., WIESTNER, A. 2013. B-cell receptor signaling as a driver of lymphoma development and evolution. *Seminars in cancer biology.* 2013;23(6):410-421.
- NISHIO, M., ENDO, T., TSUKADA, N., OHATA, J., KITADA, S. & REED, J.C. 2005. Nurselike cells express BAFF and APRIL, which can promote survival of chronic lymphocytic leukeamia cells via a paracrine pathway distinct from that of SDF-1alpha. *Blood*, 106, 1012-1020.
- NOELLE, R. J.,MCCANN, J., MARSHALL, L. AND BARTLETT, W. C. 1989. Cognateinteractions between helper T cells and B cells. III. Contact-dependent, lymphokine-independent induction of B cell cycle entry by activated helper T cells. *J. Immunol*. 143: 1807–1814.

- O'HAYRE, M., SALANGA, C. L., KIPPS, T. J., D. 2010. Elucidating the CXCL12/CXCR4 signaling network in chronic lymphocytic leukeamia through phosphoproteomics analysis. *PLoS One*, 5, 117-116.
- O'NEILL, S.K., GETAHUN, A., GAULD S.B., MERRELL, K.T, TAMIR, I., SMITH M.J, 2011. Monophosphorylation of CD79a and CD79b ITAM Motifs Initiates a SHIP1 Phosphatase-Mediated Inhibitory Signaling Cascade Required for B Cell Anergy. *Immunity,* 35, 746–56.
- OKKENHAUG, K., BILANCIO, A., FARJOT, G., PRIDDLE, H., SANCHO, S., PESKETT, E., PEARCE, W., MEEK, S.E., SALPEKAR, A., WATERFIELD. M.D, Smith A.J., Vanhaesebroeck B. 2002. Impaired B and T cell antigen receptor signaling in p110delta PI 3-kinase mutant mice. *Science* 7(5583):1031-4.
- OLIVER P.M, VASS T., KAPPLER J., MARRACK P. 2006. Loss of the proapoptotic protein, Bim, breaks B cell anergy. J Exp Med;203(3):731–41
- ONG, C.J., MING-LUM, A., NODWELL, M., GHANIPOUR, A., YANG, L., WILLIAMS, D.E, et al. 2007. Small-molecule agonists of SHIP1 inhibit the phosphoinositide 3-kinase pathway in hematopoietic cells. *Blood* ;110:1942–1949
- PALMER, S., HANSON, C.A., ZENT, C.S., PORRATA, L.F., LAPLANT, B. & GEYER, S.M. 2008. Prognostic importance of T and NK-cells in a consecutive series of newly diagnosed patients with chronic lymphocytic leukaemia. *British Journal of Haematology,* 141, 607-614.
- PAO, L.I., LAM, K.P., HENDERSON, J.M., KUTOK, J.L., ALIMZHANOV, M. & NITSCHKE, L. 2007. B cell-specific deletion of protein-tyrosine phosphatase Shp1 promotes B-1a cell development and causes systemic autoimmunity. *Immunity*, 27, 35–48.
- PARK, C. S. & CHOI, Y. S. 2005. How do follicular dendritic cells interact intimately with B cells in the germinal centre? *Immunology,* 114, 1, 2–10.
- PARSONS, R. 2004. Human cancer, PTEN and the PI-3 kinase pathway. *Semin Cell Dev Biol,* 15:171–6
- PATTEN, P.E. 2008. CD38 expression in chronic lymphocytic leukeamia is regulated by the tumor microenvironment. *Blood,* 111, 10, 5173–81.
- PAULS, S. D,. AND MARSHALL, A. J. (2017), Regulation of immune cell signaling by SHIP1: A phosphatase, scaffold protein, and potential therapeutic target. *Eur. J. Immunol*., 47: 932-945. doi:
- PEDERSEN, I. M., KITADA, S., LEONI, L. M., ZAPATA, J. M., KARRAS, J. G., TSUKADA, N. & KIPPS, T. J. 2002. Protection of CLL B cells by a follicular dendritic cell line is dependent on induction of Mcl-1. *Blood,* 100, 1795-1801.
- PEDERSEN, I.M., OTERO, D. & KAO, E. 2009. Onco-miR-155 targets SHIP1 to promote TNFα-dependent growth of B cell lymphomas. *EMBO Molecular Medicine*, 1, 5, 288-295.
- PENHEITER, S. G., MITCHELL, H., GARAMSZEGI, N., EDENS, M., DORÉ, J. J., JR, & LEOF, E. B. (2002). Internalization-dependent and -independent requirements for transforming growth factor beta receptor signaling via the Smad pathway. *Molecular and cellular biology*, 22(13), 4750–4759. doi:10.1128/mcb.22.13.4750-4759.2002
- PEREIRA, J. P., KELLY, L. M., & CYSTER, J. G. (2010). Finding the right niche: B-cell migration in the early phases of T-dependent antibody responses. International *immunology*, 22(6), 413–419. doi:10.1093/intimm/dxq047
- PETLICKOVSKI, A. 2007. Sustained signaling through the B-cell receptor induces Mcl-1 and promotes survival of chronic lymphocytic leukeamia B cells.*Blood*, 105, 12, 4820–7.2005

- PFEIFER, M., GRAU, M., LENZE, D. 2013. PTEN loss defines a PI3K/AKT pathway-dependent germinal center subtype of diffuse large B-cell lymphoma.Proceedings of the National Academy of Sciences of the United States of America, 110, 30,12420-12425.
- PORSTMANN T., SANTOS C.R., GRIFFITHS B., CULLY M., WU M., LEEVERS S., GRIFFITHS J.R., CHUNG Y.L., SCHULZE A. 2008. SREBP activity is regulated by mTORC1 and contributes to Akt-dependent cell growth. Cell Metab.;8:224–236.
- PUENTE, X.S., PINYOL, M., QUESADA, V., CONDE, L., ORDÓÑEZ, G.R., VILLAMOR, N., ET AL 2011. Whole-genome sequencing identifies recurrent mutations in chronic lymphocytic leukaemia. *Nature*. 15():707-47
- QUIROGA, M. P., BALAKRISHNAN, K. & KURTOVA, A.V. 2009. B-cell antigen receptor signaling enhances chronic lymphocytic leukeamia cell migration and survival: specific targeting with a novel spleen tyrosine kinase inhibitor, R406. *Blood*, 114, 5, 1029–1037.
- R. NEGRO, S. GOBESSI, P. G. LONGO. 2012. Overexpression of the autoimmunity-associated phosphatase PTPN22 promotes survival of antigen-stimulated CLL cells by selectively activating AKT, Blood, vol. 119, no. 26, pp. 6278–6287.
- RAMANATHAN. S., DI PAOLO, J.A., JIN, F., SHAO, L., SHARMA, S., ROBESON, M., KEARNEY, B.P. 2016. *Clinical Drug Investigation*, 37(2): 195-205
- RAMSAY, A.G. & GRIBBEN, J.G. 2010. The 3 Rs in CLL immune dysfunction. Blood, 115, 13, 2563–4.
- RANHEIM, E.A. & KIPPS, T.J. 1993. Activated T cells induce expression of B7/BB1 on normal or leukemic B cells through a CD40-dependent signal. J Exp Med, 177, 4, 925–35.
- RAO, A., LUO, C., HOGAN, P.G.1997. Transcription factors of the NFAT family: regulation and function. *Annu Rev Immunol*, 15():707-47.
- REDONDO-MUNOZ, J. 2006. MMP-9 in B-cell chronic lymphocytic leukeamia is up-regulated by alpha4beta1 integrin or CXCR4 engagement via distinct signaling pathways, localizes to podosomes, and is involved in cell invasion and migration. *Blood*, 108, 9, 3143–51.
- REDONDO-MUNOZ, J. 2010. Matrix metalloproteinase-9 promotes chronic lymphocytic leukeamia b cell survival through its hemopexin domain. *Cancer Cell,* 17, 2, 160–72.
- REX, E.B., KIM, S., WIENER, J., RAO, N.L., MILLA, M.E. & DISEPIO, D. 2015. Phenotypic Approaches to Identify Inhibitors of B Cell Activation. *Journal of Biomolecular Screening*, 20, 7, 876-886.
- RICHARDSON, S.J., MATTHEWS, C., CATHERWOOD, M.A., ALEXANDER, H.D., CAREY, B.S., FARRUGIA, J. 2006 .ZAP-70 expression is associated with enhanced ability to respond to migratory and survival signals in B-cell chronic lymphocytic leukeamia (B-CLL). *Blood*, 107(9):3584–92
- RICHES, J.C. ,DAVIES, J.K. ,MCCLANAHAN, F., FATAH, R., IQBAL, S. & AGRAWAL, S. 2013. Tcells from CLL patients exhibit features of T-cell exhaustion but retain capacity for cytokine production. *Blood*, 121,1612.
- RINGSHAUSEN, I., SCHNELLER, F., BOGNER, C. 2002. Constitutively activated phosphatidylinositol-3 kinase (PI-3K) is involved in the defect of apoptosis in B-CLL: association with protein kinase Cdelta. *Blood*, 100(10):3741-8.

- Rozman, C., Montserrat, E., Rodríguez-Fernández, J.M., Ayats, R., Vallespí, T,. Parody. R,, Ríos, A., Prados, D., Morey, M., Gomis, F. 1983 . Bone marrow biopsy in chronic lymphocytic leukaemia: a study of 208 cases. *Haematologia*, 5(3):642-8.
- RUAN, J. 2006. Magnitude of stromal hemangiogenesis correlates with histologic subtype of non-Hodgkin's lymphoma. Clin Cancer Res, 12, 19, 5622–31.
- RUI, L., VINUESA, C.G., BLASIOLI, J., GOODNOW, C.C. 2003. Resistance to CpG DNA-induced autoimmunity through tolerogenic B cell antigen receptor ERK signaling. *Nat Immunol*, 4(6):594–600
- RULAND, J., MAK, T.W. 2003. Transducing signals from antigen receptors to nuclear factor kappaB. *Immunol Rev* ;193:93–100.
- RUNMIN, G., JIAMEI, J., ZHILIANG, J., YONGHUA, C., ZHIZHOU, S., GUIZHOU, T., & SHUGUANG, L. (2017). Genetic variation of CXCR4 and risk of coronary artery disease: epidemiological study and functional validation of CRISPR/Cas9 system. *Oncotarget*, 9(18), 14077–14083. doi:10.18632/oncotarget.23491
- SAGIV-BARFI, I., KOHRT, H.E.K., CZERWINSKI, D.K., NG, P.P., CHANG, B.Y., LEVY, R. 2015. Therapeutic antitumor immunity by checkpoint blockade is enhanced by ibrutinib, an inhibitor of both BTK and ITK. Proceedings of the National Academy of Sciences of the United States of America.p112(9):E966-E972.
- SAINT-GEORGES, S., QUETTIER, M., BOUYABA, M., LE COQUIL, S., LAURIENTÉ, V., GUITTAT, L., LÉVY, V., AJCHENBAUM-CYMBALISTA, F., VARIN-BLANK, N., LE ROY, C., & LEDOUX, D. 2016. Protein kinase D-dependent CXCR4 down-regulation upon BCR triggering is linked to lymphadenopathy in chronic lymphocytic leukaemia. *Oncotarget*, 7, 27, 41031-41046.
- SALMENA, L., CARRACEDO, A., PANDOLFI, P.P. 2008. Tenets of PTEN tumor suppression. *Cell*, 133:403–14.
- SANKANAGOUDAR, S. H., SINGH, G., MAHAPATRA, M., KUMAR, L., & CHANDRA, N. 2017. Cholesterol Homeostasis in Isolated Lymphocytes: a Differential Correlation Between Male Control and Chronic Lymphocytic Leukeamia Subjects. Asian Pacific journal of cancer prevention : APJCP, 18(1), 23–30. doi:10.22034/APJC.18.1.23
- SCHMID, C. & ISAACSON, P.G. 1994. Proliferation centres in B-cell malignant lymphoma, lymphocytic (B-CLL): an immunophenotypic study. Histopathology, 24,5, 445–51.
- SCHULMAN I. G. (2017). Liver x receptors link lipid metabolism and inflammation. FEBS letters, 591(19), 2978–2991. doi:10.1002/1873-3468.12702
- SEVERIN F., FREZZATO F., MARTINI V., RAGGI F., TRIMARCO V., MARTINELLO L., VISENTIN A,, FACCO M., SEMENZATO G., TRENTIN. 2016. Inhibition of JAK2/STAT3 Pathway Leads to Apoptosis in Chronic Lymphocytic Leukeamia Cells. *Blood*; 128 (22): 2023.
- SHEN Y., BURGOYNE D.L. Efficient Synthesis of IPL576,092: A Novel Anti-Asthma Agent. *J Org Chem*. 2002;67:3908–3910
- SIMON-GABRIEL, C., BENKIßER-PETERSEN, M., UMEZAWA, K. 2014. Potential of NF-κB Inhibition in the Treatment of Chronic Lymphocytic Leukeamia. Blood, 124(21),
- SMITH, A., HOWELL, D., PATMORE, R., JACK, A., ROMAN, E. 2011. Incidence of haematological malignancy by sub-type: a report from the Haematological Malignancy Research Network. British Journal of Cancer ;105(11):1684-1692.
- SNAPPER, C. M. AND MOND, J. J., 1993. Towards a comprehensive view of immunoglobulin class switching. *Immunol.* Today. 14: 15–17.

- SONG, M.S, SALMENA, L. & PANDOLFI, P.P. 2012. The functions and regulation of the PTEN tumour suppressor. *Nature Reviews Molecular Cell Biology*.
- SOUERS A.J., LEVERSON J.D., BOGHAERT E.R, et al. 2013. ABT-199, a potent and selective BCL-2 inhibitor, achieves antitumor activity while sparing platelets. *Nat Med*.;19(2):202–208. 10.1038/nm.3048
- STALIN CHELLAPPA, KUSHI KUSHEKHAR, LUDVIG A. MUNTHE, GEIR E. TJØNNFJORD, EINAR M. AANDAHL, KLAUS OKKENHAUG AND KJETIL TASKÉN. 2019. The PI3K p110δ Isoform Inhibitor Idelalisib Preferentially Inhibits Human Regulatory T Cell Function. *J Immunol* January 28, ji1701703;
- STENTON G.R, MACKENZIE L.F, TAM P, CROSS J.L, HARWIG C, RAYMOND J, TOEWS J, CHERNOFF D., MACRURY T., SZABO C. 2013. Characterization of AQX-1125, a small-molecule SHIP1 activator. Part 2. Efficacy studies in allergic and pulmonary inflammation models in vivo. Br J Pharmacol.;168:1519–1529.
- STENTON G.R, MACKENZIE L.F., TAM P, CROSS J.L., HARWIG C, RAYMOND J., TOEWS J, WU J., OGDEN N., MACRURY T., SZABO C. 2013. Characterization of AQX-1125, a small-molecule SHIP1 activator. Part 1. Effects on inflammatory cell activation and chemotaxis in vitro and pharmacokinetic characterization in vivo. Br *J Pharmacol*.;168:1506–1518.
- SUGIYAMA, T., KOHARA, H., NODA, M., NAGASAWA, T. 2006. Maintenance of the hematopoietic stem cell pool by CXCL12-CXCR4 chemokine signalling in bone marrow stromal cell niches. Immunity
- SUZUKI A., YAMAGUCHI M.T., OHTEKI T., SASAKI T., KAISHO T., KIMURA Y., YOSHIDA R., WAKEHAM A., HIGUCHI T., FUKUMOTO M. 2001. T cell-specific loss of Pten leads to defects in central and peripheral tolerance. *Immunity*. 14:523–534 10.1016/S1074-7613(01)00134-0
- SUZUKI, A., KAISHO, T., OHISHI, M., TSUKIO-YAMAGUCHI, M., TSUBATA T., KONI P.A., SASAKI T., MAK T.W., NAKANO T. 2003. Critical roles of Pten in B cell homeostasis and immunoglobulin class switch recombination. J. Exp. Med. 197:657–667 10.1084/jem.20021101
- SWERDLOW, S. H., CAMPO, E., PILERI, S. A., HARRIS, N. L., STEIN, H., SIEBERT, R., ADVANI, R., GHIELMINI, M., SALLES, G. A., ZELENETZ, A. D., & JAFFE, E. S. The 2016 revision of the World Health Organization classification of lymphoid neoplasms. *Blood*, 2016. 127(20), 2375-2390.
- TAKATA, M., SABE, H., HATA, A. 1994. Tyrosine kinases LYN and SYK regulate B cell receptor-coupled Ca2+ mobilization through distinct pathways,13(6):1341-9
- TE RAA GD, et al. The impact of SF3B1 mutations in CLL on the DNA-damage response. Leukemia. 2015;29:1133–1142.
- TILL, K. J., LIN, K., ZUZEL, M. & CAWLEY, J. C. 2002. The chemokine receptor CCR7 and alpha4 integrin are important for migration of chronic lymphocytic leukeamia cells into lymph nodes. *Blood,* 99, 2977–84.
- TILL, K. J., PETTITT, A. R., & SLUPSKY, J. R. (2015). Expression of functional sphingosine-1 phosphate receptor-1 is reduced by B cell receptor signaling and increased by inhibition of PI3 kinase δ but not SYK or BTK in chronic lymphocytic leukemia cells. Journal of immunology (Baltimore, Md. : 1950), 194(5), 2439–2446. doi:10.4049/*jimmunol*.1402304
- TREANOR B. B-cell receptor: from resting state to activate. Immunology. 2012;136(1):21–27. doi:10.1111/j.1365-2567.2012.03564.x

- VANGAPANDU, H. V., HAVRANEK, O., AYRES, M. L., KAIPPARETTU, B. A., BALAKRISHNAN, K., WIERDA, W. G. GANDHI, V. (2017). B-cell Receptor Signaling Regulates Metabolism in Chronic Lymphocytic Leukemia. Molecular cancer research : MCR, 15(12), 1692–1703. doi:10.1158/1541-7786.MCR-17-0026
- VAISITTI, T., AYDIN, S., ROSSI, D., COTTINO, F., BERGUI, L., D'ARENA, G., BONELLO, L. 2010. CD38 increases CXCL12-mediated signals and homing of chronic lymphocytic leukeamia cells. *Leukeamia*. 24: 958-969.
- VAISITTI, T., GAUDINO, F., OUK, S., MOSCVIN, M., VITALE, N., SERRA, S., … DEAGLIO, S. (2017). Targeting metabolism and survival in chronic lymphocytic leukeamia and Richter syndrome cells by a novel NF-κB inhibitor. Haematologica, 102(11), 1878–1889. doi:10.3324/haematol.2017.173419
- VAN DANG, C., & MCMAHON, S. B. (2010). Emerging Concepts in the Analysis of Transcriptional Targets of the MYC Oncoprotein: Are the Targets Targetable?. Genes & cancer, 1(6), 560–567. doi:10.1177/1947601910379011
- VANGAPANDU, H. V., HAVRANEK, O., AYRES, M. L., KAIPPARETTU, B. A., BALAKRISHNAN, K., WIERDA, W. G., … GANDHI, V. (2017). B-cell Receptor Signaling Regulates Metabolism in Chronic Lymphocytic Leukeamia. Molecular cancer research : MCR, 15(12), 1692–1703. doi:10.1158/1541-7786.MCR-17-0026
- VIERNES D.R, CHOI L.B., KERR W.G., CHISHOLM J.D. Discovery and development of small molecule SHIP phosphatase modulators. *Med Res Rev*. 2014;34(4):795–824. 10.1002/med.21305
- VIERNES, D. R., CHOI, L. B., KERR, W. G., & CHISHOLM, J. D. (2014). Discovery and development of small molecule SHIP phosphatase modulators. *Medicinal research reviews*, 34(4), 795–824.10.1002/med.21305
- WALLISER C., HERMKES E., SCHADE A, et al. The Phospholipase Cgamma2 Mutants R665W and L845F Identified in Ibrutinib-resistant Chronic Lymphocytic Leukeamia Patients Are Hypersensitive to the Rho GTPase Rac2 Protein. *J Biol Chem*. 2016. October 14;291(42):22136–22148.
- WANG, J., GUAN, E., RODERIQUEZ, G., CALVERT, V., ALVAREZ, R., AND NORCROSS M.A. 2001 .Role of Tyrosine Phosphorylation in Ligand-independent Sequestration of CXCR4 in Human Primary Monocytes-Macrophages., *JBC,* 2001, 10.1074
- WANG, L., LAWRENCE, M.S., WAN, Y., STOJANOV, P., SOUGNEZ, C., STEVENSON, K., et al 2011. SF3B1 and other novel cancer genes in chronic lymphocytic leukeamia. N Engl J Med. 2011;365(26):2497–506.
- WARDEMANN, H., YURASOV, S., SCHAEFER, A., YOUNG, J.W., MEFFRE, E. & NUSSENZWEIG, M.C. 2003. Predominant Autoantibody Production by Early Human B Cell Precursors. *Science*, 301, 1374–7.
- WAYNER, E.A., GARCIA-PARDO, A. & HUMPHRIES, M.J. 1989. Identification and characterization of the T lymphocyte adhesion receptor for an alternative cell attachment domain (CS-1) in plasma fibronectin. J Cell Biol, 109, 1321–1330.
- WHITLOCK, C,A,, WITTE, O.N. 1982 Long-term culture of B lymphocytes and their precursors from murine bone marrow. *Proc Natl Acad Sci* U S A 79(11):3608-3612.
- WOYACH, J.A., BOJNIK, E. & RUPPERT, A.S. 2014. Bruton's tyrosine kinase (BTK) function is important to the development and expansion of chronic lymphocytic leukeamia (CLL). *Blood*, 123, 8, 1207-1213.
- WOYACH, J.A., FURMAN, R.R,, LIU. T.M. 2014. Resistance mechanisms for the Bruton's tyrosine kinase inhibitor ibrutinib. N Engl J Med, 370(24):2286-2294.

- XING, D., RAMSAY, A.G., GRIBBEN, J.G., DECKER, W.K., BURKS, J.K., MUNSELL, M. 2010. Cord Blood natural killer cells exhibit impaired lytic immunological synapse formation that is reversed with IL-2 ex vivo expansion. *Journal of Immunotherapy,* 33, 684-696.
- YEGANEH B., WIECHEC E., ANDE S.R., SHARMA P., MOGHADAM A.R., POST M., FREED D.H., HASHEMI M., SHOJAEI S., ZEKI A.A., GHAVAMI S. Targeting the mevalonate cascade as a new therapeutic approach in heart disease, cancer and pulmonary disease. *Pharmacol Ther*. 2014;143:87–110.
- YEOMANS, A., THIRDBOROUGH, S. M., VALLE-ARGOS, B., LINLEY, A., KRYSOV, S., HIDALGO, M. S., LEONARD, E., ISHFAQ, M., WAGNER, S. D., WILLIS, A. E., STEELE, A. J., STEVENSON, F. K., FORCONI, F., COLDWELL, M. J. & PACKHAM, G. 2016. Engagement of the B-cell receptor of chronic lymphocytic leukeamia cells drives global and MYC-specific mRNA translation. *Blood,* 127, 449-57.
- YONEKAWA, K. & HARLAN, J. M. 2005. Targeting leukocyte integrins in human diseases. *Journal of Leukocyte Biology,* 77, 129-140.
- ZENG, Z., SAMUDIO, I.J., MUNSELL, M., AN, J., HUANG, Z., ESTEY, E., ANDREEFF, M. & KONOPLEVA, M. 2006. Inhibition of CXCR4 with the novel RCP168 peptide overcomes stroma-mediated chemoresistance in chronic and acute leukeamias. *Molecular Cancer Therapeutics*, 5, 3113–3121.
- ZHUANG. J., HAWKINS, S.F., GLENN, M.A., LIN, K., JOHNSON, G.G., CARTER, A., CAWLEY, J.C., PETTITT, A.R. 2010.AKT is activated in chronic lymphocytic leukeamia cells and delivers a pro-survival signal: the therapeutic potential of AKT inhibition. *Haematologica (*1):110-8.
- ZUCCHETTO, A., BENEDETTI, D., TRIPODO, C., BOMBEN, R., DAL BO, M., MARCONI, D., BOSSI, F., LORENZON, D., DEGAN, M., ROSSI, F. M., ROSSI, D., BULIAN, P., FRANCO, V., DEL POETA, G., DEAGLIO, S., GAIDANO, G., TEDESCO, F., MALAVASI, F. & GATTEI, V. 2009. CD38/CD3, the CCL3 and CCL4 chemokines, and CD49d/vascular cell adhesion molecule-1 are interchained by sequential events sustaining chronic lymphocytic leukeamia cell survival. *Cancer* Res, 69, 4001-4009.
- ZUCCHETTO, A., VAISITTI, T., BENEDETTI, T., TISSINO, E., BERTAGNOLO, V. & ROSSI, D. 2012. The CD49d/CD29 complex is physically and functionally associated with CD38 in B-cell chronic lymphocytic leukeamia cells. *Leukeamia*, 26,1301-1312.

Appendix

Appendix A

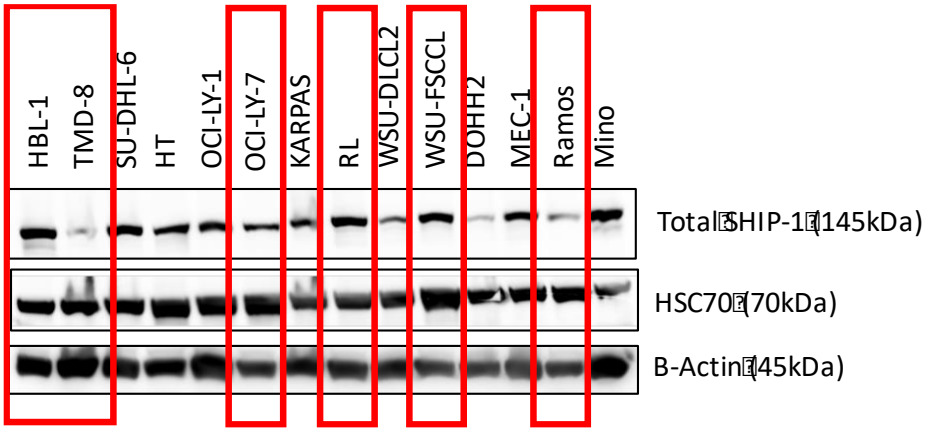

Figure A1. Immunoblot data showing basal expression of SHIP1 and loading controls in a panel of B-cell lines. Data from Dr Alison Yeomans. Cell lines used in the current study are indicated.

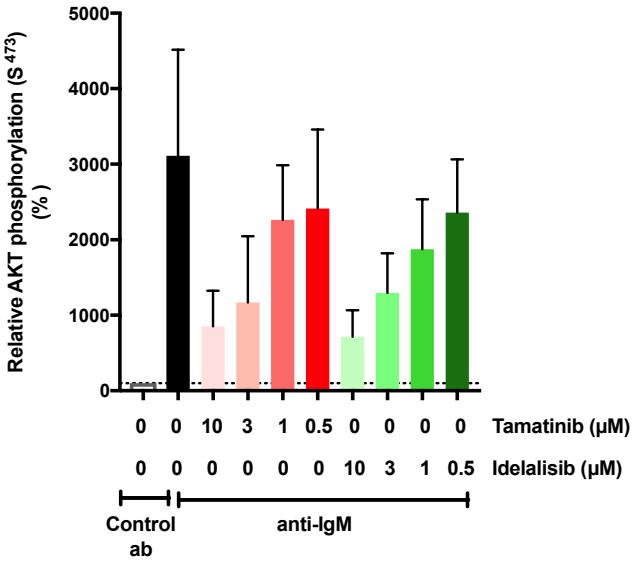

Figure A2. Immunoblot quantification of effect of Tamatinib and Idelalisib on anti-IgM induction of Akt phosphorylation (N=3).

Appendix B

Outline of bioinformatics analysis performed by Dr Dean Bryant

Raw data in the form of fastq files were aligned against the hg19 reference genome using BWA (Li et al., 2009 https://academic.oup.com/bioinformatics/article/25/14/1754/225615). Initial data quality control was performed using FastQC (Babraham bioinformatics https://www.bioinformatics.babraham.ac.uk/projects/fastqc/). Counts matrices were produced using HTseq-count (Anders et al., 2015) and exported for differential expression analysis in EdgeR (McCarthy et al., 2012; Chen et al., 2012). "Differential expression analysis of multifactor RNA-Seq experiments with respect to biological variation." Nucleic Acids Research, 40(10), 4288-4297.). Transcriptomic data were fitted to multifactor GLM models and tested for differential expression using quasi-likelihood f-tests. Multiple testing correction was performed using the Benjamini Hochberg procedure.

Table B1. IPA canonical pathways enriched (P<0.05) in the anti-IgM-induced gene expression signature.

Ingenuity Canonical Pathways[a]	Rank	p-value	Ratio	z-score[b]
tRNA Charging	1	2.51189E-14	0.513	4.472
Sirtuin Signaling Pathway	2	6.30957E-11	0.175	1.095
Unfolded protein response	3	1.09648E-10	0.357	NaN
Protein Ubiquitination Pathway	4	1.86209E-08	0.162	NaN
Antigen Presentation Pathway	5	4.36516E-08	0.368	NaN
Endoplasmic Reticulum Stress Pathway	6	2.13796E-07	0.476	NaN
Type I Diabetes Mellitus Signaling	7	5.01187E-07	0.207	3.207
Purine Nucleotides De Novo Biosynthesis II	8	1.1749E-06	0.636	2.646
Th1 and Th2 Activation Pathway	9	2.5704E-06	0.162	NaN
RAN Signaling	10	4.16869E-06	0.471	NaN
Th1 Pathway	11	5.12861E-06	0.178	2.982
TNFR2 Signaling	12	1.07152E-05	0.333	2.646
Induction of Apoptosis by HIV1	13	2.51189E-05	0.23	1.604
NRF2-mediated Oxidative Stress Response	14	3.0903E-05	0.146	3.411
Dendritic Cell Maturation	15	5.01187E-05	0.144	5.196
T Helper Cell Differentiation	16	5.24807E-05	0.205	NaN

Hypoxia Signaling in the Cardiovascular System	17	7.24436E-05	0.2	2.828
Nur77 Signaling in T Lymphocytes	18	7.58578E-05	0.22	NaN
Cysteine Biosynthesis III (mammalia)	19	8.31764E-05	0.333	2.828
Role of Macrophages, Fibroblasts and Endothelial Cells in Rheumatoid Arthritis	20	9.54993E-05	0.122	NaN
EIF2 Signaling	21	0.000141254	0.132	0
Crosstalk between Dendritic Cells and Natural Killer Cells	22	0.000158489	0.18	NaN
OX40 Signaling Pathway	23	0.00020893	0.176	0.378
Th2 Pathway	24	0.000245471	0.147	2.111
5-aminoimidazole Ribonucleotide Biosynthesis I	25	0.000263027	1	NaN
Inosine-5'-phosphate Biosynthesis II	26	0.000263027	1	NaN
Methionine Degradation I (to Homocysteine)	27	0.000323594	0.318	2.646
Superpathway of Methionine Degradation	28	0.000446684	0.243	3
ERK5 Signaling	29	0.000616595	0.181	3.051
Autoimmune Thyroid Disease Signaling	30	0.000812831	0.208	NaN
Graft-versus-Host Disease Signaling	31	0.000812831	0.208	NaN
Cholesterol Biosynthesis I	32	0.000912011	0.385	2.236
Cholesterol Biosynthesis II (via 24,25-dihydrolanosterol)	33	0.000912011	0.385	2.236
Cholesterol Biosynthesis III (via Desmosterol)	34	0.000912011	0.385	2.236
TREM1 Signaling	35	0.000912011	0.173	3.606
GADD45 Signaling	36	0.000912011	0.316	NaN
Role of PKR in Interferon Induction and Antiviral Response	37	0.000977237	0.22	NaN
Allograft Rejection Signaling	38	0.001	0.165	NaN
Cell Cycle: G1/S Checkpoint Regulation	39	0.001071519	0.179	-1.414
Aldosterone Signaling in Epithelial Cells	40	0.001174898	0.131	2.236
IL-10 Signaling	41	0.001380384	0.174	NaN
TWEAK Signaling	42	0.001412538	0.229	0
IL-17A Signaling in Fibroblasts	43	0.001412538	0.229	NaN
CD40 Signaling	44	0.001513561	0.165	1.387
Superpathway of Cholesterol Biosynthesis	45	0.00162181	0.25	2.646
B Cell Development	46	0.001737801	0.222	NaN
Aryl Hydrocarbon Receptor Signaling	47	0.001778279	0.135	1.5
Altered T Cell and B Cell Signaling in Rheumatoid Arthritis	48	0.001778279	0.156	NaN
Neuroinflammation Signaling Pathway	49	0.001778279	0.109	5.145
CD27 Signaling in Lymphocytes	50	0.001819701	0.189	1.134
PI3K/AKT Signaling	51	0.001819701	0.137	3.153
D-myo-inositol (1,4,5,6)-Tetrakisphosphate Biosynthesis	52	0.002238721	0.132	4.359
D-myo-inositol (3,4,5,6)-tetrakisphosphate Biosynthesis	53	0.002238721	0.132	4.359

Tetrahydrofolate Salvage from 5,10-methenyltetrahydrofolate	54	0.002398833	0.6	NaN
3-phosphoinositide Biosynthesis	55	0.002570396	0.119	4.899
Parkinson's Signaling	56	0.002630268	0.312	NaN
April Mediated Signaling	57	0.002951209	0.205	0.707
Iron homeostasis signaling pathway	58	0.003019952	0.131	NaN
Tumoricidal Function of Hepatic Natural Killer Cells	59	0.003467369	0.25	1.342
4-1BB Signaling in T Lymphocytes	60	0.003630781	0.219	2
B Cell Activating Factor Signaling	61	0.004073803	0.195	2
Spermine Biosynthesis	62	0.004168694	1	NaN
Spermidine Biosynthesis I	63	0.004168694	1	NaN
TNFR1 Signaling	64	0.004168694	0.18	2.828
Role of JAK family kinases in IL-6-type Cytokine Signaling	65	0.004265795	0.24	NaN
Pyruvate Fermentation to Lactate	66	0.004570882	0.5	NaN
CD28 Signaling in T Helper Cells	67	0.004786301	0.129	2.828
Circadian Rhythm Signaling	68	0.005248075	0.206	NaN
Superpathway of Inositol Phosphate Compounds	69	0.005248075	0.11	5.099
iCOS-iCOSL Signaling in T Helper Cells	70	0.005495409	0.13	3.606
Adipogenesis pathway	71	0.005623413	0.127	NaN
3-phosphoinositide Degradation	72	0.006309573	0.12	4.359
Phagosome Maturation	73	0.00691831	0.122	NaN
iNOS Signaling	74	0.007413102	0.178	2.646
Pentose Phosphate Pathway (Non-oxidative Branch)	75	0.007585776	0.429	NaN
Glucocorticoid Receptor Signaling	76	0.008912509	0.0986	NaN
Calcium-induced T Lymphocyte Apoptosis	77	0.009120108	0.152	3
Antioxidant Action of Vitamin C	78	0.009332543	0.13	-3.464
PKCθ Signaling in T Lymphocytes	79	0.01	0.115	4.243
Phenylalanine Degradation IV (Mammalian, via Side Chain)	80	0.01	0.286	2
γ-glutamyl Cycle	81	0.01	0.286	2
PPAR Signaling	82	0.012589254	0.129	-3.051
PI3K Signaling in B Lymphocytes	83	0.014125375	0.118	3.873
IL-1 Signaling	84	0.014791084	0.13	3.317
Hepatic Cholestasis	85	0.014791084	0.112	NaN
Death Receptor Signaling	86	0.015848932	0.129	1.155
D-myo-inositol-5-phosphate Metabolism	87	0.016595869	0.111	4.243
Folate Transformations I	88	0.016595869	0.333	NaN
Small Cell Lung Cancer Signaling	89	0.019952623	0.129	1.633
Stearate Biosynthesis I (Animals)	90	0.021379621	0.159	2.646

Regulation of IL-2 Expression in Activated and Anergic T Lymphocytes	91	0.021877616	0.128	NaN
Pancreatic Adenocarcinoma Signaling	92	0.021877616	0.117	2.111
Heme Degradation	93	0.022908677	0.5	NaN
Glutathione Redox Reactions II	94	0.022908677	0.5	NaN
Proline Biosynthesis I	95	0.022908677	0.5	NaN
Differential Regulation of Cytokine Production in Macrophages and T Helper Cells by IL-17A and IL-17F	96	0.025118864	0.222	NaN
p53 Signaling	97	0.025703958	0.117	1.134
Lymphotoxin β Receptor Signaling	98	0.026915348	0.134	1.89
Cell Cycle Regulation by BTG Family Proteins	99	0.029512092	0.162	0
Pentose Phosphate Pathway	100	0.029512092	0.273	NaN
Dolichyl-diphosphooligosaccharide Biosynthesis	101	0.029512092	0.273	NaN
Remodeling of Epithelial Adherens Junctions	102	0.032359366	0.13	NaN
Osteoarthritis Pathway	103	0.032359366	0.0991	1.606
Prostate Cancer Signaling	104	0.033113112	0.117	NaN
Molecular Mechanisms of Cancer	105	0.033113112	0.0888	NaN
Acute Phase Response Signaling	106	0.034673685	0.102	2.668
CMP-N-acetylneuraminate Biosynthesis I (Eukaryotes)	107	0.036307805	0.4	NaN
Myo-inositol Biosynthesis	108	0.036307805	0.4	NaN
dTMP De Novo Biosynthesis	109	0.036307805	0.4	NaN
Folate Polyglutamylation	110	0.036307805	0.4	NaN
Assembly of RNA Polymerase I Complex	111	0.03801894	0.25	NaN
Acyl-CoA Hydrolysis	112	0.03801894	0.25	NaN
BER pathway	113	0.03801894	0.25	NaN
Cdc42 Signaling	114	0.040738028	0.102	2.828
Communication between Innate and Adaptive Immune Cells	115	0.041686938	0.116	NaN
IL-4 Signaling	116	0.041686938	0.116	NaN
Sumoylation Pathway	117	0.044668359	0.115	-0.707
Fatty Acid Activation	118	0.046773514	0.231	NaN
Choline Biosynthesis III	119	0.046773514	0.231	NaN
Opioid Signaling Pathway	120	0.047863009	0.0931	2.132
Activation of IRF by Cytosolic Pattern Recognition Receptors	121	0.047863009	0.127	0
Wnt/Ca+ pathway	122	0.047863009	0.127	2.828
Polyamine Regulation in Colon Cancer	123	0.048977882	0.182	NaN

[a]IPA canonical pathway analysis was performed using genes that were significantly up-regulated (log_2FC >1.0, FDR<0.05) in anti-IgM-treated samples. Of the 1663 significantly up-regulated genes, 1508 were included in the IPA analysis. [b]NaN, no activity pattern predicted.

Table B2. IPA canonical pathways enriched (P<0.05) in the anti-IgM-down-regulated gene expression signature.

Ingenuity Canonical Pathways[a]	Rank	p-value	Ratio	z-score
B Cell Receptor Signaling	1	3.16228E-08	0.196	-3.657
Phospholipase C Signaling	2	2.75423E-07	0.172	-4.902
PI3K Signaling in B Lymphocytes	3	7.24436E-06	0.191	-4.082
Primary Immunodeficiency Signaling	4	8.51138E-06	0.286	NaN
Axonal Guidance Signaling	5	1.23027E-05	0.131	NaN
Opioid Signaling Pathway	6	3.54813E-05	0.15	-4
Sphingosine-1-phosphate Signaling	7	4.46684E-05	0.184	-3.411
Endothelin-1 Signaling	8	5.24807E-05	0.158	-4.49
G-Protein Coupled Receptor Signaling	9	6.16595E-05	0.142	NaN
Phagosome Formation	10	9.54993E-05	0.176	NaN
Dendritic Cell Maturation	11	0.000245471	0.149	-5.292
Cellular Effects of Sildenafil (Viagra)	12	0.00025704	0.168	NaN
Neuropathic Pain Signaling In Dorsal Horn Neurons	13	0.000301995	0.174	-4.472
Role of NFAT in Cardiac Hypertrophy	14	0.00030903	0.142	-4.811
CREB Signaling in Neurons	15	0.000380189	0.142	-4.69
cAMP-mediated signaling	16	0.000389045	0.14	-3.772
Reelin Signaling in Neurons	17	0.000398107	0.185	NaN
Inflammasome pathway	18	0.00040738	0.35	-2.646
Adrenomedullin signaling pathway	19	0.000416869	0.145	-5.385
Thrombin Signaling	20	0.00042658	0.143	-3.962
Fcγ Receptor-mediated Phagocytosis in Macrophages and Monocytes	21	0.000457088	0.183	-4.123
Role of NFAT in Regulation of the Immune Response	22	0.000467735	0.146	-4.6
Leptin Signaling in Obesity	23	0.000549541	0.186	-2.828
p70S6K Signaling	24	0.000549541	0.159	-2.985
UVA-Induced MAPK Signaling	25	0.00057544	0.17	-3.464
FAK Signaling	26	0.000707946	0.171	NaN
Tec Kinase Signaling	27	0.000812831	0.147	-4.243
GP6 Signaling Pathway	28	0.000912011	0.157	-4.583
Ceramide Signaling	29	0.000954993	0.172	-1
Leukocyte Extravasation Signaling	30	0.001	0.137	-3.53
Telomerase Signaling	31	0.001	0.162	-2.324
IL-7 Signaling Pathway	32	0.001023293	0.176	-2.324
Amyotrophic Lateral Sclerosis Signaling	33	0.001380384	0.162	-2.5

FcγRIIB Signaling in B Lymphocytes	34	0.001412538	0.176	-2.714
Relaxin Signaling	35	0.001479108	0.146	-3.464
Chemokine Signaling	36	0.001479108	0.182	-3.207
P2Y Purigenic Receptor Signaling Pathway	37	0.001584893	0.15	-4.472
Molecular Mechanisms of Cancer	38	0.00162181	0.117	NaN
Phospholipases	39	0.001819701	0.194	-3.464
Gαq Signaling	40	0.001905461	0.143	-3.838
Fc Epsilon RI Signaling	41	0.002238721	0.152	-3.441
ERK/MAPK Signaling	42	0.002511886	0.132	-3.657
Sperm Motility	43	0.002691535	0.15	-4.359
14-3-3-mediated Signaling	44	0.002818383	0.146	-2.982
D-myo-inositol (1,4,5)-Trisphosphate Biosynthesis	45	0.002951209	0.259	-2.646
Glioblastoma Multiforme Signaling	46	0.003311311	0.137	-3.962
TREM1 Signaling	47	0.003388442	0.173	-3.051
Integrin Signaling	48	0.003548134	0.128	-5.099
Synaptic Long Term Depression	49	0.003890451	0.133	-3.674
Aryl Hydrocarbon Receptor Signaling	50	0.003981072	0.142	-1.265
Cardiac β-adrenergic Signaling	51	0.003981072	0.142	-1.5
Estrogen-Dependent Breast Cancer Signaling	52	0.004265795	0.163	-3.317
Systemic Lupus Erythematosus Signaling	53	0.004466836	0.124	NaN
Docosahexaenoic Acid (DHA) Signaling	54	0.004466836	0.192	NaN
PDGF Signaling	55	0.004786301	0.156	-3.873

[a]IPA canonical pathway analysis was performed using genes that were significantly down-regulated (log_2FC <1.0; FDR<0.05) in anti-IgM-treated cells. Of the 2187 significantly down-regulated genes, 1845 were included in the IPA analysis.

Appendix C

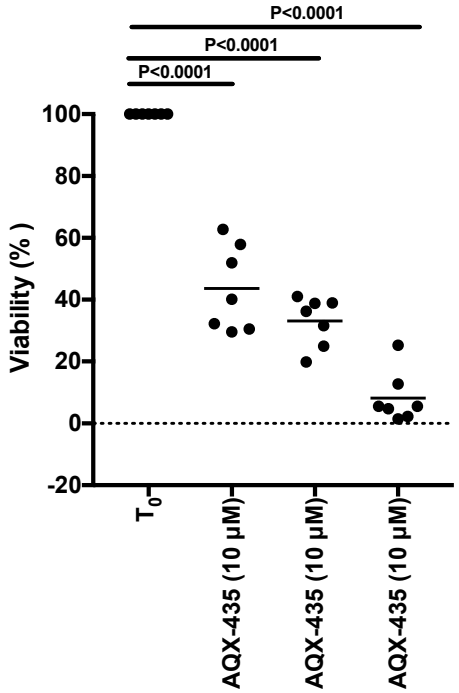

Figure C. AQX-435-induced apoptosis in CLL cells.

CLL samples (n=8) were treated with the indicated concentrations of AQX-435. After 24 hours, cell viability was measured using Annexin-V/PI staining. Cell viability was also analysed at the start of the experiment (0 hours). Graph shows mean and individual date points for relative viability ($AnnexinV^-/PI^-$ cells) with values for cells at the start of the experiment (T_0) set to 100 %. The statistical significance indicate the effect of AQX-435 induced apoptosis (paired Student's t-test).